

Figure 17 Variation of void ratio with mean effective pressure during the drained triaxial compression tests of Figs. 15 and 16.

As shown in Figs. 18, the failure envelopes of dense and loose Sacramento River sand are generated by the Mohr circles at the peak failure states of Figs. 15 and 16. These failure envelopes are both curved over a large range of normal effective stress σ' , but can be approximated by straight segments in smaller ranges of σ' . The values of cohesion intercept c' , friction angle ϕ'_p , and stress ranges σ' are listed in Table 3. For $6.5 < \sigma' < 35$ MPa, c' is equal to 0.2 MPa to fit the curved failure envelope, which does not imply that the sand is cohesive as fine-grained materials. The dense sand has a larger and more curved failure envelope than loose sand in the lower σ' range, but about the same strength in the higher σ' range, as loose sands become denser under large pressure.

The failure envelope of Sacramento River sand can also be defined in $s'-t$ space. This envelope is curved and can be approximated by straight segments defined by the values of ξ' and a' in Table 3. As shown in Fig. 19, the failure envelope in $p'-q$ space is also slightly curved, and is larger for dense sand than for loose sand for $p' < 4$ MPa. Figure 20 represents the variation of ϕ'_p calculated by using Eq. 5 with the mean pressure p'_f at peak failure for the dense and loose sands. For $p'_f < 10$ MPa, ϕ'_p linearly varies with the logarithm of p'_f and depends on the sand density. However, for $p'_f > 10$ MPa, ϕ'_p coincides for dense and loose sands.

TABLE 3

Variation of cohesion c' , friction angle ϕ'_p , and parameters ξ' and a' with normal effective stress σ' for loose and dense Sacramento River sand.

State	Effective normal stress (MPa)	Friction angle ϕ'_p (deg)	Cohesion c' (kPa)	ξ' (deg)	a' (kPa)
Loose	0.0–6.5	33.0	0	28.6	0
	6.5–35.0	29.7	207	26.4	180
Dense	0.0–3.0	37.2	0	31.2	0
	3.0–10.0	30.2	393	26.7	340
	10.0–35.0	32.7	0	28.4	0

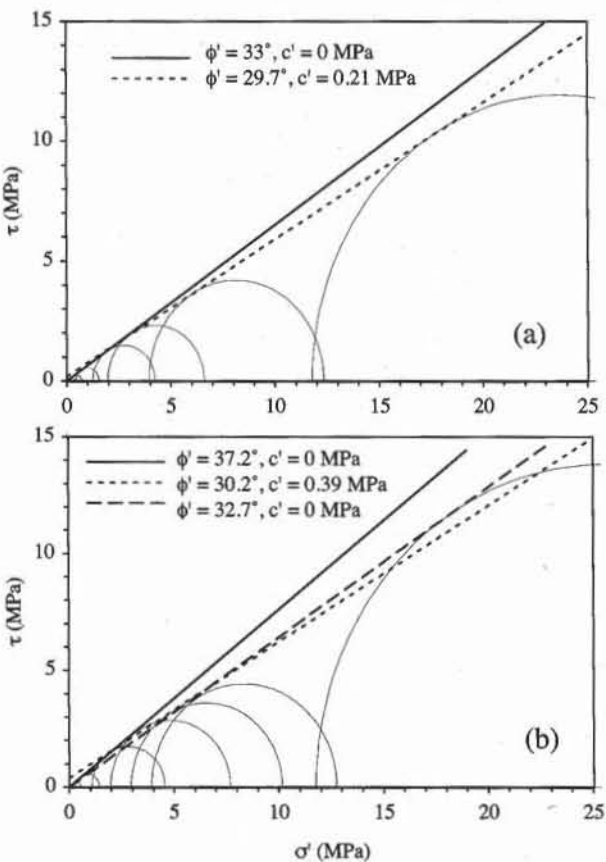


Figure 18 Peak failure envelope of (a) dense and (b) loose Sacramento River sand obtained from the results of Figs. 15 and 16.

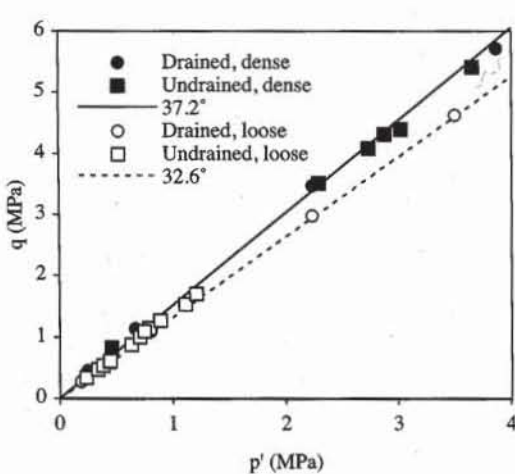


Figure 19 Peak failure envelope in p' - q space obtained for loose and dense Sacramento River sand from CD and CU triaxial compression tests at various confining pressures.

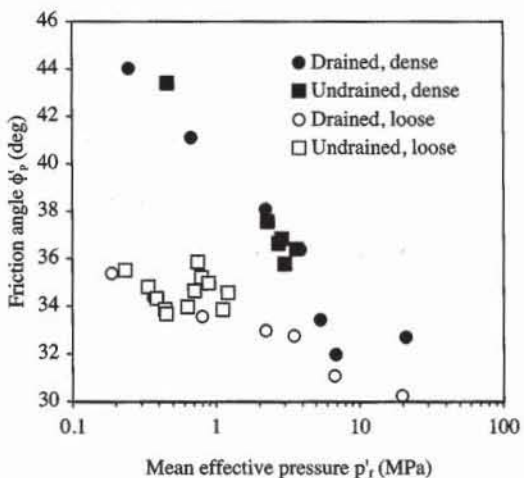


Figure 20 Variation of peak friction angle with mean effective pressure at failure for loose and dense Sacramento River sand during drained and undrained triaxial compression tests.

Undrained Triaxial Tests on Sacramento River Sand

Figures 21 and 23 show the stress-strain response, variation of excess pore pressure, and effective $p'-q$ stress paths for the loose and dense Sacramento River sand subjected to CU triaxial compression tests at various confining pressures σ_3 .

As shown in Figs. 15 and 21, the stress-strain responses of loose Sacramento River sand are quite different during CU and CD tests performed at the same cell pressure. For instance, for CD and CU tests at $\sigma_3 = 1.2$ MPa, the maximum value of q is about 2.9 and 1.1 MPa, respectively. As shown in Fig. 22, this reduction in strength in CU tests is caused by the increase in pore pressure and decrease in p' , compared to CD tests in which there is no pore pressure and p' increases.

As shown in Fig. 23, in the case of dense sands, the $p'-q$ effective stress paths are also curved due to changes in pore pressure. However, the shear strength increases because p' increases due to a decrease in pore pressure. During the undrained tests at $\sigma_3 = 0.1$, 1., and 1.5 MPa, the pore pressure becomes equal to minus atmospheric pressure (i.e., -0.1 MPa), which puts the water under vac-

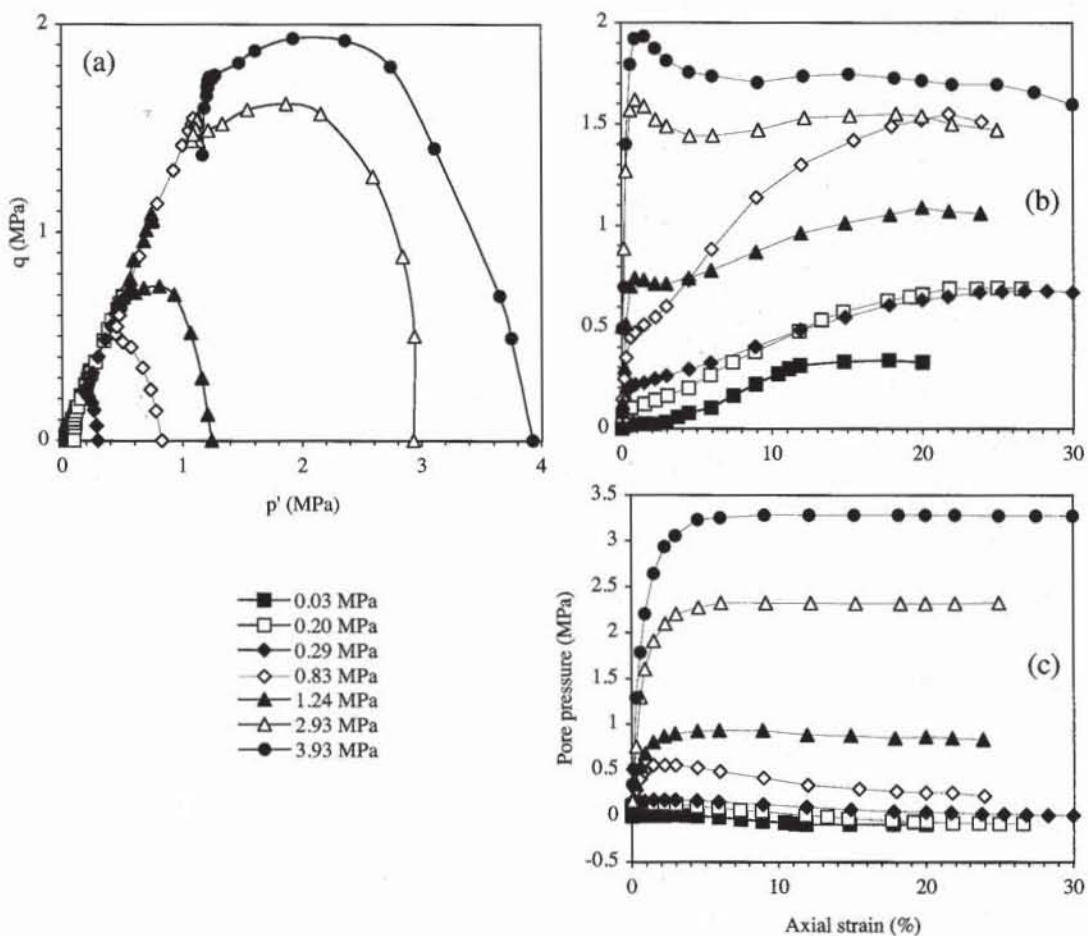


Figure 21 Results of CU triaxial compression tests on loose Sacramento River sand at various confining pressures: (a) effective stress paths, (b) variation of deviator stress q versus axial strain, and (c) variation of pore pressure versus axial strain (data after Seed and Lee, 1967).

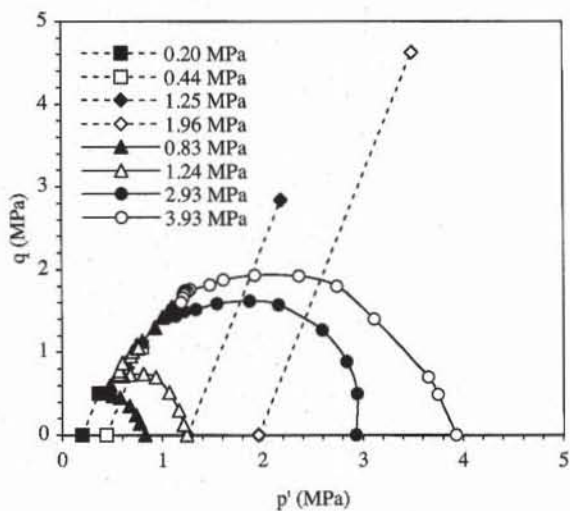


Figure 22 Effective stress path during the CD (dashed) and CU (solid) triaxial tests of Figs. 15 and 21.

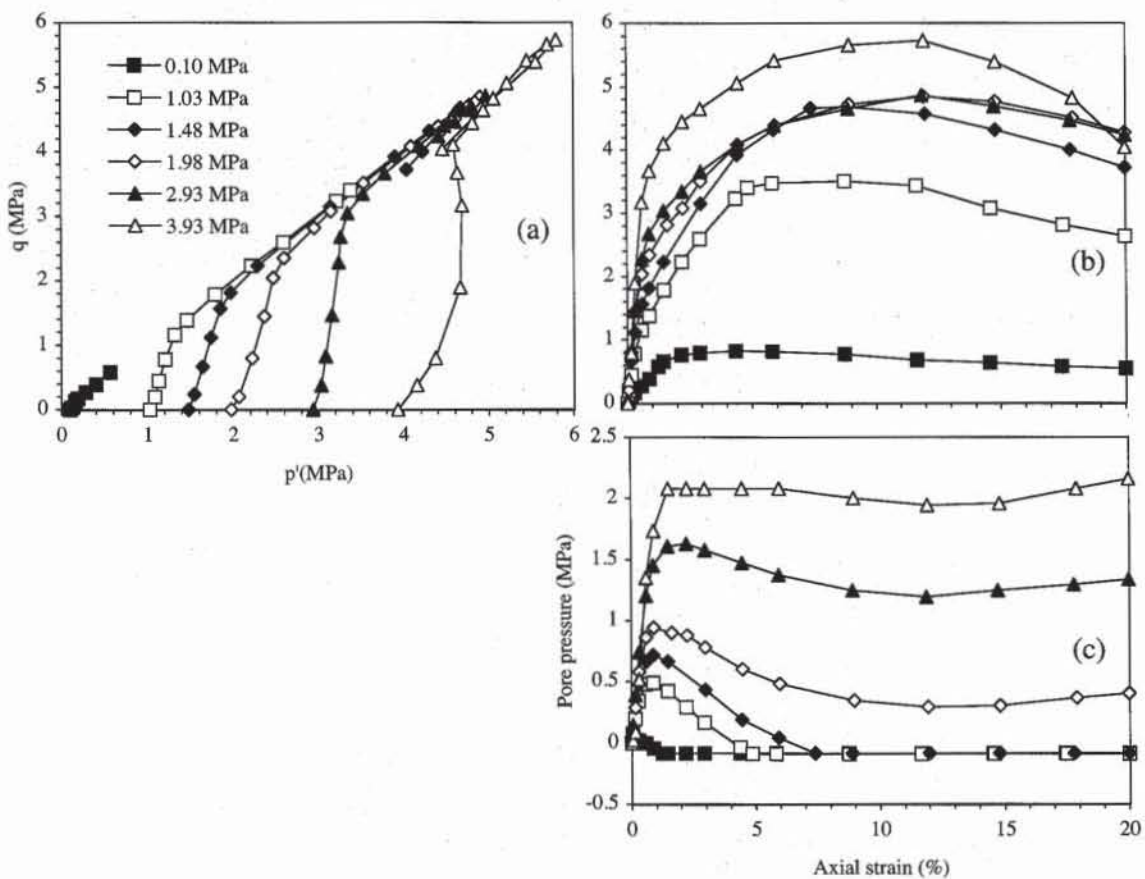


Figure 23 Results of CU triaxial compression tests on dense Sacramento River sand at various confining pressures: (a) effective stress paths, (b) variation of deviator stress q versus axial strain, and (c) variation of pore pressure versus axial strain (data after Seed and Lee, 1967).

uum. The pore pressure can no longer decrease because air bubbles form in water due to cavitation. When the pore pressure reaches -0.1 MPa, the CU triaxial test is no longer undrained, but drained as cavitation allows for volume changes. Cavitation may be avoided by increasing the back pressure (see Chapter 7-6).

Figures 19 and 20 compare the peak failure envelope obtained from CD and CU triaxial tests for the loose and dense Sacramento River sands. Both drained and undrained failure envelopes coincide. In term of effective stress, the failure envelopes of the Sacramento River sand are identical during drained and undrained conditions. This remark reconciles the apparent difference between the drained and undrained shear strength of sands, and demonstrates the advantage of expressing the failure of soils in terms of effective stress.

Undrained Triaxial Tests on Banding Sand

Figure 24 shows the stress-strain response and pore-pressure response of Banding sand subjected to CU triaxial compression tests, and compare them to drained responses during CD tests. The CU tests are performed at three different relative densities $D_r = 30\%$, 44% , and 47% , and the CD test at $D_r = 30\%$. All tests are performed at the same confining pressure $\sigma_3 = 400$ kPa. The undrained shear strength is smaller than the drained shear strength for $D_r = 30\%$ and 44% , but becomes larger for $D_r = 47\%$. For $D_r = 30\%$, the residual undrained shear strength is very small, which corresponds to the catastrophic phenomenon of liquefaction. Additional information on liquefaction can be found in Ishihara (1993).

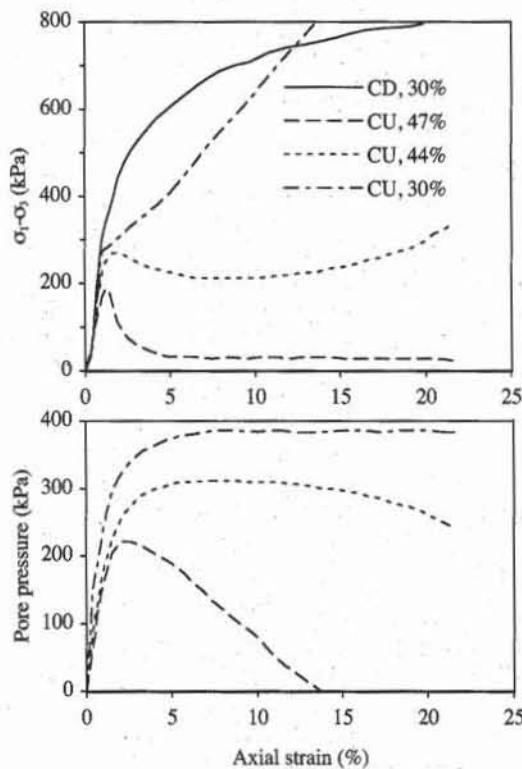


Figure 24 Stress-strain and pore pressure responses of three CU tests and one CD test on Banding sand with various relative density D_r , but identical confining pressure $\sigma_3 = 400$ kPa (after Castro, 1969).

**Typical Characteristics for Shear Strength
of Coarse-Grained Soils**

The shear strength of sands and gravels are influenced by many factors, including mean effective pressure, void ratio, particle shape, grain size distribution, water, particle size, intermediate principal stress, and overconsolidation pressure.

Table 4 shows an early attempt to tabulate the variation of friction angle with density. The peak friction angle ϕ'_p varies from 28 to 48° depending on density. The residual friction angle ϕ'_r varies from 26 to 36°, independently of density. Table 5 includes the additional effects of void ratio, grain angularity, grain size and coefficient of uniformity on ϕ'_p for various soils, and extends the range of variation of ϕ'_p from 28 and 60°. Well-graded soils have a larger ϕ'_p than poorly-graded soils. In Tables 3 and 4, ϕ'_p increases with the grain angularity and density.

TABLE 4

Peak and residual friction angle of cohesionless soils (after Hough, 1957).

Classification	Friction angle ϕ'_p at peak strength (deg)		Friction angle ϕ'_r at ultimate strength (deg)
	Medium	Dense	
Silt (nonplastic)	28–32	30–34	26–30
Uniform fine to medium sand	30–34	32–36	26–30
Well-graded sand	34–40	38–46	30–34
Sand and gravel	36–42	40–48	32–36

TABLE 5

Friction angle of cohesionless soils (Holtz and Kovacs, 1981).

Soil type	Grain shape	D_{10} (mm)	C_u	Loose		Dense	
				e	ϕ'_p (deg)	e	ϕ'_p (deg)
Ottawa standard sand	Well rounded	0.56	1.2	0.7	28	0.5	35
Sand from St Peter sandstone	Rounded	0.16	1.7	0.69	31	0.5	37
Beach sand from Plymouth, MA	Rounded	0.18	1.5	0.89	29		
Silty sand from Franklin Falls dam site, NH	Subrounded	0.03	2.1	0.85	33	0.7	37
Silty sand from vicinity of John Martin dam, CO	Subangular to subrounded	0.04	4.1	0.65	36	0.5	40
Slightly silty sand, Ft. Peck dam, MT	Subangular to subrounded	0.13	1.8	0.84	34	0.5	42
Screened glacial sand, Manchester, NH	Subangular	0.22	1.4	0.85	33	0.6	43
Beach sand of hydraulic fill dam, Quabbin Project, MA	Subangular	0.07	2.7	0.81	35	0.5	46
Artificial, well-graded mixture of gravel with sands	Subangular to subrounded	0.16	68	0.41	42	0.1	57
Sand from Great Salt Lake fill (dust gritty)	Angular	0.07	4.5	0.82	38	0.5	47
Well-graded, compacted crushed rock	Angular					0.2	60

Figures 25 to 27 show that ϕ'_p is significantly influenced by void ratio e . As shown in Fig. 25, ϕ'_p decreases from 40 to 32° when e increases, but remains larger than the friction angle between particles (e.g., $\phi_\mu = 26^\circ$). Similar influence of void ratio on ϕ'_p is observed for various types of granular soils including grav-

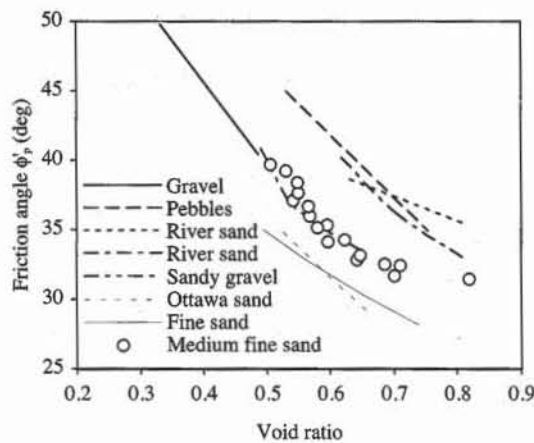


Figure 25 Variation of friction angle versus void ratio for several granular soils (data after Lambe and Whitman, 1979; and Rowe, 1962).

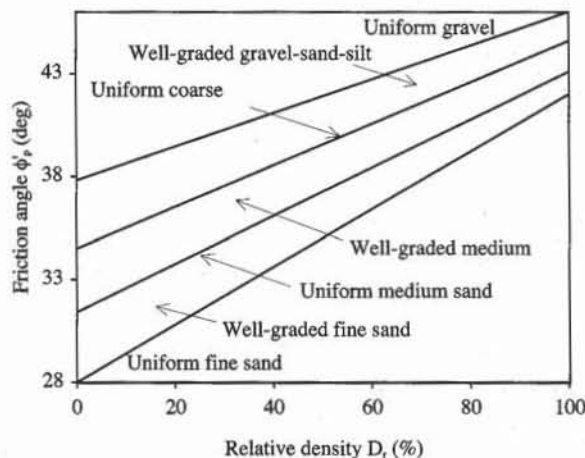


Figure 26 Variation of friction angle ϕ'_p with relative density D_r (Schertmann, 1978)

els and fine sands. As shown in Fig. 26, ϕ'_p varies with relative density D_r and coefficient of uniformity. As shown in Fig. 27, ϕ'_p can be correlated to dry unit weight, relative density, and USCS classification.

Figure 28 shows the effects of confining pressure σ'_3 on ϕ'_p in coarse-grained soils subjected to triaxial compression tests. These effects which were noticed for loose and dense Sacramento River sand are also observed in other sands, and can account for a decrease in ϕ'_p from 45 to 32°.

Using a database of clean sands, Bolton (1986) shows that the peak and residual friction angles ϕ'_p and ϕ'_r are related through

$$\phi'_p = \phi'_r + \alpha \max [0, D_r [Q - \ln(p'_f)] - R] \quad (16)$$

where α depends on the type of loading (3 for triaxial compression, and 5 for plane strain compression), D_r is the relative density, Q the soil mineralogy and compressibility coefficient (10 for quartz and feldspar, 8 for limestone, 7 for anthra-

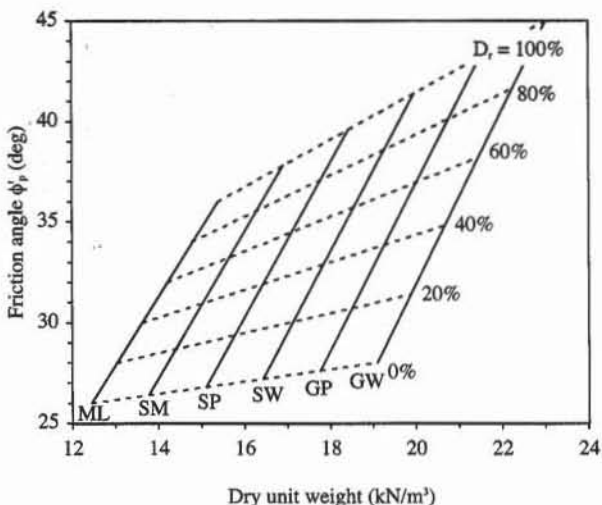


Figure 27 Correlation between friction angle, dry unit weight, relative density, and USCS classification for coarse-grained soils without plastic fines (NAVFAC, 1982).

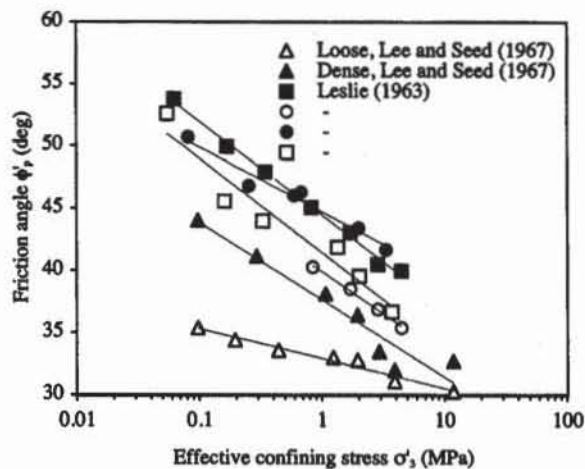


Figure 28 Variation of friction angle with confining pressure in tri-axial compression test (data after Leslie, 1963).

cite, 5.5 for chalk), R a fitting coefficient (equal to 1 for the data of Fig. 29), and $p_f' = (\sigma'_1 + \sigma'_2 + \sigma'_3)/3$ the mean effective pressure at failure. As shown in Fig. 29, Eq. 16 is capable of describing the variation of $\phi'_p - \phi'$, with density and mean pressure for loose and dense Sacramento River sands.

The residual friction angle ϕ' , in Eq. 16 can be evaluated from the relation proposed by Koerner (1970):

$$\phi'_r = 36^\circ + \Delta\phi_1 + \Delta\phi_2 + \Delta\phi_3 + \Delta\phi_4 + \Delta\phi_5 \quad (17)$$

where $\Delta\phi_1, \Delta\phi_2, \Delta\phi_3, \Delta\phi_4$, and $\Delta\phi_5$ depend on the grain shape, grain size, gradation, density and mineral hardness as specified in Table 6. By decreasing order of importance, the factors influencing ϕ' , are particle size, particle shape, mineral hardness, density, and gradation.

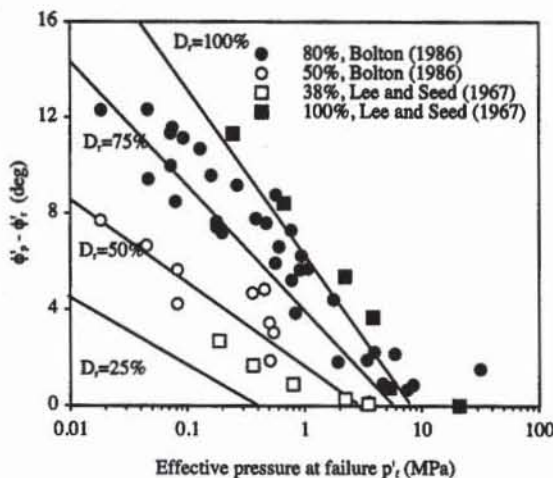


Figure 29 Variation of $\phi'_f - \phi'_r$ with effective mean pressure p'_f at failure (Bolton, 1986).

TABLE 6

Variation of friction angle ϕ'_r with particle shape, grain size, gradation, density, and mineral (Koerner, 1970).

Factor	Description	Correction factor (deg)				
		$\Delta\phi_1$	$\Delta\phi_2$	$\Delta\phi_3$	$\Delta\phi_4$	$\Delta\phi_5$
Particle shape	Low sphericity and angular shape	2				
	High sphericity and subrounded shape	-6				
Grain size	Fine sand, $0.2 > D_{10} > 0.06$ mm		0			
	Medium sand, $0.6 > D_{10} > 0.2$ mm		-4			
Gradation	Coarse sand, $2.0 > D_{10} > 0.6$ mm		-9			
	Gravel, $D_{10} > 2$ mm		-11			
Density	Poorly-graded soil, $C_u < 2$		0			
	Medium uniformity, $C_u = 10$		-1			
Mineral	Well-graded soil, $C_u > 2$		-2			
	Loose packing, $0 < D_r < 50\%$			-1		
	Medium density, $50 < D_r < 75\%$			0		
	Dense packing, $D_r > 75\%$			4		
	Quartz				0	
	Feldspar, calcite, chlorite				4	
	Muscovite, mica				6	

Influence of intermediate principal stress. The effect of intermediate principal stress σ'_2 on shear strength can be characterized by introducing the parameter b

$$b = \frac{\sigma'_2 - \sigma'_3}{\sigma'_1 - \sigma'_3} \quad (18)$$

where σ'_1 and σ'_3 are the major and minor principal effective stress, respectively. b varies from 0 to 1 when σ'_2 varies from σ'_3 to σ'_1 , $b = 0$ in triaxial compression tests ($\sigma'_2 = \sigma'_3$), and $b = 1$ in triaxial extension tests ($\sigma'_2 = \sigma'_1$).

The investigation of the effect of σ'_2 on friction angle ϕ'_p requires advanced testing apparatus, some of which are described in Chapter 5-4. As shown in Fig. 30 for various sands, b influences the friction angle ϕ'_p calculated from the measured values of σ'_1 and σ'_3 (Eq. 5). It is minimum for $b = 0$, sharply increases for

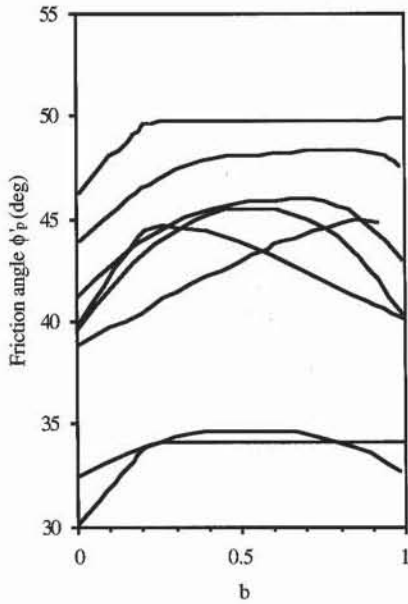


Figure 30 Variation of friction angle ϕ'_p with parameter b measured on various sands (after Biarez and Hicher, 1994).

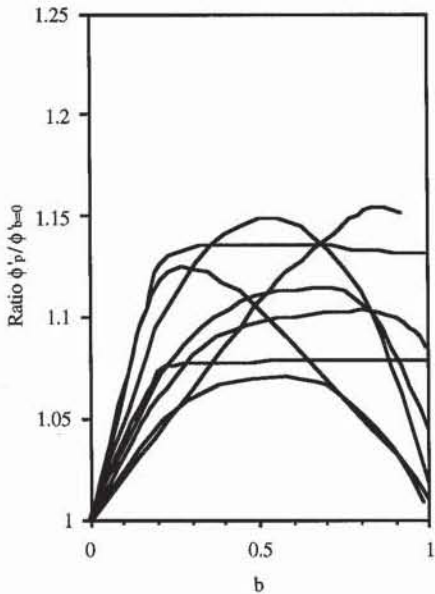


Figure 31 Variation of normalized friction angle $\phi'_p / \phi'_{b=0}$ with parameter b corresponding to Fig. 30.

$0 < b < 0.3$, then keeps increasing or start to decrease depending on data sets. Biarez and Hicher (1994) attributed this scatter in experimental results to the diversity of testing conditions. In most cases, ϕ'_p is larger in extension ($b = 1$) than in compression ($b = 0$). Figure 31 shows the variation of $\phi'_p / \phi'_{b=0}$ with b , in which ϕ'_p is normalized by its values $\phi'_{b=0}$ in triaxial compression ($b = 0$). ϕ'_p can be 15% larger than $\phi'_{b=0}$.

The effect of intermediate principal stress σ'_2 on ϕ' is not accounted for in the three-dimensional Mohr–Coulomb failure surface (Eq. 9). To account for this effect, Lade and Duncan (1975) suggested the following failure envelope:

$$I_1^3 - \eta_1 I_3 = 0 \quad \text{and} \quad \eta_1 = \frac{(3 - \sin \phi')^3}{(1 - \sin \phi') \cos^2 \phi'} \quad (19)$$

while Matsuoka and Nakai (1974) proposed:

$$I_1 I_2 - \eta_2 I_3 = 0 \quad \text{and} \quad \eta_2 = \frac{9 - \sin^2 \phi'}{1 - \sin^2 \phi'} \quad (20)$$

where I_1 , I_2 and I_3 are the stress invariants defined in Chapter 5-1, and ϕ' is calculated for $b = 0$. In the σ_1 – σ_2 – σ_3 principal stress space of Fig. 6a, the failure surfaces of Eqs. 19 and 20 are smooth cones which encompass the angular Mohr–Coulomb surface. As shown in the deviatoric plane of Fig. 32, these failure surfaces have similar cross-sections.

Figure 33 and 34 shows the variations of ϕ' and $\phi'_p / \phi'_{b=0}$ with b which are calculated by introducing b in Eqs. 19 and 20. The variations corresponding to Mohr–Coulomb are not represented; they are horizontal lines. Equation 20 predicts the measured variation of ϕ' better than Eq. 19. However, Eq. 20 does not describe the change in ϕ' observed between triaxial compression and extension. In

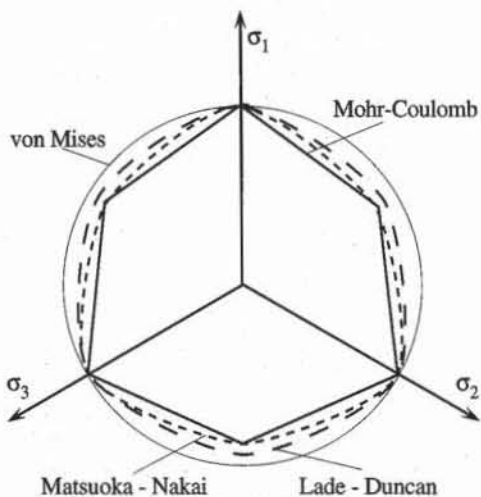


Figure 32 Failure surfaces in deviatoric plane: Mohr-Coulomb, von Mises, Lade-Duncan, and Matsuoka-Nakai.

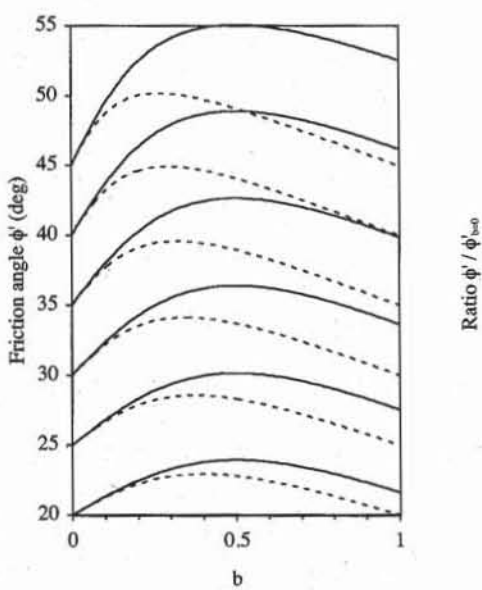


Figure 33 Variation of friction angle ϕ' with parameter b predicted by Lade and Matsuoka-Nakai failure surface for various friction angle in triaxial compression.

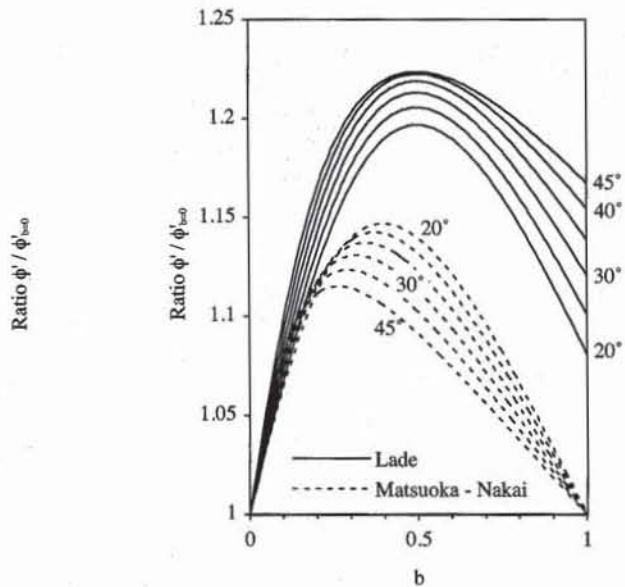


Figure 34 Variation of normalized friction angle $\phi'/\phi'_{b=0}$ with parameter b corresponding to Fig. 33.

In addition to Eqs. 19 and 20, there are other failure envelopes (e.g., Bardet, 1990) which can account for the effects of b on ϕ' .

SHEAR STRENGTH OF FINE-GRAINED SOILS

The shear strength characteristics of fine-grained soils (e.g., clays and silts) are introduced by examining the stress-strain response of a particular clay—Weald clay—which was extensively tested under CD and CU triaxial compressions.

Isotropic Consolidation of Weald Clay

Figure 35 shows the result of an isotropic consolidation test on Weald clay. Starting from the value 0.8, the void ratio e decreases linearly with the logarithm of effective mean pressure p' . The point (p', e) moves on the *virgin consolidation line* (VCL), which has the equation

$$e = X - \lambda \ln(p') \quad (21)$$

where λ is the VCL slope, and X is the void ratio at $p' = 1$ kPa. As described in Chapter 6-1, the soil response is irreversible after a loading reversal. When p' is decreased from p'_1 , the point (p', e) moves away from the VCL along a swelling line defined by

$$e = e_1 - \kappa \ln \frac{p'}{p'_1} \quad (22)$$

where κ is the average swelling slope, and e_1 is the void ratio at $p' = p'_1$. The parameter λ and κ are related to the compression indices C_c and C_s defined in Chapter 6-1 through

$$\lambda = 0.434 C_c \quad \text{and} \quad \kappa = 0.434 C_s \quad (23)$$

where the coefficient 0.434 results from the conversion from decimal to natural logarithm. For Weald clay, $\lambda = 0.092$ and $\kappa = 0.032$.

The degree of overconsolidation of a clay is characterized by the overconsolidation ratio OCR which is

$$OCR = \frac{p'_p}{p'_0} \quad (24)$$

where p'_0 is the present mean effective pressure, and p'_p is the preconsolidation pressure, which is the largest effective pressure applied in the past. OCR is always larger or equal to 1. When the point (p'_0, e) is on the VCL, the clay is normally consolidated and $OCR = 1$. When it is on a swelling line, the clay is overconsolidated.

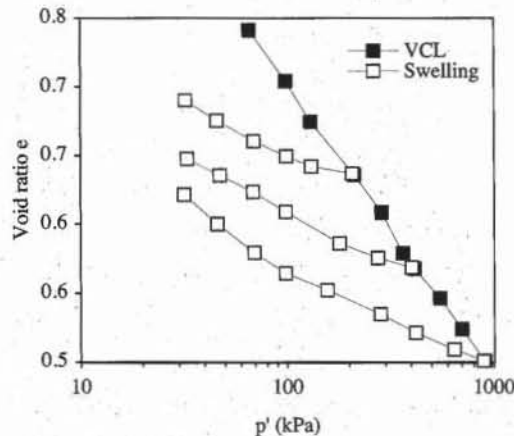


Figure 35 Results of isotropic consolidation on Weald clay (data after Parry, 1960).

dated and $OCR > 1$. For instance, a clay with an $OCR = 30$ and $p'_0 = 30$ kPa was first isotropically loaded to 900 kPa, before being unloaded to 30 kPa.

CD Triaxial Compression Tests on Weald Clay

Figure 36 shows the results of CD triaxial tests on normally consolidated and overconsolidated samples of Weald clay. At 69 kPa confining pressure, the shear strength of the overconsolidated ($OCR = 12$) sample is almost twice that of the normally consolidated sample. The overconsolidated samples initially compact then dilate during shear, whereas the normally consolidated samples compact until they fail. A similar behavior was observed for dense and loose Sacramento River sands. As shown in Fig. 36a, the failure envelope is not straight, but curved at small pressures.

CU Triaxial Compression Tests on Weald Clay

Figure 37 shows the results of CU triaxial tests on normally and over-consolidated samples of Weald clay at two different total confining pressures σ_3 . In p' - q space, the normally consolidated stress-path moves toward the origin, whereas the overconsolidated stress-path goes away from the origin, which increases p' , and makes the overconsolidated sample at $\sigma_3 = 35$ kPa almost as strong as the normally consolidated sample at $\sigma_3 = 207$ kPa.

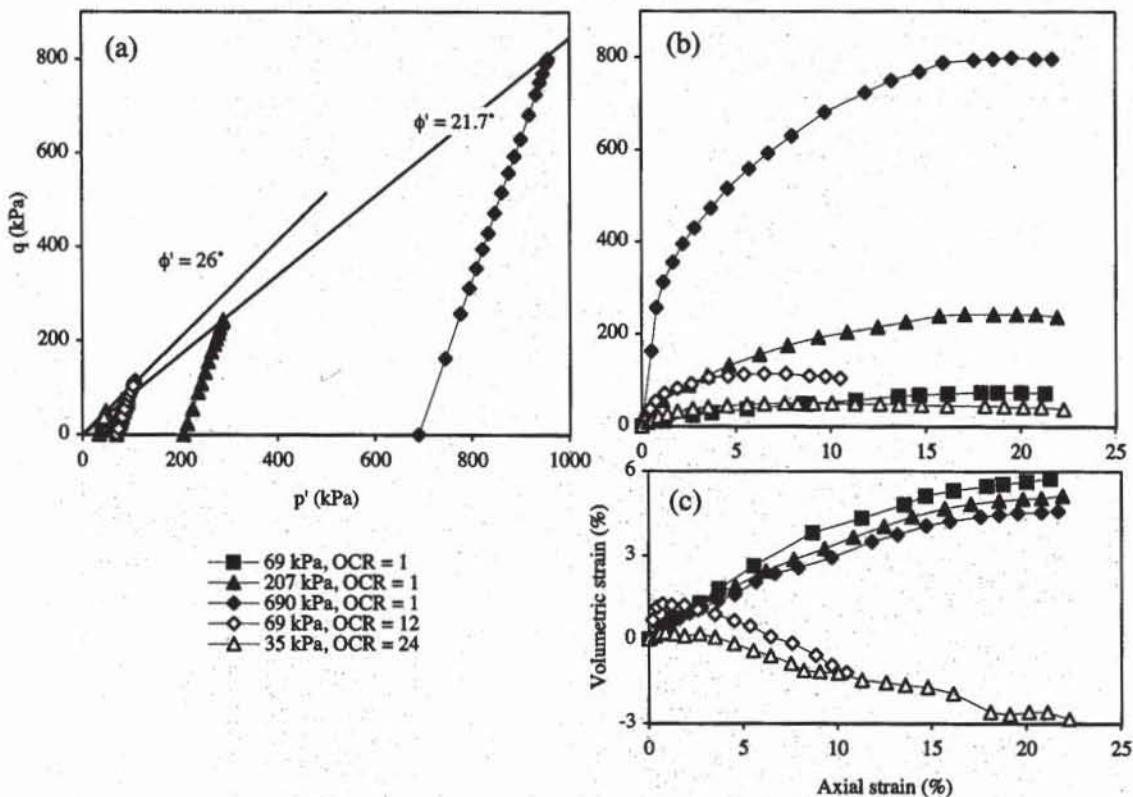


Figure 36 Results of CD triaxial tests at various confining pressures on normally consolidated ($OCR = 1$) and overconsolidated ($OCR = 12$ and 24) samples of Weald clay; (a) effective p' - q stress paths, (b) stress-strain response, and (c) volumetric response (data after Parry, 1960).

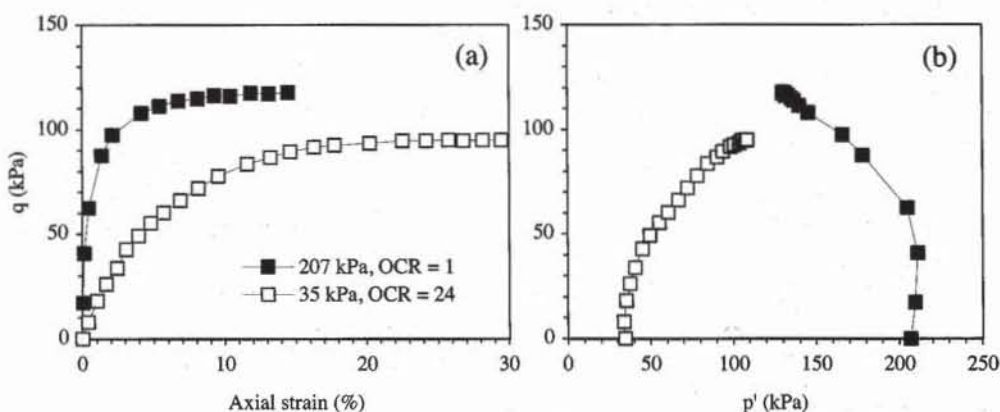


Figure 37 Results of CU triaxial tests on normally consolidated (207 kPa, $\text{OCR} = 1$) and overconsolidated sample (35 kPa, $\text{OCR} = 24$) of Weald clay: (a) stress-strain response, and (b) effective p' - q stress path (data after Parry, 1960).

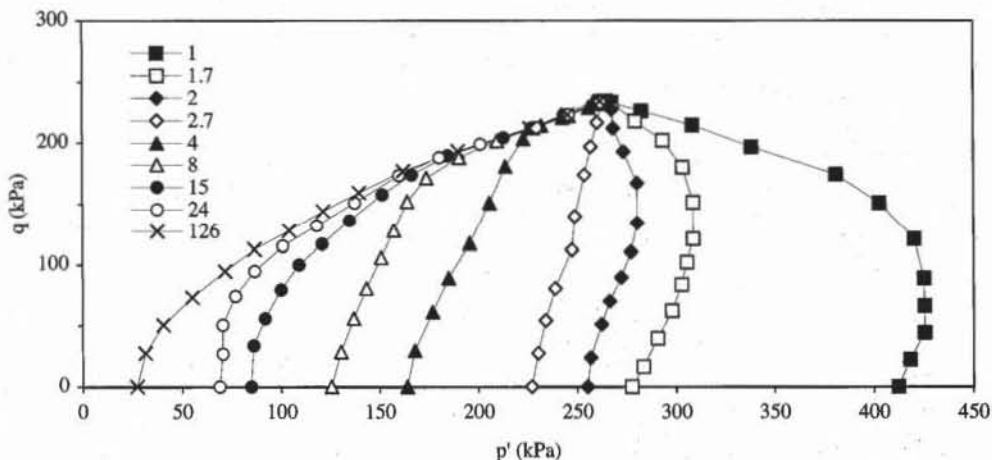


Figure 38 Effective p' - q stress paths for samples of Weald clay with the same void ratio but different overconsolidation ratios (data after Parry, 1960).

As shown in Fig. 38, the p' - q stress paths that are associated with the same void ratio but different overconsolidation ratios from 1 to 126 converge toward a common point. The undrained shear strength of Weald clay is largely determined by its initial void ratio.

Critical State Theory for Clays

The critical state theory (Schofield and Wroth, 1968) extends the Mohr-Coulomb failure theory by describing the variation of shear strength with void ratio. One of its major achievement is to relate the drained and undrained behaviors of fine-grained soils, and to predict their undrained shear strength.

In the critical state theory, soils reach their critical state when they undergo a residual failure at constant volume. The critical state is associated with residual failure, but not with peak failure, which is generally accompanied with a volume

change. The projection of the *critical state line (CSL)* onto the $p'-q$ space is

$$q = M p' \quad (25)$$

where M is related to the residual friction angle through:

$$\phi'_r = \sin^{-1} \left(\frac{3M}{6+M} \right), \quad \text{and} \quad M = \frac{6 \sin \phi'_r}{3 - \sin \phi'_r} \quad (26)$$

The projection of the critical state line in the $p'-e$ space is parallel to the virgin compression line

$$e = \Gamma - \lambda \ln(p') \quad (27)$$

where Γ is the critical void ratio at $p' = 1$ kPa. The *CSL* void ratio Γ and *VCL* void ratio X at $p' = 1$ kPa are related through

$$\Gamma = X - (\lambda - \kappa) \ln(r) \quad (28)$$

where the parameter r is usually selected equal to 2.

As shown in Figs. 39 and 40, the critical state is identical for the drained and undrained responses of normally consolidated and overconsolidated samples of Weald clay. The point (p', q, e) tends to move closer to the critical state during shear loading. A material denser than the critical void ratio dilates to reach the critical state, whereas a material looser than the critical void ratio compacts to reach the critical state.

The critical state theory has four material constants: λ , κ , ϕ' and Γ . The values of these constants are listed in Table 7 for London clay, Weald clay, and kaolin, along with their liquid and plastic limits, specific gravity and the void ratios corresponding to plastic and liquid limits.

Undrained Shear Strength from Critical State Theory

By definition, the undrained shear strength S_u is the shear stress at failure during undrained loadings. During undrained triaxial compression tests, S_u is

$$S_u = \frac{1}{2} q_f = \frac{1}{2} (\sigma_1 - \sigma_3)_f = t_f \quad (29)$$

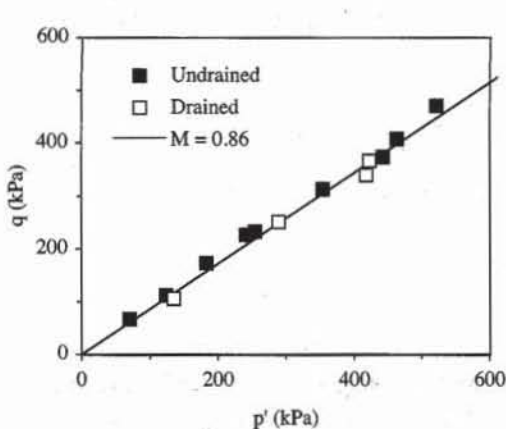


Figure 39 Critical state in $p'-q$ space from drained and undrained triaxial test results on Weald clay (data after Parry, 1960).

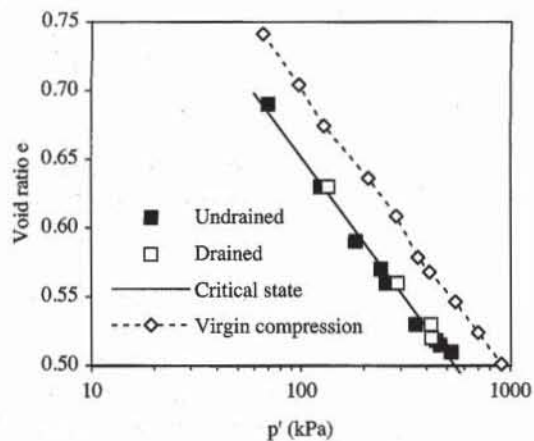


Figure 40 Critical state in $p'-e$ space from drained and undrained triaxial test results on Weald clay (data after Parry, 1960).

TABLE 7

Critical state parameters and plasticity indices for London clay, Weald clay, and kaolin (Schofield and Wroth, 1968)

Material constants	London clay	Weald clay	Kaolin
Slope of critical state line (CSL), λ	0.161	0.093	0.260
Void ratio on CSL at 1 kPa, Γ	1.759	1.060	2.767
Slope of critical state in p'/q space, M	0.88	0.95	1.02
Friction angle ϕ' at critical state (deg)	22.6	24.2	25.8
Slope of swelling line, κ	0.062	0.035	0.050
Parameter $\Lambda = (\lambda - \kappa)/\lambda$	0.615	0.624	0.808
Liquid limit LL (%)	78	43	74
Plastic limit PL (%)	26	18	42
Plasticity index PI (%)	52	25	32
Specific gravity G_s	2.75	2.75	2.61
Void ratio at LL	2.145	1.183	1.931
Void ratio at PL	0.715	0.495	1.096

At the critical state, S_u is therefore related to the effective mean pressure p'_f through

$$S_u = \frac{1}{2} M p'_f \quad (30)$$

During undrained tests, the void ratio e is constant (i.e., $e = e_0$) and is related to p'_f through Eq. 27, that is

$$e_0 = \Gamma - \lambda \ln(p'_f) \quad (31)$$

Therefore Eq. 30 becomes

$$S_u = \frac{M}{2} \exp\left(\frac{\Gamma - e_0}{\lambda}\right) \quad (32)$$

S_u can also be expressed in terms of the liquidity index LI . By definition, the liquidity index LI is

$$LI = \frac{w - PL}{PI} \quad (33)$$

where w is the water content, PL the plastic limit, PI the plasticity index ($PI = LL - PL$), and LL the liquid limit. $LI = 1$ when $w = LL$ and $LI = 0$ when $w = PL$. For saturated soils, the void ratio e_0 is related to the water content through

$$e_0 = w_0 G_s = G_s(PL + PI \times LI) \quad (34)$$

Therefore Eq. 32 becomes

$$S_u = \frac{M}{2} \exp\left[\frac{\Gamma - G_s(PL + PI \times LI)}{\lambda}\right] \quad (35)$$

The undrained shear strength S_u becomes the following function of plasticity index LI

$$S_u = S_{uPL} \left(\frac{S_{uLL}}{S_{uPL}} \right)^{LI} \quad (36)$$

where S_{uPL} and S_{uLL} are the undrained shear strength at plastic limit PL and liquid limit LL , respectively:

$$S_{uPL} = \frac{M}{2} \exp[(\Gamma - G_s PL)/\lambda] \quad \text{and} \quad S_{uLL} = S_{uPL} \exp[-G_s PI/\lambda] \quad (37)$$

Schofield and Wroth (1968) observed that the ratio S_{uPL}/S_{uLL} is practically equal to 100, which implies that the slope of the critical can approximately be related to specific gravity and plasticity index

$$\lambda = \frac{G_s PI}{\ln[S_{uPL}/S_{uLL}]} \approx 0.217 G_s PI \quad (38)$$

S_u can also be expressed in terms of OCR. An overconsolidated clay with the initial state (p'_0, e_0) corresponds to the normally consolidated state (p'_p, e_p) which is on the VCL

$$e_p = e_0 - \kappa \ln \frac{p'_p}{p'_0} = e_0 - \kappa \ln OCR = X - \lambda \ln(OCR p'_0) \quad (39)$$

Therefore e_0 is

$$e_0 = X - (\lambda - \kappa) \ln OCR - \lambda \ln p'_0 \quad (40)$$

Eq. 32 becomes

$$\frac{S_u}{p'_0} = \frac{M}{2} \exp\left(\frac{\Gamma - X}{\lambda}\right) OCR^{\frac{\lambda - \kappa}{\lambda}} \quad (41)$$

and using Eq. 28,

$$\frac{S_u}{p'_0} = \frac{M}{2} \left(\frac{OCR}{r}\right)^{\Lambda} \quad (42)$$

where the parameter Λ is

$$\Lambda = \frac{\lambda - \kappa}{\lambda} \quad (43)$$

The value of Λ is limited to be between 0 and 1, and is typically about 0.8. As mentioned previously, r depends on Γ and X and is usually selected equal to 2. The undrained shear strengths of overconsolidated and normally consolidated clays are therefore related through

$$\frac{S_u}{p'_0} = \left(\frac{S_u}{p'_0}\right)_{OCR=1} OCR^{\Lambda} \quad (44)$$

The undrained shear strength of normally consolidated clays can be approximated as

$$\left(\frac{S_u}{p'_0}\right)_{OCR=1} \approx 0.29 M = \frac{1.72 \sin \phi'_r}{3 - \sin \phi'_r} \quad (45)$$

The undrained shear strength predicted by Eqs. 36, 42, 44, and 45 is compared to experimental results later.

The normalization of Eq. 44 sets the basis of the *SHANSEP* procedure (Ladd and Foott, 1974). *SHANSEP*, which is the acronym for Stress History and Normalized Soil Engineering Properties, assumes the normalization of the undrained stress-strain response and undrained shear strength of normally and overconsolidated soils. This normalization is convenient to determine the undrained shear strength at various initial stresses p'_0 and overconsolidation ratios OCR by performing a relatively small number of tests with different values of p'_0 and OCR . Additional information on *SHANSEP* can be found in Jamiolkowski et al. (1985) and Ladd (1991).

Drained Shear Strength of Fine-grained Soils

As shown in Fig. 41, at low effective normal stress σ' , the failure envelope of overconsolidated fine-grained soils is usually more curved and larger than the failure envelope of normally consolidated material which is practically linear. As illustrated in Fig. 42, this bump *EDC* in the failure envelope originates from overconsolidation, which is represented by unloading *CDE* in the $\sigma'-e$ space. *ABCF* represents the failure envelope of normally consolidated clays, while *EDCF* denotes that of overconsolidated clays.

Table 8 gives typical values of effective cohesion intercept c' and effective friction angle ϕ' for various fine-grained soils. The values of c' range from 0 to 150 kPa, and those of ϕ' from 5 to 38°. As described previously, the failure envelope of fine-grained soils is curved, and the cohesion intercept c' varies with the range of σ' . For normally consolidated clays, c' is practically equal to zero (see Fig. 41). For overconsolidated clays, c' depends nonlinearly on σ' and OCR . In most fine-grained soils, at the exception of cemented soils, partially saturated soils, and heavily consolidated clays, the intercept of the curved failure envelope with the τ axis is small.

As shown in Figs. 43 and 44, the friction angle ϕ' of fine-grained soils decreases from 40° to 20° when the plasticity index PI varies from 20% to 100%. In the particular case on montmorillonite clay with extremely large water content (1000%), ϕ' decreases to the low value of 5°. As shown in Fig. 44, the residual friction angle ϕ'_r decreases from 33 to 5° with the clay fraction (percent by weight finer than 2 μm obtained from grain-size distribution curve). Figures 45 and 46

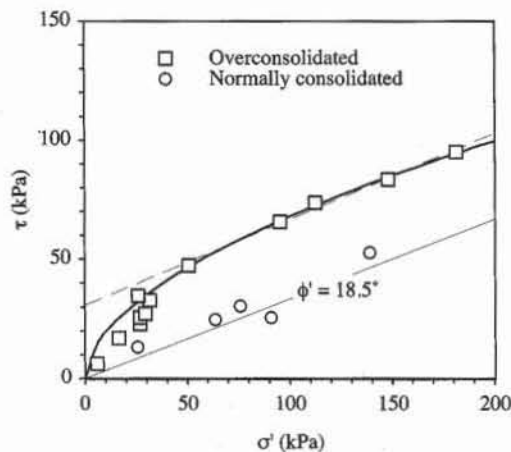


Figure 41 Failure envelopes of normally consolidated and overconsolidated clays (data from Singh et al., 1973).

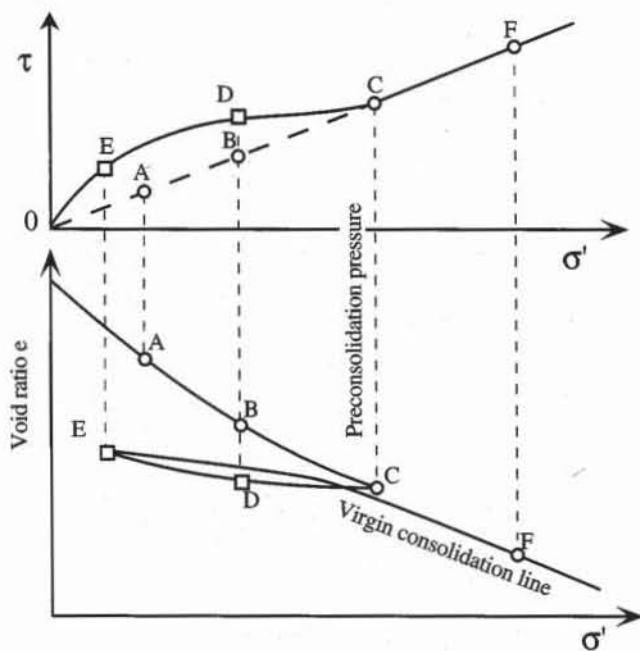


Figure 42 Effect of overconsolidation on failure envelope of fine-grained soils.

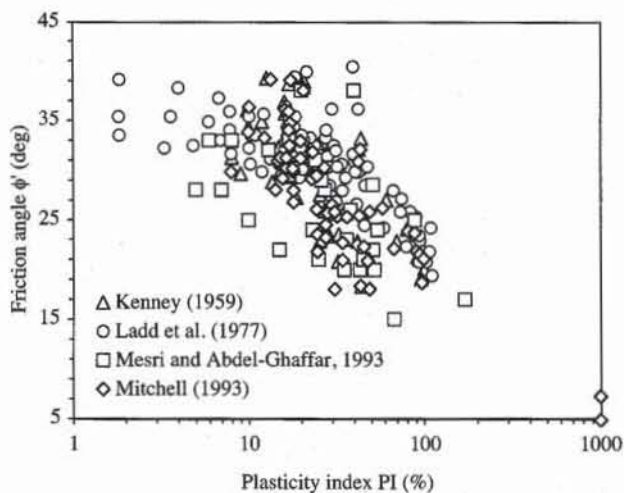


Figure 43 Relation between friction angle ϕ' and plasticity index PI on fine-grained soils (data after Kenney, 1959; Ladd et al., 1977; Mesri and Abdel-Ghaffar, 1993; and Mitchell, 1993).

show the effect of the intermediate principal stress on ϕ' . Like coarse grained soils, fine grained soils have a friction angle ϕ' that depends on the coefficient b , and may vary as much as 20% with b .

Undrained Shear Strength of Fine-grained Soils

The undrained shear strength S_u is a widely used soil parameters in geotechnical engineering. However, S_u is not a fundamental soil property like the effective

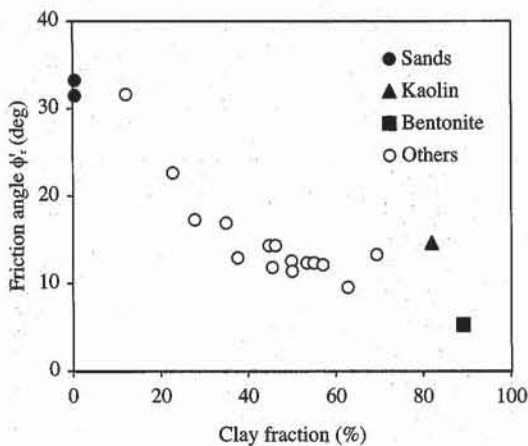


Figure 44 Relation between residual friction angle ϕ' and clay fraction from ring shear tests and field studies (Skempton, 1985).

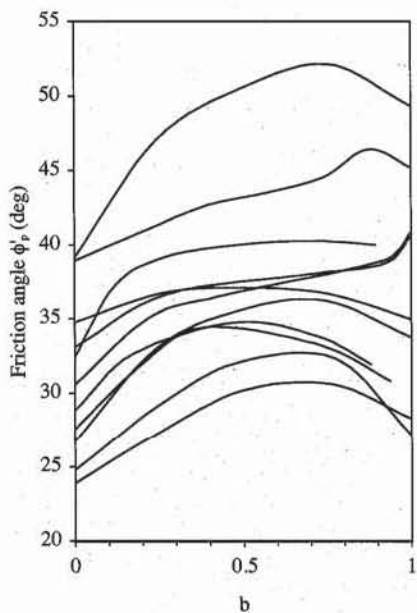


Figure 45 Variation of friction angle ϕ' with parameter b measured on various clays (after Biarez and Hicher, 1994).

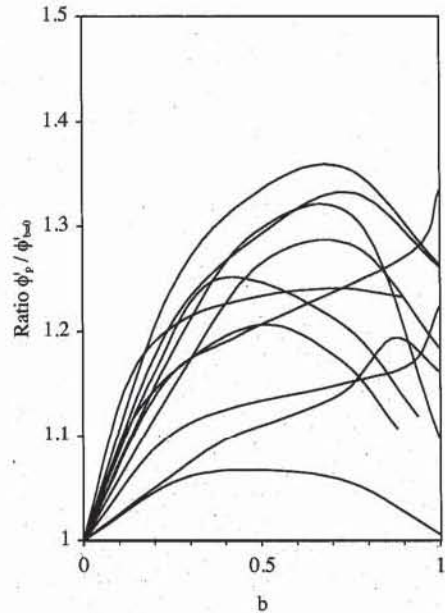


Figure 46 Variation of normalized friction angle $\phi'_p / \phi'_{b=0}$ with parameter b corresponding to Fig. 45.

friction angle ϕ . S_u is influenced by many factors including the mode of testing, rate of loading, confining stress level, initial stress states, and other variables. Hereafter, we present typical values of S_u obtained in a standard or reference test—CU triaxial tests with isotropic consolidation—and examine the relations between S_u and plasticity index, overconsolidation ratio, liquidity index, and sensitivity.

Table 9 lists values of S_u for various soils as well as additional properties, including liquid and plastic limits and water content. The values for S_u in Table 9 range from 10 to 300 kPa.

TABLE 8

Values of cohesion intercept c' and friction angle ϕ' obtained for various soils (Mesri and Abdel-Ghaffar, 1993)

Case record	Water content (%)	Plasticity index PI (%)	Liquidity index LI	c' (kPa)	ϕ' (deg)
Kimola Canal	53	27	1	4.9	28
Lake Michigan bluffs	-	2-14	Stiff	8-20	31-35
Trondheim embankment	22-25	3-7	>1	22	28
Selnes landslide	34	5	3.4	4.9	28
Selnes landslide	-	7	1	14.9	28
Voitaggio landslide	8	10	-1.1	20	25
Slope failure in China	22	20	0.05	11.8	38
Saguling power station	-	15	Stiff	26	22
Slope failure in Sri-Lanka	-	24	Stiff	10.4	31
Slope failures in varigated clay shale	20	24	-0.58	7.4	24
Slope failures in varigated clay shale	-	-	-	5.3	25
Jackfield landslide	30	25	0.4	7.2	21
Selset landslide	12	13	-0.8	8.6	32
Lodalen slide	31	17	0.75	9.8-12	27-32
Drammen River slide	32-38	17	1	0-2	33
Ullensaker landslide	30	6	1.3	1.5-2.3	32-34
S. Barbara coal mine	43	35	-0.6	150	20
Carsington Dam	40	43	0.19	10	20
Shellmouth test fill	39	38	0.48	12.4	26
Seven Sisters Dikes	48	67	0.27	13.8	15
North Ridge Dam	37	51	0.31	24.8	22
London clay failures	31	52	0	12	20
Lias clay failures, weathered	18-28	31-41	<0	17	23
Field test in Oslo clay	30-38	23	>0.5	8.8	24
Lesueur landslide	-	170	Stiff	29	17
Failure at Wettern	-	88	0	8	25
Amuay slides	15-20	40	0.15	6.9	38
Bosse-Galine test cut	55	51	0.61	10-12	26-31
River Albedosa slide	29	26	0.17	55	29
Genesse embankment	20-45	45	0.2-0.4	10-20	21
Oxford test embankment	31	54	0	10	24

Influence of Test Conditions

As mentioned in Chapter 5-4, the soil samples are not consolidated before being sheared in UU triaxial tests. In Table 9, the undrained shear strength measured from UU tests is denoted $S_u(UU)$, and that measured from CU tests is denoted by S_u , assuming that the CU tests are the reference laboratory tests to determine the undrained shear strength. As shown in Fig. 47, at the exception of a few cases, $S_u(UU)$ is systematically smaller than S_u . Detailed studies (e.g., Ladd et al., 1977) have shown that the UU tests are often in gross error because of sampling disturbance effects and omission of reconsolidation phase.

Influence of PI. Various empirical correlations were proposed to relate the undrained shear strength S_u and plasticity index PI . The most common correlation for normally consolidated clays (Skempton, 1957) is

$$\frac{S_u}{\sigma'_0} = 0.11 + 0.0037 PI \quad (46)$$

where σ'_0 is the effective vertical stress, and PI the plasticity index. As shown in Fig. 48, Eq. 46 applies to the soils tested by Bjerrum (1954) and Leonards (1962), but not to those of Osterman (1960) which have large plasticity index, and are difficult to sample in the field and test in the laboratory.

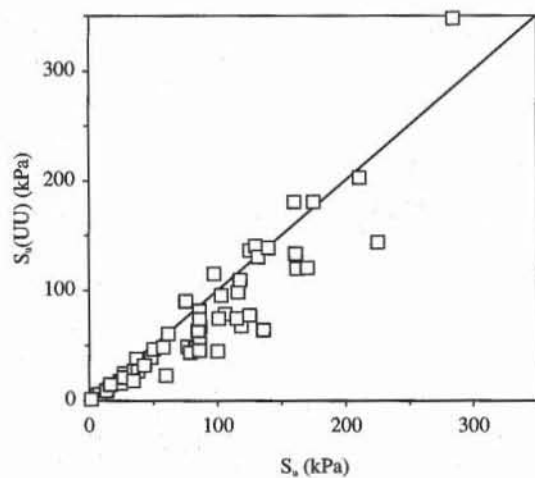


Figure 47 Relation between undrained shear strength $S_u(\text{UU})$ measured in UU triaxial tests and undrained shear strength S_u measured in CU triaxial tests on various soils (data after Chen and Kulhawy, 1993).

TABLE 9

Database for undrained shear strength of various clays from CU and UU tests (Chen and Kulhawy, 1993)

Site	Soil description	Total unit weight					Sensitivity	Depth (m)	OCR	S_u (kPa)	$S_u(\text{UU})/S_u$	S_u/σ'_0
		LL (%)	PL (%)	w (%)	(kN/m ³)							
Boston	Medium blue clay	49	25	35	18.7			12.2	4	106	0.74	0.8
		49	26	38	18.4			18.3	1.8	86.6	0.77	0.48
		39	21	36	19.3			27.4	1	84.5	0.58	0.32
Lagunillas	High plasticity clay	61	24					6.2	1.3	23.5	0.75	0.4
		61	24					6.4	1.3	24.3	0.64	0.41
Kawasaki	High plasticity clay	65	34		15.1			20.5	1.2	76.6	0.64	0.49
		68	32		15.1			25	1.2	82.8	0.58	0.45
		70	27		15.6			35	1.2	118.7	0.57	0.48
Beau-mont	High plasticity clay with fissures and slickensides	61	21	25	19.8			0-8	7.5	75	1.2	1.58
Mont-gomery	Light grey sandy clay with dessication	31	15	20	20.9			9-17		162	0.74	1.14
Hamilton	Firm to stiff grey silty clay	32	18	30				3-6	3.2	47.8	0.82	1.16
		44	24	31				6-9	2.2	50.2	0.93	0.73
		39	22	33				11	1.2	78.9	0.55	0.78
Lackland	Expansive black to gray clay Fissured expansive	60	18					0-3	5	57.4	0.84	1.48
		73	24	30				3-6	4.8	86.	0.95	1.12
		86	28	29				6-9	6.5	160	1.13	1.6
Rio de Janero Guana-barabaya	Clay shale Soft gray clay	95	27	29				9-12	8.5	211	0.96	1.47
		135	50	170	13.2	2.6		2-4	2.1	6.2	0.83	0.62
		125	60	140	13.2	2.6		4-6	2	8.1	0.73	0.1
South Padre	Medium to stiff clay	110	45	125	13.2	2.6		6-8	1.7	13.5	0.69	0.46
		90	35	110	13.2	2.6		8-10	1.7	13.2	0.65	0.44
		57	26	29				6-12	1.2	86.1	0.61	0.6

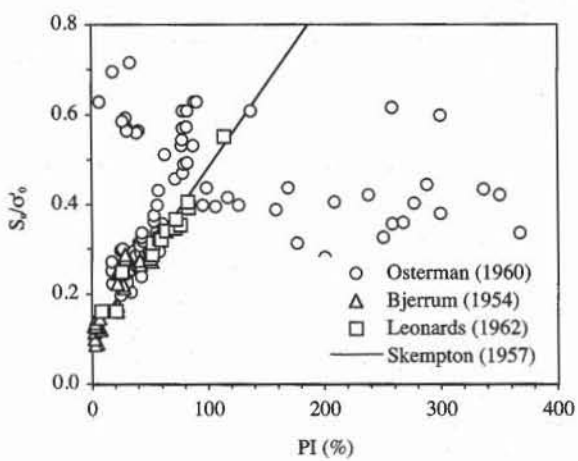


Figure 48 Variation of S_u/σ'_0 with plasticity index PI for normally consolidated clays (after Holtz and Kovacs, 1981).

TABLE 9 (CONT.)

Database for undrained shear strength of various clays from CU and UU tests (Chen and Kulhawy, 1993)

Site	Soil description	LL (%)	PL (%)	w (%)	Total unit weight (kN/m ³)	Sensitivity	Depth (m)	OCR	S_u (kPa)	S_u (UU) / S_u	S_u / σ'_0
Island St Alban	Soft to medium silty clay	55	27	26	15.3 17 16.8	5-10 5-10 5-10	15-18	1.1	136	0.47	0.51
		48	23	100			2.1	2.1	16.3	0.89	0.99
		40	18	62			55	2.3	27.4	0.89	0.85
		30	14	48			7.2	2.4	37	1.02	0.93
Boston	Lean and moderately sensitive blue clay	38	18			5-10		18		0.87	1.7
		38	18			5-10		3.2		0.75	0.72
		38	18			5-10		1		0.56	0.32
		45	35					9	125	1.09	1.28
Laboratory results	Overconsolidated kaolinite	45	35								
Hackensack	Varved clay	44	9				7.9-15	9	101	0.74	1.03
Valley								1.8	61.6	0.98	0.6
Santa Barbara	Firm Pleistocene clay	63	28	45			20-60	1.6	85	0.75	0.36
channel	Hard silty clay	55	27	30			100-140	1.2	225	0.64	0.26
Lakeland	Cohesive slimes	32	22	32	18.8		0-33	1.1	100	0.45	0.41
San Francisco	Soft gray clay (new)	88	43	92	14		6-10	1.4	27	0.77	0.43
Bay mud	Bay mud)	90	45	95	14.7		10-15	1.3	35	0.77	0.44
San Francisco	Sandy clay	83	45	92	14.5		6-9	1.4	38	0.71	0.55
Boston	Soft gray clay	70	40	72	15		9-12	1.2	43	0.75	0.49
	Marine illitic blue clay	41	20					4		0.68	0.91
		41	20					2		0.65	0.55
Anacostia	Dark organic silty clay	67	32	60	15.7		4-6	2.1	34.2	0.53	0.46
Tuckerton	Dark gray plastic clay	83	57	80	13.6		6-9	2.1	59.7	0.38	0.32
		42	22	42			16	8	130	1.08	2.03
		57	37	55			17	5.2	86	0.86	1.17
Ottawa	Dark gray plastic clay	78	28	58			18-23	4	116	0.85	1.16
	Leda clay - moderately preconsolidated clay with high plasticity	46	14	72		26	6-9	3.1	97.5	1.18	1.08
		33	8	68		80	9-12	2.2	117.5	0.93	1.02
		34	9	51		114	2-15	2	125	0.62	0.95
Madingley	and sensitivity	38	28	52		84	18-21	1.6	115	0.65	0.68
	Gray fissure Gault clay with heavily overconsolidated clay	67	23	31	18.4		3-4	20	103	0.93	2.33
		68	26	30	18.6		4-6	18	132	0.99	2.27
		74	29	29	18.8		6-7	14	140	0.99	2
South-eastern Texas	Very stiff clay with high plasticity	67	30	30			15.2	6.5	175.5	1.03	0.87
		64	23	23			18.3	5.8	170	0.71	0.75
		61	12	26			21.3	2.9	161	0.83	0.64
Empire Chicago	Fine gray clay	83	26	45			36.6	12	86.1	0.53	0.27
	Hard silty clay	29	16	13	19.6		10	22	285	1.22	2.35

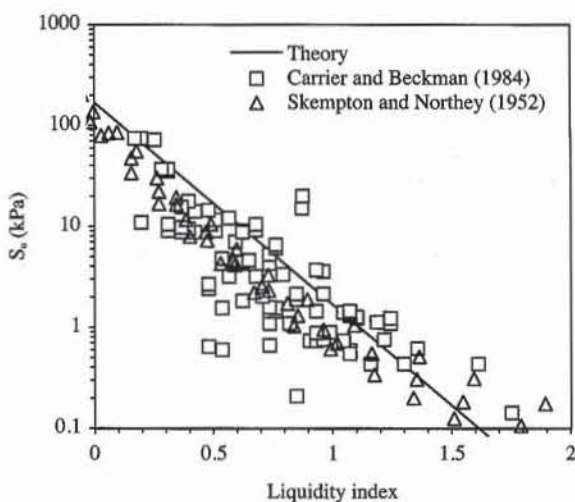


Figure 49 Relation between liquidity index and undrained shear strength S_u of clays (experimental data after Skempton and Northey, 1952; and Carrier and Beckman, 1984).

Influence of LI. As shown in Fig. 49, S_u decreases from about 100 to 0.1 kPa when LI increases from 0 to 2. Remarkably, S_u is almost 100 times larger at the plastic limit ($LI = 0$) than at the liquid limit ($LI = 1$). S_u is practically smaller than 1 kPa when $LI > 1$. The critical state theory (Eq. 36) describes the variation of S_u with LI as follows

$$S_u = S_{uPL} 10^{-2LI} \quad (47)$$

where S_{uPL} is the undrained shear strength at plastic limit, which is selected equal to 170 kPa in Fig. 49. As shown in Fig. 49, the values of S_u predicted by Eq. 47 are in agreement with measured values.

Influence of OCR. Figure 50 shows the variation of S_u/σ'_0 with overconsolidation ratio OCR . Jamiolkowski et al. (1985) suggested the following relation

$$\frac{S_u}{\sigma'_0} = (0.23 \pm 0.04) OCR^{0.8} \quad (48)$$

where σ'_0 is the initial vertical effective stress in the field. Eq. 48 can be obtained from Eq. 44 when $\Lambda = 0.8$, ϕ'_r varies from 17 to 24°, and σ'_0 is assumed equal to the mean effective pressure p'_0 . As shown in Fig. 50, Eq. 48 slightly overpredicts the measured variation of S_u/σ'_0 with OCR . As shown in Fig. 51, assuming that $\sigma'_0 = p'_0$, Eq. 44 predicts well the measured variation of normalized undrained shear strength with OCR .

Influence of Sensitivity. As shown in Fig. 52, the undrained shear strength is lower for remolded samples than for undisturbed samples. This change in S_u is characterized by the sensitivity S_t , which is the ratio of undrained shear strengths in the undisturbed and remolded states at the same water content:

$$S_t = \frac{S_{u(undisturbed)}}{S_{u(remolded)}} \quad (49)$$

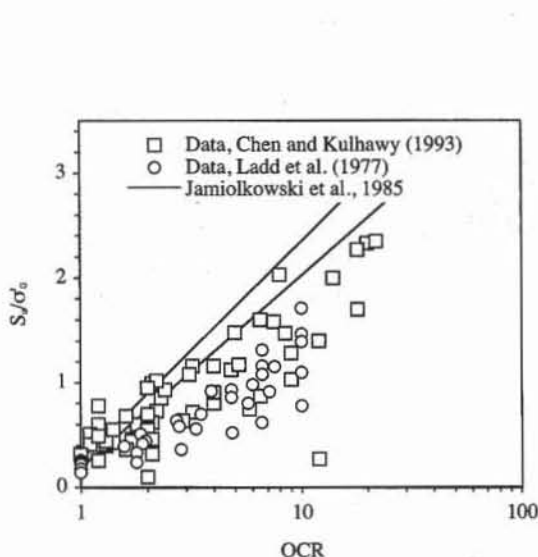


Figure 50 Variation of S_u/σ'_0 with overconsolidation ratio OCR for overconsolidated clays (data from Chen and Kulhawy, 1993, and Ladd et al., 1977).

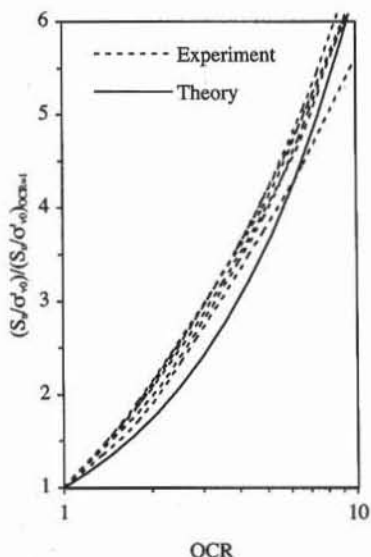


Figure 51 Variation of normalized S_u/σ'_0 with overconsolidation ratio OCR (data from Ladd et al., 1977; and theory of Eq. 44).

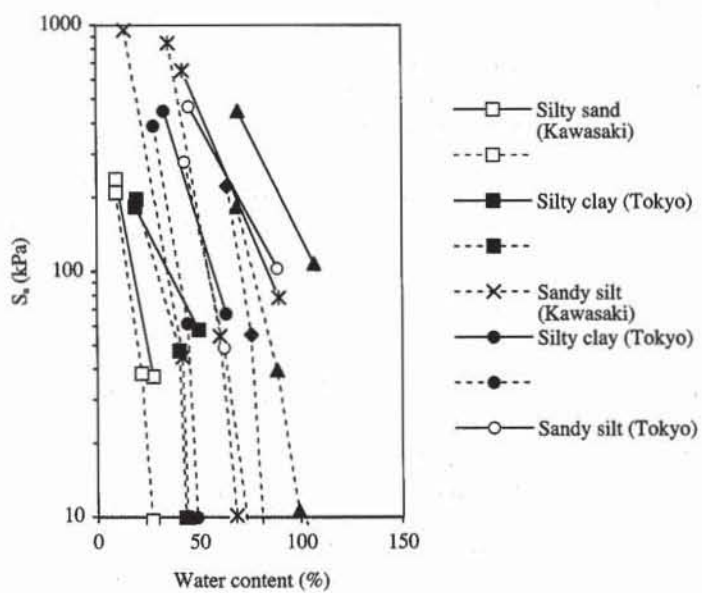


Figure 52 Relation between undrained shear strength S_u and water content for various undisturbed (solid lines) and remolded (dashed lines) samples of Japanese clays (Yoshinari, 1967).

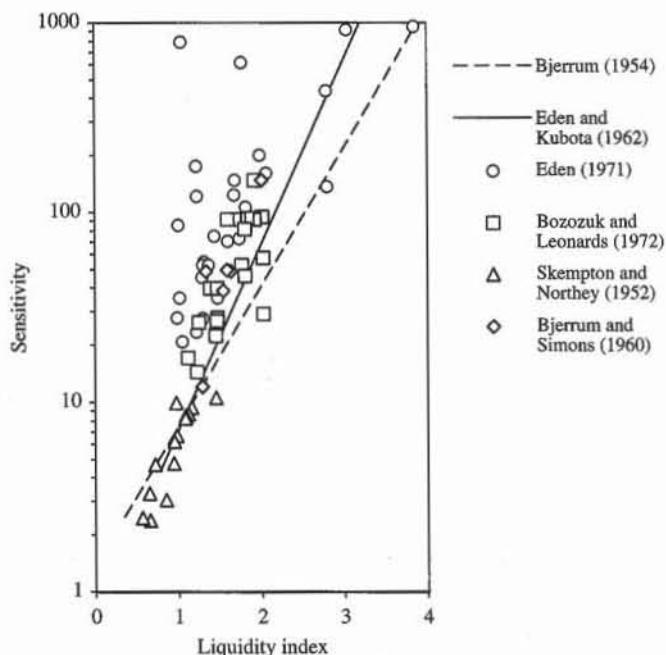


Figure 53 Relation between sensitivity and liquidity index for Scandinavian, British, Canadian, and some U.S. clays (after Holtz and Kovacs, 1981).

As shown in Fig. 53, S_t increases rapidly with liquidity index LI . S_t is generally less than 10 when LI is less than 1. Table 10 indicates the ranges of S_t commonly found in the United States, where highly sensitive clays are rare, and in eastern Canada and Scandinavia, where sensitive clays are more common.

TABLE 10
Typical values of sensitivity S_t
(after Holtz and Kovacs, 1981)

Condition	Range of S_t	
	United States	Sweden
Low sensitive	2–4	< 10
Medium sensitive	4–8	10–30
Highly sensitive	8–16	> 30
Quick	16	> 50
Extra quick		> 100

Relation between Elastic modulus and Undrained Shear Strength

The elastic Young's modulus can be compared to the undrained shear strength. As shown in Fig. 54, the ratio E_{max}/S_u for four different clays varies between 2500 and 500, where E_{max} is the elastic Young's modulus obtained for strain amplitudes smaller than 0.001%. The ratio E_{max}/S_u may become smaller than 500 when Young's modulus is determined for larger strain amplitude (see Chapter 5-5).

TOTAL STRESS FAILURE CRITERION

The failure envelopes of soils, which have been described in terms of effective stress until now, can also be represented in terms of total stress. In this case they

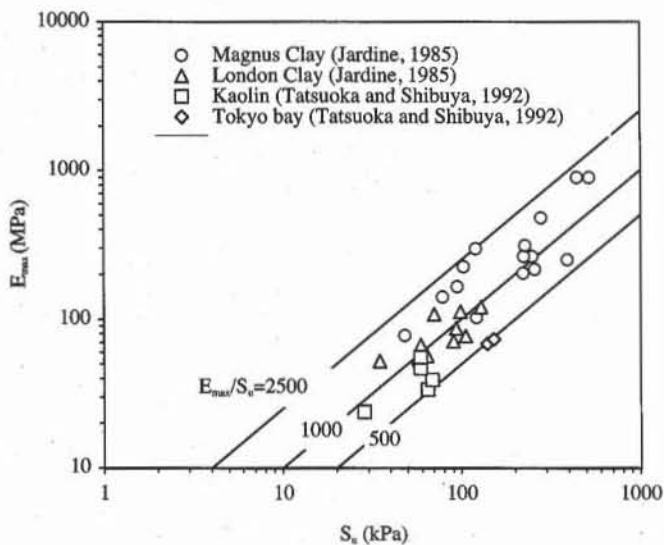


Figure 54 Relation between Young's modulus E_{max} measured at small strain amplitude ($< 10^{-3}\%$) and undrained shear strength S_u for several clays (after Tatsuoka and Shibuya, 1992).

are referred to as apparent. The apparent failure envelope in σ - τ space are constructed by enveloping the Mohr circles of total stress at failure during undrained tests, for instance as shown in Fig. 55 by enveloping circles A , B and C .

As shown in Fig. 55, in the case of CU tests, the apparent failure envelope has an apparent cohesion c_a and apparent friction angle ϕ_a which characterizes the increase in undrained shear strength S_u with the total normal stress σ (i.e., $S_u = c_a + \sigma \tan \phi_a$). When the pore pressures u_A , u_B , and u_C are known at failure, the effective failure envelope can also be constructed by drawing the effective stress circles A' , B' and C' from the total stress Mohr circles A , B , and C . This construction is impossible without pore pressure measurement.

In the case of UU tests, the apparent failure envelope can be constructed in the same way as for CU tests, for instance by using the circles A , D and E of Fig. 56. The apparent UU failure envelope is generally a straight horizontal line, and S_u is independent of σ . In the UU tests, the external pressure, which is applied to the saturated soil samples, is entirely taken by the pore pressure, and not by the

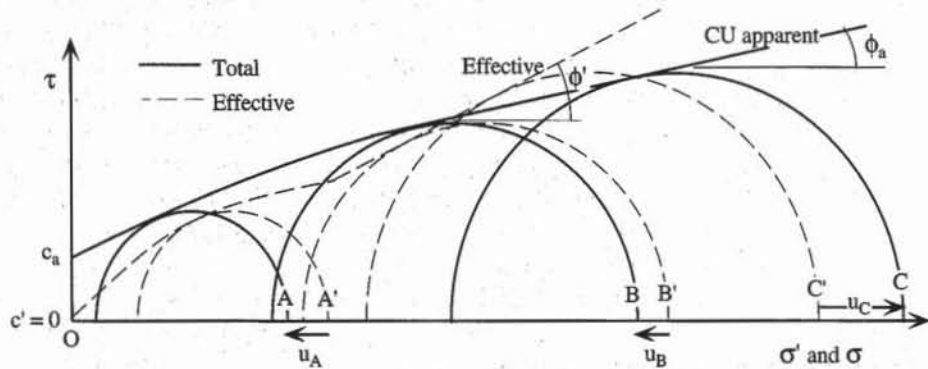


Figure 55 Apparent failure envelope constructed from CU tests, and effective failure envelope.

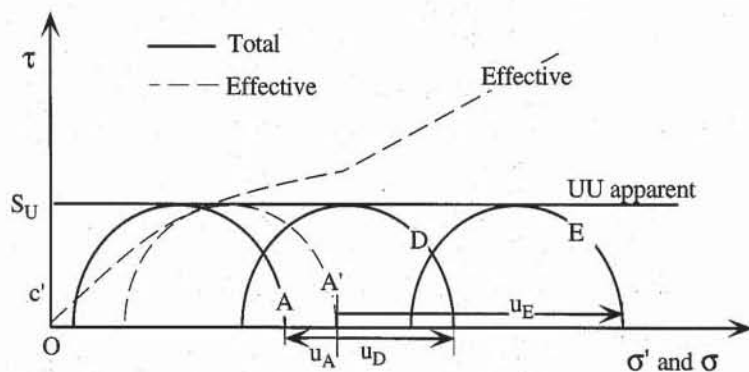


Figure 56 Apparent failure envelope constructed from UU tests, and effective failure envelope.

soil grains. At failure, the total stress Mohr circles *A*, *D*, and *E* have the same size because they correspond to the same effective stress Mohr circle *A'*, which is unfortunately unknown as the pore pressure is not measured.

REFERENCES

- BARDET, J. P., 1990, Lode dependences for isotropic pressure-sensitive elastoplastic materials, *J. Applied Mech.*, ASME, Vol. 57, pp. 498–506.
- BISHOP, A. W., 1966, The strength of soils as engineering materials, *Géotechnique*, Vol. 16, No. 2, pp. 91–128.
- BOLTON, M. D., 1986, The strength and dilatancy of soils, *Géotechnique*, Vol. 36, No. 1, pp. 65–78.
- CARRIER, W. D. III, and J. F. BECKMAN, 1984, Correlations between index tests and the properties of remoulded clays, *Géotechnique*, Vol. 34, No. 2, pp. 211–218.
- CHEN, Y. J. and F. H. KULHAWY, 1993, Undrained strength interrelationships among CIUC, UU, and UC tests, *J. Geotech. Eng.*, ASCE, Vol. 119, No. 11, pp. 1732–1750.
- CHEN, W. F., and A. F. SALEEB, 1982, *Constitutive Equations for Engineering Materials*, John Wiley & Sons, New York, pp. 441–559.
- COULOMB, C. A., 1776, Essai sur une application des règles de maximus et minimus à quelques problèmes de statique, relatifs à l'architecture, *Mémoires de Mathématique et de Physique, Présentés à l'Académie Royale des Sciences, par divers savants, et lus dans ses Assemblées*, Paris, Vol. 7, pp. 343–382.
- GOLDER, H. Q., and A. W. SKEMPTON, 1948, The angle of shearing resistance in cohesive soils for tests at constant water content, *Proceedings of the Second International Conference on Soil Mechanics and Foundation Engineering*, Rotterdam, Netherlands, Vol. 1, pp. 185–192.
- HOLTZ, R. D., W. D. KOVACS, 1981, *An Introduction to Geotechnical Engineering*, Prentice-Hall, Englewood Cliffs, NJ, pp. 449–519.
- HOUGH, B. K., 1957, *Basic Soil Engineering*, The Ronald Press Company, New York.
- ISHIHARA, K., 1993, Liquefaction and flow failure during earthquakes, The 33rd Rankine lecture, *Géotechnique*, Vol. 43, No. 3, pp. 351–415.
- JAMIOLKOWSKI, M., C. C. LADD, J. T. GERMAINE, and R. LANCELOTTO, 1985,

- New developments in field and laboratory testing of soils, *Proceedings of the 11th International Conference on Soil Mechanics and Foundation Engineering*, San Francisco, CA, Vol. 1, pp. 57-154.
- JARDINE, R. J., 1985, *Investigations of pile-soil behaviour with special reference to the foundation of offshore structures*, Ph. D. thesis, University of London, UK.
- KENNEY, T. C., 1959, Discussion of "Geotechnical properties of glacial lake clays," by T. H. Wu, *J. Soil Mech. Found. Div.*, ASCE, Vol. 85, No. SM3, pp. 67-79.
- KEZDI, A., 1974, *Handbook of Soil Mechanics, Volume 2: Soil Testing*, Elsevier Publishing, Hungary, 258 p.
- KOERNER, R. M., 1970, Effect of particle characteristics on soil strength, *J. Soil Mech. Found. Eng. Div.*, ASCE, Vol. 96, No. SM4, pp. 1221-1234.
- LADD, C. C., R. FOOTT, K. ISHIHARA, F. SCHLOSSER, and H. G. Poulos, 1977, Stress-deformation and strength characteristics, State-of-the-Art report, *Proceedings of the Ninth International Conference on Soil Mechanics and Foundation Engineering*, Tokyo, Vol. 2, pp. 421-494.
- LADD, C. C., and R. FOOTT, 1974, New design procedures for stability of soft clays, *J. Geotech. Eng.*, ASCE, Vol. 100, No. 7, pp. 763-786.
- LADD, C. C., 1991, Stability evaluation during staged construction (the twenty-second Karl Terzaghi lecture), *J. Geotech. Eng.*, ASCE, Vol. 117, No. 4, pp. 540-615.
- LADE, P. V., and J. M. DUNCAN, 1973, Cubical triaxial tests on cohesionless soils, *J. Soil Mech. Found. Eng. Div.*, ASCE, Vol. 99, No. 10, pp. 793-812.
- LADE, P. V., and J. M. DUNCAN, 1975, Elasto-plastic stress strain theory for cohesionless soils, *J. Geotech. Eng.*, ASCE, Vol. 101, No. 10, pp. 1037-1053.
- LAMBE, T. W., and R. V. WHITMAN, 1979, *Soil Mechanics*, John Wiley & Sons, pp. 116-121 and 135-150.
- LEE, K. L. and H. B. SEED, 1967, Drained strength characteristics of sands, *J. Soil Mech. Found. Eng. Div.*, ASCE, Vol. 93, No. SM6, pp. 117-141.
- LESLIE, D. D., 1963, Large-scale triaxial tests on gravelly soils, *Proceedings of the 2nd Pan American Conference on Soil Mechanics and Foundation Engineering*, Brazil, Vol. 1, pp. 181-202.
- MATSUOKA, H., and T. NAKAI, 1974, Stress-deformation and strength characteristics of soil under three different principal stresses, *Proceedings of the Japanese Society of Civil Engineers*, Vol. 32, pp. 59-70.
- MESRI, G., and M. E. M. ABDEL-GHAFFAR, 1993, Cohesion intercept in effective stress-stability analysis, *J. Geotech. Eng.*, ASCE, Vol. 119, No. 8, pp. 1229-1249.
- NAVFAC, 1982, *Soil Mechanics*, Naval Facilities Engineering Command, Design Manual DM-71, Alexandria, 355 p.
- PARRY, R. H. G., 1960, Triaxial compression and extension tests on remoulded saturated clay, *Géotechnique*, Vol. 10, pp. 166-180.
- ROWE, 1962, The stress-dilatancy relation for static equilibrium of an assembly of particles in contacts, *Proceedings of the Royal Society*, London, A 269, pp. 500-527.
- SAADA, A. S., and F. C. TOWNSEND, 1981, State of the Art: Laboratory strength testing of soils, *Laboratory Shear Strength of Soils*, ASTM Special Technical Publication 740, R. N. Yong and F. C. Townsend, eds., American Society for Testing and Materials, pp. 7-77.
- SCHERTMANN, J. H., 1978, Guidelines for cone penetration test performance and design, *Report FHWA-TS-78-209*, U.S. Department of Transportation, Washington, 145 p.

- SCHOFIELD, A. and C. P. WROTH, 1968, *Critical state soil mechanics*, McGraw-Hill, New York.
- SEED, H. B. and K. L. LEE, 1967, Undrained strength characteristics of cohesionless soils, *J. Soil Mech. Found. Eng. Div.*, ASCE, Vol. 93, No. SM6, pp. 333–360.
- SINGH, R., HENKEL, D. J., and D. A. SANGREY, 1973, Shear and K_0 swelling of overconsolidated clays, *Proceedings of the 8th International Conference on Soil Mechanics and Foundation Engineering*, Vol. 1.2, pp. 367–376.
- SKEMPTON, A. W., 1985, Residual strength of clays in landslides, folded strata, and the laboratory, *Géotechnique*, Vol. 35, No. 1, pp. 3–18.
- SOWERS, G. B. , and B. F. SOWERS, 1951, *Introductory Soil Mechanics*, MacMillan, New York.
- TATSUOKA, F., and S. SHIBUYA, 1992, *Deformation characteristics of soils and rocks from field and laboratory tests*, Report of The Institute of Industrial Science, The University of Tokyo, Vol. 37, No. 1, pp. 106–112.
- TAYLOR, 1939, A comparison of results of direct shear and cylindrical compression tests, *Proc. ASTM*.
- YOSHINARI, M., 1967, Compressive strength versus water content, *Proceedings of the Third Asian Regional Conference on Soil Mechanics and Foundation Engineering*, Haifa, Vol. 1, pp. 327–330.

REVIEW QUESTIONS

1. What is the most commonly used theory to describe the failure of soils?
2. Describe the Mohr-Coulomb theory.
3. Draw the evolution of the Mohr circle during an unconfined compression test.
4. Define peak and residual failures.
5. How does the Mohr-Coulomb theory define the orientation of the failure surfaces?
6. Among all the factors influencing the friction angle of coarse-grained soils, which factor has the largest effect?
7. Does the friction angle increase or decrease when the void ratio increases?
8. What is the range of variation for the friction angle in coarse-grained soils?
9. What is the effect of grain angularity on the friction angle of coarse-grained soils?
10. Is the failure envelope of soil strictly obeying the Mohr-Coulomb theory?
11. Define the s and t coordinates, and express the Mohr-Coulomb failure line in terms of s and t .
12. What is the relation between the parameters of the Mohr-Coulomb failure line in $\sigma-\tau$ and $s-t$ spaces.
13. Which is the most reliable conventional laboratory test to determine the failure envelope of soils?
14. Sketch the principles of the triaxial test.
15. What are the different types of triaxial tests?
16. What is the purpose of the consolidation phase in the CD and CU triaxial tests?
17. Define CD, CU and UU triaxial tests.
18. What is the relation between the total and effective stress paths?
19. What are the minimum and maximum values for the friction angle in coarse-grained soils?
20. Is the friction angle different in drained and undrained triaxial tests on coarse-grained soils?

21. Rank the following factors by decreasing order of their influence on the friction angle-confining pressure, void ratio, angularity, and grain size distribution curve.
22. What is the virgin consolidation line?
23. Define the critical state theory.
24. What is the difference between the critical state theory and the Mohr-Coulomb theory?
25. Which are the material parameters of the critical state theory?
26. Give a range of value for the undrained shear strength of fine-grained soils.
27. Does the friction angle increase or decrease with the plasticity index?
28. What is the effect of the liquidity index on the shear strength of fine-grained soils?
29. What is the meaning of apparent and true failure criteria?
30. Draw the typical apparent failure line obtained from UU tests.

7-2 Principles of the Unconfined Compression Test

DEFINITION

As introduced in Chapter 5-4, the unconfined compression test is a rapid means to obtain an approximate value of undrained shear strength S_u for fine-grained soils. As shown in Fig. 1a, the cylindrical soil specimen is loaded axially without a lateral support. The top and bottom areas are assumed to be frictionless (i.e., free of shear stress) and transmit only the axial stress σ_1 , while the lateral surface is free of stress. As schematized in Fig. 1b, a small cubical element inside the specimen undergoes a compressive axial stress σ_1 and no lateral stresses (i.e., $\sigma_2 = \sigma_3 = 0$). In practice, the stresses are not uniform within the sample, mainly due to the effects of shear stresses on the loading caps which are not frictionless. Using Fig. 2, the axial strain ϵ_1 and axial total stress σ_1 are defined as positive in compression:

$$\epsilon_1 = \frac{\Delta H}{H_0} \quad \text{and} \quad \sigma_1 = \frac{F}{A} \quad (1)$$

where H_0 is the initial sample height, H the present sample height, $\Delta H = H_0 - H$ the change in sample height, F the applied axial load, and A the average cross-section area of sample.

The soil samples which are tested in unconfined compression are usually made of fine-grained soils, fully or partially saturated, with low permeability. When these soils are loaded rapidly, they deform practically at constant volume under undrained conditions, and undergo pore pressure changes that do not have enough time to dissipate. The unconfined compression test is a particular unconsolidated undrained (UU) triaxial test without confining pressure.

FAILURE DURING UNCONFINED COMPRESSION TEST

Figure 3a shows a typical stress-strain response of soils subjected to unconfined compression tests. At the beginning of loading, the axial stress and strain are both

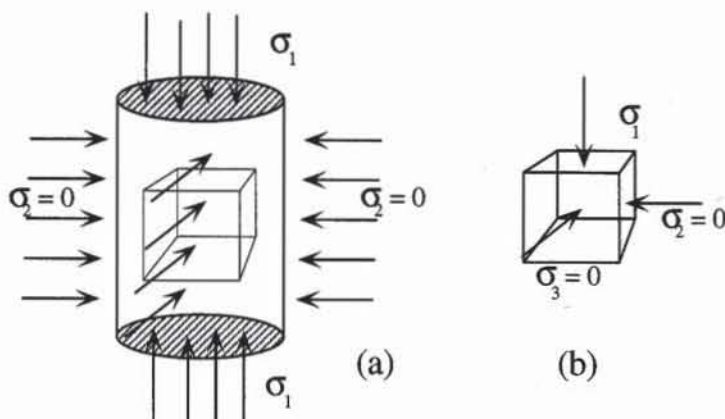


Figure 1 Stresses within a soil sample subjected to the unconfined compression test.

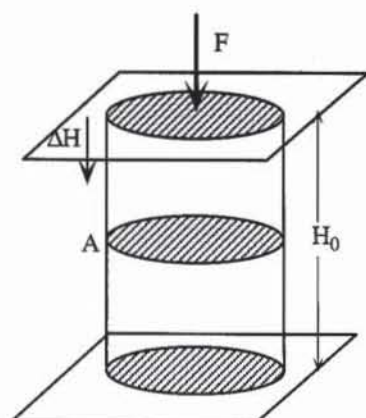


Figure 2 Initial height and change in height of sample.

equal to zero, and the Mohr circle is reduced to point O in Fig. 3b. When the axial stress σ_1 is increased, the sample deforms. At points A , B , and C , the Mohr circle passes through point O and gradually increases size until σ_1 reaches the maximum value $2S_u$ at point C . During loading, pole O of Mohr circle does not move. The unconfined compression test provides only one Mohr circle at failure, which is insufficient to determine the failure envelope in σ - τ space. It is also irrelevant to determine the effective failure envelope because no pore pressure is measured.

When the failure envelope is assumed to be purely cohesive (i.e., $\phi = 0$) as shown in Fig. 3b, the Mohr circle at failure is tangent to the horizontal line $\tau = S_u$. Using pole O as shown in Fig. 3c, the failure surfaces are inclined at 45° with respect to the horizontal direction, and $\sigma = \tau = S_u$ on the failure surface. As shown in Fig. 3d, the Mohr circle of effective stress at failure is obtained by shifting the Mohr circle of total stress by the pore pressure u , the value of which can only be assumed since it is not measured. As established in Chapter 7-1, the effective failure envelope of soils is not purely cohesive. The effective stress Mohr circle at failure is tangent to a failure line of slope $\tan \phi'$ at points (σ'_f, τ_f) where σ'_f and τ_f are the effective normal and shear stresses acting on the failure surface. The inclination of the failure surfaces which is found from pole O and point (σ'_f, τ_f) is $45^\circ + \phi'/2$ instead of 45° . Therefore, the failure planes which are observed in unconfined compression tests are not inclined at 45° as is commonly assumed in practice. Unfortunately, the failure planes are influenced by many factors and do not provide a reliable assessment of ϕ' .

TYPICAL VALUES OF UNDRAINED SHEAR STRENGTH FROM UNCONFINED COMPRESSION TEST

Table 1 classifies the consistency of soils in terms of their undrained shear strength S_u . S_u varies from 3 kPa for soils close to their liquid state, to more than 400 kPa for very hard soils. Table 2 shows compiled results on the undrained shear strength of various clays measured in the unconfined compression (UC) tests, unconsolidated undrained (UU) triaxial tests, and consolidated undrained (CU) triaxial tests. In Table 2, $S_u(\text{CU}) = S_u$, $S_u(\text{UU})$, and $S_u(\text{UC})$ are the undrained shear strength in CU, UU, and UC tests, respectively. $S_u(\text{UC})$ is also referred to as the unconfined shear strength.

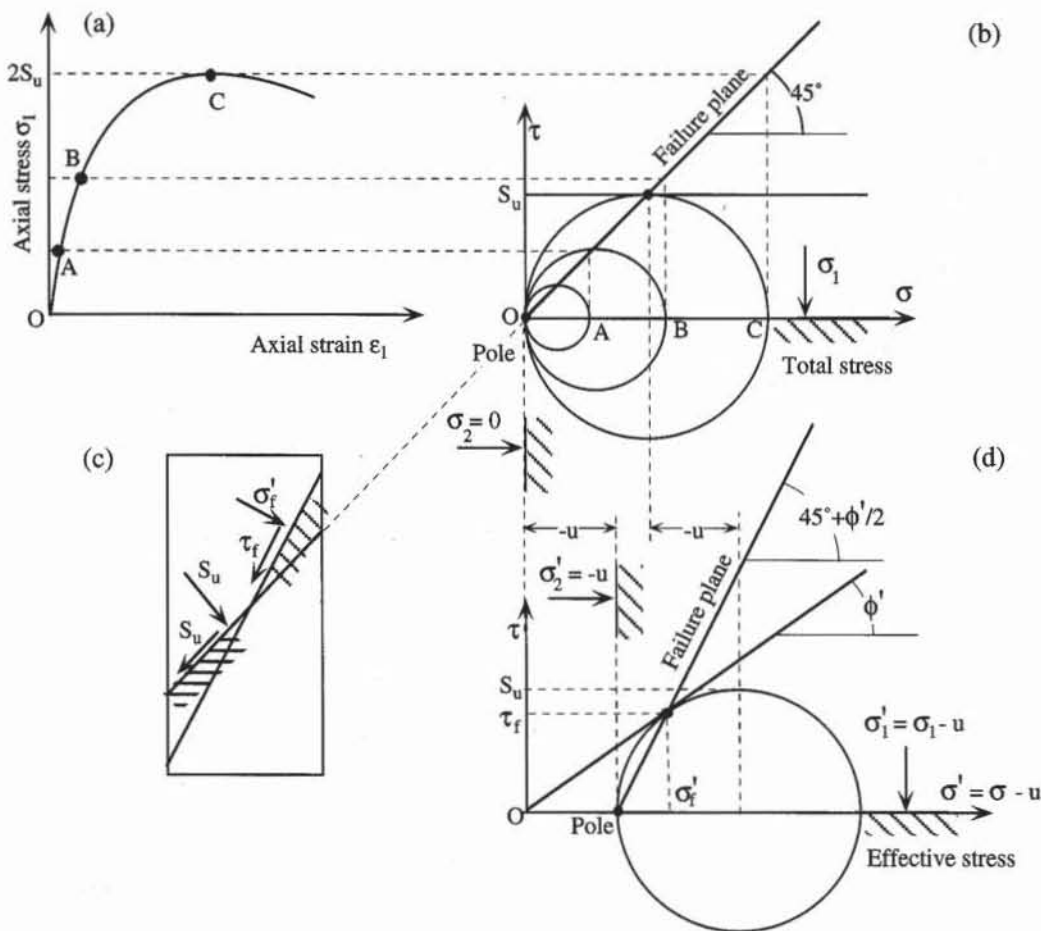


Figure 3 (a) A typical stress-strain response during the unconfined compression test, (b) the corresponding evolution of the Mohr circle in the total stress space, (c) the Mohr circle of effective stress at failure, and (d) the total and effective stresses on the failure planes.

As shown in Fig. 4, $S_u(\text{UC})$ and $S_u(\text{UU})$ are similar, because the data points fall close to the line $S_u(\text{UU}) = S_u(\text{UC})$. This result is expected because the unconfined compression test is a UU test without confining pressure. As shown in Fig. 5, $S_u(\text{UC})$ is generally smaller than the undrained shear strength S_u measured from CU triaxial tests. Most points with coordinates $S_u(\text{UC})$ and S_u fall beneath the line $S_u = S_u(\text{UC})$. $S_u(\text{UC})$ is only larger than S_u for some exceptional cases in which soil samples may not have been fully saturated, and had gained strength by drying out.

There can be considerable error in evaluating the undrained shear strength of soils from unconfined compression tests because of sample disturbance and omission of reconsolidation during testing (e.g., Ladd and Lambe, 1963; Noorany and Seed, 1965; Ladd et al., 1977; Ladd, 1991; and Tavenas and Leroueil, 1987). However, in many circumstances such as in the evaluation of older case histories with limited data, the results of more accurate tests (e.g., CU tests) are not available, and the only data available is the unconfined shear strength.

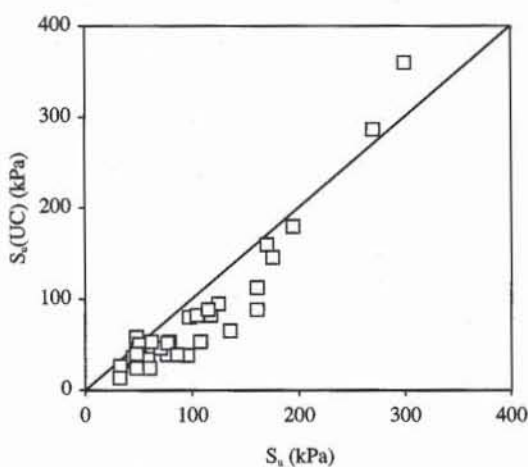


Figure 4 Comparison of the undrained shear strengths S_u measured from unconfined compression (UC) tests and CU triaxial tests (data after Chen and Kulhawy, 1993).

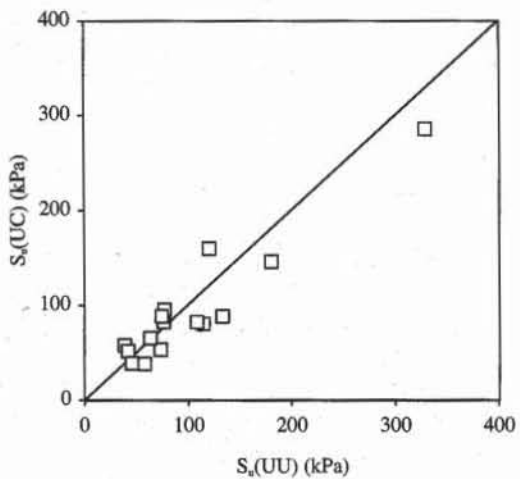


Figure 5 Comparison of the undrained shear strengths S_u measured from unconfined compression (UC) tests and UU triaxial tests (data after Chen and Kulhawy, 1993).

TABLE 1

Typical values of undrained shear strength from unconfined compression tests (Karol, 1969)

Relative consistency	S_u (kPa)
Liquid limit	3
Very soft	5
Medium soft	5-10
Ball moisture	48
Firm or stiff	48-96
Medium hard	96-192
Hard	192-383
Very hard	> 383

EFFECT OF DISTURBANCE ON UNDRAINED SHEAR STRENGTH

Figure 6 shows an example of stress-strain responses for undisturbed and remolded clay samples (Lambe, 1951) in the unconfined compression test. The undisturbed sample is stronger and much stiffer than the remolded sample. The variation in undrained shear strength is characterized by sensitivity S_t , which is the ratio of the undrained shear strengths in the undisturbed and remolded states at the same water content. In Fig. 6, S_t is equal to 7.6, corresponding to the undrained shear strength of 76 and 10 kPa for the undisturbed and remolded specimens, respectively. Additional information on the effect of sensitivity on undrained shear strength can be found in Chapter 7-1.

TABLE 2

Database for the undrained shear strength of various clays measured from unconfined compression tests, and UU and UC triaxial tests (Chen and Kulhawy, 1993).

Site	Soil description	LL (%)	PL (%)	w (%)	Sensitivity	Depth (m)	OCR	S_u (UC) (kPa)	S_u (kPa)	S_u (UU) (kPa)
Gulf of Mexico	Soft plastic clay	111	31	71	2-3	0-6	3.5	26.4	33	
	Firm to stiff plastic clay with silt and sand	73	23	43	2-3	18-32	1.1	39.1	76.6	
		85	20	43	2-3	32-50	1.2	52.8	107.7	
Skabo	Plastic clay with high salt content				5	10.6-16	1.2	32.2	46	
Gotta valley	Lilla Edet clay: marine late glacial			68	50	4-6.8	12	40.8	48	
	plastic clay with high sensitivity	58	25	78	50	10-12.3	1.8	34.2	58	
		58	29	70	50	16.2-18	1.5	46.2	70	
Drammen	Soft silty clay with thin seams of silt and fine sand	31	16	34	9	5-12	1.3	36.0	45	
		33	19	32	9	18	1.1	24.0	60	
Sault Ste Marie	Varved glacial lake clay with flocculent structure	51	23	45	8	9	1.2	24.0	48	
Hamilton	Firm to stiff grey silty clay (surface desiccated and fissured)	36	24	33		5	3.2	57.8	47.8	
		28	16	26		7	2.5	50.2	50.2	
		45	25	32		11	1.5	52.9	78.9	73.4
		46	27	36		15	1.1	51.6	77	42.4
South Padre Island	Medium to stiff clay	57	26	29		8	1.2	38.2	95.5	58.3
		55	27	25		15	1.2	65.3	136	63.9
		57	29	24		19	6.4	112.7	161	
Kars	Cemented Leda clay	51	23	45		2.5-6	7	52.7	62	
	dark gray plastic clay	56	38	65		6-12	2.5	39.8	48	
Ottawa	Leda clay: moderately preconsolidated clay with high plasticity and sensitivity	46	14	72	26	6-9	3.1	80.0	97.5	115.1
		33	8	68	80	9-12	2.2	82.3	117.5	109.3
		34	9	51	114	12-15	2	95.0	125	77.5
		27	5	36	128	15-18	2	81.9	105	76.7
		38	28	52	84	18-21	1.6	88.6	115	74.8
Southeastern Texas	Very stiff clay with high plasticity	67	30	30		15.2	6.5	145.8	175.7	181.0
		64	23	23		18.3	5.8	159.8	170	120.7
		61	12	26		21.3	2.9	88.6	161	133.6
Empire	Fine gray clay	83	26	46		36.6	1.2	38.7	86.1	45.6
Chicago	Hard silty clay	31	14	43		3.7	17	179.4	195	
		29	16	13		9	20	286.2	270	329.4
		23	14	10		11.6	39	360.0	300	

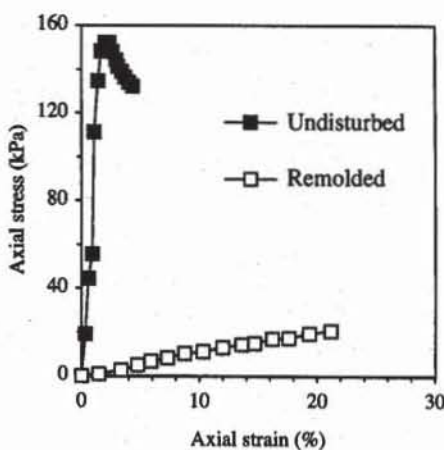


Figure 6 Results of unconfined compression tests on undisturbed and remolded samples of gray silty clay (data after Lambe, 1951).

REFERENCES

- CHEN, Y.-T., and F. H. KULHAWY, 1993, Undrained strength interrelationships among CIUC, UU, and IUC tests, *J. Geotech. Eng.*, ASCE, Vol. 119, No. 11, pp. 1732–1750.
- KAROL, R. H., 1969, *Soils and Soil Engineering*, Prentice-Hall, New Jersey, 195 p.
- LADD, C. C., 1991, Stability evaluation during staged constructions, *J. Geotech. Eng.*, ASCE, Vol. 117, No. 4, pp. 540–615.
- LADD, C. C., R. FOOTE, K. ISHIHARA, F. SCHLOSSER, and H. G. Poulos, 1977, Stress-deformation and strength characteristics, *Proceedings of the 9th International Conference on Soil Mechanics and Foundation Engineering*, Vol. 2, Tokyo, pp. 421–494.
- LADD, C. C., and T. W. LAMBE, 1963, The strength of “undisturbed” clay determined from undrained tests, *Laboratory shear testing of soils*, Special Technical Publication No. 361, ASTM, Philadelphia, PA, pp. 342–371.
- LAMBE, T. W., 1951, *Soil testing for engineers*, John Wiley & Sons, New York, 165 p.
- LAMBE, T. W., and R. V. WHITMAN, 1979, *Soil Mechanics, SI Version*, John Wiley & Sons, New York, 553 p.
- NOORANY, I., and H. B. SEED, 1965, In-Situ strength characteristics of soft clay, *J. Soil Mech. Found. Eng. Div.*, ASCE, Vol. 91, No. 2, pp. 49–80.
- TAVENAS, F., and S. LEROUEIL, 1987, State-of-the-art on laboratory and in-situ stress-strain-time behavior of soft clays, *Proceedings of the International Symposium on Geotechnical Engineering of Soft Soils*, Mexico City, pp. 1–46.

REVIEW QUESTIONS

1. What soil properties are determined from the unconfined compression test?
2. Draw the evolution of the Mohr circle in parallel to a typical stress-strain curve during an unconfined compression test.
3. Does the pole of the Mohr circle move during the unconfined compression test?
4. What is the theoretical inclination of failure planes predicted for purely cohesive material during an unconfined compression test?

5. Define the axial strain from the displacement and sample height.
6. What is the range of unconfined shear strength for soils?
7. What is the relation between the unconfined shear strength and the undrained shear strength measured from UU and CU triaxial compression tests?
8. What is the effect of the water content on the unconfined shear strength?
9. Define the sensitivity S_t of a clay. What is the range of S_t ? Which clays give the largest values of S_t ?
10. How can Young's modulus be calculated from the results of unconfined compression tests?

EXERCISES

1. Calculate the unconfined shear strengths from the following unconfined compression test results on undisturbed and remolded samples of gray silty clay (data after Lambe, 1951).

Undisturbed		Remolded	
Axial strain (%)	Axial stress (kPa)	Axial strain (%)	Axial stress (kPa)
0.00	0	0.00	0
0.30	19	1.45	1
0.60	44	3.36	2
0.90	56	4.74	5
1.10	111	5.90	7
1.43	135	7.27	8
1.70	148	8.78	10
2.00	152	10.34	11
2.30	152	12.03	13
2.60	148	13.63	14
2.90	144	14.69	15
3.10	141	16.20	17
3.40	139	17.62	17
3.70	136	19.36	19
4.00	134	21.18	20
4.30	132		

2. Calculate Young's modulus for the undisturbed and remolded samples of gray silty clay from the unconfined compression results of Exercise 1. Compare your results with those reported in Chapter 5-5.

Unconfined Compression Test

OBJECTIVE

The unconfined compression test is used to measure the unconfined shear strength of fine-grained soils, which is an approximate value of their undrained shear strength. This test is applicable only to cohesive materials such as saturated clays or cemented soils that retain an intrinsic strength without a confining pressure. It is not applicable to dry or cohesionless soils, such as gravels and sands.

EQUIPMENT

The equipment for the unconfined compression test includes:

- Loading device (see Fig. 12), either hand operated or machine driven, capable of providing rates of loading in the range 0.5 to 5 mm/min and with a maximum load capacity of 5 kN.
- Loading ring with 2 kN capacity, accurate to 1 N. The loading ring is equipped with a dial indicator or a LVDT transducer for computer data acquisition.
- Dial indicator or LVDT transducer for measuring axial displacement, having a full range of 25 mm and accurate to 0.01 mm.
- Vernier calipers, suitable for measuring the dimensions of the specimens to the nearest 0.1 mm.
- Trimming frame. A typical trimming frame for 3.5-cm-diameter specimens is shown in Fig. 1. A motorized soil lathe may also be used.
- Sampling tube with extractor with cutting edges to prepare cylindrical specimens.
- Wire saws and knives.
- Miter box or cradle (see Fig. 3) for cutting specimens.
- Watch or clock.



Figure 1 The sample is installed on a trimming frame. The vertical guides are adjusted to obtain the desired sample diameter.

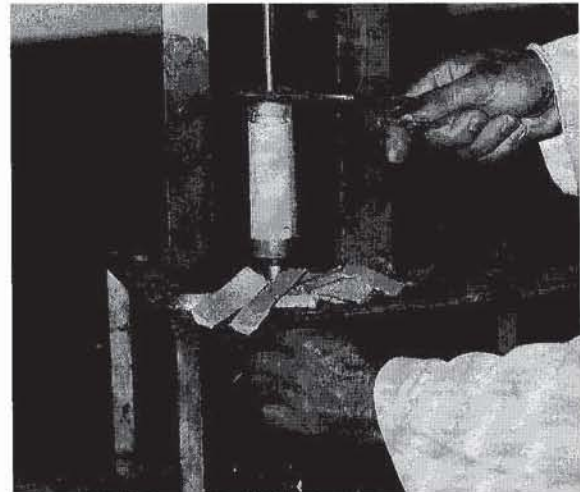


Figure 2 Fragments and scraps from cutting are used to determine the sample water content.

- Balances, sensitive to 0.1 g.
- Equipment necessary to determine water content.

PREPARATION OF SPECIMENS

The test specimens are cut into cylinders which are usually 3.5 cm in diameter. Specimens of larger diameter (e.g., 7 cm) are recommended for undisturbed soils with stratification and cracks. The largest particle in the test specimens should be smaller than 6 mm. The height-to-diameter ratio of the sample should be larger than 2. The specimens may be undisturbed or remolded.

Undisturbed Specimens

Undisturbed specimens are prepared from undisturbed samples of larger size taken in the field. Undisturbed samples are carefully transported and handled in sealed containers that retain the field water content. The test specimens are cut into cylinders by trimming or extruding them:

Trimming specimens

1. Cut a chunk from the undisturbed soil mass which is large enough to cut a specimen. Make a note about the orientation of the vertical direction in the field.
2. Trim the specimen to the required diameter using a trimming device (Fig. 1). The specimen is trimmed by pressing the wire saw against the adjustable

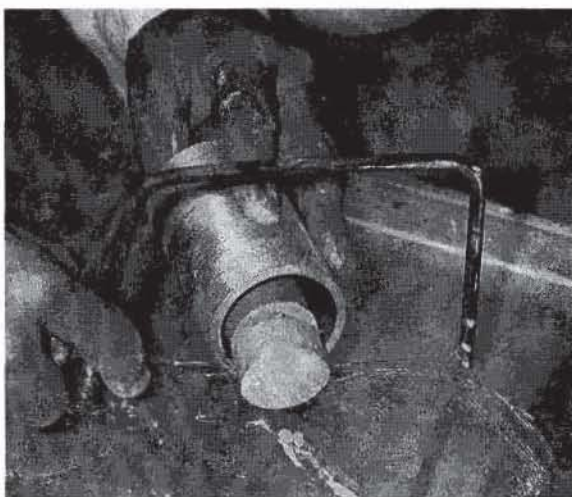


Figure 3 The top and bottom surfaces are cut perpendicular to the specimen axis using a wire saw.



Figure 4 The sample is marked to the desired height.

edges of the trimming frame and by sliding it down. For stiff clays, move the wire saw from the top and bottom toward the middle of the specimen to prevent breaking off pieces at the ends. Remove any small pebbles and fill voids in the specimen with soil from the trimmings. The trimmed specimen is shown in Fig. 2.

3. Cut the specimen to the required length (usually 7 to 9 cm for 3.5-cm-diameter specimens) by using a miter box (Figs. 3 and 4).
4. Measure the weight, height, and diameter of the sample.
5. Test the specimen immediately to prevent loss of moisture.

Extruding specimens

1. Push into the soil the sampling tube, which has a lower cutting edge (Fig. 5), and then remove it with a twisting motion. The soil specimen should now be in the sampling tube (Fig. 6).



Figure 5 The sampling tube with a cutting edge is pushed into the soil.

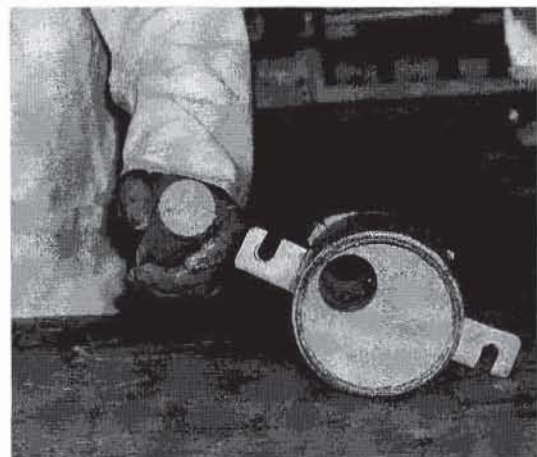


Figure 6 The soil specimen is now in the sampling tube.



Figure 7 The extractor is assembled to extrude the soil from the sampling tube.



Figure 8 After extruding about 1 cm of soil from the sampling tube, the bottom surface of the sample is cut with a wire saw.

2. Reassemble the extractor and extrude the sample from the sampling tube (Fig. 7).
3. After extruding about 1 cm of soil from the sampling tube, cut the bottom surface of the sample by using a wire saw (Fig. 8).
4. Cut the sample to the desired length by extruding the right amount from the sampling tube (Fig. 9).
5. Same as steps 4 and 5 for trimming specimens.

Remolded Specimens

Remolded specimens are prepared from remolded field samples or specimens that have already been tested. For a meaningful comparison of undisturbed and remolded responses, their water content should be similar to that of the undisturbed specimens.

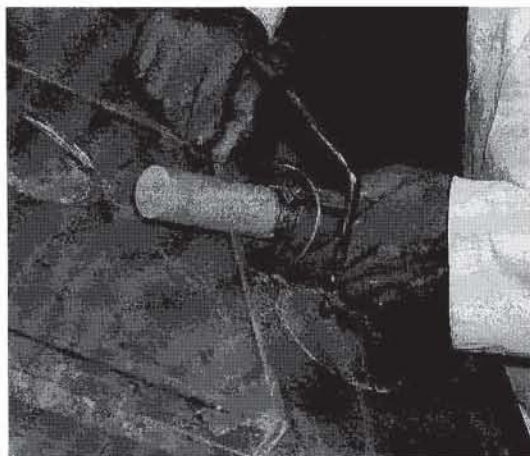


Figure 9 The sample, which is extruded from the sampling tube, is cut to the desired length.



Figure 10 The remolded specimen, which has been compacted in the compaction cylinder, is cut to the desired length.

1. Knead the specimen with the fingers to remold it completely. Avoid trapping air in the specimen.
2. Compact the soil in a cylindrical mold having the internal diameter of the test specimen.
3. Carefully extrude the specimen from the mold, preferably by means of a piston, and plane off the top and bottom of the specimen (Fig. 10).
4. Same as steps 4 and 5 for trimming specimens.

The remolded sample may also be prepared in compaction molds which are larger than the test specimen, and then trimmed and cut as for undisturbed samples.

TEST PROCEDURE

1. Measure the water content of the specimen by using the soil trimmings (see Fig. 2), and measure the specimen weight.
2. Measure the height and diameter of the specimen. When the sample is well trimmed, its diameter D_0 is measured only at its center. When the sample is more irregular, as shown in Fig. 11, the average diameter D_0 is

$$D_0 = \frac{1}{4} (D_1 + 2D_2 + D_3) \quad (1)$$

where D_1 , D_2 , and D_3 are the diameters measured at the top, center, and bottom, respectively, of the specimen.

3. Without delay, to avoid loss of water content, place the specimen on the loading device (Fig. 12). Lower the upper platen or raise the bottom platen so that the upper platen barely touches the specimen and triggers a slight response of the load sensor. Attach the dial indicator or LVDT transducer to the loading device to measure the axial deformation of the specimen.
4. Adjust the rate of axial displacement to obtain a strain rate of about 1% per minute. The complete loading lasts about 20 min to apply 20% of axial strain, which is generally sufficient to reach the unconfined shear strength. Very stiff or brittle materials that fail for small deformations may be tested at a slower rate of strain.

5. As shown in Fig. 13, record simultaneously the axial displacement and load at close time intervals at the beginning, and then at larger intervals. Stop the test when the axial load remains constant or after 20% axial strain.

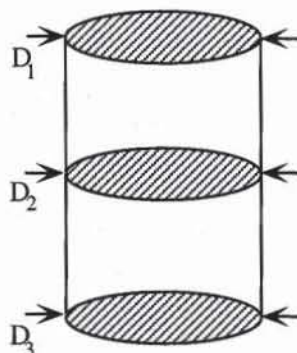


Figure 11 Determination of average diameter of test specimen.



Figure 12 Typical unconfined compression test apparatus. The specimen is placed on the loading frame, and the displacement and force dial gages are adjusted and initialized.

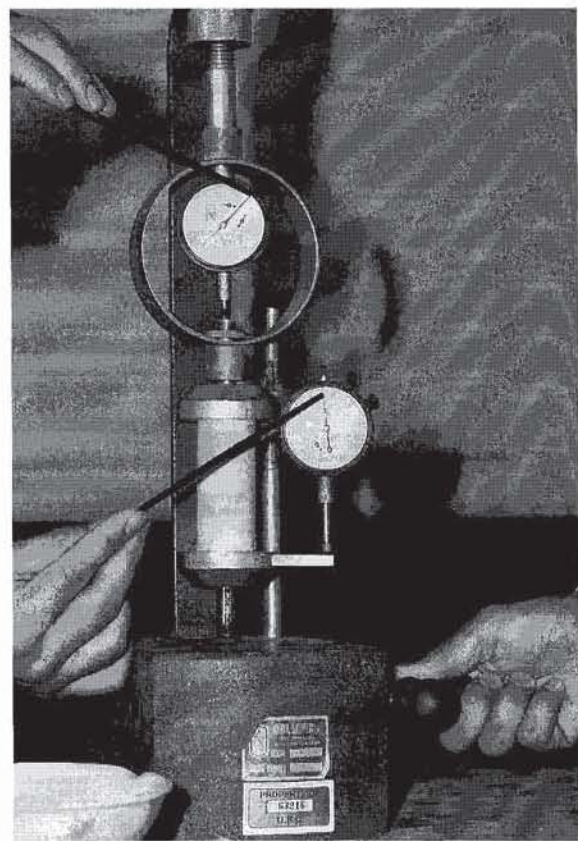


Figure 13 The loading platen is raised by turning the crank at constant speed. Both displacement and force dial readings are recorded at representative time intervals.

6. Record the time to reach the peak strength and the type of failure pattern (e.g., shear or bulge failure), and sketch the failed specimen. Determine the inclination and spacing of the shear bands, if any, in the specimen (Figs. 14 and 15).
7. After the test, determine the water content using the entire specimen or a representative portion of it.

COMPUTATION

The initial state of the tested soil is identified by its water content, total and dry unit weights, void ratio, and degree of saturation. The water content w is

$$w = \frac{W_i - W_d}{W_d} \times 100 \quad (\%) \quad (2)$$

where W_i is the initial weight and W_d is the dry weight of the complete sample or some sample trimmings. The total unit weight γ is

$$\gamma = \frac{W_i}{V_i} \quad (3)$$



Figure 14 When a shear plane occurs, its angle should be recorded. Other modes of failure may also occur and should be reported.



Figure 15 A closer look at the failure plane of the sample of Fig. 14 after lifting up the top part of the sample.

where W_i is the initial sample weight, and V_i is the initial sample volume. The dry unit weight γ_d , void ratio e , and degree of saturation S_r are

$$\gamma_d = \frac{\gamma}{1+w}, \quad e = \frac{G_s \gamma_w}{\gamma_d} - 1, \quad \text{and} \quad S_r = \frac{G_s w}{e} \quad (4)$$

where G_s is the soil specific gravity. The axial strain ϵ is

$$\epsilon = \frac{\Delta H}{H_0} \times 100 \quad (\%) \quad (5)$$

where H_0 is the initial sample height and ΔH is the change of sample height. The compressive axial stress σ is

$$\sigma = \frac{F}{A_c} \quad \text{and} \quad A_c = \frac{A_i}{1-\epsilon} \quad (6)$$

where F is the axial load applied to the sample, A_c the corrected area, A_i the initial cross-sectional area of the soil sample, and ϵ the axial strain in real value (not in %). The cross-sectional area of the sample changes during the compression test and is corrected assuming that the sample volume is constant. The unconfined compressive strength of the specimen is the maximum or peak of compressive

stress. When the unconfined shear strength is measured for undisturbed and remolded samples, the sensitivity ratio S_t is also calculated.

EXAMPLE

Figure 16 shows the stress-strain response curves obtained for the unconfined compression test of a clay sample, Fig. 17 shows the input/output data of Fig. 16, and Fig. 18 shows the formulas used in Fig. 17. In reports, the failure mode of the sample should also be sketched. If a failure plane is observed, its orientation must be measured and reported.

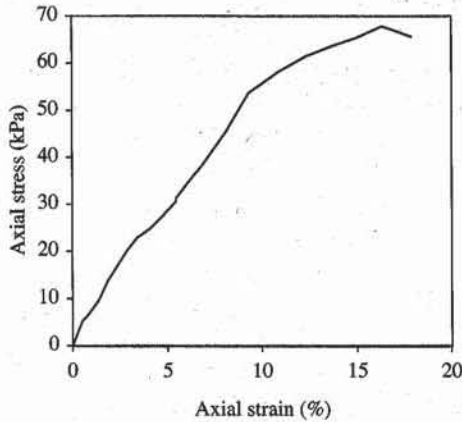


Figure 16 Stress-strain response curve obtained in an unconfined compression test.

REVIEW QUESTIONS

1. What is the purpose of the unconfined compression test?
2. To which types of soil is the unconfined compression test applicable?
3. What are undisturbed and remolded samples?
4. What method can you use to prepare undisturbed samples?
5. What is the typical loading rate for the unconfined compression test?

EXERCISE

1. Derive the relation between the corrected area, initial area, and axial strain (Eq. 6)

	A	B	C	D
1	Unconfined compression test			
2	Analyst name: Sean Smith			
3	Test date: 4/13/1993			
4	Sample description: Aardvack modelling clay			
5				
6	Initial height $h_0 = 7.28$ cm			
7	Initial diameter $d_0 = 3.39$ cm			
8	Mass of wet sample and tare $M_t = 593.80$ g			
9	Mass of dry sample and tare $M_d = 572.80$ g			
10	Mass of tare $M_t = 466.30$ g			
11	Specific gravity $G_s = 2.65$			
12	Initial water content $w = 19.72\%$			
13	Initial unit weight $\gamma = 19.09$ kN/m ³			
14	Initial dry unit weight $\gamma_d = 15.95$ kN/m ³			
15	Initial void ratio $e_0 = 0.63$			
16	Initial degree of saturation $S_r = 83.12\%$			
17	Young's modulus $E = 616.54$ kPa			
18	Unconfined shear strength $S_u = 35.03$ kPa			
19				
20	Displacement (mm)	Force (N)	Strain (%)	Stress (kPa)
21	Δh	F	e	s
22	0.00	0.00	0.0	0.0
23	0.37	4.68	0.5	5.2
24	0.62	6.08	0.9	6.7
25	1.02	8.88	1.4	9.7
26	1.37	12.62	1.9	13.8
27	1.75	15.90	2.4	17.2
28	2.09	18.70	2.9	20.2
29	2.49	21.31	3.4	22.9
30	2.98	23.37	4.1	24.9
31	3.37	25.45	4.6	27.0
32	3.96	29.11	5.4	30.6
33	4.00	29.92	5.5	31.4
34	4.49	33.53	6.2	34.9
35	4.99	36.93	6.9	38.2
36	5.90	44.41	8.1	45.3
37	6.78	53.29	9.3	53.7
38	7.97	58.90	11.0	58.3
39	8.98	63.11	12.3	61.4
40	9.99	66.38	13.7	63.6
41	10.93	69.19	15.0	65.3
42	11.91	72.93	16.4	67.7
43	13.06	71.99	17.9	65.6
44	14.08	77.14	19.4	69.1
45	15.09	79.01	20.7	69.5
46	16.05	79.01	22.1	68.4
47	16.67	81.81	22.9	70.1

Figure 17 Example of data set for an unconfined compression test.

	B	C	D
12	Initial water content $w = (M_i - M_d) / (M_d - M_t)$		
13	Initial unit weight $\gamma = (M_i - M_t) / (h_0 \cdot \pi \cdot d_0^2 / 4) \cdot 9.81$		kN/m^3
14	Initial dry unit weight $\gamma_d = g / (1 + w)$		kN/m^3
15	Initial void ratio $e_0 = G_s \cdot 9.8 / \gamma_d - 1$		
16	Initial degree of saturation $S_r = G_s \cdot w / e_0$		
17	Young's modulus $E = \text{SLOPE}(D22:D30, C22:C30) \cdot 100$	kPa	
18	Unconfined shear strength $S_u = \text{MAX}(s) / 2$		kPa

	C	D
20	Strain (%)	Stress (kPa)
21	e	s
22	$=Dh/h_0 \cdot 10$	$=F / (\pi \cdot d_0^2 / 4) \cdot (1 - e/100) \cdot 10$
23	$=Dh/h_0 \cdot 10$	$=F / (\pi \cdot d_0^2 / 4) \cdot (1 - e/100) \cdot 10$

Figure 18 Formulas used in Fig. 17.

7-4 Principles of the Direct Shear Test

DIRECT SHEAR TEST

As introduced in Chapter 5-4, the direct shear test is used to determine the shear strength of soils on predetermined failure surfaces. The principles of the direct shear test is illustrated in Fig. 1. The soil sample confined inside the upper and lower rigid boxes is subjected to the normal load N and is sheared by the shear force T . If A is the area of surface CD , the shear stress τ acting on surface CD is equal to T/A , and the normal stress σ is equal to N/A . The soil shear strength is the shear stress τ that causes the soil to slip on surface CD . It can be defined by Mohr-Coulomb theory:

$$\tau = c + \sigma \tan\phi \quad (1)$$

where c is the cohesion and ϕ is the friction angle.

STRESS IN THE DIRECT SHEAR TEST

During the direct shear test, the stress state is not completely defined: σ and τ are only measured on the horizontal surface, but are undetermined on other surfaces. Therefore, the stress path during direct shear test cannot be represented in $s-t$ space. However, the Mohr circle can be drawn at failure, assuming that the failure plane is horizontal and the stress state is uniform. As shown in Fig. 2, point M represents the stress on the horizontal surface, and point N the stress on the vertical surface. Pole P is on the same horizontal line as point M when the failure plane is horizontal. The Mohr circle at failure is tangent to AM , and its center B is given by line MB perpendicular to AM . Therefore, the normal stresses σ_y and σ_x acting on horizontal and vertical surfaces, respectively, are related through

$$\sigma_x = 2c \tan\phi + K_s \sigma_y \quad \text{and} \quad K_s = 1 + 2 \tan^2\phi \quad (2)$$

As shown in Fig. 3, K_s is larger than 1, increases with ϕ , but remains smaller than

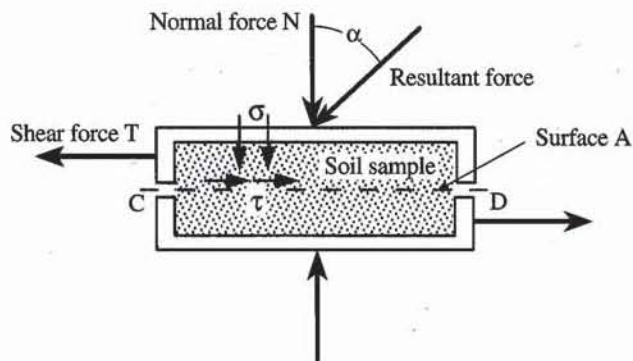


Figure 1 Soil sample in the direct shear box.

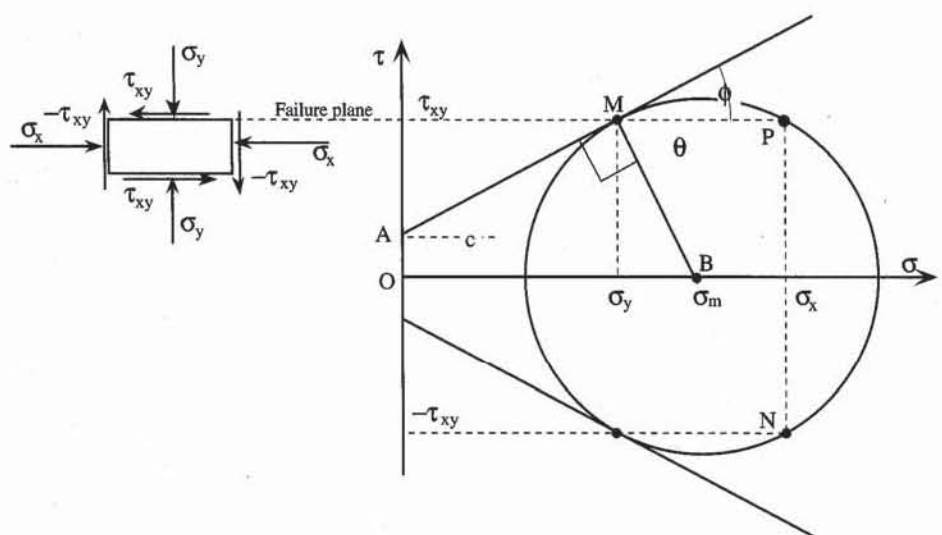


Figure 2 Stress state at failure in direct shear test and its Mohr representation.

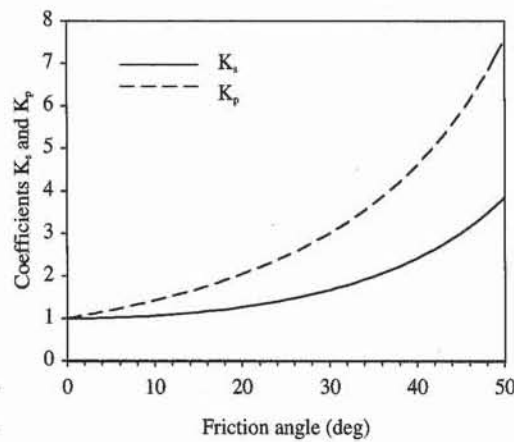


Figure 3 Variation of coefficients K_s and K_p with friction angle.

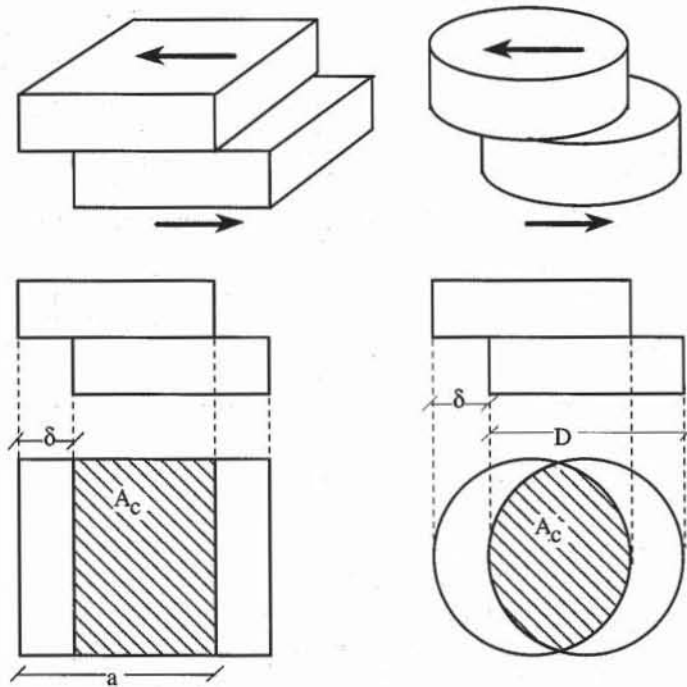


Figure 4 Corrected area for the calculation of shear and normal stresses.

the coefficient K_p of the Rankine theory for passive earth pressure ($K_p = (1 + \sin\phi)/(1 - \sin\phi)$).

As shown in Fig. 4, the contact area between the two specimen halves varies with the relative displacement δ between the lower and upper boxes. The corrected area A_c of the sheared specimen is for the square box of length a ,

$$A_c = a(a - \delta) \quad (3)$$

and for the cylindrical box of internal diameter D ,

$$A_c = \frac{D^2}{2} \left(\theta - \frac{\delta}{D} \sin \theta \right) \quad (4)$$

where $\theta = \cos^{-1} \left(\frac{\delta}{D} \right)$ in radians.

The shear stress τ and normal stress σ on the horizontal surface are calculated from the corrected area A_c , measured lateral force T , and normal force N :

$$\tau = \frac{T}{A_c} \quad \text{and} \quad \sigma = \frac{N}{A_c} \quad (5)$$

The error on the stresses resulting from the error on the contact area is for a square box ($A = a^2$),

$$\frac{\Delta A}{A} = \frac{A - A_c}{A} = \frac{\delta}{a} \quad (6)$$

and for a cylindrical box ($A = \frac{\pi D^2}{4}$),

$$\frac{\Delta A}{A} = \frac{A - A_c}{A} = 1 - \frac{2\theta}{\pi} + \frac{2\delta}{\pi D} \sin \theta \quad (7)$$

For a typical sample diameter $D = 6.3$ cm, the error on shear and normal stresses may reach 20% when $\delta = 1$ cm.

STRAIN IN THE DIRECT SHEAR TEST

In the direct shear test, the material response is reported versus shear displacement instead of shear strain, because it is not possible to evaluate shear strain. The direct shear test is therefore not suited for studying the stress-strain relationships of soils.

Figure 5a shows the specimen in its initial state before it is sheared in the direct shear test. The vertical lines in Fig. 5 represent the initial and distorted positions of soil grains which are marked to stand out from the rest of the sample. If the shear strain was uniform, the sheared specimen would become uniformly slanted, as in Fig. 5b. However, the shear strains are never uniform in the direct shear test. As shown in Fig. 5c and d, the deformation is concentrated within the thick or thin shear zones at the interface between the upper and lower boxes. The soil fails at the edges of the box before it fails at the specimen center.

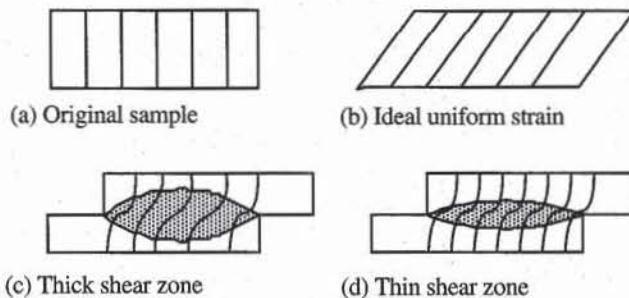


Figure 5 Idealized and observed displacements in the direct shear test (after Lambe, 1951).

DIRECT SHEAR OF COARSE-GRAINED SOILS

Figure 6 shows the typical response of a loose sand subjected to direct shear test. It represents the variation of τ/σ with shear displacement and the corresponding variation of normal displacement. The sand first compacts then dilates under shear.

Figure 7 illustrates the effect of density on the soil response during direct shear tests. For small shear displacement, dense sands have a larger shear strength than loose sands. However, after undergoing a peak failure, dense sands soften with shear strain until they gradually get the same residual strength as loose sands. The peak failure is characterized by the peak friction angle ϕ_p , and the residual failure by the residual friction angle ϕ_r . The peak friction angle ϕ_p is

$$\phi_p = \tan^{-1} \left(\frac{\tau_{\max}}{\sigma} \right) = \tan^{-1} \left(\frac{T_{\max}}{N} \right) \quad (8)$$

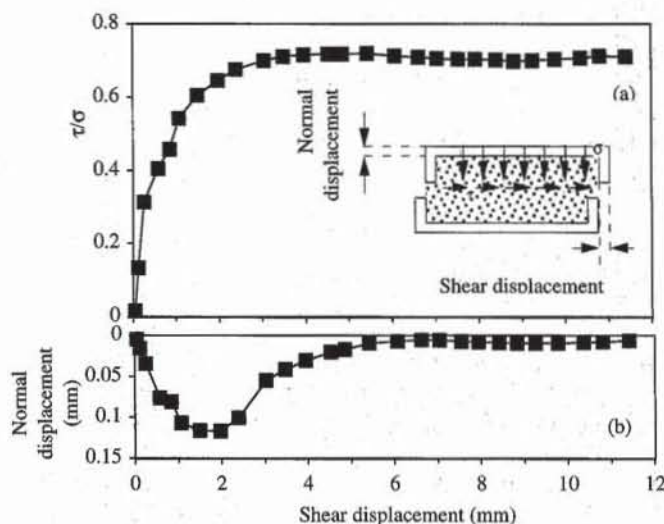


Figure 6 Typical results from a direct shear test on a loose sand (Lambe, 1951).

where τ_{\max} is the maximum shear stress, σ the normal stress, T_{\max} the maximum shear force, and N the normal load. The residual friction angle ϕ_r is

$$\phi_r = \tan^{-1} \left(\frac{\tau_r}{\sigma} \right) = \tan^{-1} \left(\frac{T_r}{N} \right) \quad (9)$$

where τ_r is the residual shear stress and T_r is the corresponding residual shear force at large lateral displacement. τ/σ is also equal to T/N , which eliminates calculation of the corrected area A_c .

The influence of soil density on ϕ_p is described by the concept of critical void ratio. By definition, the void ratio is critical when the soil fails without a volume change, as shown in Fig. 7. When the void ratio is smaller than critical (e.g., a dense soil), the soil dilates at peak failure. With increasing shear displacement, the void ratio increases until it becomes critical, and the shear stress decreases and gradually merges with the residual shear strength. When the void ratio is larger than critical (e.g., a loose soil), the soil compacts until the void ratio becomes critical, and the shear stress reaches the residual shear strength.

The peak friction angle ϕ_p of coarse-grained soils is also influenced by the normal load amplitude, grain size and shape, grain mineral, and grain size distri-

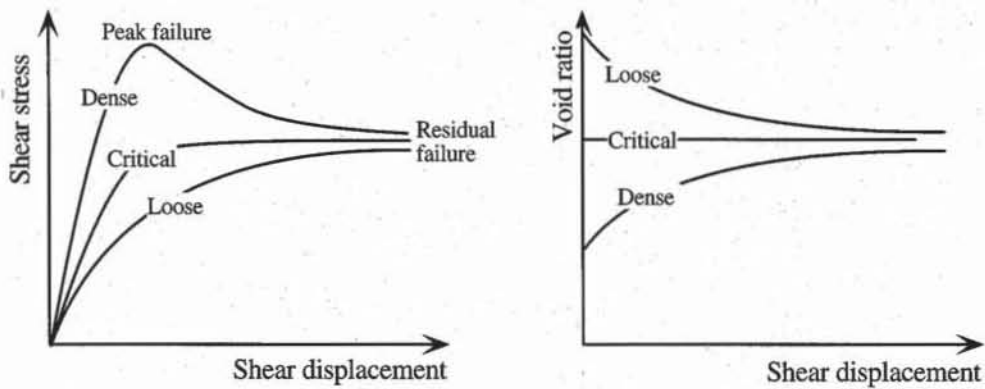


Figure 7 Influence of density on the response of soils subjected to direct shear tests.

bution. Smoothness, rounded corners, and uniform size of the soil grains tend to give lower friction angles. The contributions of these various factors, and typical values of friction angles are presented in Chapter 7-1.

DIRECT SHEAR OF FINE-GRAINED SOILS

Figure 8 shows the typical responses of undisturbed and remolded samples of inorganic clay from Maine which were subjected to the unconsolidated undrained (UU) direct shear test. The samples were sheared in 7 min., which left little time for the excess pore pressure to dissipate. The tests were performed under undrained conditions, without measuring the pore pressure. The undrained shear strength S_u of the remolded and undisturbed specimen is 5 and 40 kPa ($S_u = \tau_{\max}$). The value of the sensitivity S_t is 8.

In the case of consolidated drained (CD) direct shear tests, the shearing rate can be selected by following ASTM guidelines (ASTM 3080). The minimum time t_f required to reach failure is

$$t_f = 50 t_{50} = 11.7 t_{90} \quad (10)$$

where t_{50} and t_{90} are the times to complete 50 and 90% of the primary compression, respectively. t_{50} and t_{90} are determined before the application of shear loading, by measuring the settlement of soil samples with time under the constant normal load (see Chapter 6-1). Once t_f is calculated, the lateral displacement δ that is required to reach the soil peak strength is estimated to be 1 to 2 mm for hard clay, 2 to 5 mm for stiff clay, and 8 to 10 mm for plastic clay. The maximum rate v of shearing displacement is then chosen so that it takes at least the time t_f to reach the lateral displacement δ . Typical values of the undrained shear strength, friction angle, and cohesion intercept for various soils can be obtained from Chapter 7-1.

FRICTION ANGLE IN DIRECT SHEAR TEST

Many comparisons have been made between the values of ϕ' measured from direct shear and triaxial tests. Earlier studies (e.g., Taylor, 1939) indicate that the friction angle ϕ'_{DS} during direct shear is generally greater by about 2° than the peak friction angle ϕ'_p during triaxial compression, especially for dense sands. Re-

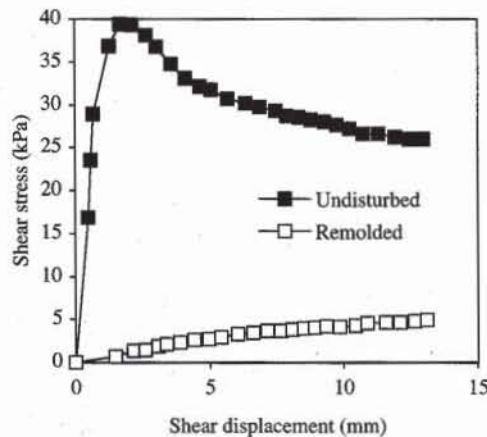


Figure 8 Typical results from a direct shear test on undisturbed and remolded samples of clay (Lambe, 1951).

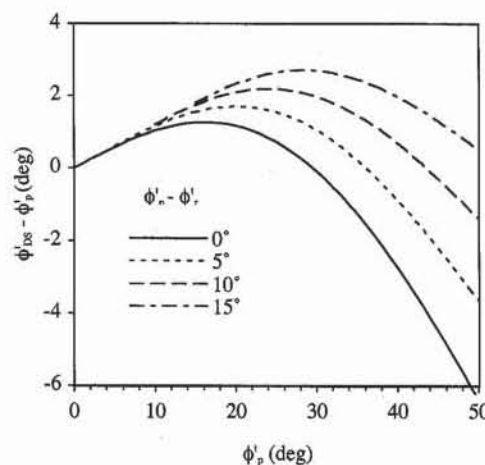


Figure 9 Variation of difference $\phi'_{DS} - \phi'_p$ with ϕ'_p for various values of $\phi'_p - \phi'_r$.

cent studies (e.g., Rowe, 1969; and Kulhawy and Mayne, 1990) show that ϕ'_{DS} is related to ϕ'_p through

$$\phi'_{DS} = \tan^{-1} [\tan(1.12 \phi'_p) \cos \phi'_r] \quad (10)$$

where ϕ'_r is the residual friction angle. In the case of sands, ϕ'_p can be related to ϕ'_r , relative density D_r , and stress level as explained in Chapter 7-1. Figure 9 shows the variation of $\phi'_{DS} - \phi'_p$ with ϕ'_p , where ϕ'_{DS} is calculated from Eq. 10, for various constant values of $\phi'_p - \phi'_r$. For small values of ϕ'_p , ϕ'_{DS} can be 2° larger than ϕ'_p , but for larger values of ϕ'_p , ϕ'_{DS} can become 6° smaller than ϕ'_p . Therefore, the friction angle during triaxial compression may be larger or smaller than the friction angle during direct shear, depending on the values of ϕ'_r , relative density and stress level.

There are pros and cons for measuring the shear strength of soils with the direct shear test. The direct shear is inexpensive and reliable for simulating the long term drained failure of fine-grained soils on predetermined failure surfaces. However, it is less reliable for fine-grained soils under undrained conditions, because it does not allow a complete control of the drainage conditions.

REFERENCES

- See Introduction for references to ASTM procedures (pages 4 to 6).
- KULHAWY, F. H., and P. W. MAYNE, 1990, *Manual on Estimating Soil Properties for Foundations Design*, Report EL-9800 to Electric Power Research Institute, Cornell University, Ithaca, New York.
- LAMBE, T. W., 1951, *Soil Testing for Engineers*, John Wiley & Sons, New York, pp. 88-97.
- ROWE, P. W., 1969, The relation between the shear strength of sands in triaxial compression, plane strain and direct shear, *Géotechnique*, Vol. 19, No. 1, pp. 75-86.
- TAYLOR, D. W., 1939, A comparison of results of direct shear and cylindrical compression tests, *Proc. ASTM*.

REVIEW QUESTIONS

- For which types of engineering analyses do you need the results of direct shear tests?
- Why is the shear strength of dense sands higher than that of loose sands?
- Is it possible to plot the evolution of the Mohr stress circle during a direct shear test?
- Is it possible to determine the state of strain of the tested sample during the direct shear test?
- Under which assumptions can we determine the normal failure stress on the vertical surface of a sheared sample?
- What is the effect of the change in the contact area during a direct shear test?
- In which parts of the soil sample are the strains concentrated during a direct shear test?
- What is the effect of density on the friction angle of sands?
- Define *peak* and *residual friction angles*.
- What is the critical state theory in the case of the direct shear test on sand?

EXERCISES

- Plot the shear stress and normal displacement versus shear displacement from the direct shear test results on a loose sand shown in Table E1. Calculate the friction angle.

TABLE E1

Shear displacement (mm)	τ/σ	Normal displacement (mm)
0.04	0.02	0.005
0.12	0.13	0.016
0.25	0.31	0.035
0.57	0.40	0.076
0.85	0.46	0.081
1.07	0.54	0.107
1.50	0.60	0.117
1.97	0.64	0.117
2.39	0.68	0.100
3.04	0.70	0.055
3.49	0.71	0.041
3.96	0.72	0.030
4.53	0.72	0.021
4.85	0.72	0.018
5.43	0.72	0.010
6.07	0.71	0.007
6.62	0.71	0.005
7.04	0.71	0.006
7.54	0.70	0.007
7.94	0.70	0.008
8.41	0.70	0.009
8.83	0.70	0.009
9.25	0.70	0.009
9.77	0.70	0.009
10.37	0.71	0.009
10.82	0.71	0.008
11.41	0.71	0.007

2. Given the direct shear test results of Table E1, calculate the normal and shear stresses that are acting at failure on the horizontal and vertical surfaces, provided that the failure plane is horizontal and that the stresses are uniform. The normal stress on the horizontal surface is 50 kPa.
3. Derive the relation between the normal stresses on vertical and horizontal surfaces at failure assuming that the stress state is uniform, and that the failure plane is horizontal.
4. Plot the relative error on the contact area versus the shear displacement for a circular shear box of 6.35 mm diameter. Define the range of displacement for which the relative error on the contact area is less than 5%.
5. Calculate the undrained shear strength of the undisturbed and remolded samples whose direct shear test results are shown in Table E2.

TABLE E2

Undisturbed		Remolded	
Shear displacement (mm)	Shear stress (kPa)	Shear displacement (mm)	Shear stress (kPa)
0.00	0.00	0.00	0.00
0.49	16.82	1.48	0.67
0.57	23.54	2.16	1.32
0.68	28.91	2.59	1.45
1.26	36.89	3.06	1.89
1.68	39.39	3.38	2.11
2.10	39.31	3.88	2.35
2.63	38.10	4.41	2.58
3.01	36.78	4.96	2.72
3.57	34.75	5.41	2.95
4.11	33.13	6.05	3.30
4.64	32.12	6.60	3.43
5.07	31.74	7.13	3.67
5.68	30.74	7.63	3.69
6.34	30.16	8.08	3.82
6.87	29.77	8.51	3.95
7.49	29.29	8.90	4.08
7.88	28.69	9.35	4.20
8.34	28.51	9.86	4.13
8.79	28.23	10.44	4.27
9.29	28.05	10.89	4.60
9.74	27.66	11.58	4.64
10.22	27.17	12.11	4.67
10.73	26.58	12.66	4.80
11.31	26.62	13.11	4.93
11.94	26.24		
12.45	25.96		
12.98	25.99		

Normal stress = 31.92 kPa

7-5 Direct Shear Test

OBJECTIVE

The direct shear test is used to measure the friction angle, cohesion, and undrained shear strength of soils for stability analysis of foundations, slopes, and retaining walls.

EQUIPMENT

The equipment for the direct shear test includes:

- Direct shear loading machine with a counterbalance system for the application of normal load (see Figs. 1 and 6).
- Direct shear box (see Figs. 3 to 5).
- Assortment of slotted weights for applying the normal load. The total weight should be at least 100 kg. For the typical 6.35-cm-diameter shear box, it takes a mass of 32.3 kg to create a normal stress equal to 100 kPa.
- Two dial gages for measuring vertical and horizontal displacements sensitive to 0.01 mm with a full range of 2.5 cm. The dial gages may be replaced by calibrated LVDT transducers of similar range and sensitivity.
- One calibrated load ring for measuring the shear force. A capacity of 2 kN is suitable for most purposes. A larger capacity (e.g., 5 or 10 kN) may be required for larger normal loads. The load ring may be replaced by a load transducer of similar range.
- A 2.5-cm ball bearing for applying the normal load to the sample cap.
- Specimen cutter for trimming samples of cohesive soil.
- Tamper for compacting cohesionless soil.
- Balance, sensitive to 0.1g.
- Timer and calipers.
- Spoons and straightedge.

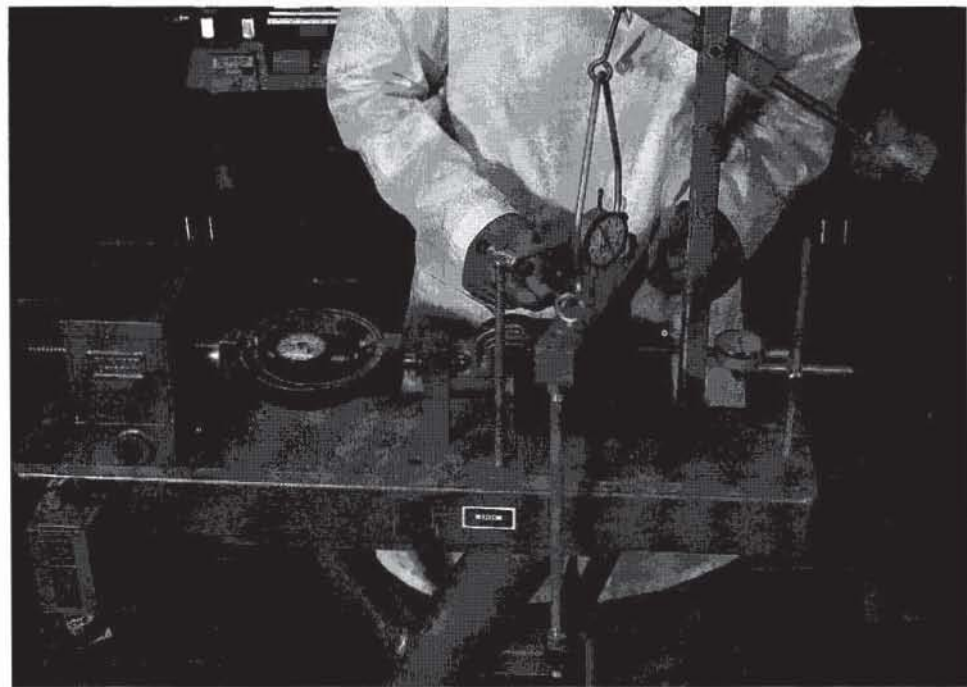


Figure 1 General view of the direct shear equipment.

Direct Shear Box

As shown in Figs. 2 and 3, the direct shear box is made of a lower part (base) and an upper part with a swan neck yoke. The sample is between two porous stones, which are toothed or serrated as shown in Fig. 4 to minimize the slippage at the interface between soil and shear box and to improve the transfer of the shear load to the soil. The porous stones are also used to drain water from saturated samples. The setscrews are used to adjust the spacing between the upper and lower parts of the shear box. Two mounting pins maintain the position of these two parts during the sample fabrication and are removed before the beginning of the shear phase. The base is fixed to the loading frame and occasionally contains water when the soil sample is to remain saturated. The normal load is applied to the soil sample through a ball bearing and a rigid cap. The lateral load is applied to the upper part through the swan neck yoke.

As shown in Fig. 5, some particular shear boxes are designed to simplify preparation of cohesive soil samples. They take samples right out of the field sam-

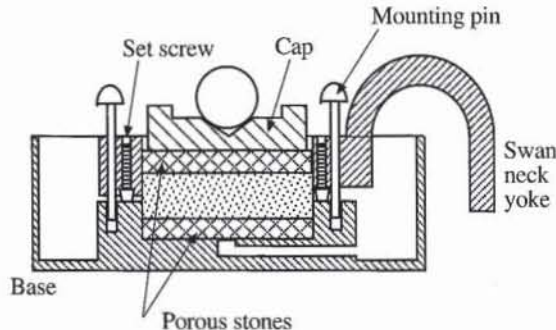


Figure 2 Schematic view of the direct shear box.

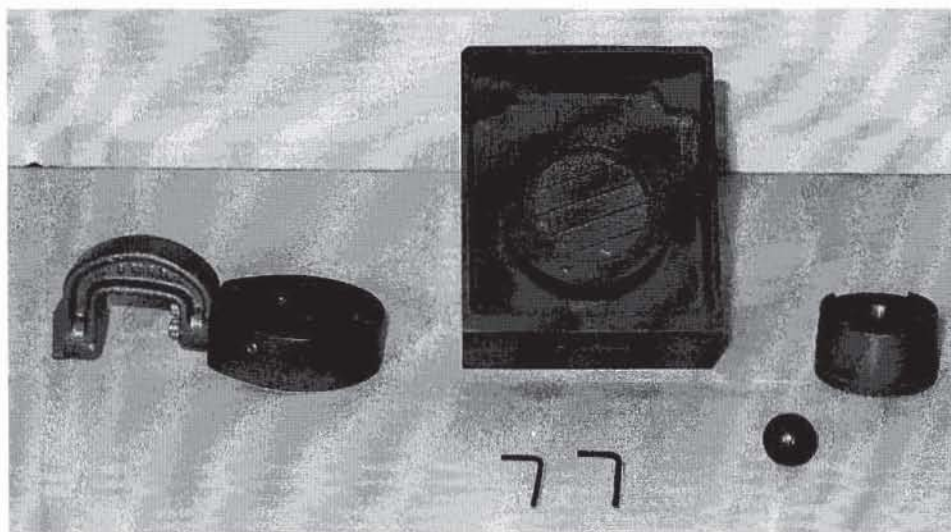


Figure 3 Shear box components.



Figure 4 Detail of (a) serrated and (b) toothed porous stones for the direct shear box.

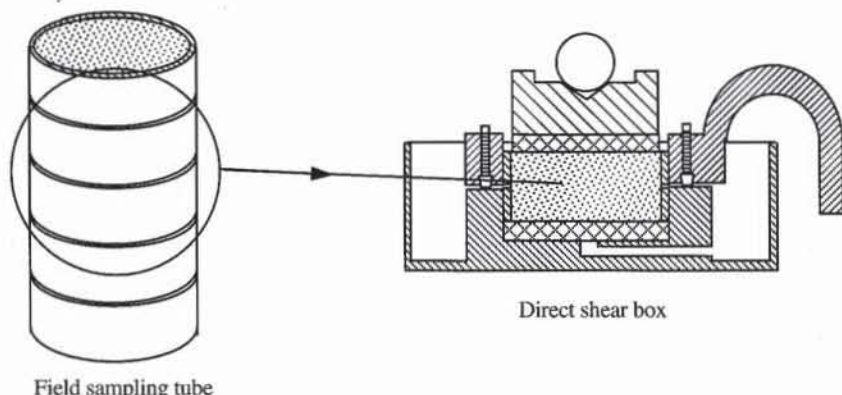


Figure 5 Shear box assorted to field sampling tube.

pling tubes. During field exploration, a stack of rings is first placed in the field sampling tube, which becomes filled with the soil to be tested when it is pushed into the ground. In the laboratory, two full rings are sliced from the field sample using a wire saw and are directly mounted in the shear box.

Loading Unit

The direct shear test can be controlled by either displacement or force. When it is force controlled, the shear force is gradually increased at a prescribed rate and the resulting displacement is measured. When displacement controlled, the upper part of the shear box is laterally pushed at a specified rate and the resulting shear

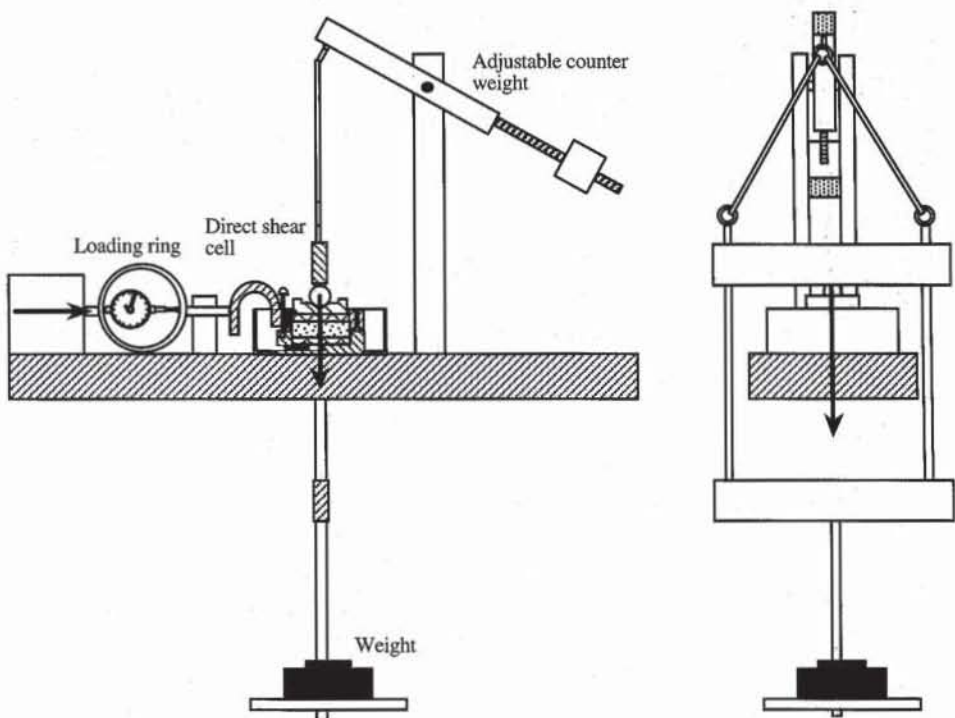


Figure 6 The loading unit and its counterweight mechanism.

force is measured. Displacement-controlled units are preferred because they give the residual shear strength of soils.

Good displacement-controlled equipment has a controllable rate of lateral displacement ranging from 5 to 0.0005 mm/min and a full displacement of about 10 mm. With this range of speed, it takes from 2 min to about 14 days to move 10 mm. A rate of 0.5 to 1 mm/min is appropriate to perform a quick test in 10 to 20 min. The rate of displacement is generally controlled by an electrical motor and a gearbox. As shown in Fig. 6, the shear force is measured by the proving ring attached to the yoke of the direct shear box. The lateral and vertical displacements are measured with dial gages or LVDT transducers.

As shown in Fig. 6, the loading unit also applies normal force to the soil specimen. The counterweight system is balanced so that the empty weight hanger applies no normal force to the sample. The normal load is then obtained directly by adding weights suspended on a weight hanger.

TEST PROCEDURE

There are two different test procedures, depending on whether the soil to be tested is coarse grained (e.g., sands), or fine grained (e.g., clays and silts).

Coarse-Grained Soil

1. Measure the internal diameter of the cylindrical cell (or the internal side length for square cell).
2. Balance the counterweight system so that it applies a small but negligible normal force.

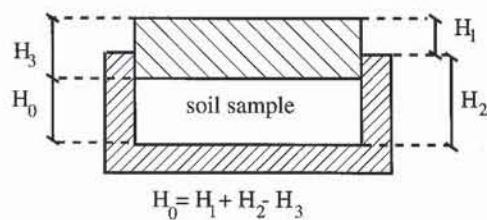


Figure 7 Determination of the initial height H_0 of sample.

3. Weigh the cap and the ball bearing, as their weight is not counterbalanced by the counterweight mechanism and must be added to the weights on the weight hanger.
4. Assemble the direct shear box, and mount it on the direct shear machine. Insert the mounting pins to align the upper and lower parts of the direct shear box.
5. Adjust the gap between the two parts of the shear box by turning the set-screws. In theory, the spacing should be larger than the diameter of the largest particle to prevent the top part from riding up on the grains that get caught in the gap. In practice, a spacing of approximately 0.5 mm is satisfactory. Too close a spacing is indicated by a snapping and crushing of grains, accompanied by jerky readings.
6. Measure the depth H_2 of the shear box and the height H_3 of the top cap as shown in Fig. 7.
7. Weigh the dish filled with the sand to be tested.
8. While the pins hold the two parts of the shear box together, pour in the sand slowly to obtain a loose specimen (Fig. 8). Compact the sand with a tamper or vibrate the container to obtain denser specimens. The cell should be filled with enough material so that the top cap is quite above the shear plane (Fig. 9).



Figure 8 Filling the shear box with sand.



Figure 9 The specimen should be thick enough for the bottom of the loading cap to be quite above the plane separating the upper and lower parts of the shear box.

9. Weigh the dish and the leftover sand to determine the weight of the soil used in the test.
10. Level the soil surface inside the shear cell, put on the cap and ball bearing, and position the counterweight system (Figs. 10 and 11).
11. Put the amount of dead weight on the balanced mechanism which is required to apply the desired normal load.
12. Measure the initial height H_0 of the soil specimen by measuring the distance H_1 as shown in Fig. 7.
13. Attach the dial gages or displacement transducers that measure shear and normal displacements as shown in Fig. 10.

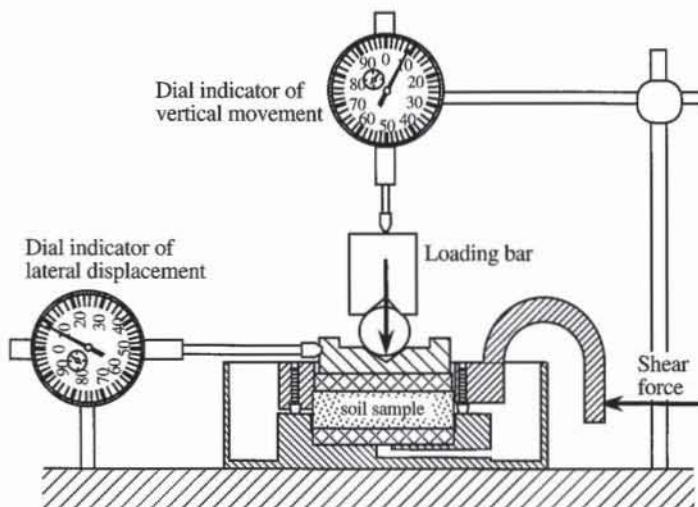


Figure 10 The shear box and the dial gages.

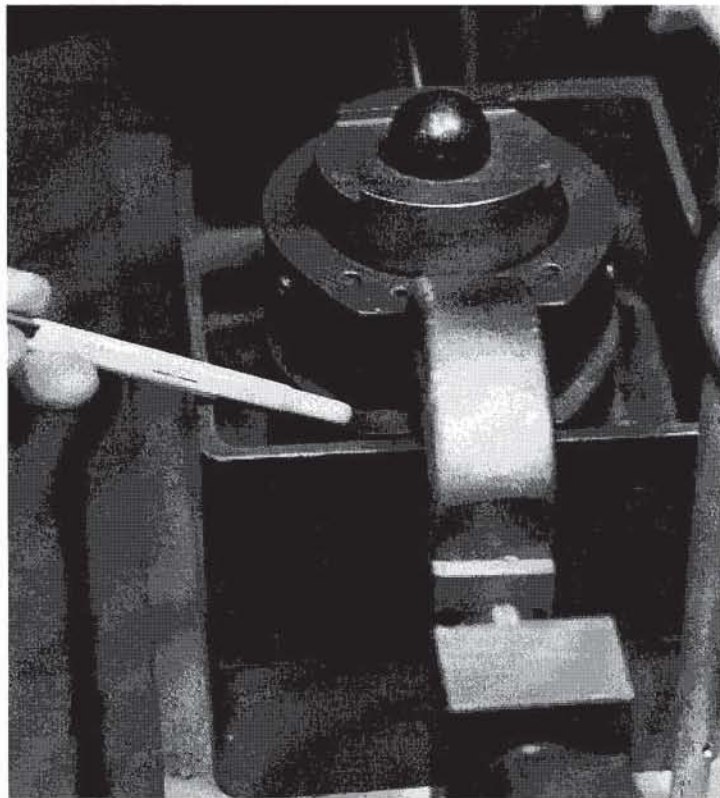


Figure 11 The shear box is assembled and the two mounting pins are removed.

14. Before beginning the shear loading, carefully check that no pin or screw is left to hold the two parts of the shear box together.

15. Adjust the rate of shear displacement to approximately 1 mm/min. If dial gages are used to measure displacement and forces, select a rate of shearing that is convenient for reading the dial gages simultaneously. For a maximum lateral displacement of 1 cm and a rate of 1 mm/min, the test duration is 10 min. For sands, the effect of the displacement rate on the friction angle is generally negligible within the range 3 to 0.1 mm/min.

16. Start the loading. Measure the shear force, time, and shear and normal displacements at convenient time intervals. Continue the test until the horizontal displacement becomes approximately 1 cm or until the shear force becomes constant, whichever comes first.

Fine-Grained Soil

In the case of fine-grained soils, the direct shear test can be performed under CU or CD conditions (see Chapter 5-4). In the CU test, the sample is first consolidated under the action of the normal load, and then quickly sheared. In the CD test, the sample is consolidated as for the CU test, but is sheared very slowly so that no excess pore pressure builds up.

CU test

1. Same as steps 1 to 4 for coarse-grained soils.

2. Turn the set screws so that there is no gap at all between the two parts of the shear box.
3. Measure the depth H_2 of the shear box and the height H_3 of the top cap as shown in Fig. 7.
4. Put the amount of dead weight on the balanced mechanism to apply the desired normal load.
5. Measure the initial height H_0 of the soil specimen by measuring the distance H_1 as shown in Fig. 7.
6. Add water in the direct shear box to cover the soil specimen completely.
7. Attach the dial gages or displacement transducers that measure shear and normal displacements (Fig. 10), and record their initial readings.
8. Measure the vertical settlement of the sample with time until the end of the primary consolidation is detected (see Chapter 6-1).
9. Adjust the gap between the two parts of the shear box to the smallest possible setting that minimizes the friction resistance between these two parts.
10. Check that no pin or screw holds together the two parts of the shear box.
11. Adjust the rate of shearing displacement to approximately 1 mm/min. The loading rate should be fast enough to approach the undrained condition.
12. Start the shear loading. Measure the shear force, time, and shear and normal displacements at convenient time intervals. Continue the test until the horizontal displacement becomes approximately 1 cm.

CD test. The CD test is similar to the CU test, except for the determination of the shearing rate that prevents the excess pore pressure from building up in the sample.

1. Same as steps 1 to 7 of the CU test.
2. Measure the vertical settlement of the sample with time, and determine the time t_{90} to reach 90% of the primary consolidation (see Chapter 6-1).
3. Same as steps 9 to 10 of the CU test.
4. Estimate the lateral displacement δ required to reach the soil peak strength. Typically, $\delta = 1$ to 2 mm for hard clay, $\delta = 2$ to 5 mm for stiff clay, and $\delta = 8$ to 10 mm for plastic clay. Calculate the minimum time t_f required for failure by using the empirical relation $t_f = 11.7 t_{90}$ (ASTM D3080). Calculate the maximum rate v of shearing displacement so that it takes the time t_f to reach the lateral displacement δ (i.e., $v = \delta/t_f$). Select the shearing rate of the equipment that is closest to v .
5. Start the shear loading. Measure the shear force, time, and shear and normal displacements at convenient time intervals. Continue the test until the lateral displacement becomes approximately 1 cm or until the shear force becomes constant, whichever comes first.

COMPUTATIONS

The results of the direct shear test should identify the characteristics of the tested soil. For dry soil specimens of coarse grain, the dry unit weight γ_d and void ratio e are

$$\gamma_d = \frac{W_i}{V_i} \quad \text{and} \quad e = \frac{G_s \gamma_w}{\gamma_d} - 1 \quad (1)$$

where γ_w is the water unit weight, W_i the initial sample weight, V_i the initial sample volume, and G_s the soil specific gravity. For wet specimens of fine-grained soils, the water content w is

$$w = \frac{W_i - W_d}{W_d} \times 100 \quad (\%) \quad (2)$$

where W_i is the initial weight and W_d is the dry weight of the complete sample or some sample trimmings. The total unit weight γ , dry unit weight γ_d , void ratio e , and degree of saturation S_r of wet soil samples are

$$\gamma = \frac{W_i}{V_i}, \quad \gamma_d = \frac{\gamma}{1+w}, \quad e = \frac{G_s \gamma_w}{\gamma_d} - 1, \quad \text{and} \quad S_r = \frac{G_s w}{e} \quad (3)$$

For coarse-grained soils and fine-grained soils tested under CD conditions, the results of a direct shear test should include the peak and residual friction angles, the shear displacements at which they are observed, and the graphs τ/σ and normal displacement versus shear displacement. The shear stress τ , normal stress σ , and ratio τ/σ are

$$\sigma = \frac{N}{A_c}, \quad \tau = \frac{T}{A_c}, \quad \text{and} \quad \frac{\tau}{\sigma} = \frac{T}{N} \quad (4)$$

where T is the measured lateral force, N the normal force, and A_c the corrected area of the sheared specimen, which is a function of the shear displacement δ . In contrast to τ and σ , τ/σ is determined without A_c . The peak friction angle ϕ_p and residual friction angle ϕ_r are

$$\phi_p = \tan^{-1} \frac{T_{\max}}{N} \quad \text{and} \quad \phi_r = \tan^{-1} \frac{T_r}{N} \quad (5)$$

where T_{\max} is the maximum shear force and T_r is the residual shear force.

For fine-grained soils tested under CU conditions, the results of the direct shear test should include the undrained shear strength, the shear displacements at which it is observed, and graphs of τ/σ versus shear displacement.

EXAMPLE

Figures 12 to 15 show results obtained for a dense fine uniform sand. Figures 12 and 13 show graphs of τ/σ and normal displacement versus shear displacement, Fig. 14 shows the corresponding input/output data, and Fig. 15 lists the formulas used in Fig. 14. During shear, the dense material first compacts, then dilates.

REFERENCES

See Introduction for references to ASTM procedures (pages 4 to 6).

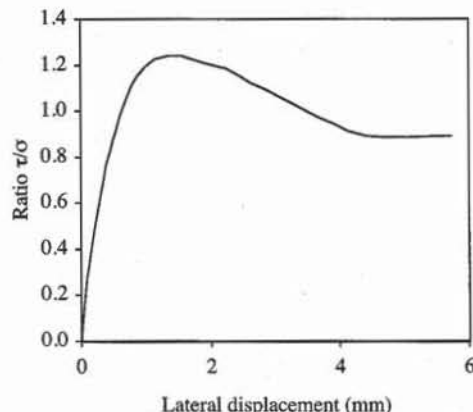


Figure 12 Variation of τ/σ with lateral displacement during a direct shear test of dense fine sand.

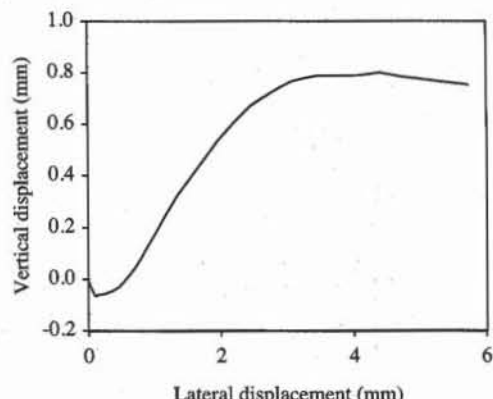


Figure 13 Variation of vertical displacement with lateral displacement corresponding to Fig. 12.

	B	C	D										
6	Mass of specimen M = 84		g										
7	Vertical load N = =19.392*9.8		N										
8	Specific gravity $G_s = 2.65$												
9	Initial height $h_0 = 1.545$		cm										
10	Diameter $d_0 = 6.33$		cm										
11	Dry unit weight $\gamma_d = =M*9.81/(PI()*H0*D0^2/4)$		kN/m ³										
12	Void ratio e = =Gs*9.8/gd-1												
13	Maximum friction angle $\phi_p = =ATAN(MAX(ratio))*180/PI()$		deg										
14	Displacement at peak $\delta_p = =INDEX(d,MATCH(MAX(ratio),ratio,0))$	mm											
15	Residual friction angle $\phi_r = =ATAN(D61)*180/PI()$	deg											
16	Displacement at residual $\delta_r = =A61$	mm											
17	Normal stress $\sigma = =N*9.81/(PI()*D0^2/4)$		kPa										
			<table border="1" style="width: 100%; border-collapse: collapse;"> <thead> <tr> <th style="text-align: center;">D</th> <th style="text-align: center;">Ratio</th> </tr> </thead> <tbody> <tr> <td style="text-align: center;">19</td> <td style="text-align: center;">τ/σ</td> </tr> <tr> <td style="text-align: center;">20</td> <td style="text-align: center;">$=T/N$</td> </tr> <tr> <td style="text-align: center;">21</td> <td style="text-align: center;">$=T/N$</td> </tr> <tr> <td style="text-align: center;">22</td> <td style="text-align: center;">$=T/N$</td> </tr> </tbody> </table>	D	Ratio	19	τ/σ	20	$=T/N$	21	$=T/N$	22	$=T/N$
D	Ratio												
19	τ/σ												
20	$=T/N$												
21	$=T/N$												
22	$=T/N$												

Figure 15 Formulas used in Fig. 14.

REVIEW QUESTIONS

- What is the purpose of a direct shear test? Which soil properties does it measure?
- Why do we use mounting pins in a direct shear test? Can you predict what will happen if you do not remove them during the test?
- Why are the porous stones of a direct shear box serrated or provided with teeth?
- What is the rationale for determining the spacing between the two parts of a direct shear box? What are the effects of a poorly selected spacing?
- What is the purpose of the counterweight mechanism in direct shear apparatus?
- What is the range of the rate of shear displacement that is typically achievable with a direct shear loading device?
- Under which circumstances and for which soils should a very slow shearing speed be used?
- Give an approximate duration for a very slow direct shear test.

	A	B	C	D
1	Direct Shear Test			
2	Analyst name: Robertus B. Kurniawan			
3	Test date: April 20, 1993			
4	Sample Description: Dense uniform sand			
5				
6	Mass of specimen M = 84.00	g		
7	Vertical load N = 190.04	N		
8	Specific gravity G_s = 2.65			
9	Initial height h_0 = 1.55	cm		
10	Diameter d_0 = 6.33	cm		
11	Dry unit weight γ_d = 16.95	kN/m³		
12	Void ratio e = 0.53			
13	Maximum friction angle φ_p = 51.11	deg		
14	Displacement at peak δ_p = 1.35	mm		
15	Residual friction angle φ_r = 41.73	deg		
16	Displacement at residual δ_r = 5.74	mm		
17	Normal stress σ = 59.24	kPa		
18				
19	Lateral displacement (mm)	Vertical displacement (mm)	Lateral force (N)	Ratio
20	d		T	t/g
21	0.00	0.00	0.0	0.00
22	0.02	-0.02	13.7	0.07
23	0.05	-0.04	30.8	0.16
24	0.08	-0.05	46.5	0.24
25	0.09	-0.06	52.4	0.28
26	0.12	-0.06	61.5	0.32
27	0.15	-0.06	72.6	0.38
28	0.19	-0.06	86.4	0.45
29	0.23	-0.06	99.5	0.52
30	0.27	-0.06	110.6	0.58
31	0.31	-0.05	122.4	0.64
32	0.35	-0.05	132.9	0.70
33	0.39	-0.04	145.3	0.76
34	0.46	-0.03	157.7	0.83
35	0.50	-0.02	166.2	0.87
36	0.55	-0.01	174.1	0.92
37	0.59	0.01	182.6	0.96
38	0.64	0.02	190.5	1.00
39	0.70	0.05	200.9	1.06
40	0.79	0.08	211.4	1.11
41	0.88	0.12	219.3	1.15
42	1.00	0.17	227.1	1.20
43	1.14	0.24	233.0	1.23
44	1.35	0.32	235.6	1.24
45	1.55	0.39	235.6	1.24
46	1.97	0.54	229.1	1.21
47	2.25	0.62	225.1	1.18
48	2.45	0.67	219.3	1.15
49	2.62	0.70	213.4	1.12
50	2.87	0.74	207.5	1.09
51	3.07	0.76	201.6	1.06
52	3.27	0.78	196.3	1.03
53	3.47	0.79	190.5	1.00
54	3.68	0.79	184.6	0.97
55	3.91	0.79	179.3	0.94
56	4.12	0.79	173.4	0.91
57	4.42	0.80	169.5	0.89
58	4.72	0.79	168.2	0.89
59	5.02	0.77	168.2	0.89
60	5.33	0.77	168.9	0.89
61	5.74	0.75	169.5	0.89

Figure 14 Example of data set for a direct shear test.

9. Is the shear strength of coarse-grained soils influenced by the rate of shearing in a direct shear test? On what basis is the rate of shearing selected for coarse-grained soils?
10. How many and which types of direct shear tests are possible to perform on fine-grained soils?
11. What are the basic steps of a CU direct shear test on a fine-grained soil?
12. What are the basic steps of a CD direct shear test on a fine-grained soil?
13. How is the shearing rate determined for the CD direct shear tests of fine-grained soils?

EXERCISES

1. Plot the exact and approximate variation of area correction and define the range of displacement for which the error on the contact area is less than 5%.
2. Process the following results of a direct shear test on a loose and a dense sample of fine sand.

Sample description	Dense uniform sand	Loose uniform sand
Weight of specimen	84.00 g	68.00 g
Vertical load	190.04 N	190.04 N
Specific gravity	2.65	2.65
Initial height	1.53 cm	1.51 cm
Initial diameter	6.35 cm	6.35 cm
Normal stress	58.92 kPa	58.92 kPa

Dense uniform sand				Loose uniform sand			
Lateral displacement (mm)	Vertical displacement (mm)	Lateral force (N)	τ/σ	Lateral displacement (mm)	Vertical displacement (mm)	Lateral force (N)	τ/σ
0.00	0.00	0.00	0.00	0.00	0.00	0.00	0.00
0.02	0.00	15.05	0.08	0.05	0.01	17.02	0.09
0.04	0.00	29.45	0.15	0.09	0.01	29.45	0.15
0.06	0.00	45.16	0.24	0.14	0.01	41.89	0.22
0.08	0.00	54.98	0.29	0.18	0.01	50.40	0.27
0.10	0.00	66.76	0.35	0.23	0.01	61.52	0.32
0.14	0.00	85.08	0.45	0.30	0.01	75.92	0.40
0.20	0.00	103.41	0.54	0.40	0.01	93.59	0.49
0.26	-0.01	117.81	0.62	0.49	0.00	107.99	0.57
0.30	-0.02	130.24	0.69	0.53	0.00	121.74	0.64
0.34	-0.03	138.10	0.73	0.55	0.00	129.59	0.68
0.40	-0.04	147.92	0.78	0.60	0.00	140.06	0.74
0.44	-0.04	153.81	0.81	0.63	0.00	145.95	0.77
0.54	-0.06	163.62	0.86	0.70	-0.01	155.77	0.82
0.60	-0.07	167.55	0.88	0.72	-0.02	159.70	0.84
0.68	-0.10	173.44	0.91	0.76	-0.03	165.59	0.87
0.74	-0.11	177.37	0.93	0.80	-0.04	169.51	0.89
0.80	-0.12	179.33	0.94	0.82	-0.04	171.48	0.90
0.89	-0.14	183.26	0.96	0.86	-0.04	175.40	0.92
0.99	-0.17	183.91	0.97	0.88	-0.05	177.37	0.93
1.09	-0.20	185.22	0.97	0.90	-0.05	179.33	0.94
1.29	-0.25	185.22	0.97	0.96	-0.07	183.26	0.96
1.48	-0.30	185.88	0.98	1.12	-0.10	186.53	0.98
1.58	-0.32	185.88	0.98	1.16	-0.11	188.49	0.99

(cont.)

Dense uniform sand				Loose uniform sand			
Lateral displacement (mm)	Vertical displacement (mm)	Lateral force (N)	τ/σ	Lateral displacement (mm)	Vertical displacement (mm)	Lateral force (N)	τ/σ
1.79	-0.36	187.18	0.98	1.31	-0.15	187.84	0.99
1.89	-0.38	186.53	0.98	1.42	-0.17	187.18	0.98
2.01	-0.40	182.60	0.96	1.56	-0.20	184.57	0.97
2.13	-0.41	179.33	0.94	1.69	-0.22	180.64	0.95
2.33	-0.43	176.71	0.93	1.86	-0.25	176.71	0.93
2.51	-0.45	172.13	0.91	2.06	-0.25	171.48	0.90
2.74	-0.47	168.20	0.89	2.23	-0.27	166.90	0.88
2.89	-0.48	166.24	0.87	2.51	-0.27	159.04	0.84
2.99	-0.49	166.24	0.87	2.62	-0.28	157.73	0.83

7-6 Principles of Triaxial Tests

INTRODUCTION

As introduced in Chapter 5-4, the triaxial test is used to determine the stress-strain-strength characteristics of soils under drained or undrained conditions. This test reproduces in the laboratory the initial effective stresses and stress changes of soils in the field, in a more realistic way than unconfined compression and direct shear tests. Here we review the principles of triaxial tests, check the saturation of triaxial specimens, and select the loading rate of triaxial tests. Typical triaxial test results can be found in Chapter 7-1.

TYPES OF TRIAXIAL TEST

As shown in Fig. 1, in a triaxial test the cylindrical soil specimen is encased within a rubber sleeve inside a pressure chamber. The lower and upper loading platens have porous disks connected to the drainage system for saturating and/or draining the soil specimen. The confining pressure σ_3 is applied by adjusting the chamber pressure, and the axial stress σ_1 is applied by pushing the piston. There are three main types of triaxial test, which are labeled CD, UU, and CU. The first letter, C or U, refers to the consolidation stage and stands for *consolidated* or *unconsolidated*. The second letter, D or U, refers to the drainage condition during shear and stands for *drained* or *undrained*. Hereafter we present only the CD, CU and UU triaxial compression tests with isotropic consolidation. Information on other types of triaxial test in Chapter 5-4 can be found in Head (1986).

During CD and CU tests, the soil sample is first consolidated to an initial effective stress state. Consolidation is an important step in testing frictional materials, whose elastic properties and shear strength depend largely on effective stresses. As shown in Fig. 1, during an isotropic consolidation, the soil specimen is subjected to hydrostatic pressure. The drainage is opened, and the interstitial water filling the soil voids can drain freely. The time required to complete consolidation is almost negligible for coarse-grained soils with high permeability, but can

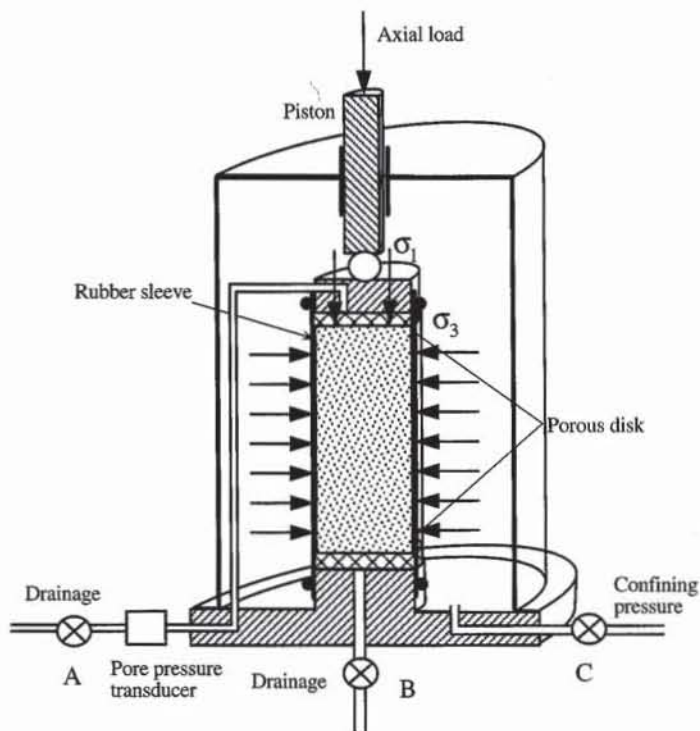


Figure 1 Experimental setup of triaxial test.

be long for fine-grained soils with low permeability.

Figure 2 schematizes the stress loading in σ - τ and s - t spaces during the axial compression after consolidation. As shown in Fig. 2, the axial stress σ_1 is increased while σ_3 is kept constant. The Mohr circle of total stress expands from point A (Fig. 2b) and the corresponding total stress path is AB in s - t space (Fig. 2c).

During CD tests, the drainage is opened and the excess pore pressure remains equal to zero. The total stress path AB is also an effective stress path. For fine-grained soils, the axial loading must be applied very slowly so that the excess pore pressure has time to dissipate through the drainage system.

CU triaxial tests are similar to CD tests except for the drainage which is closed during axial compression. This lack of drainage constrains the volume change of fully saturated specimens and creates an excess pore pressure. As shown in Fig. 2c, the prescribed total stress path AB does not coincide with the nonlinear effective stress path AB'. The effective stress path AB' and effective Mohr circles are related to their total stress counterparts through the measured excess pore pressure as shown in Fig. 2b and c.

During UU triaxial tests, the consolidation phase is omitted and the sample is sheared without knowing its effective stress, but the compression phase is the same as that of CU tests.

SATURATION OF SPECIMENS

The triaxial specimen must be fully saturated to measure its volume change in drained tests and to generate pore pressure in undrained tests. Its degree of saturation S_r is checked directly in the triaxial cell by determining the coefficient B

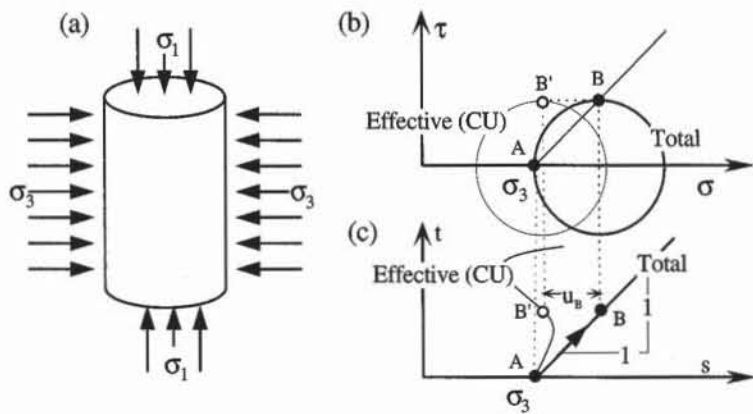


Figure 2 CU and CD triaxial compressions: (a) applied stresses, (b) effective and total stress Mohr circles in σ - τ space, and (c) effective and total stress paths in s - t space.

$$B = \frac{\Delta u}{\Delta \sigma_3} \quad (3)$$

where $\Delta \sigma_3$ is a small increase in confining pressure applied to the sample, and Δu is the resulting change in pore pressure measured under undrained conditions. $\Delta \sigma_3$ should be small enough (e.g., 5 to 10 kPa) to prevent the consolidation of partially saturated specimens. During the total stress increase $\Delta \sigma_3$, the volume change ΔV_{sk} of the sample is equal to the volume change ΔV_f of interstitial water

$$\Delta V_{sk} = V_{sk} \frac{\Delta \sigma'_3}{B_s} = V_{sk} \frac{\Delta \sigma_3 - \Delta u}{B_s} = \Delta V_f = V_f \frac{\Delta u}{B_f} = n V_{sk} \frac{\Delta u}{B_f} \quad (4)$$

where $\Delta \sigma'_3$ is the change in effective stress, V_{sk} the initial volume of soil, B_s the bulk modulus of soil, $V_f = n V_{sk}$ the initial volume of water, B_f the bulk modulus of interstitial water, and n the porosity. Using Eq. 4, B is

$$B = \frac{1}{1 + n \frac{B_s}{B_f}} \quad (5)$$

The interstitial water of nearly saturated soils is a mixture of water and gas which has the following bulk modulus B_f (Bardet and Sayed, 1993):

$$\frac{1}{B_f} = \frac{1}{B_w} + \frac{1 - S_r}{p_B} \quad (6)$$

where S_r is the degree of saturation, B_w the bulk modulus of pure water (2,200 MPa), and p_B the absolute fluid pressure, also referred to as backpressure. $p_B = 101$ kPa for water at atmospheric pressure. As shown in Fig. 3, Eq. 6 predicts that B_f is strongly influenced by S_r . Using Eqs. 5 and 6, and neglecting B_s compared to B_w , B and S_r are related through

$$B \approx \frac{1}{1 + n \frac{B_s}{p_B} (1 - S_r)} \quad \text{and} \quad S_r = 1 - \frac{p_B}{n B_s} \left(\frac{1}{B} - 1 \right) \quad (7)$$

Figure 4 shows the effect of S_r on B at various ratios B_s/p_B . These effects are especially important for soils with large bulk modulus. Under undrained conditions, this effect is reduced, but not eliminated with large back pressure p_B .

Eq. 7 implies that the sample is fully saturated when $B = 1$. In practice, $B \geq 99.5\%$ is satisfactory for undrained tests, and $B \geq 98\%$ is acceptable for drained tests. When B is too small, S_r can be increased under drained conditions by increasing the back pressure p_B and introducing additional deaired water into the voids, which will force some air to be absorbed into solution. p_B and σ_3 should be simultaneously increased so that the differential pressure across the triaxial membrane does not change. The increase in backpressure Δp_B required to increase S_r from an initial value S_0 to a final value S_f is given by Lowe and Johnson (1960):

$$\frac{\Delta p_B}{p_B} = \frac{0.98 (S_f - S_0)}{100 - 0.98 S_f} \quad (8)$$

where p_B is the initial back pressure, and S_f and S_0 are in percent. For instance, Eq. 9 indicates that the backpressure p_B should be increased by 495 kPa to get a final saturation $S_f = 100\%$, when $S_0 = 90\%$ and p_B was initially atmospheric ($p_B = 101$ kPa).

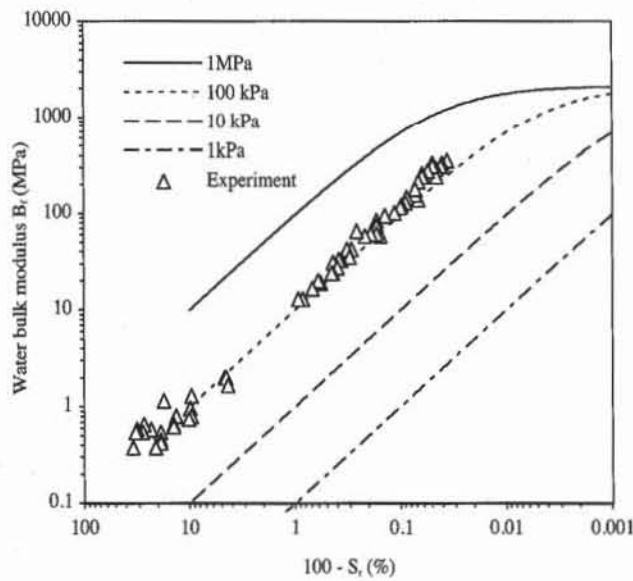


Figure 3 Variation of bulk modulus of water with water pressure and degree of saturation S_r (after Bardet and Sayed, 1993).

RATE OF LOADING FOR CU AND CD TESTS

In CU and CD triaxial tests, the loading rate is selected so that the pore pressure remains uniform within the tested specimen.

In the CD test, the excess pore pressure should remain negligible. The loading rate must be slow enough to allow for the excess pore pressure to dissipate through the pervious boundaries. The loading rate of the CD triaxial test is selected by first determining the time t_f required to reach failure by from Table 1

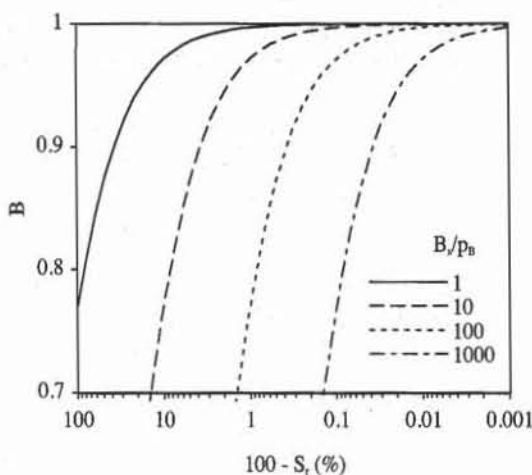


Figure 4 Variation of coefficient B versus degree of saturation S_r ($n = 0.3$) for various normalized values of soil bulk moduli B_s/p_B .

(after Head, 1986). In Table 1, t_{100} is the time to complete the primary compression, which can be determined by measuring the volume change during the consolidation phase of the triaxial test (see Chapter 6-1 for the determination of t_{100}). The side drain of Table 1 refers to a thin filter paper which is wrapped around the sample to shorten the duration of the consolidation phase.

The axial strain ϵ_p required to reach the soil peak strength is then estimated. The maximum rate v of axial displacement is chosen so that axial strain ϵ_p is reached after time t_f :

$$v = \frac{\epsilon_p H_0}{12.7 t_{100}} \quad (9)$$

where H_0 is the initial sample height.

TABLE 1
Time t_f to reach failure (after Head, 1986)

Type of test	No side drain	With side drain
CU	$0.51 \times t_{100}$	$1.8 \times t_{100}$
CD	$8.5 \times t_{100}$	$14 \times t_{100}$

In the CU test, the pore pressure should be distributed uniformly, although its overall value varies when the sample is sheared. The loading rate is determined by using Table 1 as for CD tests. The loading rate of CU tests is about 10 times faster than those of CD tests. During CU tests, the pore water is practically immobile, and the excess pore pressure is more rapidly and uniformly distributed than during CD tests.

REFERENCES

- BARDET, J. P., and H. SAYED, 1993, Velocity and attenuation of compressional waves in nearly saturated soils, *Soil Dyn. Earthquake Eng.*, Vol. 12, No. 7, pp. 391–402.

- BISHOP, A. W., and D. J. HENKEL, 1962, *The Measurement of Soil Properties in the Triaxial Test*, 2nd ed., Edward Arnold, London, pp. 228.
- HEAD, K. H., 1986, *Manual of Soil Laboratory Testing, Volume 3: Effective Stress Tests*, John Wiley & Sons, New York, pp. 951–956, 1001–1053.
- HOLTZ, R. D., and W. D. KOVACS, 1981, *An Introduction to Geotechnical Engineering*, Prentice-Hall, Englewood Cliffs, NJ, pp. 449–519.
- LAMBE, T. W., and R. V. WHITMAN, 1979, *Soil Mechanics, SI Version*, John Wiley & Sons, pp. 116–121, 135–150.
- LOWE, J., and T. C. JOHNSON, 1960, Use of backpressure to increase degree of saturation of triaxial test specimens, *Proceedings of the ASCE Research Conference on Shear Strength of Cohesive Soils*, Boulder, CO, pp. 819–836.

REVIEW QUESTIONS

1. How many types of triaxial tests are there?
2. Define UU, CU, and CD triaxial tests.
3. Sketch a typical triaxial cell with its basic components.
4. Define the B coefficient. What is it used for?
5. How is the rate of loading defined for CD triaxial tests?

Triaxial Tests on Coarse-Grained Soils

OBJECTIVE

There are two main types of triaxial tests for coarse-grained soils: CU and CD tests. CD tests are used to determine the cohesion and friction angle for various densities and confining pressures, while CU tests are used to calculate the undrained shear strength. UU triaxial tests are not performed on coarse-grained soils.

EQUIPMENT

The equipment for triaxial tests on coarse-grained soils includes:

- Loading frame with a 50 kN capacity (Fig. 1). Strain- or stress-controlled loading devices may be used to load the soil specimen. Strain-controlled devices compress the specimen at a predetermined rate of displacement, whereas stress-controlled devices vary the axial load at a fixed rate. Strain-controlled devices are preferable because they are capable of detecting the strain-softening properties of soils. Strain-controlled devices should have a loading speed of about 1 mm/min.
- Triaxial cell. As shown in Fig. 2, the triaxial cell consists primarily of a head plate, a baseplate, and a transparent plastic cylinder. The baseplate has an inlet to pressurize the chamber and two inlets to saturate and drain the specimen through its base and cap. The head plate has a vent valve to let air out when the chamber is filled with fluid. The cylinder, head plate, and baseplate are tightly held together by tie rods, and their joints are sealed with rubber gaskets. The piston friction is reduced using linear ball bushings. Leakage around the piston is reduced by means of O-rings. For cohesionless soils, the sample diameter is about 7.5 cm.
- Calibrated load ring for measuring the axial force. A capacity of 20 kN is suitable for most purposes. A larger capacity (e.g., 50 kN) may be required for high confining pressure. The load ring may be replaced by a load transducer of similar capacity.

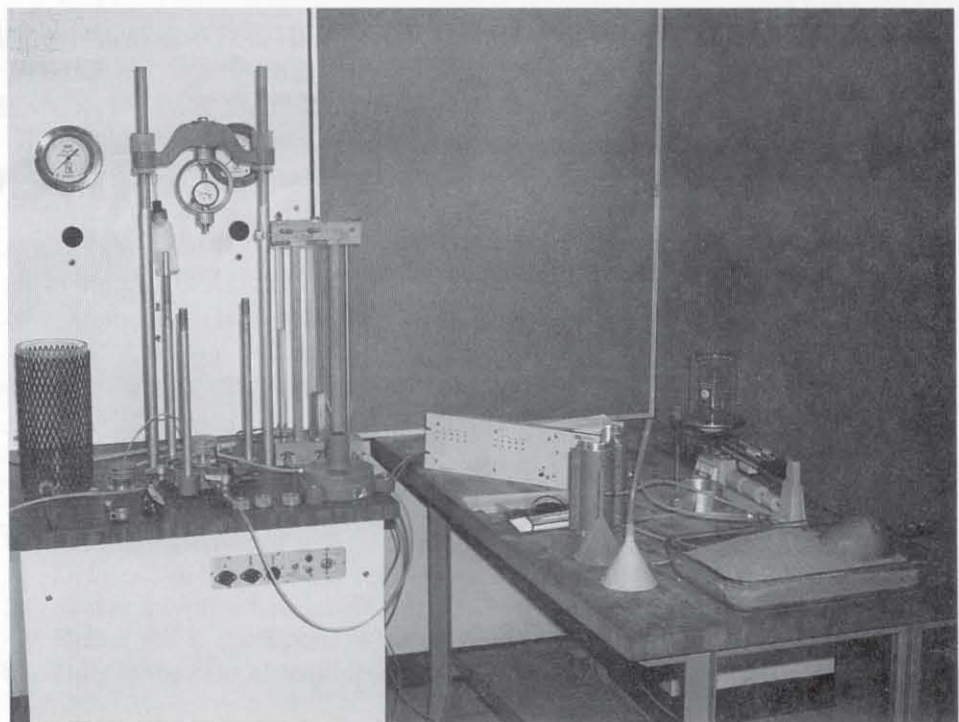


Figure 1 Loading frame device and triaxial test equipment. On the left table, the dismantled triaxial cell includes the upper and lower caps, the head plate, the base plate, and the transparent plastic cylinder reinforced with a steel mesh. On the left table, the equipment for the sample fabrication includes the split mold, membranes and O-rings, vacuum grease, funnels of various sizes, and a scale.

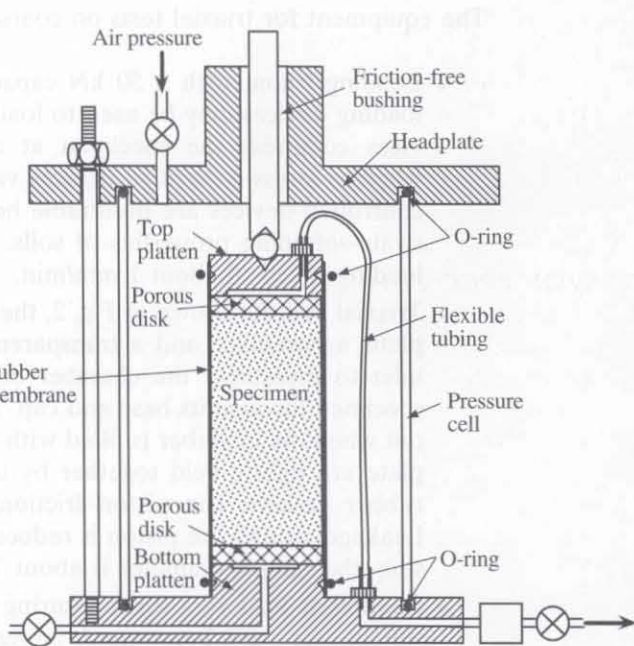


Figure 2 Components of the triaxial cell.

- Pressure transducer for measuring the pore pressure during CU tests. The transducer range should be 0 to 1000 kPa. It should have a bleed valve for saturation.
- Two pressure gages for measuring the confining pressure and backpressure, with a capacity of 1000 kPa.
- Dial gage for measuring the axial displacements sensitive to 0.01 mm and having a full range of 2.5 cm. The dial gage may be replaced by a calibrated LVDT transducer having similar range and sensitivity.
- Base and head caps. These are constructed of a lightweight noncorrosive material and have porous stones and drainage connections.
- Rubber sleeves. These encase the specimen and provide a reliable protection against leakage, with the minimum lateral restraint to the specimen. Membrane thickness ranges from 0.05 to 0.25 mm. They should be carefully inspected prior to use and should be discarded if they have flaws or pin-holes.
- Four O-rings of diameter slightly smaller than the base and head caps are required to fasten the membrane.
- Equipment for preparing specimens. A split mold is required to hold the rubber sleeve and construct cohesionless soils (see Fig. 4). The internal diameter of the mold (e.g., 7.5 cm) will give the approximate diameter of the specimen. A funnel or spoon for placing the material inside the mold, and a tamping hammer or vibratory equipment are also necessary.
- Saturation equipment. An air regulator and a pressure gage for controlling the backpressure, similar to those used to control the chamber pressure. A calibrated burette or standpipe capable of measuring volume changes. This burette, which is connected to the backpressure line, measures the volume change of the specimen during the isotropic and shear phases of the triaxial test.

Other items of equipment are as follows:

- Deaired water produced as in Chapter 4-2.
- Vacuum grease.
- Vacuum and air pressure supply.
- Balance sensitive to 0.01 g.
- Equipment necessary to determine specific gravity.

PREPARATION OF SPECIMENS

1. Weigh an amount of material slightly larger than the one to be used for the test specimen.
2. Place the membrane with two O-rings on the bottom platen, then assemble and mount the split mold. Fold back the membrane on the top rim of the mold as shown in Fig. 3.
3. Evacuate the air between the membrane and the membrane stretcher using a vacuum pump (see Fig. 3).
4. Pour the sand inside the forming jacket by means of a funnel or a spoon (see Fig. 4 and the sample construction in Chapter 4-2). The desired density may be achieved by vibrating the specimen. A specimen that is properly formed generally deforms in a symmetric way when it is tested.

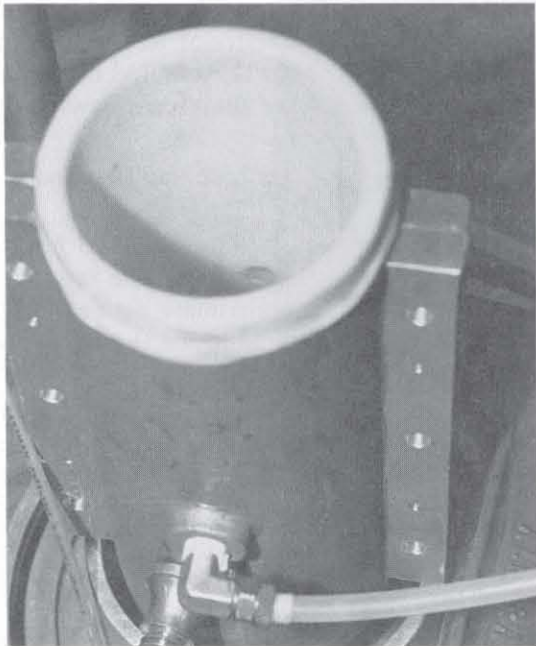


Figure 3 The split mold is mounted on the bottom cap. The membrane is stretched in place by applying vacuum.



Figure 4 Loose samples are constructed by pouring sand into the mold with a funnel. Denser samples are obtained by tamping or vibrating.

5. Weigh the unused material to calculate the dry sample weight.
6. After having filled the forming jacket with sand to the desired height, place the specimen cap on top of specimen, roll the membrane over the specimen cap and base, and fasten it with O-rings (see Fig. 5).
7. As shown in Fig. 6, open valve *D*, close valve *E*, and connect connector *I* to the vacuum line. This applies vacuum to the inside of the sample through valve *D*. If there is a leak or hole in the membrane, bubbles will keep forming in the bubble trap. If the leak is too important, the sample must be discarded and a new sample must be prepared. In the absence of bubbles, open and remove the split mold (see Fig. 7). The sample is now held together by an internal vacuum. Its initial height and diameter are now measured. The vacuum intensity should be kept to a small value (e.g., -20 kPa) to avoid the consolidation of the specimen.
8. Assemble the triaxial chamber (see Fig. 8) and place it on the loading device.
9. Disconnect connector *G* and open valve *F* to fill the triaxial cell with water (Fig. 9).

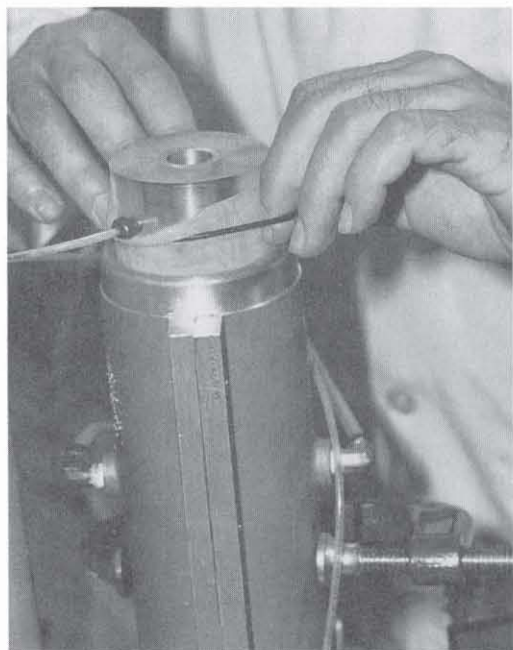


Figure 5 After placing the cap on top of the specimen, the membrane is rolled over the top cap and is fastened by using O-rings.

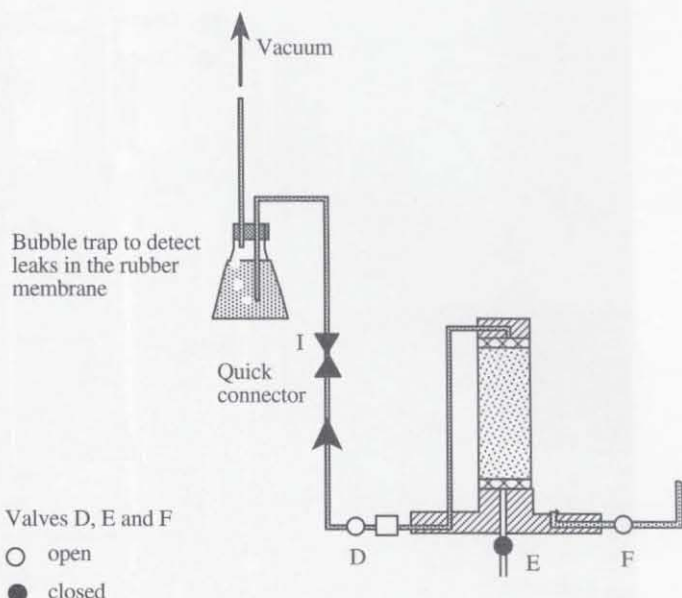


Figure 6 Application of vacuum inside the sample.



Figure 7 Once the vacuum is applied internally to the sample, the spilt mold is removed.

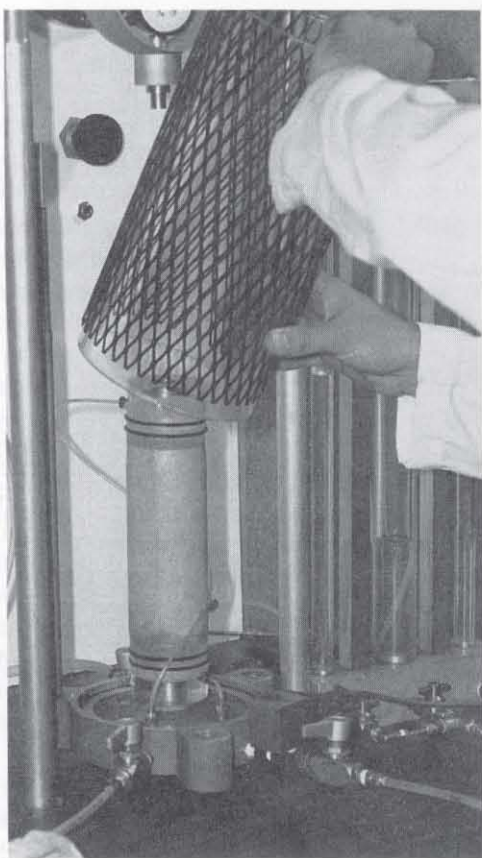


Figure 8 The triaxial cell is assembled by adding the transparent chamber and the top plate, and by securing the mounting bolts firmly.

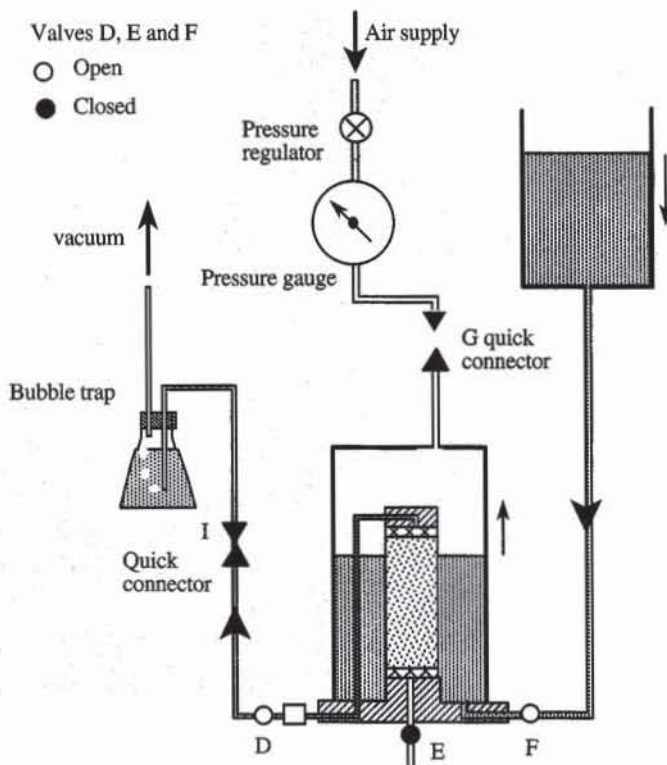


Figure 9 Filling of triaxial cell with water, and application of a small confining pressure to hold the sample together.

10. When the triaxial chamber is almost completely filled with water, close valve *F* and connect the *G* connector.

11. Apply a small amount of confining pressure with the pressure regulator (e.g., 20 kPa), then close valve *D*. At this stage the sample is held together by the external confining pressure, no longer by the internal vacuum.

SATURATION OF SPECIMENS

The triaxial samples for CU and CD triaxial tests must be fully saturated before being isotropically consolidated and sheared. The saturation is tested by closing the drainage system, by applying a small increase $\Delta\sigma_3$ in confining pressure, and by measuring the resulting change in pore pressure Δu . The sample is fully saturated when the coefficient $B = \Delta u/\Delta\sigma_3 = 1$, and partially saturated when $B < 1$.

For CU tests, complete saturation ($B \geq 99.5\%$) is required to generate a meaningful pore pressure. Otherwise, a partial saturation results in erroneous pore pressure and undrained shear strength. The degree of saturation can be increased by increasing the backpressure and confining pressure simultaneously so that the soil effective stress and differential pressure across the sample membrane do not change.

For CD tests, saturation is not as critical as for CU tests because it is used only to measure volume change. Partial saturation leads only to slightly underestimating the volume change. $B \geq 98\%$ is satisfactory for drained tests.

The drainage lines and porous disks should be fully saturated with deaired water. The drainage lines are as short as possible and made of thick-walled, small-

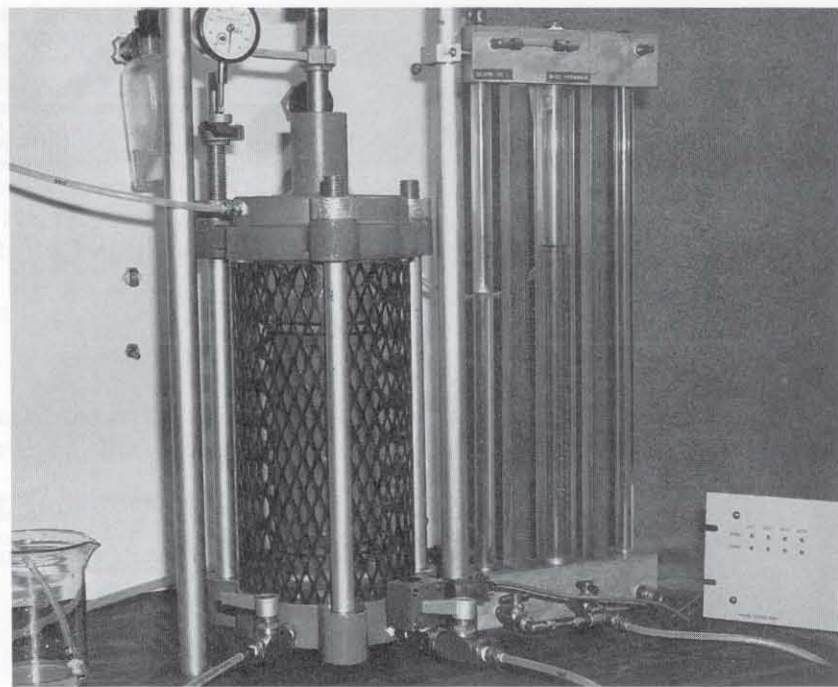


Figure 10 Triaxial cell and volume-change and saturation burette.

bore tubing to ensure minimum changes in volume when the applied pressure varies. During the saturation phase, the chamber pressure should be only slightly higher than the backpressure (e.g., 20 kPa) in order to hold the specimen without consolidating it. The specimen is saturated as follows:

1. Fill the saturation burette (Fig. 10) with deaired water. As shown in Fig. 11, disconnect connector *H*, close valve *B*, and open valve *A*. Close valve *A* when the saturation burette is almost full.
2. Open valves *E* and *D* and close valve *C*. Reconnect connector *H* to the backpressure line and apply 20 kPa of backpressure. Open valve *B*. As shown in Fig. 11, the water of the saturation burette is pushed through the soil specimen until there are no more air bubbles in the saturation line. If necessary, the saturation burette may be refilled with deaired water.
3. To check the saturation, close valves *B*, *D*, and *E*, increase the confining pressure by 10 kPa, measure the resulting increase in pore pressure Δu , and calculate the *B* coefficient. If its value is not satisfactory, repeat steps 1 and 2.
4. If the repetition of steps 1 and 2 does not increase the *B* coefficient, open valves *E* and *B* and apply equal increments of confining pressure and back-pressure simultaneously. Check the *B* coefficient again and if necessary, increase confining and backpressures within reasonable limits. The backpressure must always remain slightly smaller than the confining pressure: otherwise, the sample either consolidates or collapses. If the value of *B* is not satisfactory, repeat steps 2 to 4. One may also saturate the samples after the consolidation phase.
5. Open valve *A* to adjust the water level at the middle of the volume-change burette. Close valve *A*, open valves *C* and *E*, and record the level in the measuring burette. The saturation phase is now completed.

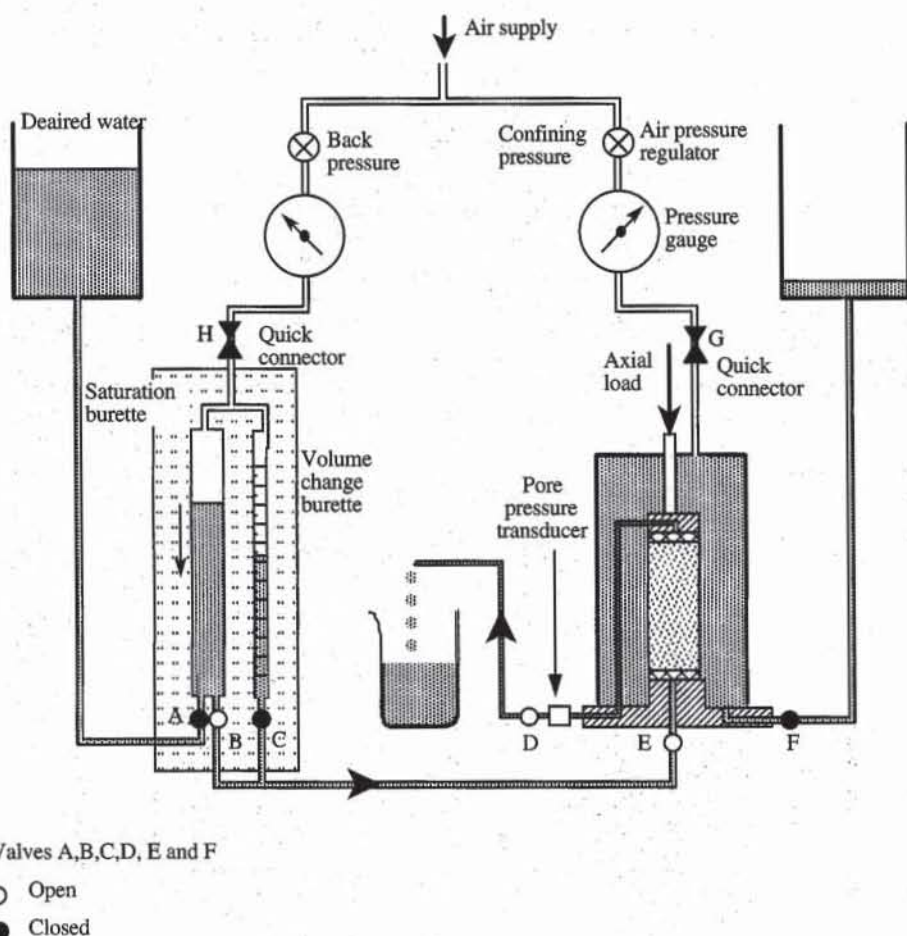


Figure 11 Schematic diagram showing the saturation of soil sample.

CONSOLIDATION PHASE

After saturation, the sample can be isotropically or K_0 consolidated.

For isotropic consolidation, keep the backpressure constant, and increase the cell pressure until the difference between the cell pressure and backpressure becomes equal to the desired confining pressure. Open valves C and E , and let the specimen consolidate under the applied confining pressure. Measure the volume change in the volume-change burette.

For K_0 consolidation, the vertical effective stress σ'_1 is increased with the radial effective stress σ'_3 to reach the initial effective stress state at which $\sigma'_1 = K_0 \sigma'_3$ where K_0 is the coefficient of earth pressure at rest. K_0 consolidation is not covered in this book. Additional information can be found in Head (1986).

SHEAR PHASE

For drained triaxial tests, valves B and D are closed and valves C and E are open. The volume change of the sample is measured in the volume-change burette. For undrained tests, valves D and E are closed and the pore pressure is measured using the pore pressure transducer.

1. Select a loading rate, about 0.5% of axial strain per minute.
2. Start loading and record simultaneously the applied axial load, piston displacement, and volume change for drained tests (porewater pressure for undrained tests).
3. After having completed the axial loading (20 to 25% axial strain), release the back pressure and decrease the confining pressure to 30 kPa. Open valve F to flush the pressure fluid gently from the pressure cell. Close valve F when the chamber is empty, remove the confining pressure, and then dismantle the triaxial cell.

COMPUTATIONS

Figure 12 shows the height, average area, and total volume of the sample after construction, after saturation, after consolidation, and during shear.

After Construction

The initial dry density γ_{d0} and void ratio e_0 of the sample are

$$\gamma_{d0} = \frac{W}{V_0} \quad \text{and} \quad e_0 = \frac{G_s \gamma_w}{\gamma_{d0}} - 1 \quad (1)$$

where W is the dry weight of the sample, $V_0 = H_0 A_0$ the initial sample volume, $A_0 = \pi D_0^2 / 4$ the average cross-sectional area of the initial sample, D_0 the initial diameter, G_s the soil specific gravity, and γ_w the water unit weight.

After Saturation

During the saturation phase, the sample size is assumed to be constant. There is no accurate way to measure its volume change while it is saturated. As shown in Fig. 12, the heights, average areas, and volumes of the samples are the same after construction and after saturation. As mentioned previously, the upward flow of interstitial water must be slow to prevent the sample from expanding or compacting while it is saturated.

After Consolidation

The volume V_c of the sample after the isotropic consolidation is

$$V_c = V_0 - \Delta V_c \quad (2)$$

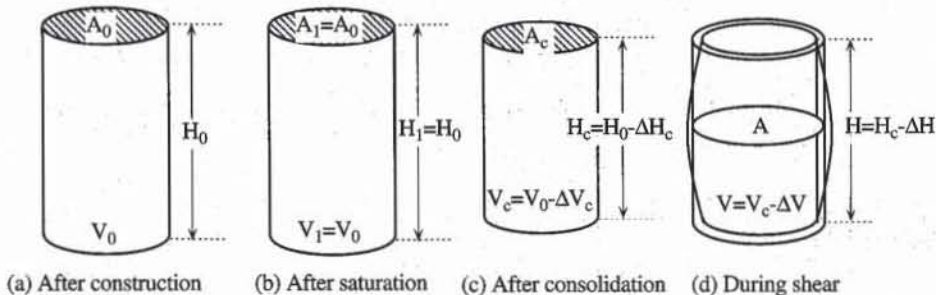


Figure 12 Height, average area, and volume of sample after the construction phase, saturation phase, and consolidation phase, and during the shear phase.

where ΔV_c is the volume change caused by consolidation and measured on the volume-change burette. The specimen height H_c and average area A_c after consolidation are calculated by assuming that axial and radial strains are equal:

$$H_c = H_0 \left(1 - \frac{1}{3} \frac{\Delta V_c}{V_0}\right) \quad \text{and} \quad A_c = \frac{V_c}{H_c} = A_0 \frac{1 - \Delta V_c/V_0}{1 - \Delta V_c/3V_0} \quad (3)$$

After consolidation, the dry unit weight γ_{dc} and void ratio e_c are

$$\gamma_{dc} = \frac{W}{V_c} \quad \text{and} \quad e_c = \frac{G_s \gamma_w}{\gamma_{dc}} - 1 \quad (4)$$

During Shear

During the shear phase, the volume V and height H of the specimen are

$$V = V_c - \Delta V \quad \text{and} \quad H = H_c - \Delta H \quad (5)$$

where ΔV is the volume change and ΔH is the height change. Both ΔV and ΔH are measured from the beginning of the shear phase. ΔV is positive when the sample compacts, and ΔH is positive when the sample shortens. The axial strain ε_1 and volumetric strain ε_v are

$$\varepsilon_1 = \frac{\Delta H}{H_c} \quad \text{and} \quad \varepsilon_v = \frac{\Delta V}{V_c} \quad (6)$$

The average cross-sectional area A of the sample is

$$A = \frac{V}{H} = \frac{V_c - \Delta V}{H_c - \Delta H} = \frac{V_c}{H_c} \frac{1 - \frac{\Delta V}{V_c}}{1 - \frac{\Delta H}{H_c}} = A_c \frac{1 - \varepsilon_v}{1 - \varepsilon_1} \quad (7)$$

The shear stress t and normal stress s are

$$t = \frac{1}{2} (\sigma_1 - \sigma_3) = \frac{P}{A} \quad \text{and} \quad s = \frac{1}{2} (\sigma_1 + \sigma_3) = t + \sigma_3 \quad (8)$$

where P is the net applied axial load, σ_1 the axial stress, and σ_3 the constant confining pressure. $P = 0$ at the beginning of the shear phase. During the drained test, total and effective stresses are equal because there is no pore pressure (i.e., $u = 0$):

$$s' = s \quad \text{and} \quad t' = t \quad (9)$$

Young's modulus is calculated from the initial slope of the $t - \varepsilon_1$ curve:

$$E = 2 \frac{\Delta t}{\Delta \varepsilon_1} \quad (10)$$

where Δt is the increase in t corresponding to the increase $\Delta \varepsilon_1$ in ε_1 . The Poisson ratio is calculated from the initial slope of the $\varepsilon_v - \varepsilon_1$ curve:

$$\nu = \frac{1}{2} \left(1 - \frac{\Delta \varepsilon_v}{\Delta \varepsilon_1}\right) \quad (11)$$

where $\Delta\epsilon_v$ is the increase in ϵ_v corresponding to $\Delta\epsilon_1$. The residual and peak friction angles are calculated using the following relation (assuming $c' = 0$):

$$\phi' = \sin^{-1} \left(\frac{\sigma'_1 - \sigma'_3}{\sigma'_1 + \sigma'_3} \right) = \sin^{-1} \left(\frac{t}{s'} \right) = \sin^{-1} \left(\frac{t}{t + \sigma_3 - u} \right) \quad (12)$$

During the undrained triaxial test ($\epsilon_v = 0$), Eq. 7 becomes

$$A = \frac{A_c}{1 - \epsilon_1} \quad (13)$$

The effective shear stress t' and normal stress s' are

$$s' = s - u, \quad \text{and} \quad t' = t \quad (14)$$

The shear modulus G is calculated from the initial slope of the $t - \epsilon_1$ curve:

$$G = \frac{1}{6} \frac{\Delta t}{\Delta \epsilon_1} \quad (15)$$

where Δt is the increase in t corresponding to $\Delta\epsilon_1$. The peak friction angle is calculated from the maximum ratio t'/s' by using the following relation:

$$\phi'_p = \sin^{-1} \left(\frac{t'}{s'} \right)_{\max} \quad (16)$$

Example of a Drained Triaxial Test

The results of the drained triaxial test are summarized by reporting the initial dry unit weight and void ratio of the specimen and by plotting the variation of shear stress t and volumetric strain ϵ_v versus axial strain ϵ_1 . The results should include the initial Young's modulus and Poisson ratio, the peak and residual friction angles, the failure modes of the specimen, and the inclination of shear bands, if any.

Figures 13 to 15 show an example of drained triaxial test results on a fine uniform sand in a loose state. Figure 13 shows the stress-strain and volumetric responses versus axial strain, Fig. 14 shows the input/output data, and Fig. 15 lists the formulas used in Fig. 14.

Example of a Undrained Triaxial Test

The results of the undrained triaxial test are summarized by reporting the initial dry unit weight and void ratio of the specimen and by plotting the variation of shear stress t and pore pressure u versus axial strain ϵ_1 , and the $s'-t$ stress path. The results should include the initial shear modulus, the peak and residual undrained shear strengths, the peak and residual friction angles ϕ'_p and ϕ'_r , the failure modes of the specimen, and the inclination of shear bands, if any.

Figures 16 to 18 show an example of undrained triaxial test results on a fine uniform sand in a loose state. Figure 16 shows the stress-strain and pore pressure responses versus axial strain, and the effective $s'-t$ stress path, Fig. 17 shows the input/output data, and Fig. 18 lists the formulas used in Fig. 17. As shown in Fig. 16, the loose sand undergoes a peak failure, softens, and then hardens as the pore pressure decreases. The residual undrained shear strength is larger than the peak undrained shear strength.

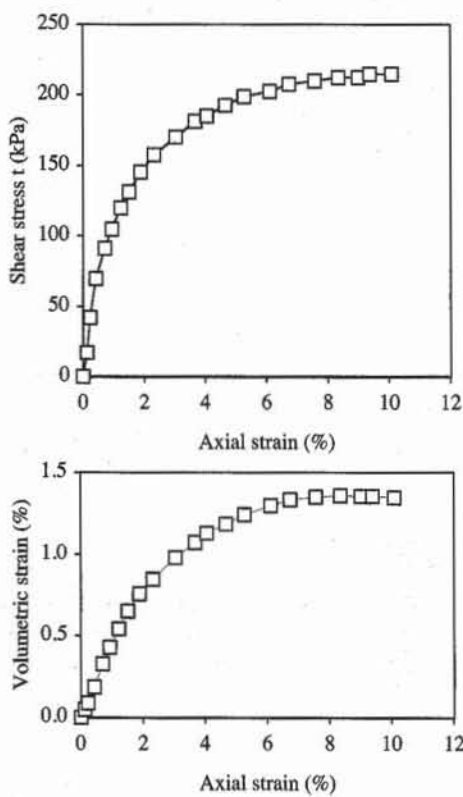


Figure 13 Stress-strain and volumetric responses of loose Hostun sand during drained triaxial test.

REVIEW QUESTIONS

1. Which soil properties are determined from CD and CU triaxial tests on coarse-grained sand?
2. Describe briefly the preparation of a sand specimen.
3. What is the purpose of the split mold?
4. Why do we use a rubber membrane in triaxial tests?
5. How is it possible to detect a small leak in a rubber membrane?
6. Why should the vacuum be kept to a low level during sample construction?
7. How is saturation checked in triaxial tests?
8. Why should the sample be saturated in CU and CD tests?
9. How is the corrected area defined in a CD triaxial test?

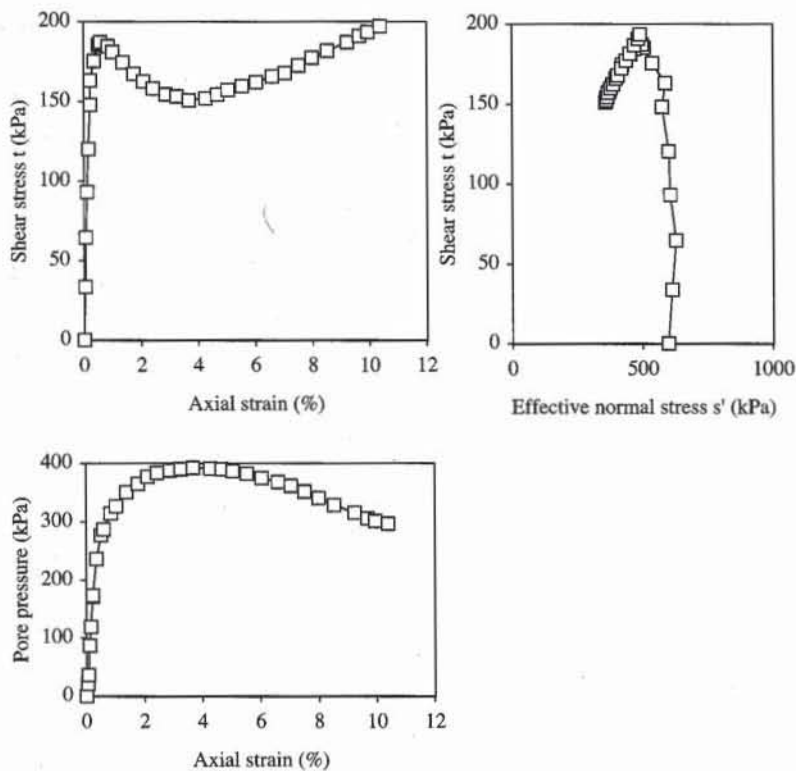
	A	B	C	D	E	F
1	Drained triaxial test					
2						
3						
4						
5						
6	Weight of dry sample W =	1164	g			
7	Initial height of sample h_0 =	19.5	cm			
8	Initial sample diameter D_0 =	6.95	cm			
9	Soil specific gravity G_s =	2.65				
10	Confining pressure σ_3 =	200	kPa			
11	Back pressure σ_b =	0	kPa			
12	Saturation coefficient B =	99	%			
13	Rate of loading v =	2	mm/min			
14	Initial void ratio e_0 =	0.684				
15	Initial dry unit weight γ_{d0} =	15.42	kN/m ³			
16	Volume change during consolidation ΔV_c =	1.00	cm ³			
17	Void ratio after consolidation e_c =	0.682				
18	Dry unit weight after consolidation γ_d =	15.44	kN/m ³			
19	Height after consolidation h_c =	19.49	cm			
20	Volume after consolidation V_c =	738.77	cm ³			
21	Area after consolidation A_c =	37.90	cm ²			
22	Initial Young's modulus E =	37.14	MPa			
23	Initial Poisson ratio v =	0.30				
24	Peak friction angle ϕ_p =	31.19	deg			
25	Residual friction angle ϕ_r =	31.19	deg			
26						
27	Axial displacement (mm)	Axial force (kN)	Volume change (cm ³)	Axial strain (%)	Shear stress (kPa)	Volumetric strain (%)
28	Δh	F	ΔV	eps	t	e_v
29	0.00	0.000	0.00	0.00	0.0	0.00
30	0.02	0.127	-0.36	0.12	16.8	0.05
31	0.04	0.319	-0.67	0.22	42.0	0.09
32	0.08	0.529	-1.36	0.43	69.6	0.18
33	0.14	0.692	-2.43	0.71	91.0	0.33
34	0.18	0.799	-3.17	0.94	104.8	0.43
35	0.24	0.915	-4.01	1.23	119.9	0.54
36	0.29	1.003	-4.82	1.51	131.2	0.65
37	0.37	1.112	-5.58	1.89	145.0	0.76
38	0.45	1.212	-6.24	2.33	157.6	0.84
39	0.59	1.317	-7.22	3.05	170.1	0.98
40	0.72	1.412	-7.91	3.67	181.4	1.07
41	0.79	1.446	-8.33	4.06	185.1	1.13
42	0.91	1.513	-8.76	4.67	192.6	1.19
43	1.03	1.571	-9.16	5.27	198.8	1.24
44	1.19	1.614	-9.59	6.12	202.6	1.30
45	1.32	1.665	-9.84	6.76	207.5	1.33
46	1.48	1.699	-9.97	7.58	210.0	1.35
47	1.63	1.733	-10.03	8.36	212.4	1.36
48	1.76	1.746	-10.01	9.02	212.4	1.36
49	1.83	1.774	-9.99	9.40	214.9	1.35
50	1.97	1.787	-9.95	10.10	214.8	1.35

Figure 14 Example of data set for drained triaxial test on sand.

	D	E	F
14	Initial void ratio $e_0 = =Gs*9.8/gd0-1$		
15	Initial dry unit weight $\gamma_{d0} = =W/(PI())^d0^2/4*h0)*9.8$	kN/m^3	
16	Volume change during consolidation $\Delta V_c = 1$	cm^3	
17	Void ratio after consolidation $e_c = =Gs*9.8/gd-1$		
18	Dry unit weight after consolidation $\gamma_d = =W/(PI())^d0^2/4*h0-DVc)*9.8$	kN/m^3	
19	Height after consolidation $h_c = =h0*(1-DVc/(h0*PI())^d0^2/4)/3$	cm	
20	Volume after consolidation $V_c = =h0*PI()^d0^2/4-DVc$	cm^3	
21	Area after consolidation $A_c = =Vc/hc$	cm^2	
22	Initial Young's modulus $E = =SLOPE(E29:E31,D29:D31)*2/10$	MPa	
23	Initial Poisson ratio $\nu = =(1-SLOPE(F29:F31,D29:D31))/2$		
24	Peak friction angle $\phi_p = =ASIN(MAX(q)/(MAX(q)+sc))*180/PI()$	deg	
25	Residual friction angle $\phi_r = =ASIN(E50/(E50+sc))*180/PI()$	deg	

	D	E	F
27	Axial strain (%)	Shear stress (kPa)	Volumetric strain (%)
28	eps	t	e_v
29	=Dh/hc*100	=F/Ac*(1-eps/100)/(1-ev/100)/2*10000	=-DV/Vc*100
30	=Dh/hc*100	=F/Ac*(1-eps/100)/(1-ev/100)/2*10000	=-DV/Vc*100

Figure 15 Formulas used in Fig. 14.

Figure 16 Stress-strain and pore pressure responses, and effective $s'-t$ stress path of loose Hostun sand during undrained triaxial test.

	A	B	C	D	E	F	G
1	Undrained triaxial test						
2	Analyst name: A. Comet Date: Apr-78						
3	Sample identification: Loose Hostun sand						
4	Weight of dry sample W =	1185 g					
5	Initial height of sample h_0 =	20.1 cm					
6	Initial sample diameter D_0 =	6.92 cm					
7	Soil specific gravity G_s =	2.65					
8	Confining pressure σ_3 =	600 kPa					
9	Back pressure σ_b =	0 kPa					
10	Saturation coefficient B =	99 %					
11	Rate of loading v =	2 mm/min					
12	Initial void ratio e_0 =	0.691					
13	Initial dry unit weight γ_{d0} =	15.36 kN/m ³					
14	Volume change during consolidation ΔV_c =	2.00 cm ³					
15	Void ratio after consolidation e_c =	0.686					
16	Dry unit weight after consolidation γ_d =	15.40 kN/m ³					
17	Height after consolidation h_c =	20.08 cm					
18	Volume after consolidation V_c =	753.96 cm ³					
19	Area after consolidation A_c =	37.54 cm ²					
20	Shear modulus G =	14.45 MPa					
21	Peak friction angle ϕ_p =	25.14 deg					
22	Residual friction angle ϕ_r =	23.20 deg					
23	Peak undrained shear strength S_u =	197.09 kPa					
24	Residual undrained shear strength S_{ur} =	197.09 kPa					
25							
26							
27							
28	Axial displacement (mm)	Axial force (kN)	Pore pressure (kPa)	Axial strain (%)	Shear stress (kPa)	Effective normal stress (kPa)	t/s'
29	Δh	F	u	eps	t	s'	ratio
30	0.00	0.000	0.00	0.00	0.0	600.0	0.00
31	0.01	0.252	20.80	0.04	33.6	612.8	0.05
32	0.01	0.486	36.29	0.07	64.6	628.3	0.10
33	0.02	0.700	87.26	0.12	93.1	605.8	0.15
34	0.03	0.905	118.72	0.15	120.3	601.6	0.20
35	0.04	1.114	171.12	0.22	148.0	576.9	0.26
36	0.04	1.228	173.14	0.22	163.2	590.1	0.28
37	0.07	1.323	236.03	0.35	175.6	539.6	0.33
38	0.10	1.399	276.99	0.52	185.3	508.3	0.36
39	0.12	1.413	286.83	0.59	187.0	500.2	0.37
40	0.17	1.397	314.12	0.85	184.5	470.4	0.39
41	0.20	1.373	326.23	1.01	181.0	454.8	0.40
42	0.28	1.329	350.02	1.38	174.5	424.5	0.41
43	0.36	1.280	364.59	1.77	167.4	402.8	0.42
44	0.42	1.245	376.39	2.10	162.3	385.9	0.42
45	0.49	1.215	383.18	2.44	157.9	374.7	0.42
46	0.58	1.194	387.56	2.88	154.5	366.9	0.42
47	0.66	1.188	390.58	3.26	153.1	362.5	0.42
48	0.74	1.177	391.76	3.69	151.0	359.2	0.42
49	0.86	1.194	391.00	4.29	152.2	361.2	0.42
50	0.94	1.216	389.66	4.88	154.4	364.7	0.42
51	1.01	1.243	387.17	5.05	157.2	370.0	0.42
52	1.11	1.270	381.83	5.55	159.8	377.9	0.42
53	1.22	1.297	374.22	6.05	162.2	388.0	0.42
54	1.33	1.333	367.74	6.61	165.7	398.0	0.42
55	1.42	1.355	360.89	7.06	167.7	406.8	0.41
56	1.51	1.401	351.01	7.53	172.5	421.5	0.41
57	1.61	1.446	340.13	8.00	177.2	437.1	0.41
58	1.72	1.492	328.77	8.54	181.7	453.0	0.40
59	1.86	1.546	315.49	9.24	186.9	471.4	0.40
60	1.95	1.588	305.09	9.69	191.0	485.9	0.39
61	2.00	1.615	301.25	9.97	193.7	492.4	0.39
62	2.09	1.652	296.85	10.40	197.1	500.2	0.39

Figure 17 Example of data set for undrained triaxial test on sand.

	D	E	F
14	Initial void ratio $e_0 = =Gs*9.8/gd0-1$		
15	Initial dry unit weight $\gamma_{d0} = =W/(PI()*D0^2/4*h0)*9.8$	kN/m ³	
16	Volume change during consolidation $\Delta V_c = 2$	cm ³	
17	Void ratio after consolidation $e_c = =Gs*9.8/gd-1$		
18	Dry unit weight after consolidation $\gamma_d = =W/(PI()*D0^2/4*h0-DVc)*9.8$	kN/m ³	
19	Height after consolidation $h_c = =h0*(1-DVc/(h0*PI()*D0^2/4))/3$	cm	
20	Volume after consolidation $V_c = =h0*PI()*D0^2/4-DVc$	cm ³	
21	Area after consolidation $A_c = =Vc/Hc$	cm ²	
22	Shear modulus G = =SLOPE(E30:E32,D30:D32)/6/10	MPa	
23	Peak friction angle $\phi_p = =ASIN(MAX(ratio)*180/PI())$	deg	
24	Residual friction angle $\phi_r = =ASIN(G62)*180/PI()$	deg	
25	Peak undrained shear strength $S_u = =MAX(q)$	kPa	
26	Residual undrained shear strength $S_{ur} = =E62$	kPa	

	D	E	F	G
28	Axial strain (%)	Shear stress (kPa)	Effective normal stress (kPa)	t/s'
29	eps	t	s'	ratio
30	=Dh/Hc*100	=F/Ac*(1-eps/100)*10000/2	=sc+q-u	=q/p
31	=Dh/Hc*100	=F/Ac*(1-eps/100)*10000/2	=sc+q-u	=q/p

Figure 18 Formulas used in Fig. 17.

EXERCISES

- From elasticity theory, derive the relation between Young's modulus E and the Poisson ratio ν and the initial slopes of the $t-\epsilon_1$ and $\epsilon_v-\epsilon_1$ curves for CD triaxial tests.
- From elasticity theory, derive the relation between shear modulus G and the initial slope of the $t-\epsilon_1$ curve for CU triaxial tests.

7-8 Triaxial Tests on Fine-Grained Soils

OBJECTIVE

There are three different types of triaxial tests for fine-grained soils: UU, CU, and CD tests. The CD tests are used to determine the friction angle for various densities and confining pressures, while UU and CU tests are used to define the undrained shear strength.

EQUIPMENT

The equipment for fine-grained soils is similar to that of coarse-grained soils described in Chapter 7-7. The differences are

- Loading devices. For CU and UU tests, the loading rate is about 0.05 to 2 mm/min. For CD tests, the loading speed should cover a wider range (i.e., 1 to 0.0005 mm/min).
- Triaxial cell. Smaller than for cohesionless soils. The sample diameter is about 2.5 to 3 cm.
- Membrane stretcher (Fig. 1).
- Trimming equipment similar to that used for the unconfined compression test.

PREPARATION OF SPECIMENS

The test specimen is trimmed into a cylinder as described in Chapter 7-3. As shown in Fig. 1a, two O-rings are mounted on the suction membrane stretcher, and the rubber membrane is placed as shown in Fig. 1b. The rubber membrane is drawn tightly to the membrane by applying suction (Fig. 1c) and is lowered around the soil sample (Fig. 1d). When the membrane stretcher is at the position shown in Fig. 1d, the suction is released so that the membrane sticks to the spec-

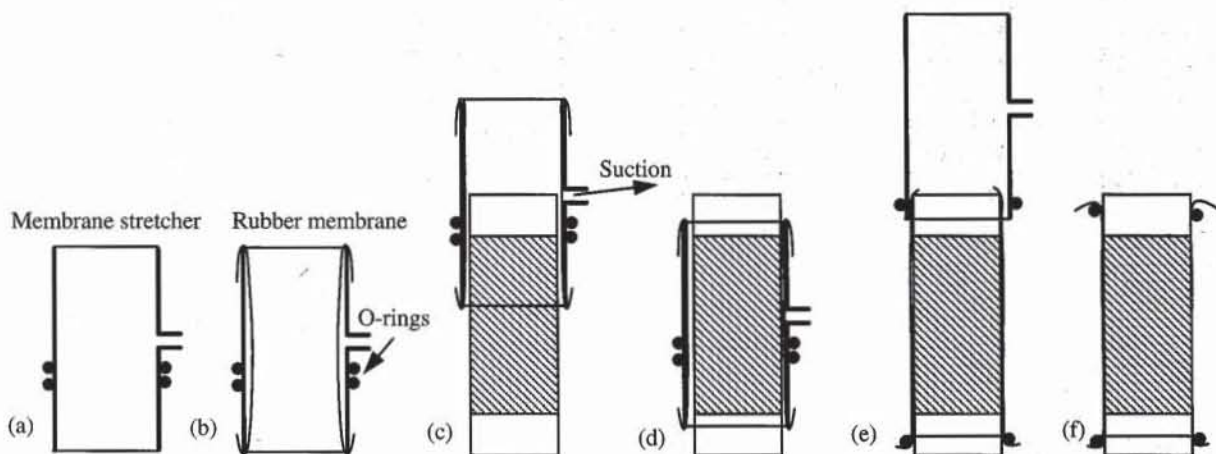


Figure 1 Successive stages to fit the rubber membrane to the cylindrical soil specimen.

imen. The membrane is rolled on the head and base caps and fastened on the base cap with an O-ring (Fig. 1e). The membrane stretcher is removed and the upper O-ring positioned on the head plate.

SATURATION OF SPECIMENS

The triaxial samples for UU, CU, and CD triaxial tests must be fully saturated before being isotropically consolidated and sheared. The saturation phase of fine-grained soils is simpler than that of coarse-grained soils, provided that the specimens were initially saturated and remain saturated during trimming. The saturation of partially saturated specimens may be extremely tedious otherwise. The saturation is checked as for cohesionless soils, by calculating the B coefficient from an isotropic increment. For CU tests, $B \geq 99.5\%$ is required to generate meaningful pore pressure. For CD and UU tests, the saturation is not as critical as for CU tests. $B > 98\%$ is considered satisfactory for drained tests.

UU, CU AND CD TRIAXIAL TESTS

The consolidation and shear phases of the CU and CD tests for fine-grained soils are similar to those of coarse-grained soils. In UU tests, the consolidation phase is performed rapidly, with closed rather than opened drainage. The pore pressure is generally not recorded during UU tests.

EXAMPLE

The results of CU tests are summarized by reporting the initial dry unit weight, water content, and void ratio of the specimen, and by plotting the variation of shear stress t and pore pressure u versus axial strain ϵ_1 , and the $s'-t$ stress path. The results should include the initial shear modulus, the peak and residual undrained shear strengths, the failure modes of the specimen, and the inclination of shear bands, if any. The results of UU tests are reported as those of CU tests but without the pore pressure variation and effective stress paths. The results of CD tests are reported as those for coarse-grained soils.

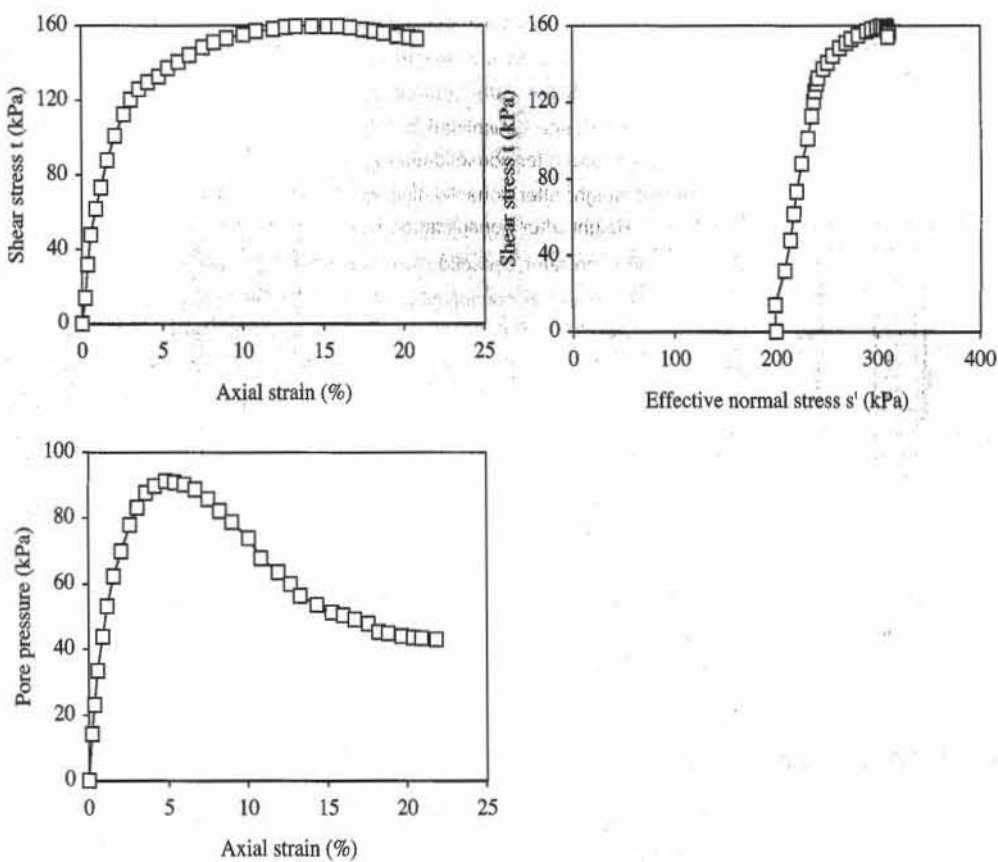


Figure 2 Stress-strain response, pore pressure response, and effective stress path of kaolinite during CU triaxial test.

Figures 2 to 4 show an example of CU triaxial test results on a normally consolidated clay. Figure 2 shows the stress-strain response, pore pressure response, and effective $s'-t$ stress path, Fig. 3 shows the input/output data, and Fig. 4 lists the formulas used in Fig. 3.

	A	B	C	D	E	F	G
12		Saturation coefficient B =	99 %				
13		Rate of loading v =	0.5 mm/min				
14		Initial void ratio e_0 =	0.696				
15		Initial wet density γ_0 =	19.30 kN/m ³				
16		Initial dry unit weight γ_{d0} =	15.37 kN/m ³				
17		Initial water content w_0 =	25.55%				
18		Volume change during consolidation ΔV_c =	0.40 cm ³				
19		Void ratio after consolidation e_c =	0.686				
20		Dry unit weight after consolidation γ_d =	15.46 kN/m ³				
21		Height after consolidation h_c =	7.09 cm				
22		Volume after consolidation V_c =	65.97 cm ³				
23		Area after consolidation A_c =	9.31 cm ²				
24		Shear modulus G =	1.49 MPa				
25		Peak friction angle ϕ_p =	34.41 deg				
26		Residual friction angle ϕ_r =	29.43 deg				
27		Peak undrained shear strength S_u =	159.80 kPa				
28		Residual undrained shear strength S_{ur} =	151.55 kPa				
29							
30	Axial displacement (mm)	Axial force (kN)	Pore pressure (kPa)	Axial strain (%)	Shear stress (kPa)	Effective normal stress (kPa)	t/s'
31	Δh	F	u	eps	t	s'	ratio
32	0.00	0.000	0.0	0.00	0.0	200.0	0.00
33	0.01	0.026	14.1	0.18	13.8	199.7	0.07
34	0.03	0.059	23.0	0.35	31.7	208.7	0.15
35	0.04	0.089	33.4	0.57	47.7	214.3	0.22
36	0.06	0.116	43.9	0.87	61.7	217.8	0.28
37	0.08	0.138	53.2	1.18	73.4	220.3	0.33
38	0.11	0.166	62.3	1.58	87.8	225.5	0.39
39	0.15	0.192	69.9	2.08	100.8	230.9	0.44
40	0.19	0.215	78.1	2.64	112.7	234.6	0.48
41	0.22	0.231	83.3	3.07	120.2	236.9	0.51
42	0.25	0.243	87.8	3.59	125.8	238.0	0.53
43	0.30	0.252	89.9	4.17	129.7	239.9	0.54
44	0.34	0.259	91.3	4.84	132.6	241.3	0.55
45	0.38	0.270	90.9	5.40	137.3	246.4	0.56
46	0.43	0.279	90.2	6.04	140.7	250.5	0.56
47	0.48	0.288	88.8	6.72	144.3	255.5	0.56
48	0.54	0.299	85.7	7.54	148.5	262.8	0.57
49	0.59	0.306	82.1	8.24	151.0	268.9	0.56
50	0.64	0.313	78.8	9.02	153.1	274.3	0.56
51	0.71	0.321	73.9	10.06	155.0	281.1	0.55
52	0.77	0.328	67.8	10.85	156.9	289.1	0.54
53	0.85	0.334	63.6	11.95	158.1	294.4	0.54
54	0.90	0.339	59.9	12.71	159.1	299.2	0.53
55	0.95	0.343	56.4	13.33	159.5	303.0	0.53
56	1.02	0.347	53.7	14.35	159.4	305.8	0.52
57	1.09	0.351	51.2	15.29	159.8	308.6	0.52
58	1.13	0.353	50.4	15.97	159.5	309.1	0.52
59	1.19	0.355	49.2	16.72	158.7	309.5	0.51
60	1.25	0.356	47.8	17.54	157.6	309.8	0.51
61	1.29	0.357	45.4	18.20	157.0	311.7	0.50
62	1.33	0.358	44.9	18.79	156.0	311.1	0.50
63	1.40	0.358	44.0	19.67	154.3	310.2	0.50
64	1.45	0.359	43.7	20.37	153.6	309.9	0.50
65	1.48	0.360	43.5	20.91	152.9	309.4	0.49
66	1.55	0.361	43.1	21.86	151.6	308.5	0.49

Figure 3 Example of data set for CU triaxial test on clay.

	C	D	E
14	Initial void ratio $e_0 = =Gs*9.8/gd0-1$		
15	Initial wet density $\gamma_0 = =Ww/(PI()*D0^2/4*h0)*9.8$	kN/m ³	
16	Initial dry unit weight $\gamma_{d0} = =Wd/(PI()*D0^2/4*h0)*9.8$	kN/m ³	
17	Initial water content $w_0 = =(Ww-Wd)/Wd$		
18	Volume change during consolidation $\Delta V_c = 0.4$	cm ³	
19	Void ratio after consolidation $e_c = =Gs*9.8/gd-1$		
20	Dry unit weight after consolidation $\gamma_d = =Wd/(PI()*D0^2/4*h0-DVc)*9.8$	kN/m ³	
21	Height after consolidation $h_c = =h0*(1-DVc/(h0*PI()*D0^2/4)/3)$	cm	
22	Volume after consolidation $V_c = =h0*PI()*D0^2/4-DVc$	cm ³	
23	Area after consolidation $A_c = =Vc/hc$	cm ²	
24	Shear modulus G = =SLOPE(E32:E34,D32:D34)/6/10	MPa	
25	Peak friction angle $\phi_p = =ASIN(MAX(G32:G66))*180/PI()$	deg	
26	Residual friction angle $\phi_r = =ASIN(G66)*180/PI()$	deg	
27	Peak undrained shear strength $S_u = =MAX(E32:E66)$	kPa	
28	Residual undrained shear strength $S_{ur} = =E66$	kPa	

	D	E	F	G
30	Axial strain (%)	Shear stress (kPa)	Effective normal stress (kPa)	t/s'
31	eps	t	s'	ratio
32	=Dh/h0*100	=F/Ac*(1-eps/100)*10000/2	=sc+q-u	=q/p
33	=Dh/h0*100	=F/Ac*(1-eps/100)*10000/2	=sc+q-u	=q/p

Figure 4 Formulas used in Fig. 3.

8

Elements of Experimental Techniques

-
- 8-1** Review of data modeling
 - 8-2** Review of statistics
 - 8-3** Error analysis
 - 8-4** Dimensions and units
 - 8-5** Report writing

Review of Data Modeling

INTRODUCTION

The modeling of data is a common exercise in engineering and science. It consists of determining the parameters of theoretical relations that give the best agreement between theoretical and experimental results. Four methods are presented here: linear regression, polynomial regression, interpolation, and nonlinear optimization.

LINEAR REGRESSION

Linear regression finds the straight line that best fits a set of data points, thus providing a linear relationship between two variables. Linear regression consists of fitting a set of n data points (x_i, y_i) to the straight-line model

$$y = Ax + B \quad (1)$$

where A is the slope and B is the intercept of the straight line with the y axis. The accuracy of fit between the straight line and data points can be evaluated by defining the total deviation E , which is the sum of the squared distances between data points and fitted points:

$$E = \sum_{i=1}^n (Ax_i + B - y_i)^2 \quad (2)$$

The best fit is obtained when E is minimum, that is, when

$$\frac{\partial E}{\partial A} = 0 \quad \text{and} \quad \frac{\partial E}{\partial B} = 0 \quad (3)$$

Equations 2 and 3 imply that

$$\frac{\partial E}{\partial A} = 2 \sum_{i=1}^n x_i (Ax_i + B - y_i) = 0 \quad \text{and} \quad \frac{\partial E}{\partial B} = 2 \sum_{i=1}^n (Ax_i + B - y_i) = 0 \quad (4)$$

Equation 4 is a system of two linear equations with two unknowns, A and B :

$$\begin{aligned} A \sum_{i=1}^n x_i^2 + B \sum_{i=1}^n x_i &= \sum_{i=1}^n x_i y_i \\ A \sum_{i=1}^n x_i + B n &= \sum_{i=1}^n y_i \end{aligned} \quad (5)$$

The values of A and B are

$$A = \frac{n \sum_{i=1}^n x_i y_i - \sum_{i=1}^n x_i \sum_{i=1}^n y_i}{n \sum_{i=1}^n x_i^2 - \left(\sum_{i=1}^n x_i \right)^2} \quad \text{and} \quad B = \frac{\sum_{i=1}^n y_i \sum_{i=1}^n x_i^2 - \sum_{i=1}^n x_i \sum_{i=1}^n x_i y_i}{n \sum_{i=1}^n x_i^2 - \left(\sum_{i=1}^n x_i \right)^2} \quad (6)$$

In Excel, linear regression is carried out by using the built-in functions SLOPE, INTERCEPT, and LINEST.

POLYNOMIAL REGRESSION

Linear regression analysis is generalized to nonlinear regression by using polynomials of order m :

$$P(x) = a_m x^m + a_{m-1} x^{m-1} + \cdots + a_1 x + a_0 \quad (7)$$

where the $m + 1$ coefficients a_m, a_{m-1}, \dots, a_1 , and a_0 define a polynomial of order m . Equation 7 may also be written

$$P(x) = \sum_{j=0}^m a_j x^j \quad (8)$$

Polynomial regression consists of fitting a set of n data points (x_i, y_i) to a polynomial model. Linear regression is a particular polynomial regression corresponding to $m = 1, A = a_1$, and $B = a_0$. The accuracy of the fit between the polynomial line and data points is evaluated by the sum E of the squared distances between data points and fitted points:

$$E = \sum_{i=1}^n [P(x_i) - y_i]^2 \quad (9)$$

The best fit is obtained when E is minimum, that is, when the following $m + 1$ equations are satisfied:

$$\frac{\partial E}{\partial a_j} = 0 \quad \text{for } j = 0, 1, \dots, m \quad (10)$$

Equation 10 implies that

$$\sum_{i=1}^n [P(x_i) - y_i] \frac{\partial P(x_i)}{\partial a_j} = 0 \quad \text{for } j = 0, 1, \dots, m \quad (11)$$

Equation 11 becomes, after some algebraic manipulations:

$$\sum_{k=0}^m \sum_{i=1}^n x_i^{k+j} a_k = \sum_{i=1}^n y_i x_i^j \quad \text{for } j = 0, 1, \dots, m \quad (12)$$

Equation 12 can also be written

$$\sum_{k=0}^m G_{jk} a_k = H_j \quad \text{for } j = 0, 1, \dots, m \quad (13)$$

where $G_{jk} = \sum_{i=1}^n x_i^{k+j}$ and $H_j = \sum_{i=1}^n y_i x_i^j$. By using a matrix notation, Eq. 13 becomes

$$\mathbf{GA} = \mathbf{H} \quad (14)$$

The polynomial coefficients are therefore

$$\mathbf{A} = \mathbf{G}^{-1} \mathbf{H} \quad (15)$$

where \mathbf{G}^{-1} is the inverse matrix of \mathbf{G} , and $A_j = a_j$. For a quadratic polynomial,

$$\mathbf{A} = \begin{pmatrix} a_0 \\ a_1 \\ a_2 \end{pmatrix}, \quad \mathbf{G} = \begin{pmatrix} n & \sum_{i=1}^n x_i & \sum_{i=1}^n x_i^2 \\ \sum_{i=1}^n x_i & \sum_{i=1}^n x_i^2 & \sum_{i=1}^n x_i^3 \\ \sum_{i=1}^n x_i^2 & \sum_{i=1}^n x_i^3 & \sum_{i=1}^n x_i^4 \end{pmatrix}, \quad \text{and} \quad \mathbf{H} = \begin{pmatrix} \sum_{i=1}^n y_i \\ \sum_{i=1}^n x_i y_i \\ \sum_{i=1}^n x_i^2 y_i \end{pmatrix} \quad (16)$$

and for a cubic polynomial,

$$\mathbf{A} = \begin{pmatrix} a_0 \\ a_1 \\ a_2 \\ a_3 \end{pmatrix}, \quad \mathbf{G} = \begin{pmatrix} n & \sum_{i=1}^n x_i & \sum_{i=1}^n x_i^2 & \sum_{i=1}^n x_i^3 \\ \sum_{i=1}^n x_i & \sum_{i=1}^n x_i^2 & \sum_{i=1}^n x_i^3 & \sum_{i=1}^n x_i^4 \\ \sum_{i=1}^n x_i^2 & \sum_{i=1}^n x_i^3 & \sum_{i=1}^n x_i^4 & \sum_{i=1}^n x_i^5 \\ \sum_{i=1}^n x_i^3 & \sum_{i=1}^n x_i^4 & \sum_{i=1}^n x_i^5 & \sum_{i=1}^n x_i^6 \end{pmatrix}, \quad \text{and} \quad \mathbf{H} = \begin{pmatrix} \sum_{i=1}^n y_i \\ \sum_{i=1}^n x_i y_i \\ \sum_{i=1}^n x_i^2 y_i \\ \sum_{i=1}^n x_i^3 y_i \end{pmatrix} \quad (17)$$

Besides E , the R^2 values are used to measure the quality of fitting:

$$R^2 = 1 - \frac{\sum_{i=1}^n [y_i - P(x_i)]^2}{\sum_{i=1}^n y_i^2 - \frac{1}{n} \left(\sum_{i=1}^n y_i \right)^2} \quad (18)$$

R^2 varies from 0 to 1, the best fitting corresponding to $R^2 = 1$.

EXAMPLE OF REGRESSION USING BUILT-IN AND USER-DEFINED FUNCTIONS

Figure 1 shows a series of data points. The x coordinate is the temperature, and the y coordinate is the water unit mass. In Excel, regression analysis may be performed by using built-in functions or user-defined functions.

Figure 2 shows the linear, quadratic, and cubic fits of the data points of Fig. 1, which were obtained by using the built-in function Trendline. Trendline is based on Eqs. 1 to 18. The optimum regression coefficients and the R^2 values are also shown in Fig. 2. The quadratic and cubic regressions fit data better than the linear regression. In Fig. 2, their fitted results are so similar that they can only be distinguished by their R^2 values, which indicate a small advantage for the cubic regression.

	A	B
1	Temperature ('C)	Unit mass (g/cm ³)
2	x	y
3	4	1.00000
4	16	0.99897
5	17	0.99880
6	18	0.99862
7	19	0.99844
8	20	0.99823
9	21	0.99802
10	22	0.99780
11	23	0.99757
12	24	0.99733
13	25	0.99708
14	26	0.99682
15	27	0.99655
16	28	0.99627
17	29	0.99598
18	30	0.99568

Figure 1 Example of series of data point for regression analysis.

The calculations of linear, quadratic, and cubic regression analysis are detailed in the user-defined functions FIT1, FIT2, and FIT3 of Fig. 3. The arrays X and Y represent the cell ranges containing the x and y data, respectively. The coefficients of \mathbf{G} and \mathbf{H} are calculated using the built-in functions COUNT, SUM, and SUMPRODUCT; then

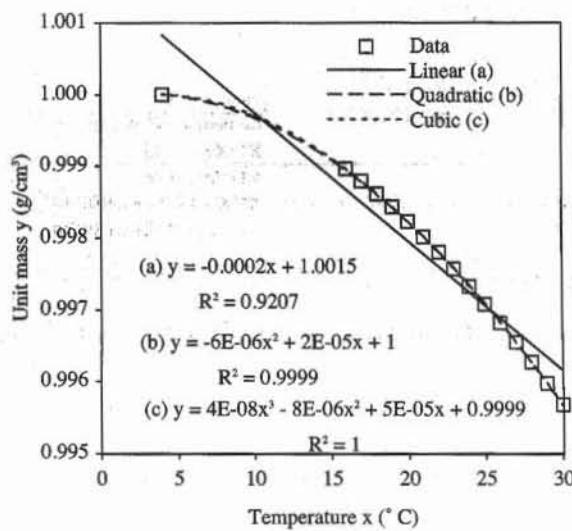


Figure 2 Regression analysis with Trendline.

$$n = \text{COUNT}(X), \sum_{i=1}^n x_i = \text{SUM}(X), \sum_{i=1}^n x_i^2 = \text{SUMPRODUCT}(X, X), \quad (19)$$

$$\sum_{i=1}^n x_i y_i = \text{SUMPRODUCT}(X, Y), \text{ and } \sum_{i=1}^n x_i^2 y_i = \text{SUMPRODUCT}(X, X, Y), \text{ etc.}$$

The matrix \mathbf{G} is inverted using the built-in function MINVERSE, and \mathbf{G}^{-1} and \mathbf{H} are multiplied using MMULT. Figure 4 shows the coefficients calculated using FIT1, FIT2, and FIT3, and Fig. 5 shows the formulas of Fig. 4. FIT1, FIT2, and FIT3 determine exactly the same coefficients as Trendline.

INTERPOLATION

In some engineering calculations, it is only necessary to interpolate a set of tabulated data, without the need for a regression analysis. The problem is to find y corresponding to a known value x , based on n tabulated data points (x_i, y_i) , where x_i either continuously increases (i.e., $x_1 \leq x_2 \leq \dots \leq x_{n-1} \leq x_n$) or decreases (i.e., $x_1 \geq x_2 \geq \dots \geq x_{n-1} \geq x_n$). The linearly interpolated value of y corresponding to x is

$$y = y_i + \frac{y_{i+1} - y_i}{x_{i+1} - x_i} (x - x_i) \quad \text{if } (x - x_i)(x - x_{i+1}) \leq 0 \quad \text{and } x_i \neq x_{i+1} \quad (20)$$

In some instances, such as the determination of grain size corresponding to 10% by weight finer on a grain size distribution curve, the linear interpolation is carried out on a semilogarithmic graph having a logarithmic y axis. In this case, referred to as semilog interpolation, Eq. 20 becomes

	A	B	C	D
1	FIT1	Name of function		
2	=RESULT(64)	Result of function is an array		
3	=ARGUMENT("X",64)	Input X-array		
4	=ARGUMENT("Y",64)	Input Y-array		
5	=COUNT(X)	n= number of element in X and Y		
6	=SUM(X)	X1+X2+...+Xn		
7	=SUM(Y)	Y1+Y2+...+Yn		
8	=SUMPRODUCT(X,X)	X1*X1+X2*X2+...+Xn*Xn		
9	=SUMPRODUCT(X,Y)	X1*Y1+X2*Y2+...+Xn*Yn		
10	=A5*A8-A6*A6			
11	=IF(A10=0,RETURN("ERR"))			
12	=(A7*A8-A6*A9)/A10			
13	=(A5*A9-A6*A7)/A10			
14	=RETURN(A12:A13)			
15				
16	FIT2	Fit quadratic polynomial by linear regression		
17	=RESULT(64)	Input X-array		
18	=ARGUMENT("X",64)	Input Y-array		
19	=ARGUMENT("Y",64)			Space for vector
20	=COUNT(X)	349	8231	15.96216
21	=SUM(X)	8231	201889	348.06384
22	=SUMPRODUCT(X,X)	201889	5095943	8207.227
23	=SET.VALUE(B20,A21)	Form matrix		
24	=SET.VALUE(C20,A22)			
25	=SET.VALUE(B21,A22)			
26	=SET.VALUE(C21,SUMPRODUCT(X,X,X))			
27	=SET.VALUE(B22,C21)			
28	=SET.VALUE(C22,SUMPRODUCT(X,X,X,X))			
29	=SET.VALUE(D20,SUM(Y))	Form vector		
30	=SET.VALUE(D21,SUMPRODUCT(X,Y))			
31	=SET.VALUE(D22,SUMPRODUCT(X,X,Y))			
32	=RETURN(MMULT(MINVERSE(A20:C22),D20:D22))			

	A	B	C	D	E
34	FIT3	Fit cubic polynomial by linear regression			
35	=RESULT(64)	Input X-array			
36	=ARGUMENT("X",64)	Input Y-array			
37	=ARGUMENT("Y",64)				Space for vector
38	=COUNT(X)	349	8231	201889	15.96216
39	=SUM(X)	8231	201889	5095943	348.06384
40	=SUMPRODUCT(X,X)	201889	5095943	131689249	8207.227
41	=SUMPRODUCT(X,X,X)	5095943	131689249	3470452391	201271.75128
42	=SET.VALUE(B38,A39)	Form matrix			
43	=SET.VALUE(C38,A40)				
44	=SET.VALUE(D38,A41)				
45	=SET.VALUE(B39,A40)				
46	=SET.VALUE(C39,A41)				
47	=SET.VALUE(D39,SUMPRODUCT(X,X,X,X))				
48	=SET.VALUE(B40,A41)				
49	=SET.VALUE(C40,D39)				
50	=SET.VALUE(D40,SUMPRODUCT(X,X,X,X,X))				
51	=SET.VALUE(B41,D39)				
52	=SET.VALUE(C41,D40)				
53	=SET.VALUE(D41,SUMPRODUCT(X,X,X,X,X,X))				
54	=SET.VALUE(E38,SUM(Y))	Form vector			
55	=SET.VALUE(E39,SUMPRODUCT(X,Y))				
56	=SET.VALUE(E40,SUMPRODUCT(X,X,Y))				
57	=SET.VALUE(E41,SUMPRODUCT(X,X,X,Y))				
58	=RETURN(MMULT(MINVERSE(A38:D41),E38:E41))				

Figure 3 User-defined functions for linear (FIT1), quadratic (FIT2), and cubic (FIT3) regressions.

	A	B	C	D
20		FIT1	FIT2	FIT3
21	a_0	1.001542072	1.000000202	0.999910033
22	a_1	-0.000179121	2.43481E-05	5.20192E-05
23	a_2		-5.63002E-06	-7.51229E-06
24	a_3			3.60518E-08

Figure 4 Results of regression analysis with FIT1, FIT2, and FIT3.

	A	B	C	D
20		FIT1	FIT2	FIT3
21	a_0	=FIT1(x,y)	=FIT2(x,y)	=FIT3(x,y)
22	a_1	=FIT1(x,y)	=FIT2(x,y)	=FIT3(x,y)
23	a_2		=FIT2(x,y)	=FIT3(x,y)
24	a_3			=FIT3(x,y)

Figure 5 Formulas used in Fig. 4.

$$\ln(y) = \ln(y_i) + \frac{\ln(y_{i+1}) - \ln(y_i)}{x_{i+1} - x_i} (x - x_i)$$

if $(x - x_i)(x - x_{i+1}) \leq 0$ and $x_i \neq x_{i+1}$ (21)

Equation 21 can also be written

$$\ln \frac{y}{y_i} = \frac{x - x_i}{x_{i+1} - x_i} \ln \frac{y_{i+1}}{y_i} \quad (22)$$

or equivalently,

$$y = y_i \left(\frac{y_{i+1}}{y_i} \right)^{(x-x_i)/(x_{i+1}-x_i)} \quad (23)$$

EXAMPLE OF INTERPOLATION

In Table 1 there are seven data points. The x component is the grain size, and the y component is the percent finer. In Fig. 6, the data are plotted using semilog axes. The problem is to find the grain size D_{30} corresponding to 30 percent finer. The solution is given in Table 1, and the EXCEL formulas are given in Fig. 7. The user-defined functions INTERL and INTER that perform the linear and semilog interpolation are listed in Fig. 8. Both INTERL and INTER check first that the input arrays are defined in columns, search the two components that bracket the input *Value*, and finally, perform a linear interpolation for the entry *Value*. As shown in Table 1 and Fig. 6, the linear and semilog interpolations give slightly different results. In contrast to the linear interpolation, the semilog interpolation gives an interpolated point that is exactly on one of the segments of Fig. 6.

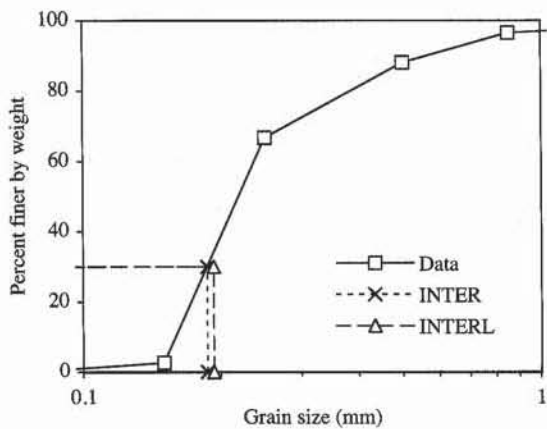


Figure 6 Graph corresponding to data of Table 1, and linear and semilinear interpolation.

	A	B
10	Semilog interpolation	
11		$D_{30} = =\text{INTER}(30, B2:B8, A2:A8)$
12		
13	Linear interpolation	
14		$D_{30} = =\text{INTERL}(30, B2:B8, A2:A8)$
15		

Figure 7 Formulas used in Fig. 6.

TABLE 1
Data set for interpolation

	A	B
	Grain size (mm)	Percent finer
1		
2	4.750	100.00
3	2.000	98.90
4	0.850	96.48
5	0.500	88.17
6	0.250	66.67
7	0.150	2.52
8	0.075	0.05
9		0.00
10	Semilog interpolation	
11		$D_{30} = 0.187 \text{ mm}$
12		
13	Linear interpolation	
14		$D_{30} = 0.193 \text{ mm}$
15		

NONLINEAR OPTIMIZATION WITH CONSTRAINTS

Some spreadsheet programs have the capabilities of performing nonlinear optimization with constraints. In principle, constrained optimization consists of finding the values of m variables p_1, p_2, \dots, p_m that minimize the function $f(p_1, p_2, \dots, p_m)$, with inequality or equality constraints on p_1, p_2, \dots, p_m . In general, the con-

	A	B
1	INTER	Linear Interpolation returns interpolated result corresponding to Value given two arrays X and Y in columns (x-logy axis)
2	=RESULT(1)	
3	=ARGUMENT("Value",1)	
4	=ARGUMENT("X",64)	
5	=ARGUMENT("Y",64)	
6	=IF(OR(ROWS(X)<>ROWS(Y),COLUMNS(X)>1,COLUMNS(Y)>1),RETURN(#VALUE!))	
7	=FOR("I",1,ROWS(X)-1)	
8	= IF(AND((INDEX(X,I+1)-Value)*(INDEX(X,I)-Value)<=0,INDEX(X,I+1)<>INDEX(X,I)))	
9	= RETURN(INDEX(Y,I)*(INDEX(Y,I+1)/INDEX(Y,I))^{((Value-INDEX(X,I))/(INDEX(X,I+1)-INDEX(X,I)))})	
10	= END.IF()	
11	=NEXT()	
12	=RETURN(#VALUE!)	
13		
14	INTERL	Linear Interpolation returns interpolated result corresponding to Value given two arrays X and Y in columns
15	=RESULT(1)	
16	=ARGUMENT("Value",1)	
17	=ARGUMENT("X",64)	
18	=ARGUMENT("Y",64)	
19	=IF(OR(ROWS(X)<>ROWS(Y),COLUMNS(X)>1,COLUMNS(Y)>1),RETURN(#VALUE!))	
20	=FOR("I",1,ROWS(X)-1)	
21	= IF(AND((INDEX(X,I+1)-Value)*(INDEX(X,I)-Value)<=0,INDEX(X,I+1)<>INDEX(X,I)))	
22	= RETURN(INDEX(Y,I)+(INDEX(Y,I+1)-INDEX(Y,I))^{((Value-INDEX(X,I))/(INDEX(X,I+1)-INDEX(X,I)))})	
23	= END.IF()	
24	=NEXT()	
25	=RETURN(#VALUE!)	

Figure 8 User-defined functions INTER and INTERL for linear and semilinear interpolations.

straints assign an admissible range of values for the variables, which eliminates unrealistic solutions. A detailed description of these numerical techniques is beyond the scope of this book. We only present an example relevant to soil mechanics.

In the case of the consolidation test, the problem is to find the values of parameters $p_1 = d_0$, $p_2 = d_{100}$, and $p_3 = C_v$ (i.e., $m = 3$) that minimize the error function $E(p_1, p_2, p_3)$:

$$E = \sum_{i=1}^n (d_i - d_i^p)^2 \quad (24)$$

between n experimental dial readings d_i at time t_i , $i = 1, \dots, n$, and the corresponding fitted dial readings d_i^p :

$$d_i^p = d_0 + (d_{100} - d_0) U(C'_v t_i) \quad \text{and} \quad U(x) = \begin{cases} \sqrt{\frac{4}{\pi}} x & \text{if } x < 0.2827 \\ 1 - \frac{8}{\pi^2} \exp\left(-\frac{\pi^2}{4} x\right) & \text{if } x \geq 0.2827 \end{cases} \quad (25)$$

We impose the following constraint on d_0 , d_{100} , and C'_v :

$$d_0 \geq d_1, \quad d_{100} \leq d_n, \quad d_{100} \geq d_0, \quad \text{and} \quad C'_v \geq 0 \quad (26)$$

where d_1 represents the first dial reading, and d_n represents the last dial reading. Figure 9 shows the data points to be fitted, and Fig. 10 lists the formulas used in Fig. 9. Figure 11 compares the experimental and fitted data points.

	A	B	C	D	E	F
1	Time (min)	Displacemen t (cm)	Fitted displacemen t (cm)			
2	0.0	0.0000	0.0350	$d_0 = 0.0350 \text{ cm}$		
3	0.3	0.0445	0.0449	$d_{100} = 0.1234 \text{ cm}$		
4	0.5	0.0483	0.0491	$C_v = 0.0400 \text{ 1/min}$		
5	1.0	0.0551	0.0549	Error E = 0.0000		
6	2.0	0.0635	0.0632			
7	4.0	0.0762	0.0748			
8	8.0	0.0912	0.0908			
9	15.0	0.1067	0.1070			
10	30.0	0.1173	0.1196			
11	60.0	0.1217	0.1232			
12	120.0	0.1232	0.1234			
13	240.0	0.1245	0.1234			
14	480.0	0.1245	0.1234			
15	1440.0	0.1245	0.1234			

Figure 9 Data set and results of nonlinear optimization with constraints.

C	
1	Fitted displacement (cm)
2	=E2+(E3-E2)*U(E4*A2)
3	=E2+(E3-E2)*U(E4*A3)
4	=E2+(E3-E2)*U(E4*A4)
5	=E2+(E3-E2)*U(E4*A5)
6	=E2+(E3-E2)*U(E4*A6)
7	=E2+(E3-E2)*U(E4*A7)
8	=E2+(E3-E2)*U(E4*A8)
9	=E2+(E3-E2)*U(E4*A9)
10	=E2+(E3-E2)*U(E4*A10)
11	=E2+(E3-E2)*U(E4*A11)
12	=E2+(E3-E2)*U(E4*A12)
13	=E2+(E3-E2)*U(E4*A13)
14	=E2+(E3-E2)*U(E4*A14)
15	=E2+(E3-E2)*U(E4*A15)

D	E
5	Error E = =SUMPRODUCT(B3:B15-C3:C15,B3:B15-C3:C15)

Figure 10 Formulas used in Fig. 9.

In Excel, the nonlinear optimization with constraints is performed using SOLVER. The parameters C_v , d_0 , and d_{100} to be optimized are in cells E2, E3, and E4, and the function to minimize is in cell E5. At the beginning of the calculations, C_v , d_0 , and d_{100} were set equal to 0.01, d_1 , and d_n . When SOLVER is called, it displays the window of Fig. 12. Set the cell to be optimized (e.g., E5), and select the minimum option. Define the cells to be changed by separating them with a comma, then add the constraints of Eq. 26. When all the input is performed, start the optimization. The calculation may take a few minutes, depending on the computer speed and the number of data points. In most cases, with the SOLVER default options, the optimization converges without a problem when the variables are properly constrained and initialized. SOLVER provides additional options for difficult optimizations (refer to the Microsoft Excel User's Manual for the options available).

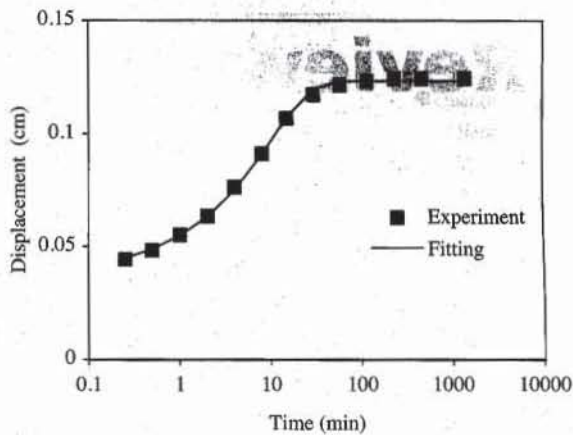


Figure 11 Comparison of experimental and fitted data points.

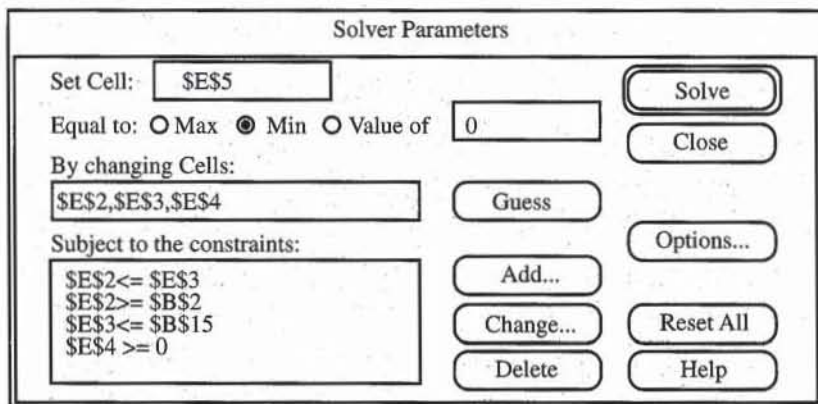


Figure 12 SOLVER's window.

REVIEW QUESTIONS

1. What is the difference between interpolation, linear regression, and nonlinear optimization?
2. What is the principle of linear regression?
3. Which quantity measures the accuracy of a linear regression fitting?
4. By using a linear interpolation, find the value of y corresponding to x between data points (x_1, y_1) and (x_2, y_2) .
5. Name the EXCEL functions that are used to perform linear regression.

8-2 Review of Statistics

In this chapter, we review some basic definitions in statistics and introduce statistical concepts relevant to grain size distributions of soils.

HISTOGRAM, FREQUENCY PLOT, AND CUMULATIVE FREQUENCY

Table 1 displays the distribution of glass beads. The glass beads are sorted in size categories; each is characterized by a minimum and a maximum size. For instance, there are 148 particles having a diameter between 12 and 14 mm, and the corresponding mass is 340.5 g. The total number of particles is 1565, and the total mass

TABLE 1

Distribution of a set of glass beads

Size (mm)	Number of glass beads	Weight (g)	Weight distribution (%)	Quantity distribution (%)	Cumulative weight distribution (%)	Cumulative quantity distribution (%)
0	0	0.00	0.0	0.00	0.00	0.00
2	141	3.99	0.2	9.01	0.20	9.01
4	183	23.95	1.2	11.69	1.40	20.70
6	362	130.03	6.5	23.13	7.90	43.83
8	325	248.11	12.4	20.77	20.30	64.60
10	230	320.58	16.0	14.70	36.32	79.30
12	148	340.50	17.0	9.46	53.34	88.75
14	85	300.41	15.0	5.43	68.36	94.19
16	47	241.81	12.1	3.00	80.44	97.19
18	24	172.39	8.6	1.53	89.06	98.72
20	13	126.08	6.3	0.83	95.36	99.55
22	6	76.45	3.8	0.38	99.18	99.94
24	1	16.36	0.8	0.06	100.00	100.00
26	0	0.00	0.0	0.00	100.00	100.00
	1565	2000.65				

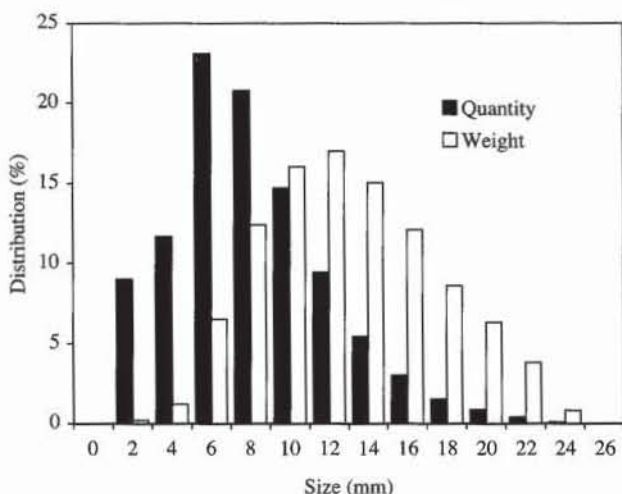


Figure 1 The histograms for the distributions of quantity and weight of the set of glass beads.

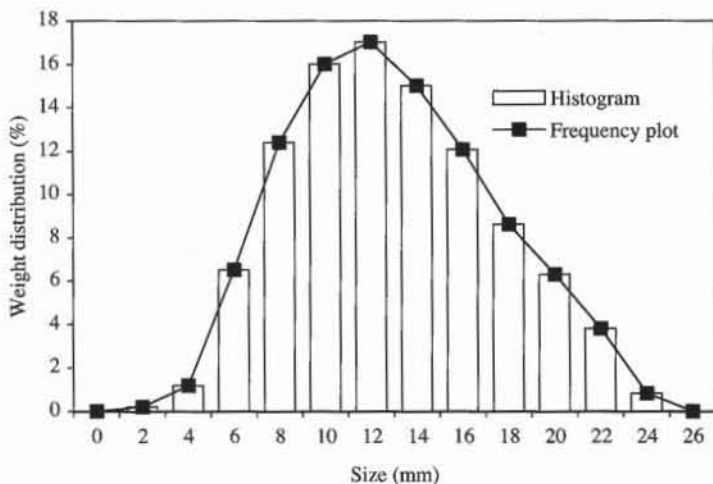


Figure 2 The histogram and frequency plot representations for the weight distribution of Table 1.

is 2000.65 g. The distributions of weight and quantity are expressed in percent. They are obtained by dividing the quantity, or mass, in each size category by the total quantity, or mass.

A distribution may be represented by using several graphical means. Figure 1 shows the histogram plot for the weight and quantity distributions. The fourth size range contains the largest number of beads, whereas the seventh size range has the largest mass. Distribution may also be represented as a frequency plot (continuous line) instead of a histogram (Fig. 2). The continuous line of the frequency plot connects the average size of each size category.

Figure 3 shows the cumulative distribution of weight and quantity. The cumulative distribution for a given size x is obtained by adding all the distributions for the category size smaller than x . While the distributions of weight and quantity vary up and down, the cumulative distributions always increase from 0 to 100.

In contrast to sets of glass beads, real soils have particles whose size varies from 0.001 to 100 mm. The smallest clay particles may reach a total number 10^{10} times larger than the number of coarser gravel particles. This large disparity in

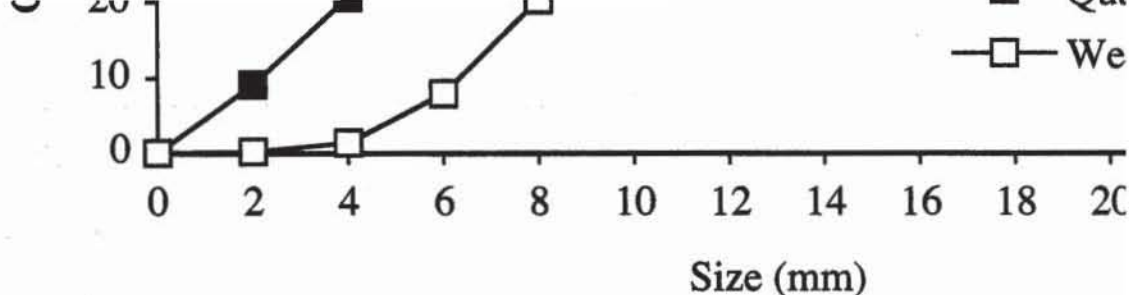


Figure 3 Cumulative frequency plots of the distribution and weight of the set of glass beads.

the quantity of particle sizes and the impossibility of course are the main reasons for selecting a weight distribution for size distribution of soils.

AND STANDARD DEVIATION

A distribution is generally characterized by three statistics: mean, and standard deviation. The range is the difference between the smallest and largest values in the data set. It is a measure of the dispersion of the data. For instance, the range is 24 mm for the distribution of glass beads shown in Table 1. If a data set sorted in M groups, each group having f_i elements with average value m_i , the mean or average value μ is

$$\mu = \frac{\sum_{i=1}^M m_i f_i}{\sum_{i=1}^M f_i}$$

In the case of glass beads, m_i and f_i are the average size and a particle size range, respectively. For instance, in the case of Table 1, $m_6 = 11$ mm and $f_6 = 16\%$ for the sixth position 1 may be simplified because the sum of coefficients

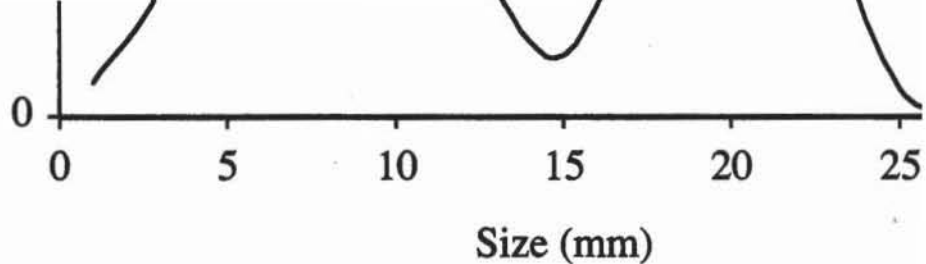


Figure 4 An example of bimodal distribution.

When $\sum_{i=1}^M f_i = 1$, Eq. 3 becomes

$$\sigma = \sqrt{\sum_{i=1}^M (m_i - \mu)^2 f_i} = \sqrt{\sum_{i=1}^M m_i^2 f_i - \mu^2}$$

By applying Eq. 4 to the data of Table 1, $\sigma = 4.43$ mm.

The mean, range, and standard deviation are generally used to characterize distributions that have a unique peak. The distribution is *unimodal*. However, the mean, range, and standard deviation are less meaningful for describing complicated distributions with several peaks. As an example of a *bimodal* distribution (i.e., two peaks), when mixing a uniform gravel and a uniform fine sand, for instance, the distribution is defined more accurately with two values for mean and standard deviation than with a single value for mean and standard deviation.

DISTRIBUTION

Several functions have been proposed to describe various distributions. Only a few examples available in spreadsheet programs are discussed here.

EXPONENTIAL DISTRIBUTION

The exponential distribution is

$$f(x, \lambda) = \lambda e^{-\lambda x}$$

WEIBULL DISTRIBUTIONS

The Weibull distribution is

$$f(x) = \frac{\alpha}{\beta^\alpha} x^{\alpha-1} e^{-(x/\beta)^\alpha} \quad (8)$$

Its cumulative distribution is

$$F(x, \alpha, \beta) = \int_0^x f(t) dt = 1 - e^{-(x/\beta)^\alpha} \quad (9)$$

When $\alpha = 1$, the Weibull distribution becomes the exponential distribution with $\lambda = 1/\beta$.

NORMAL AND LOGNORMAL DISTRIBUTIONS

The normal distribution is

$$f(x, \mu, \sigma) = \frac{1}{\sqrt{2\pi}\sigma} e^{-(x-\mu)^2/2\sigma^2} \quad (10)$$

The lognormal distribution is obtained by replacing x by $\ln(x)$ in Eq. 10.

As shown in Figs. 5 and 6, the normal distribution fits the weight distribution of Table 1. Fig. 7 gives the data set, and Fig. 8 lists the formulas used in Fig. 7. The average and standard deviation are calculated using Eqs. 2 and 4.

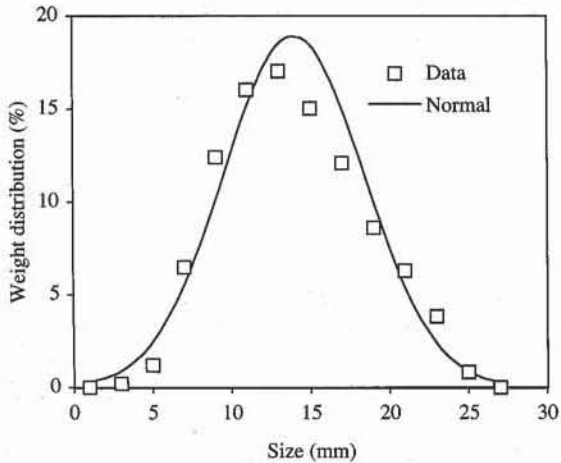


Figure 5 Weight distribution of Table 1 fitted by normal distribution.

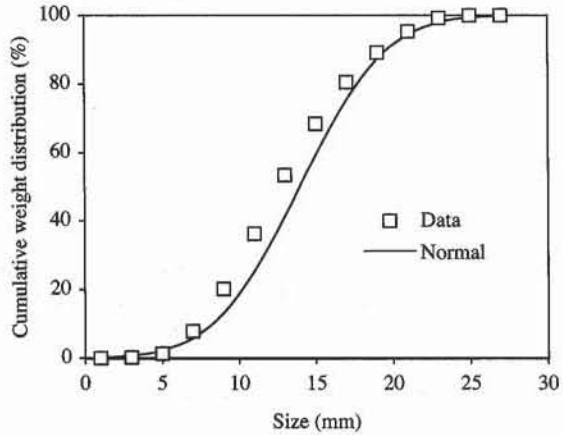


Figure 6 Weight distribution of Table 1 fitted by cumulative normal distribution.

OTHER DISTRIBUTIONS

Besides exponential, Weibull, and normal distributions, there are other types of distributions, such as gamma, Poisson, and Student-*t*.

1	A	B	C	D	E
	Data		Fitting		
2	Size (mm)	Weight distribution (%)	Cumulative weight distribution	Normal	Normal cumulative
3	d	f			
4	1	0.00	0.00	0.26	0.17
5	3	0.20	0.20	0.89	0.67
6	5	1.20	1.40	2.46	2.16
7	7	6.50	7.90	5.52	5.82
8	9	12.40	20.30	10.13	13.16
9	11	16.02	36.32	15.15	25.21
10	13	17.02	53.34	18.50	41.41
11	15	15.02	68.36	18.43	59.24
12	17	12.09	80.44	14.98	75.32
13	19	8.62	89.06	9.94	87.20
14	21	6.30	95.36	5.38	94.37
15	23	3.82	99.18	2.38	97.92
16	25	0.82	100.00	0.86	99.36
17	27	0.00	100.00	0.25	99.84
18	Average size μ =		13.96	mm	
19	Standard dev σ =		4.44	mm	

Figure 7 Examples of weight distribution fitted by a normal distribution.

	D	E
2	Normal	Normal cumulative
3		
4	=100/EXP((d-m)^2/2/s^2)/SQRT(2*PI()*s)	=NORMDIST(d,m,s,TRUE)*100
5	=100/EXP((d-m)^2/2/s^2)/SQRT(2*PI()*s)	=NORMDIST(d,m,s,TRUE)*100
18	Average size μ = =SUMPRODUCT(f,d)/100	mm
19	Standard dev σ = =SQRT(SUMPRODUCT(d,d,f)/100-m^2)	mm

Figure 8 Formulas used in Fig. 7.

REVIEW QUESTIONS

- Define *histogram* and *frequency plots* of a distribution.
- What is the relation between a distribution and a cumulative distribution? Assuming that $f(x)$ is a continuous distribution, define the cumulative distribution $F(x)$. Conversely, assuming that $F(x)$ is a cumulative distribution, define the distribution $f(x)$.
- Why is a weight distribution preferable to a quantity distribution when characterizing the grain size distribution of real soils?
- Assume that a data set is sorted in M groups of data, each having an average value x_i and each containing m_i elements. Define the average and standard deviation of the data set.
- Same as question above but assume that m_i represents the percentage of elements instead of the number of components. Simplify the definitions of the average and standard deviation of the complete data set.
- What are unimodal and bimodal distributions?
- Name three probability distributions.

EXERCISES

1. Define a weight distribution and a quantity distribution for the following set of glass beads:

5 beads of 3 mm diameter
10 beads of 5 mm diameter
20 beads of 7 mm diameter
10 beads of 9 mm diameter
5 beads of 9 mm diameter

Assume the same unit mass for all glass beads.

2. Define a cumulative weight distribution and a cumulative quantity distribution for the set of glass beads in Exercise 1.
3. Plot the distribution and cumulative distribution of a bimodal distribution that has the following averages and standard deviations: $\mu_1 = 10$ mm, $\sigma_1 = 5$ mm, and $\mu_2 = 100$ mm, $\sigma_2 = 10$ mm. Identify the shape of a gap-graded grain size distribution curve.

8-3 Error Analysis

CAUSES AND TYPES OF EXPERIMENTAL ERRORS

Errors creep into all experiments regardless of the care that is exerted. Some errors are of a random nature, and some are due to gross blunders on the part of the experimenter. The latter type may be detected and fixed after scrutinizing the experimental results, especially when they show a gross deviation from expected results. The former type of error may be systematic, which causes the readings to be incorrect by the same amount for some unknown reason, or random errors, which result from fluctuations in the measuring instruments. The random errors in reading a well-calibrated and operational instrument are generally comparable to the instrument accuracy.

UNCERTAINTY ANALYSIS

Kline and McClintock (1953) presented a method of estimating the uncertainties of experimental results based on the uncertainties of various primary experimental measurements. Consider that the result y is a function of n independent variables x_1, x_2, \dots, x_n :

$$y = y(x_1, x_2, \dots, x_n) \quad (1)$$

The variables x_1, x_2, \dots, x_n are considered independent when they are separately measured (i.e., they are not calculated one from the other). The uncertainties in the measurement of x_i are denoted Δx_i . For instance, if x_i is a weight, the uncertainty Δx_i is the scale accuracy at which the weight x_i can be measured. The accuracy of an instrument is generally specified by its manufacturer. When the uncertainties of all the independent variables are given, the uncertainty of the result is

$$\Delta y = \sqrt{\left(\frac{\partial y}{\partial x_1} \Delta x_1\right)^2 + \left(\frac{\partial y}{\partial x_2} \Delta x_2\right)^2 + \dots + \left(\frac{\partial y}{\partial x_n} \Delta x_n\right)^2} \quad (2)$$

One may also evaluate Δy by using the following alternative formula:

$$\Delta y = \left| \frac{\partial y}{\partial x_1} \Delta x_1 \right| + \left| \frac{\partial y}{\partial x_2} \Delta x_2 \right| + \cdots + \left| \frac{\partial y}{\partial x_n} \Delta x_n \right| \quad (3)$$

In both formulas, the errors generated by each independent variable add up. The more variables there are, the larger is the error. By definition, Δy is called the *absolute error* on y , whereas $\Delta y/y$ is called the *relative error* on y . The relative error is dimensionless and is expressed in percent, while the absolute value has the same dimension as y (i.e., $[\Delta y] = [y]$).

EXAMPLES

Equations 2 and 3 apply to the determination of water content w in the plastic limit test. The result $y = w$ is calculated as follows:

$$w = \frac{W_w - W_d}{W_d - W_c} \times 100 \quad (\%) \quad (4)$$

where W_c is the weight of the container, W_w the weight of the container and wet soil, and W_d the weight of the container and dry soil. The independent variables are $x_1 = W_c$, $x_2 = W_w$, and $x_3 = W_d$ because W_c , W_w , and W_d are measured independently. The partial derivatives of w with respect to W_c , W_w , and W_d are

$$\frac{\partial w}{\partial W_c} = \frac{W_w - W_d}{(W_d - W_c)^2} = \frac{w}{W_d - W_c}, \quad \frac{\partial w}{\partial W_w} = \frac{1}{W_d - W_c}, \quad \text{and} \quad \frac{\partial w}{\partial W_d} = \frac{W_c - W_w}{(W_d - W_c)^2} \quad (5)$$

Since W_c , W_w , and W_d are measured using the same scale,

$$\Delta W_c = \Delta W_w = \Delta W_d = \Delta W \quad (6)$$

Applying Eq. 2 to w , one obtains the relative error of w :

$$\begin{aligned} \frac{\Delta w}{w} &= \Delta W \sqrt{\frac{(W_w - W_d)^2 + (W_w - W_c)^2 + (W_d - W_c)^2}{(W_d - W_c)^2}} \\ &= \frac{\Delta W}{W_d - W_c} \sqrt{1 + w^2 + \left(\frac{W_w - W_c}{W_d - W_c}\right)^2} \end{aligned} \quad (7)$$

As shown in Eq. 7, the error on w is proportional to the error of the weight measurement. Figure 1 shows an example of experimental results for the liquid limit test. In this case, the error in weight measurement is set equal to the scale accuracy (i.e., $\Delta W = 0.01$ g). The relative and absolute errors for each determination of w are given in Fig. 1. Figure 2 lists the formulas used in Fig. 1.

The error can also be calculated using Eq. 3 instead of Eq. 2. First, it is convenient to take the logarithm of w :

$$\ln(w) = \ln(W_w - W_d) - \ln(W_d - W_c) \quad (8)$$

then to differentiate it:

$$\begin{aligned}\frac{dw}{w} &= \frac{d(W_w - W_d)}{W_w - W_d} - \frac{d(W_d - dW_c)}{W_d - W_c} \\ &= \frac{dW_c}{W_d - W_c} + \frac{dW_w}{W_w - W_d} - \frac{(W_w - W_c)dW_d}{(W_w - W_d)(W_d - W_c)}\end{aligned}\quad (9)$$

The infinitesimal variations dW_c , dW_w , and dW_d are then replaced by the errors ΔW_c , ΔW_w , and ΔW_d that are all set equal to ΔW , and the relative error on w becomes

$$\frac{\Delta w}{w} = \Delta W \left(\frac{1}{W_d - W_c} + \frac{1}{W_w - W_d} + \frac{|W_w - W_c|}{|W_w - W_d| |W_d - W_c|} \right) \quad (10)$$

Because $W_d > W_c$, $W_w > W_d$, and $W_w > W_c$, Eq. 10 becomes

$$\frac{\Delta w}{w} = \frac{2\Delta W(W_w - W_c)}{(W_w - W_d)(W_d - W_c)} \quad (11)$$

As shown in Fig. 1, Eq. 3 generates larger errors than Eq. 2 and therefore is a more conservative error estimate.

In Fig. 3, the absolute errors are represented by using vertical bars centered on the data points. The height of each error bar is equal to the absolute error on w . In Excel, these error bars are plotted by selecting the graph, by using **Insert Error Bars**, and by entering the range of absolute error on w as **Y Error Bars**.

Another example may be taken from the one-point liquid limit test. In this simplified procedure, the liquid limit LL is calculated from the water content w associated with N blows:

$$LL = w \left(\frac{N}{25} \right)^{A'} \quad (12)$$

where A' is the slope of flow line. The error of N can be taken to be zero, because it is improbable that the number of blows be miscounted. The independent variables are $x_1 = w$ and $x_2 = A'$. The partial derivatives of LL with respect to w and A' are

$$\frac{\partial LL}{\partial w} = \frac{LL}{w} \quad \text{and} \quad \frac{\partial LL}{\partial A'} = LL \ln \frac{N}{25} \quad (13)$$

Therefore, the error of LL is

$$\frac{\Delta LL}{LL} = \sqrt{\left(\frac{\Delta w}{w} \right)^2 + \left(\ln \frac{N}{25} \Delta A' \right)^2} \quad (14)$$

When $N = 25$, $\Delta LL/LL = \Delta w/w$. Figure 4 shows $\Delta LL/LL$ calculated by using $\Delta w/w = 1\%$ and four values of $\Delta A'$ (i.e., $\Delta A' = 0.01, 0.02, 0.05$, and 0.08). As illustrated in Fig. 4, error analysis can be used to assess the effects of each measurement on the final results and to select the optimal measurement conditions, which produce the smallest errors. In the one-point liquid limit test, it is recommended to select a blow count N as close as possible to 25 in order to decrease the error on LL . It is clear that the liquid limit cannot be determined more accurately than the water content itself.

	A	B	C	D	E	F	G	H	I	J	K
1	Liquid limit										
2	Analyst name: Henry T. Guapo										
3	Sample description: Aardvark modeling clay										
4	Scale accuracy $\Delta W = 0.01$ g										
5	set number	Container mass (g)	Mass of wet soil and container (g)	Mass of dry soil and container (g)	Number of blows	Water content (%)	Relative error on water content	Absolute error on water content (%)	Relative error on water content	Absolute error on water content (%)	Water content fitted (%)
6		W_c	W_w	W_d	N	w	$\Delta w/w$	$\Delta w/w$	$\Delta w/w$	$\Delta w/w$	
7	1	47.72	59.89	57.05	24	30.44	0.18%	0.05	0.92%	0.28	30.70
8	2	43.21	59.76	55.95	31	29.91	0.13%	0.04	0.68%	0.20	29.76
9	3	45.17	61.25	57.45	22	30.94	0.14%	0.04	0.69%	0.21	31.02
10	4	45.81	58.26	55.26	19	31.75	0.18%	0.06	0.88%	0.28	31.56

Figure 1. Example of error calculation for liquid limit test.

	F	G	H	I	J
5	Water content (%)	Relative error on water content	Absolute error on water content (%)	Relative error on water content	Absolute error on water content (%)
6	w	$\Delta w/w$		$\Delta w/w$	
7	=100*(Ww-Wd)/(Wd-Wc)	=DW*SQRT((Ww-Wd)^2+(Wd-Wc)^2+(Ww-Wc)^2)/(Wd-Wc)^2	=G7*w	=2*DW*(Ww-Wc)/(Ww-Wd)/(Wd-Wc)	=I7*w
8	=100*(Ww-Wd)/(Wd-Wc)	=DW*SQRT((Ww-Wd)^2+(Wd-Wc)^2+(Ww-Wc)^2)/(Wd-Wc)^2	=G8*w	=2*DW*(Ww-Wc)/(Ww-Wd)/(Wd-Wc)	=I8*w

Figure 2. Formulas used in Fig. 1.

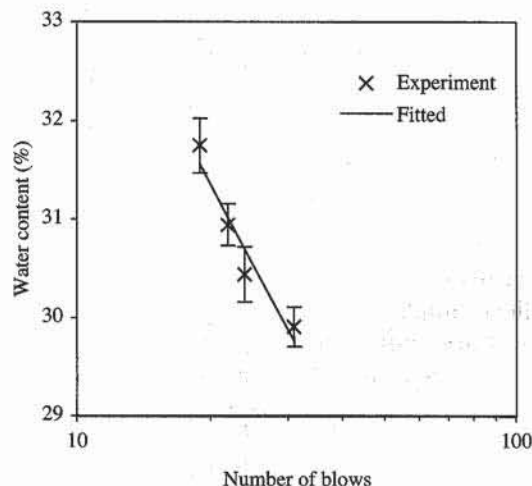


Figure 3 Error in water content resulting from error in the measurement of weight (Eq. 3).

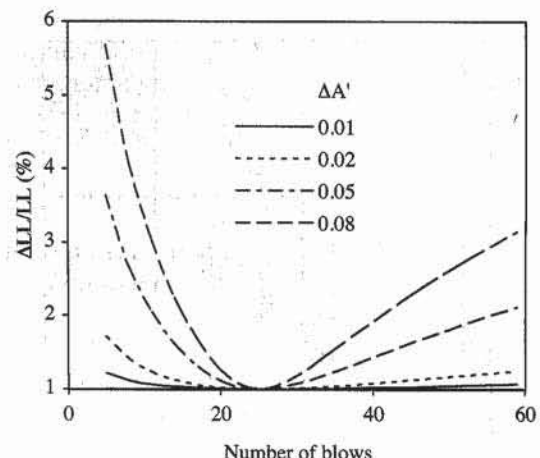


Figure 4 Variation of relative error of liquid limit versus number of blows N for various errors of coefficient A' ($\Delta A' = 0.01, 0.02, 0.05, \text{ and } 0.08$).

REFERENCE

KLINE, S. J., and F. A. MCCLINTOCK, 1953, Describing uncertainties in single-sample experiments, *Mech. Eng.*, January, p. 3.

EXERCISES

1. Define two different types of errors in experiments. Illustrate your general definitions with an example of your choice.
2. Define *relative error* and *absolute error*.
3. What is the purpose of error analysis?
4. How can error analysis be used to improve an experimental procedure?
5. In pipette analysis, the grain size D (mm) is calculated as follows:

$$D = \sqrt{\frac{30\eta H}{(G_s - 1)981\rho_w t}}$$

where t is the time (min) after the beginning of sedimentation, G_s the specific gravity of soil particles, ρ_w the unit mass of water (g/cm^3) at temperature T , η the viscosity of water ($\text{g}/\text{cm} \cdot \text{s}$) at temperature T , and H the sampling depth (cm). Calculate the relative error of D as a function of the error of each variable.

6. In pipette analysis (dry method), the percentage p by weight of particles with diameter smaller than D is

$$p = 100 \frac{V_t}{V} \frac{M_s - M_b - M_d}{M_o} \quad (\%)$$

where M_o is the total mass of oven-dried soil in suspension, M_b the mass of empty bottle used to collect the pipette sample, M_s the mass of bottle and sample of oven-dried soil, V_t the total volume of suspension, V the volume

of the pipette, and M_d the mass of the dispersing agent in volume V . Calculate the relative error of p as a function of the error of each variable.

7. In pipette analysis (wet method), the percentage p by weight of particles with diameter smaller than D is

$$p = 100 \frac{\rho_s V_t}{\rho_s V - M_{dw}} \frac{M_{sw} - M_b - M_{dw}}{M_o} \quad (\%)$$

where M_o is the total mass of oven-dried soil in suspension, M_b the mass of the empty bottle used to collect sample, M_{sw} the mass of the bottle and sample of soil suspension, V_t the total volume of suspension, V the volume of the pipette, ρ_s the unit mass of solids, and M_{dw} the mass of water and dispersing agent in volume V . Calculate the relative error of p as a function of the error of each variable.

8. In the determination of unit weight by the buoyancy method, the total unit mass of soil is

$$\rho = \rho_w \frac{M}{M_P - M_I - (\rho_w/\rho_P)(M_P - M)}$$

where M is the mass of the soil, M_P the mass of the soil and paraffin wax, M_I the immersed mass of the soil and wax, ρ_w the unit mass of water ($\rho_w \approx 1.0 \text{ g/cm}^3$), and ρ_P the unit mass of wax. Calculate the relative error of ρ as a function of the error of each variable.

8-4 Dimensions and Units

The comparison of experimental results obtained from different sources requires certain standard units of length, weight, time, temperature, and electrical quantities. The National Institute of Standards and Technologies has the primary responsibility of maintaining these standards in the United States. In this section we present the dimensions, units, and unit conversions that are useful in soil mechanics.

DIMENSIONS

A dimension is a physical variable used to describe the behavior or nature of a physical system. For instance, the length of a rod is a dimension. Dimensions are not to be confused with units. When the rod is said to be 2 meters long, the length dimension was measured with the unit *meter*. Most of the physical quantities used in soil mechanics can be expressed in terms of the following dimensions: length, mass, time, force, and temperature. Their notations are listed in Table 1.

TABLE 1
Notation of physical dimensions used in soil mechanics

Notation	Dimension
<i>L</i>	length
<i>M</i>	mass
<i>T</i>	time
Θ	temperature
<i>F</i>	force

DIMENSIONAL ANALYSIS

Physical variables can be related by physical laws. Their relations can be derived by using dimensional analysis, a simplified form of calculus that we illustrate with

a few examples. In dimensional analysis, the dimension of variable x is noted $[x]$. When x has no dimension, $[x] = 1$.

In Table 1, L , M , T , and θ are independent dimensions, but F is related to other dimensions. Using Newton's second law of motion, the mass m moving with acceleration a is subjected to the force f :

$$f = ma \quad (1)$$

The dimension of f is force (i.e., $[f] = F$). Similarly, $[m] = M$. By using dimensional analysis,

$$[f] = [m][a] \quad (2)$$

Because the acceleration a is the second-order derivative of displacement x with respect to time t , the acceleration dimension is

$$[a] = \left[\frac{d^2x}{dt^2} \right] = [x][t]^{-2} = LT^{-2} \quad (3)$$

where $[x] = L$ and $[t] = T$. Therefore, F is related to M , L , and T through

$$F = MLT^{-2} \quad (4)$$

As another example, consider Stokes' law, which gives the drag force f applied by a fluid moving with velocity v onto a sphere of radius d :

$$f = 3\pi\eta vd \quad (5)$$

where η is the fluid viscosity. Using dimensional analysis,

$$[f] = [\eta][v][d] \quad (6)$$

$[3\pi] = 1$ because 3π is dimensionless. The dimension of velocity v is

$$[v] = LT^{-1} \quad (7)$$

Therefore, the dimension of η is mass divided by length and time:

$$[\eta] = [f][v]^{-1}[d]^{-1} = FL^{-1}TL^{-1} = MLT^{-2}L^{-1}TL^{-1} = ML^{-1}T^{-1} \quad (8)$$

UNITS

Units are not be confused with dimensions. Units are used to report the measurement of dimensions. In general, there are several units for the same dimension. For instance, the length of a rod may be 2 meters, or 200 centimeters. One of the most common systems of units is the International System of units, referred to as the SI units system. Table 2 lists the names and notations of basic SI units. Table 3 gives a list of derived SI units for the physical quantities in soil mechanics.

Table 4 lists the standard multiplier prefixes used in the SI system. For instance, $1 \times 10^6 \text{ N} = 1000 \text{ kN} = 1 \text{ MN}$, or $1 \times 10^{-6} \text{ m} = 1 \mu\text{m}$.

TABLE 2
Basic SI units

Dimension	Unit	Symbol
Length	meter	m
Mass	kilogram	kg
Time	second	s
Electric current	ampere	A
Temperature	kelvin	K
Luminous intensity	candela	Cd
Plane angle	radian	rad
Solid angle	steradian	sr

TABLE 3
Derived SI units

Dimension	Unit	Symbol
Area	square meter	m^2
Volume	cubic meter	m^3
Unit mass	kilogram per cubic meter	kg/m^3
Frequency	hertz	Hz (or s^{-1})
Velocity	meter per second	m/s
Angular velocity	radian per second	rad/s
Acceleration	meter per squared second	m/s^2
Angular acceleration	radian per squared second	rad/s^2
Volumetric flow rate	cubic meter per second	m^3/s
Force	newton	N (or $\text{kg} \cdot \text{m}/\text{s}^2$)
Pressure	newton per squared meter, Pascal	N/m^2 , Pa
Surface tension	newton per meter	N/m
Work	joule, newton meter	J, $\text{N} \cdot \text{m}$
Diffusivity	meter squared per second	m^2/s

TABLE 4
Standard prefixes and multiples
in SI units (after Holman and Gadja, 1984)

Symbol	Multiple/ submultiple	Prefix
10^{12}	tera	T
10^9	giga	G
10^6	mega	M
10^3	kilo	k
10^2	hecto	h
10	deka	da
10^{-1}	deci	d
10^{-2}	centi	c
10^{-3}	milli	m
10^{-6}	micro	μ
10^{-9}	nano	n
10^{-12}	pico	p
10^{-15}	femto	f
10^{-18}	atto	a

CONVERSION OF UNITS

A physical quantity can be reported in terms of several units. It is common to convert a physical quantity from one unit system to another. For instance, a pressure can be converted from Pa to atm (atmospheric pressure). Erroneous unit

conversions can generate dramatic engineering mistakes, such as errors of several orders of magnitude. In soil mechanics in the United States, British units (e.g., pound, quart, foot, or inch) are still commonly used, although the SI units are recommended in engineering practice and required in technical publications.

Unit conversions can easily be performed with spreadsheets. The user-defined function UNITS in Chapter 9-3 performs such a conversion task. It was used in the appendix to generate the conversion factors for the units of length, area, volume, time, velocity, force stress, unit weight, and diffusivity.

REFERENCE

HOLMAN, J. P., and W. J. GADJA, Jr., 1984, *Experimental Methods for Engineers*, McGraw-Hill Book Company, New York.

REVIEW QUESTIONS

1. Define *dimension* and *unit*. Give an example of a dimension and a unit.
2. Name five basic dimensions.
3. Which is the most commonly used systems of units?
4. List 10 different units for length.
5. Find the basic dimensions of energy by using dimensional analysis.

8-5 Report Writing

INTRODUCTION

Many books have been written on the subject of report writing (e.g., Tarabian 1973). Here, we only review some basic requirements for a good report for engineering and academic purposes. The importance of good report writing and data representation cannot be overemphasized. The best experiment or the most brilliant discovery is worthless unless the information is communicated effectively to other people. In report writing, as in any communication exercise, the author must first identify his or her relative position to the reader with whom he or she intends to share the information. The author could be a student writing to the laboratory instructor, a laboratory technician to an engineering company, or an engineer to a client. The following presentation pertains primarily to the first situation, where a student has to write a report to a laboratory instructor.

ORGANIZATION OF REPORTS

The organization of a report depends largely on its volume; a 10-page report generally requires less structure than a 1000-page doctoral dissertation. Our recommendations apply to the laboratory reports that students will write to their laboratory instructor and supervisor, those reports involving generally less than a total of 10 pages. Our comments are also adapted to the generation of reports accompanied with spreadsheet results.

A carefully constructed outline is always the best starting point to write a report. It will help the writer to make sure that all pertinent information is included. The writer may decide to omit some elements of the recommended outline in particular circumstances.

Front Matter

Front matter includes the title page, with the author's name and affiliation, date of the work, sponsor of the report if any, a table of contents, and an optional list of nomenclature, tables, and figures.

- The title page should contain the minimum, but necessary, amount of information. Its main function is to identify the report. It is generally typed in larger characters that are clearly laid out.
- The table of contents should list the main headings and subheadings of the report. It is a good practice to number each page of the report and to indicate the heading page numbers in the table of contents.
- A list of nomenclature should be included when the author uses abbreviations and mathematical notations that are not common knowledge.
- A list of tables and a list of figures are required when there are numerous figures and tables throughout the text, a profusion of which may confuse everybody, including the author.

Abstracts

The abstract summarizes the main points of a report and should reflect in a few words the outcome of the work. Keep in mind that an abstract is often what people read first. Although the abstract comes first, it is generally written after the body of the report has been completed.

Introduction

The purpose of an introduction is to lay down the background of the problem that is to be solved in the report. A reference to past work on similar subjects is strongly encouraged. A good introduction should explain why a particular report has been written. It should always spell out the objectives of the present work. In practice, the objectives are generally specified by the instructor or by the client.

Experimental Apparatus and Procedure

The description of the experimental equipment and procedure may be extremely brief (e.g., ASTM D-854). It tells the reader how the test was performed. There is no need to copy a well-known procedure except when there have been deviations from it.

Results of Experiments

The results should be in clear tabular and graphical presentations. The spreadsheet programs provide added presentation benefits, of which the author should take full advantage. As a golden rule, all numbers should be reported with their units. A number without a unit implicitly assumes that the corresponding variable is dimensionless. Would you like to be paid 100 cents rather than 100 dollars? The same rule applies to the labels along the vertical and horizontal axes of a graph. Always remember that a good graph or table should stand on its own without the need for additional information.

Interpretation of Results

The interpretation of experimental results always engages the responsibility of the author, who has to answer the following question: Are my results in agreement with existing theories, or are they contradicting them? Again, remember that the experiment has been performed for a specific objective. This section should tell if the experimental results fail, meet, or exceed expectations. The reasons for failure or success should be made as clear as possible. In cases where the

author would develop an challenging or apologetic mood, it is recommended that there be a separate section entitled "Discussion." You may include in a discussion section what you did not like, or what you believe should be done.

Conclusions

An honest conclusion collects only the main points that have been made in the body of the report. It should make sure that all the objectives of the report that were spelled out in the introduction have been addressed properly. It should not bring a new topic or problem, which is bound to confuse the reader. Many readers will read only the abstract and the conclusion. In general, the conclusion and the abstract are always the last sections to be written in a report. But avoid copying the same sentences in the abstract and conclusion, at the risk of testing the patience of your readers.

Acknowledgments

Should you feel the need to recognize the contribution of some of your colleagues to your work, an acknowledgment is the appropriate place to express your gratitude. Please be precise, and acknowledge your sponsor if any. What about your laboratory partners who collected data for you during the experiment?

References

Rare, and generally poor, are the technical reports that contain no references to past work. References may be cited in the text in various ways. We recommend referring to the work by the author's last name followed by the publication year (e.g., Terzaghi 1943). Numbering the references in the text is another recognized practice. The references should be listed alphabetically in a separate section after the conclusion. They should be typed in a consistent format. You may refer to the format of the references typed in this book.

Appendix

To keep a report clear and concise, it is very often necessary to open a separate section after the main body of the report: the appendix or appendices. An appendix may contain data or graphs that are useful but not fundamental to comprehending the report. In the appendix you may include the calibration of measuring instruments, or details of the formulas you have used to perform the calculations in the spreadsheets.

EXAMPLE

Most computer programs have a wealth of features for preparing reports, which should be used sparingly with the sole goal of clarifying the report. The author should try to refrain from abusing the bells and whistles of these computer programs, an excess of which may obscure the main message. A report should have a consistent style throughout the headings, text, numbers, and figures.

Hereafter, we provide an example of a clear and well-organized report, which should meet the requirements of most instructors. It was obtained by combining the use of a word processor and a spreadsheet program: namely Microsoft Word and Excel. The word processor is used to

generate and paginate the report, and the spreadsheet program is used to perform all calculations and graphics. Once all the data have been processed into the spreadsheet, it is copied and inserted into the report for the final presentation. The report is listed in Fig. 1. The cover page is a title page, the function of which is to identify the report by stating the experiment title, name of student, date, and so on. Following the cover page, the first page contains the table of contents, the abstract, the introduction, and the experimental equipment and procedure. It accounts for the selection of a particular sieving technique (e.g., dry versus wet technique). The second page combines the experimental results and their interpretation. The measured and calculated data are reported in tables and figures that are numbered (e.g., Table 1 and Fig. 1) and that are referred to in the text by using these numbers (e.g., Table 1 and Fig. 1). All the tables and figures should have a caption that identifies them and describes their contents concisely. All the numbers in the tables have a unit (e.g., grain size in mm) unless if they are dimensionless (e.g., coefficient of uniformity). The third page presents the experimental results as a graph, with labeled axes, and gives the discussion, conclusion, and references. The fourth and fifth pages are the appendices. They contain the details of the calculations that are useful to detect the possible errors of measurement and/or data processing.

REFERENCES

TURABIAN, K. L., 1973, *A Manual for Writers*, 4th ed., University of Chicago Press, Chicago.

EXERCISES

1. Name the 10 different sections in a well-organized report.
2. What is the purpose of a table of contents?
3. What is the function of an introduction?
4. What is the main difference between an abstract and a conclusion?

Grain size analysis with sieve

CE468L laboratory report No. 1

by M. Kapuskar

7 September 1996

Civil Engineering Department
University of Southern California
Los Angeles CA 90089-2531

Figure 1 Example of a laboratory report.

Custom functions used in formulas

The grain size distribution curve of soil sample is shown in Figure 1. The soil sample was taken from the Arroyo Seco, Marin District of San Francisco, California. The soil sample was analyzed by the hydrometer method. Based on the coefficients of uniformity and curvature, the soil sample is classified as a fine-grained unconsolidated soil.

Action and objective

The objective of the report is to define
by using a sieve analysis for soil sample No. 1,
San Francisco, California. The grain size
and the relative proportion of different grain sizes.

Instrumental equipment and procedure

The experimental equipment and procedure entitled "Grain size analysis with sieve" of consists of sorting soil grains by size

50	0.250	40.90
100	0.150	122.00
200	0.075	4.70
pan		0.10

Total mass $M_{\text{tot}} = 190.20 \text{ g}$

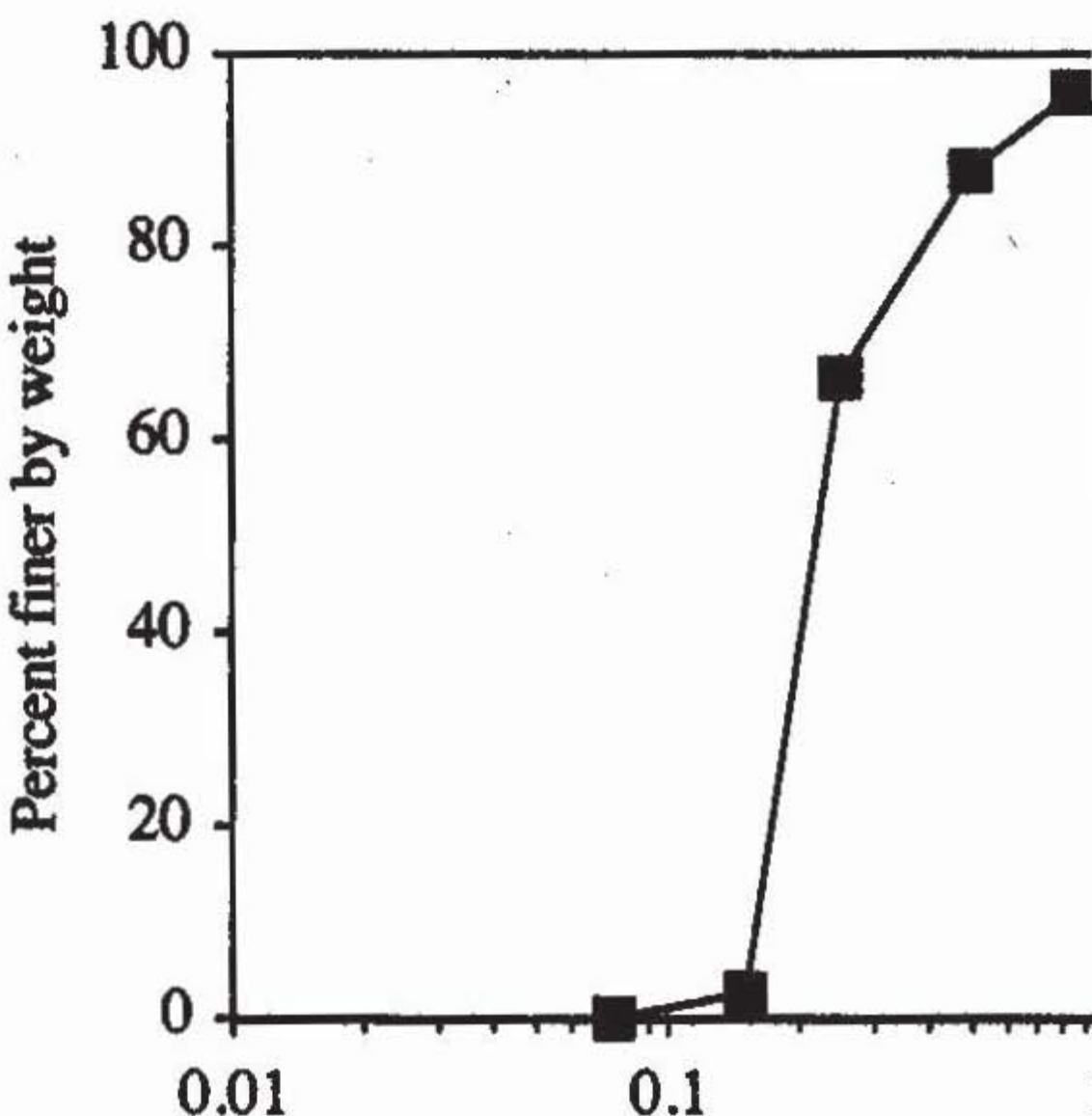
$$D_{10} = 0.159 \text{ mm}$$

$$D_{30} = 0.187 \text{ mm}$$

$$D_{60} = 0.238 \text{ mm}$$

C_u

C_c



Sample mass M_0 =

191.10

US sieve number	Sieve opening (mm)	Mass retained (g)
	d	M
4	4.750	0.00
10	2.000	2.10
20	0.850	4.60
35	0.500	15.80
60	0.250	40.90
100	0.150	122.00
200	0.075	4.70
pan		0.10

Total mass M_{tot} = 190.20 g

$D_{10} = 0.159 \text{ mm}$

 C_u

$D_{30} = 0.187 \text{ mm}$

 C_c

$D_{60} = 0.238 \text{ mm}$

Sieve analysis used in Table 1

A	B	C	
US sieve number	Sieve opening (mm)	Mass retained (g)	Mass M_a

List of variables used in Table 1

Variable name	Cell(s) location
d	=B10:B16
D.10	=B19
D.30	=B20
D.60	=B21
M	=C10:C17
M0	=B6
Mp	=D10:D17
Mtot	=C18
p	=E10:E16

Custom functions used in formulas of Table 1

A	
1	INTER
2	=RESULT(1)
3	=ARGUMENT("Value",1)
4	=ARGUMENT("X",64)
5	=ARGUMENT("Y",64)
6	=IF(OR(ROWS(X)<>ROWS(Y),ROWS(X)<1,ROWS(Y)<1),RETURN(#VALUE!))
7	=FOR("I",1,ROWS(X)-1)
8	= IF(AND((INDEX(X,I+1)-Value)*(INDEX(X,I)-Value)<=0,INDEX(X,I+1)<>INDEX(X,I)))
9	= RETURN(INDEX(Y,I)*(INDEX(Y,I+1)/INDEX(Y,I))\((Value-INDEX(X,I))/(INDEX(X,I+1)-INDEX(X,I))))
10	= END.IF()
11	=NEXT()
12	=RETURN(#VALUE!)

- 4 -

Figure 1 (cont.)

9

Data Processing with Spreadsheets

9-1 Basics of spreadsheets

9-2 User-defined functions

9-3 Worked examples

INTRODUCTION

Spreadsheet programs such as Lotus 123 and Microsoft Excel are common software for personal computers. Originally intended for business applications, spreadsheets are now capable of performing sophisticated calculations in engineering and science. Spreadsheets are convenient for entering and processing data and displaying it as two- and three-dimensional graphs. Intuitively mastered after a few hours of training, spreadsheets are becoming the most used technique for processing data in the geotechnical laboratory. In this book, we selected Excel (Microsoft Corp. 1994a,b) because it works on Apple and Windows computers. However, our spreadsheet approach to data processing is general enough to be adapted to other spreadsheet programs.

In the following section, we introduce some basic spreadsheet definitions and review their features relevant to the processing of laboratory data. This section, which may be too elementary for experienced users, ends with a list of exercises and questions to probe basic knowledge of spreadsheets. These questions may help users test their understanding and identify the features they should know. The text here applies to both the Macintosh and Windows versions of Excel. The only difference is that the COMMAND key, denoted  for Macintosh, should be replaced by the Control key (CTRL) in Windows.

WORKSHEETS AND WORKBOOKS

As shown in Fig. 1, a spreadsheet (or worksheet) is a matrix of cells to enter data, text or formulas. The columns are numbered from A to Z, then AA, AB to IV, and the rows are numbered from 1 to 16384. Cells are referenced by column then by row. For example, cell B2 is located in column B and row 2. The active cell where the action takes place is highlighted and its name is displayed in the reference area. A cell range is a group of connected cells, columns, and rows. Ranges are referred to by the cells at their extremities (e.g., B:D, 5:7, B2:E5, or C2:F2).

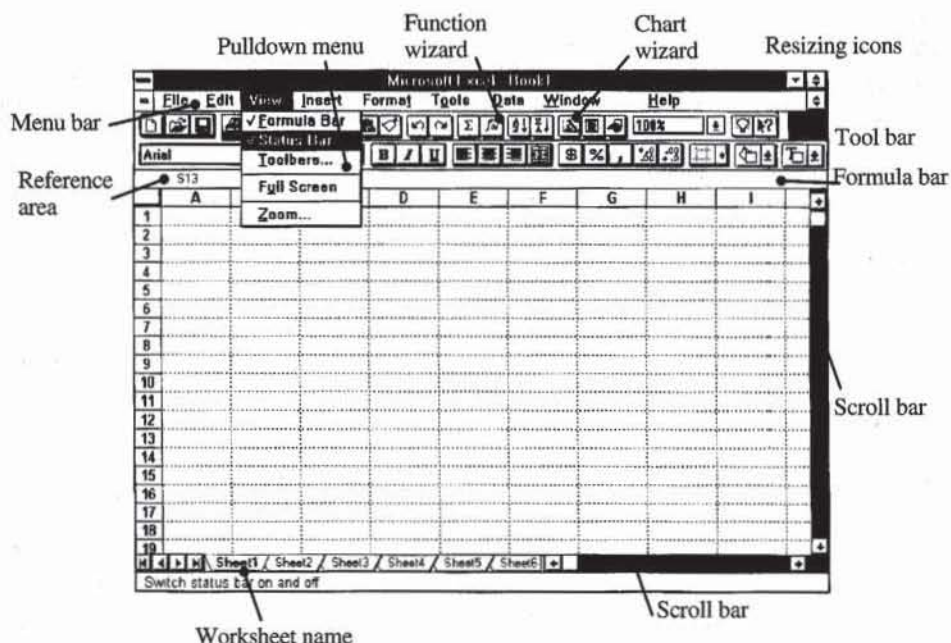


Figure 1 Typical Excel window and some of its parts.

Excel collects several worksheets into workbooks. As shown in Fig. 1, the worksheets are displayed by clicking on their names once and are renamed by clicking twice. Workbooks are useful to organize related materials (e.g., specific types of experiments and projects).

Figure 1 identifies several elements of a workbook. The menu bar displays several pull-down menus (e.g., View) with their specific commands. Some of these commands are listed in Table 1. The title bar displays the name of the workbook. The formula bar displays the data or formula in the active cell. The scroll bars are used to display the rest of the worksheet. The status bar displays various messages or information about the current command. The tool bar contains several icons of commonly used commands. The window may be resized by dragging its lower right corner or double clicking on the icon at the upper right corner.

FORMULAS

By definition, a formula is a mathematical expression that calculates a result from two or more values. Formulas consist of numbers, mathematical operators (+, -, *, /, ^), functions (e.g., COS, SIN), and references to other cells (e.g., B2) or range references (e.g., B2:D10). Cells and cell ranges may be called by using names (e.g., A). All formulas must begin with an equal sign. They are entered and edited as text or numbers. The following are examples of formulas:

- = B4 The cell containing the formula takes the values in cell B4.
- = B4/B2 Divides the contents of cell B4 by that of cell B2.
- = B4 + B2 Adds the contents of cell B4 with that of cell B2.

The mathematical operators obey the common rule of operator precedence. The order of the calculation is %, ^, * and /, +, and - . You may use parentheses to overrule this operator precedence. The result of a formula is calculated and

TABLE 1

Main functions of pull-down menus of the Macintosh version of Excel. In Windows, the COMMAND (apple) key should be replaced by the Control (CTRL) key

Name	Shortcut	Definitions
File Save	apple S	To save an existing workbook or to save and name a new one.
File Save As ...		To save the workbook under a different name or in a different folder or floppy disk.
File New	apple N	To open a new workbook.
File Open	apple O	To open an existing workbook.
File Close	apple W	To close the workbook, which can also be done by clicking on the close icon.
File Quit	apple Q	To finish using Excel. Remember to save your work from time to time when working and before closing it.
File Print	apple P	To print a worksheet.
Edit Redo	apple Y	To repeat the last action.
Edit Undo	apple Z	To undo the last action.
Edit Copy	apple C	To copy a cell or cell range to another location. You may also copy by dragging the selection with the mouse while pressing the Option key.
Edit Paste..	apple V	To paste a cell or cell range that was copied to another location. You may also paste by dragging the selection with the mouse while pressing the Option key.
Edit Cut	apple X	To cut and copy a cell or cell range that is to be pasted somewhere else. You may also move the selection by dragging it with the mouse.
Edit Insert	apple I	To insert a single cell or whole rows and columns.
Edit Clear	apple B	To clear data quickly. You can completely remove the cell contents, format, formula, or attached notes by using the options of Edit Clear.
Edit Delete	apple K	To delete cells or cell ranges. Erroneous deletions can be rectified by using Undo.
Insert Name Paste	apple F	To display the names of all defined variables or arrays.
Insert Name	apple L	To switch between the displays of formulas and results.
	Enter	To name a variable or array.
		To enter an array formula.

displayed in the active cell. You switch between the display of formulas and results by using apple F.

When a formula is copied or moved from one cell to another, the cells that it references are adjusted to compensate for the movement. For instance, as shown in Fig. 2, the formula = A4 + B5 in cell B4 becomes = C8 + D9 when copied to cell D8. The column letter and row number are both shifted, in most cases avoiding the redefinition of the formula.

When the cell reference is to remain unchanged after copying, absolute cell references are used instead of relative references. Absolute references are defined by adding \$ before the column letter and/or row number. As shown in Fig. 2, \$A\$4 is not changed by copying from cell B6 to cell D11, whereas B5 is changed. A mixed reference is partially absolute and partially relative (e.g., \$A4 in cell B8). As shown in Fig. 2, the row number changes, but not the column letter, when cell B8 is copied to cell D14.

Formulas having cells or cell ranges (e.g., B43 + C2 or SUM(A3:B40)) are more difficult to read than mathematical relations with simpler variable names (e.g., = x + t or SUM(T)). Cells or cell ranges can be assigned a name by using apple L. If the variable applies only to the present worksheet, its name should be preceded by the worksheet name and ! (e.g., Example!x for variable x in worksheet Example). The names used in the workbook are defined in the pulldown menu of the reference cell. They can also be listed with their locations by using the list option of **Insert Name Paste ...** The use of variables is highly recommended because it greatly simplifies formulas.

	A	B	C	D	E
1					
2					
3					
4		=A4+B5			
5		=\$A\$4+B5			
6		=\$A4+B7		=C8+D9	
7				=\$A\$4+D10	
8					=\\$A10+D13
9					
10					
11					
12					
13					
14					
15					
16					

Figure 2 Effect of copying formulas in spreadsheets.

BUILT-IN FUNCTIONS

Excel provides built-in functions to construct complex formulas, some of which are listed in Table 2 by categories. The mathematical, trigonometric, and statistical functions are the most commonly used in processing laboratory measurements. The built-in functions may be entered directly or by using the Formula Wizard. The Formula Wizard displays the available functions and their arguments to be completed. Additional help on built-in functions can be obtained from the interactive help.

TABLE 2

List of functions available in Excel

(a) Mathematical and trigonometric functions

<u>ABS(number)</u>	absolute value of a number
<u>ACOS(number)</u>	arccosine of a number (in radian)
<u>ACOSH(number)</u>	inverse hyperbolic cosine of a number
<u>ASIN(number)</u>	arcsine of a number (in radian)
<u>ASINH(number)</u>	inverse hyperbolic sine of a number
<u>ATAN(number)</u>	arctangent of a number
<u>ATAN2(x_num,y_num)</u>	arctangent from x- and y- coordinates
<u>ATANH(number)</u>	inverse hyperbolic tangent of a number
<u>COS(number)</u>	cosine of a number
<u>COSH(number)</u>	hyperbolic cosine of a number
<u>EVEN(number)</u>	rounds a number to the nearest integer
<u>EXP(number)</u>	exponential of a number
<u>FACT(number)</u>	factorial of a number
<u>INT(number)</u>	rounds a number down to the nearest integer
<u>LOG(number, base)</u>	logarithm of a number to a specified base
<u>LOG10(number)</u>	base-10 logarithm of a number
<u>MDETERM(array)</u>	matrix determinant of an array
<u>MINVERSE(array)</u>	matrix inverse of an array
<u>MMULT(array1,array2)</u>	matrix product of two arrays
<u>PI()</u>	value pi
<u>RAND()</u>	random number between 0 and 1
<u>SIGN(number)</u>	sign of a number
<u>SIN(number)</u>	sine of a number
<u>SINH(number)</u>	hyperbolic sine of a number

TABLE 2 (cont.)

List of functions available in Excel

(a) Mathematical and trigonometric functions	
SQRT(number)	square root of a number
SUM(number1,number2,...)	add the arguments
SUMPRODUCT(array1,array2,...)	sum of the products of corresponding components
TAN(number)	tangent of a number
TANH(number)	hyperbolic tangent of a number
(b) Information functions	
ISBLANK(value)	TRUE if the value is blank
ISLOGICAL(value)	TRUE if the value is a logical value
ISNUMBER(value)	TRUE if the value is a number
ISTEXT(value)	TRUE if the value is text
(c) Statistical functions	
AVERAGE(number1,number2,...)	average of the arguments
COUNT(value1,value2,...)	counts how many numbers are in the lists of arguments
COUNTA(value1,value2,...)	counts how many values are in the lists of arguments
GROWTH(known_y's,known_x's,new_x's,const)	returns values of an exponential trend
LINEST(known_y's,known_x's,const,stat)	returns the parameters of a linear trend
LOGEST(known_y's,known_x's,const,stat)	returns the parameters of an exponential trend
MAX(number1,number2,...)	maximum value in a list of arguments
MIN(number1,number2,...)	minimum value in a list of arguments
SLOPE(known_y's,known_x's)	slope of the linear regression line
INTERCEPT(known_y's,known_x's)	intercept of the linear regression line
TREND(known_y's,known_x's,new_x's,const)	returns values along a linear trend
(d) Lookup and reference functions	
COLUMNS(array)	returns the number of columns of an array
INDEX(array, row_num,column_num)	chooses a component of an array
ROWS(array)	returns the number of rows of an array
TRANSPOSE(array)	returns the transpose of an array
(e) Logical functions	
AND(logical1, logical2,...)	returns TRUE if all its arguments are TRUE
FALSE()	returns the logical value FALSE
IF(logical1, value_if_true,value_if_false)	TRUE if the value is not text
NOT(logical)	reverses the logic of its arguments
OR(logical1, logical2,...)	returns TRUE if any argument is TRUE
TRUE()	returns the logical value TRUE
(f) Text functions	
CHAR(number)	returns the character specified by the code number
EXACT(text1,text2)	check to see if two text values are identical
FIND(find_text, within_text,start)	finds one text value within another (case sensitive)
LEFT(text, num_chars)	returns the leftmost characters from a text string
LEN(text)	returns the number of characters in a text string
LOWER(text)	convert text to lower case
RIGHT(text, num_chars)	returns the rightmost characters from a text string
TRIM(text)	removes spaces from text
UPPER(text)	convert text to upper case

ARRAY FORMULAS

An array formula produces an output array (i.e., a cell range). For instance, the built-in linear regression function LINEST fills in several cells for output instead of a single cell. Array formulas are displayed in the formula bar between braces { }.



	A	B
1	x	y
2	1	-1.00
3	2	-0.64
4	3	-0.18
5	4	-0.79
6	5	-0.07
7	6	-0.02
8	7	-0.31
9	8	-0.25
10	9	-0.22
11	10	-0.01
12	Slope	y-intercept
13	0.080	-0.783

	A	B
1	x	y
2	1	=RAND()
3	2	=RAND()
4	3	=RAND()
5	4	=RAND()
6	5	=RAND()
7	6	=RAND()
8	7	=RAND()
9	8	=RAND()
10	9	=RAND()
11	10	=RAND()
12	Slope	y-intercept
13	=LINEST(B2:B10, A2:A10)	=LINEST(B2:B10, A2:A10)

Figure 3 Example of results and array formula for linear regression.

{ } [e.g., {=LINEST(B2:B11,A2:A11)}]. Array formulas are edited by selecting a cell range, entering the formula, and using instead of Enter. As shown in Fig. 3, the array formula {=LINEST(B2:B11,A2:A11)} in cells A13:B13 calculates the slope and intercept of a linear regression for a series of x and y data. The left figure shows the results, and the right one displays the formulas.

FORMATS

The column width and row height may be adjusted by dragging the pointer at the top right edge of the column heading (or bottom edge of the row heading). The column width (or row height) may be optimized by double clicking. Columns or rows may also be hidden by using **Format Row Hide** or **Format Column Hide**.

As shown in Table 3, numbers can be displayed by using various formats of **Format Cells Numbers**. When ##### is displayed, the column width is too narrow for the selected format. The text alignment may be defined by using the left, right, or center options of the **Format Cells Alignment**. The overwriting of cells may be prevented by selecting the **Wrap** option of **Alignment**.

TABLE 3
Examples of formats for numbers

Format	Display
0.00E+00	1.23E+03
0.00	1234.00
#,##0.00	1,234.00
#,##0.00%	123,400.00%
0.0 "m"	1234.0 m

The style (e.g., bold, italic), font (e.g., Geneva, Time, Symbol), size of font (e.g., 12 pt, 14 pt), and color of cells can be modified by using the options of **Format Cells Font**. Borders and shading can also be added by using **Format Cells Borders**. By default, grid lines are displayed on the spreadsheet screen. They may be hidden by options in **Tools Options View**. Shading and various gray levels can also be added by using **Format Cells Pattern**.

PRINTING YOUR WORKSHEET

In the dialog box of **File Page Setup...** you may select the landscape or portrait orientations, paper size, margin positions, scaling, and range of pages to be printed. You may center horizontally and/or vertically your print on each page. You may add or delete the row and column headings, grid lines, headers (e.g., titles), and footers (e.g., page numbers). You may print a smaller area of the worksheet by using **File PageSetup Set Print Area...** and define your own page breaks by using **Insert Page Break.** You may preview the print on the screen by using **File Print Preview....** While previewing, you may interactively setup the pages and margins. You may select the page range and number of copies to be printed in the Print dialog box.

CREATING CHARTS

Excel offers several types of two- or three-dimensional charts, including pie, bar, column, area, and line graphs. Charts are created by using the Chart Wizard as follows. Click on the Chart Wizard Icon, open a plotting window in the worksheet with the mouse, and enter the input as required by the Chart Wizard.

Charts can be copied, moved, and resized. They are edited by double clicking on them. A title is added to the chart or the axes by using **Insert Titles.** The font, size, orientation, and alignment of axis labels, scales, tick marks, line thicknesses, number formats, fonts, and patterns may be changed by double clicking on the axis. The same technique also applies to change the minimum and maximum intervals along the axis, to reposition the *x* and *y* axes, and to select a logarithmic axis.

Two-dimensional x-y line graphs and scattered point charts are the most commonly used for representing laboratory results. The line styles and data point symbols are changed by double clicking on them. New data sets may be added to the same chart by using **Insert New Data....** The series can also be reordered. Multiple data sets may be labeled with legends by using **Insert Legend.** The legends may be repositioned by dragging them to a new position.

REFERENCES

Microsoft Corporation, 1994a, Microsoft Excel, *User's Guide, Version 5.*

Microsoft Corporation, 1994b, Microsoft Excel, *Visual Basic User's Guide, Version 5.*

EXERCISES

1. Name 10 different parts in a spreadsheet.
2. Do you know how to:

 Resize and move a worksheet window?
 Save a worksheet with the same name or with a new name?
 Open a new or existing workbook?
 Move between worksheets?
 Close a workbook?
 Enter and edit text, numbers, dates and times?
 Fill in a series of data?

- Use undo and redo?
 - Select a cell range?
 - Copy, move, and erase data?
 - Copy or move a worksheet to another workbook?
 - Insert and delete individual cells, rows, and columns?
 - Write and enter formulas?
 - Display formulas instead of their results?
 - Copy formulas?
 - Use the formula wizard?
 - Enter an array formula?
 - Format and align numbers?
 - Define names for variables and arrays that are local to a worksheet?
 - Enter formulas with named variables?
 - List all the variables defined in the workbook?
 - Rename a variable?
 - Change the display format?
 - Change alignment?
 - Center text over multiple columns?
 - Change the font?
 - Add a border around a cell or cell range?
 - Shade a cell range?
 - Change column width and row height?
 - Apply existing styles to a cell range?
 - Change the default display format and alignment?
 - Create styles?
 - Change the print setup?
 - Choose the print area?
 - Adjust page breaks?
 - Preview a print job?
 - Print a worksheet?
 - Create and save charts?
 - Choose the chart type?
 - Print a chart?
 - Resize a chart?
 - Add a title and legend to a chart?
 - Format text on a chart?
 - Change scale and tick marks?
 - Select a logarithmic axis and change the axis intersection?
3. What are relative and absolute cell references (addresses)?
 4. What are styles for Excel spreadsheets? What are their advantages?
 5. What is an array formula?
 6. What are worksheets and workbooks?
 7. Which is the easiest way to define a formulas with built-in functions?

INTRODUCTION

A user-defined function is created by combining formulas and built-in functions, and is used as other built-in functions. A user-defined function may be created by using a macrosheet or Visual Basic. A macrosheet looks like a spreadsheet but contains functions and commands instead of input data. It is the original programming language of spreadsheets. Visual Basic is a more recent and advanced programming language that is similar to Basic and other computer languages. For instance, Fig. 1 shows the user-defined function SIND, which calculates the sine of angles in degrees, in the macrosheet language and Visual Basic.

MACROSHEET USER-DEFINED FUNCTIONS

In a macrosheet, a user-defined function is a succession of formulas, ordered in a column with a specific structure. The first line contains its name (e.g., SIND in Fig. 1). The second line defines its output type, which may be a number, a text, a logical, a reference, an error message, an array, or a combination of the above. The output type is defined by RESULT followed by a data type. The various data types are listed in Table 1. If the result is a number or a text, the data type is 3. RESULT must come before any other formulas. If you omit the data type, the data type is assumed to be 7 by default (i.e., a number, a text, or a logical). In the example of Fig. 1, the result of SIND is a number.

A	
1	SIND
2	=RESULT(1)
3	=ARGUMENT("X",1)
4	=RETURN(SIN(PI()*X/180))

```
Const Pi = 3.141592654
Function Sind(x)
Sind = Sin(Pi * x / 180)
End Function
```

Figure 1 Example of user-defined function in a macrosheet (left) and Visual Basic (right).

TABLE 1
Data type for functions
ARGUMENT and **RESULT**

Value	Data type
1	Number
2	Text
4	Logical
8	Reference
16	Error
64	Array

Like built-in functions, user-defined functions have input variables. Each input variable must individually be defined by using ARGUMENT in the column under RESULT. ARGUMENT specifies the name and type of each input variable name. The name is entered as text between double quote marks. For instance, in Fig. 1, the angle in degree is named X. ARGUMENT specifies the data type in a similar way to RESULT. This type may be a number, a text, a logical, a reference, an error message, an array, or a combination of the above.

Following ARGUMENT, the users define the formulas that perform the main operation of their function. These formulas may invoke cell references within the worksheet and names of variables defined by ARGUMENT or **AL**. For instance, the calculation is performed in cell A4 of Fig. 1 by using the variable named X by ARGUMENT. A user-defined function is terminated by using RETURN, which branches the calculation back to the worksheet.

Writing a User-Defined Function

There are two steps in defining a user-defined function: (1) creating it and (2) naming it. A new macrosheet is created within a workbook by choosing **Insert Macro MS Excel 4.0 Macro**. The same macrosheet may contain several user-defined functions. A user-defined function is named by selecting its first cell, by choosing **Insert Name Define** (or **AL**), by entering the function name in the **Name** box, and by selecting the **Function** option.

Using a User-Defined Function in a Worksheet

You may use a user-defined function by using the **Function Wizard**, which lists the active user-defined functions after the built-in functions. In the window of the Function Wizard, replace the arguments of the user-defined function with cell(s) or cell range(s). When the desired user-defined functions do not appear in this list, check that their names have been defined with **AL** and that their macrosheet is open.

VISUAL BASIC USER-DEFINED FUNCTIONS

In Visual Basic, a user-defined function is created within a workbook by **Insert Module**. It starts with **Function** followed by the function name and ends with **End Function**. The function type can be Single or Variant, depending on whether it returns a number or an array (other types besides Single and Variant are also available as specified in the Visual Basic User's Guide). On the line after **Function**, the types of the function arguments should be defined. When the arguments are undefined, they are considered as Variant. Visual Basic has its own built-in func-

```
Function MyLinest(X,Y) As Variant
    Slope = Application.SLOPE(Y,X)
    Intercept = Application.INTERCEPT(Y,X)
    MyLinest = Array(Slope,Intercept)
End Function
```

Figure 2 Example of Visual Basic function using built-in macrosheet functions.

tions, which in most cases have spellings similar to those of macrosheet built-in functions. Some built-in macrosheet functions are called from within Visual Basic by using the prefix Application (Fig. 2). Visual Basic is a powerful language that extends the capabilities of macrosheets. Its functions are linked automatically to the workbook and do not need to be defined with XL.

REFERENCE

Microsoft Corporation, 1994, Microsoft Excel, *Visual Basic User's Guide, Version 5*.

EXERCISES

1. What is a user-defined function?
2. What is a macrosheet? What is the main difference between a worksheet and a macrosheet?
3. What is the basic structure of a user-defined function in a macrosheet?
4. How do you use an existing user-defined function?
5. How do you define the input and output of a user-defined function?
6. Write a user-defined function that calculates the cosine of an angle in degrees.
7. What is Visual Basic?

9-3 Worked Examples

EXAMPLE 1: SUPERIMPOSED GRAPHS

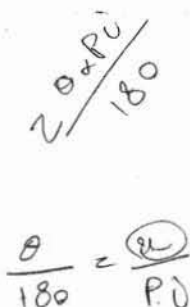
EXERCISE

Plot functions $\sin(2\theta)$ and $\cos(2\theta)$ on the same graph when angle θ varies from 0 to 180° . Format the graph as shown in Fig. 1 and tabulate the data as shown in Fig. 2.

STEPS

The table of Fig. 1 is obtained as follows:

- Create a new workbook with File New.
- Enter the table headings in cells A3, B3, and C3.
- Enter 0 in cell A4.
- Select range A4:A40 with the mouse.
- In the dialog box of **Edit Fill Series**, enter 5 for step value. Cells A4 to A40 now display the θ values.
- Press **⌘L** and enter Example1!q to name the range A4:A40 (or abcd!q if abcd is the name of your worksheet). q stands for the Greek symbol θ , which cannot be used.
- Enter = $\sin(2*Pi()/180*q)$ in cell B4 and = $\cos(2*Pi()/180*q)$ in cell C4 (Fig. 3).
- Select cells B4:C4 and press **⌘C**.
- Select range B4:C40 and press **⌘V**. All the numbers of Fig. 1 should now be displayed.
- Move to cell A43 and list the names and locations of the variables in the workbook by using **Insert Name Paste ... Paste Link**.
- Adjust the column widths by double clicking on the edges of the column headings or by dragging them.



- Select the range B4:C40 use **Format Cells Numbers ...**, or **#,###**, and enter the format 0.00.
- Select the range A3:C40 and choose the horizontal centering option of **Format Cells Alignment....**
- Edit cells A3, B3, and C3 to obtain the symbol θ with **Format Cells Font**.
- Define the table border with **Format Cells Border** so that your table looks like that of Fig. 1.

The chart of Fig. 2 is obtained as follows:

- Click on the Chart Wizard Icon and open a plotting window by dragging the mouse on the spreadsheet.
- Select the range A3:C40 by using the mouse, then press **Next >**.
- Select the XY scatter chart type, then press **Next >**.
- Select the option with connected points and linear axes, then press **Next >**.

	A	B	C
3	θ (deg)	$\sin(2\theta)$	$\cos(2\theta)$
4	0	0.00	1.00
5	5	0.17	0.98
6	10	0.34	0.94
7	15	0.50	0.87
8	20	0.64	0.77
9	25	0.77	0.64
10	30	0.87	0.50
11	35	0.94	0.34
12	40	0.98	0.17
13	45	1.00	0.00
14	50	0.98	-0.17
15	55	0.94	-0.34
16	60	0.87	-0.50
17	65	0.77	-0.64
18	70	0.64	-0.77
19	75	0.50	-0.87
20	80	0.34	-0.94
21	85	0.17	-0.98
22	90	0.00	-1.00
23	95	-0.17	-0.98
24	100	-0.34	-0.94
25	105	-0.50	-0.87
26	110	-0.64	-0.77
27	115	-0.77	-0.64
28	120	-0.87	-0.50
29	125	-0.94	-0.34
30	130	-0.98	-0.17
31	135	-1.00	0.00
32	140	-0.98	0.17
33	145	-0.94	0.34
34	150	-0.87	0.50
35	155	-0.77	0.64
36	160	-0.64	0.77
37	165	-0.50	0.87
38	170	-0.34	0.94
39	175	-0.17	0.98
40	180	0.00	1.00

Figure 1 Variation of $\sin(2\theta)$ and $\cos(2\theta)$ with θ .

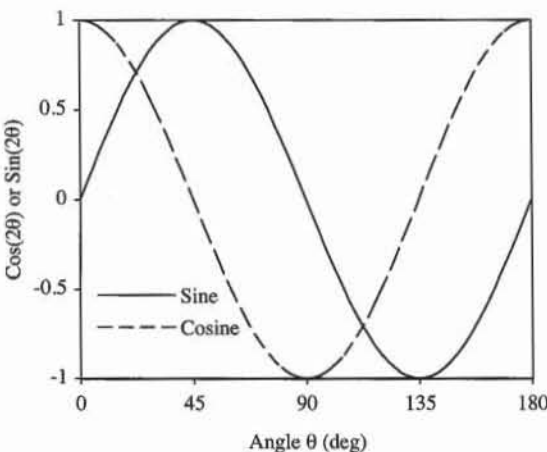


Figure 2 Plots of $\sin(2\theta)$ and $\cos(2\theta)$.

- Assign the data series in columns, using the first column for X data. Assign the legend in the first row, enter “Angle (deg)” for the X-category axis title and “Cosine or Sine” for the Y-values axis title, then press **Finish**.

A chart should now be displayed in Excel’s built-in format. In the following steps, you will modify this graph so that it looks like Fig. 2.

- Select the chart by double clicking on it.
- Double click on the shaded area to display the **Format Plot Area** dialog box. Select a border and no area, then press OK.
- Double click on the vertical axis to display the **Format Axis** dialog box. In **Patterns**, select outside major tick marks and no minor tick marks. Move to **Scale** and enter 0.5 for major unit and -1 for the value at which the X axis crosses the vertical axis. Move to **Font** and select 10-pt Times.
- Double click on the horizontal axis to display the **Format Axis** dialog box. In **Patterns**, select outside major tick marks and no minor tick marks. Move to **Scale** and enter 180 for maximum and 45 for major unit. Move to **Font** and select 10-pt Times.
- Double click on the series of Cosine data points to display the **Format Data Series** dialog box. In **Patterns**, select a solid line and no marker. In **Names and Values**, enter Cosine for name, then press OK.
- Double click on the series of Sine data points to display the **Format Data Series** dialog box. In **Patterns**, select a dashed line and no marker. In **Names and Values**, enter Sine for name, then press OK.
- Drag the box containing the series labels to the location shown in Fig. 2.
- Double click on the box to display the **Format Labels** dialog box. Select no border and no area, then press OK.
- Double click on the horizontal axis title to edit it and introduce the symbol θ . Type the letter *q*, select it, and change its font from Times to Symbol. Note that you cannot edit graph labels that are set equal to the contents of spreadsheet cells.

	A	B	C
3	θ (deg)	$\sin(2\theta)$	$\cos(2\theta)$
4	0	=SIN(2*PI()/180*q)	=COS(2*PI()/180*q)

Figure 3 Formulas used in Fig. 1.

- Double click on the vertical axis title to edit it and introduce q as shown in Fig. 2.
- You may drag the chart and scale it by using its edge points.

EXAMPLE 2: FITTING OF DATA POINTS WITH A POWER RELATION

EXERCISE

Find the power relation between U.S. sieve number N and mesh opening d in Fig. 4, and compare the fitted and original results on a log-log graph. Use the built-in functions TREND, SLOPE, INTERCEPT, and LINEST, and fit data by using Trendline.

STEPS

- In a new workbook, enter column headings in cells A8:C9 and numbers in cell range A10:B38, and format them as shown in Fig. 4.
- Assign the name N to the range A10:A38, using AL . In the same way, assign the name d to the range B10:B38. You may use the reference area or **Insert Name Paste ... Paste Link** to verify the names.
- Select the range C10:C38, type the formula as shown in cell C10 of Fig. 5, and press Enter . The cell range C10:C38 should be filled as shown in Fig. 4.
- Use the Chart Wizard, to plot the ranges C10:C38 versus A10:A38 as a solid line and the ranges B10:B38 versus A10:A38 as discrete points. Select logarithmic axes and define titles for axes as shown in Fig. 6.
- Select the range C41:D41, type the formula with LINEST in cell C41 as shown in Fig. 7, and press Enter . The results of Fig. 8 should be displayed. The final result is $d = 10^b N^a$, where d is the mesh opening (mm), N the U.S. sieve number, a the slope of linear regression ($a = -1.085$), and b the intercept of linear regression ($b = 1.360$).
- In cells C42 and C43, enter the formulas of Fig. 7 to obtain a and b by using SLOPE and INTERCEPT.
- Use the Chart Wizard to plot the ranges B10:B38 versus A10:A38 as discrete points. Format the graph as shown in Fig. 9.
- Select the data points and use **Insert Trendline...** In **Options**, select to display the equation and R^2 value on the chart. In **Type**, select the power relation. You should obtain the graph of Fig. 9, and the equation displayed by Trendline should yield the same results as those found by LINEST, SLOPE, and INTERCEPT.

Arrays

* Using

71

	A	B	C
8	US sieve number	Sieve opening (mm)	Fitted sieve opening (mm)
9	N	d	
10	4	4.750	5.098
11	5	4.000	4.002
12	6	3.350	3.284
13	7	2.800	2.778
14	8	2.360	2.404
15	10	2.000	1.887
16	12	1.700	1.548
17	14	1.400	1.310
18	16	1.180	1.133
19	18	1.000	0.997
20	20	0.850	0.890
21	25	0.710	0.699
22	30	0.600	0.573
23	35	0.500	0.485
24	40	0.425	0.420
25	45	0.355	0.369
26	50	0.300	0.329
27	60	0.250	0.270
28	70	0.212	0.229
29	80	0.180	0.198
30	100	0.150	0.155
31	120	0.125	0.127
32	140	0.106	0.108
33	170	0.090	0.087
34	200	0.075	0.073
35	230	0.063	0.063
36	270	0.053	0.053
37	325	0.045	0.043
38	400	0.038	0.035

Figure 4 U.S. sieve number, sieve opening, and fitted values.

C	
	Fitted sieve opening (mm)
8	
9	
10	=10^TREND(LOG10(d),LOG10(N),LOG10(A10))
11	=10^TREND(LOG10(d),LOG10(N),LOG10(A11))
12	=10^TREND(LOG10(d),LOG10(N),LOG10(A12))

Figure 5 Formula for defining fitted points for chart.

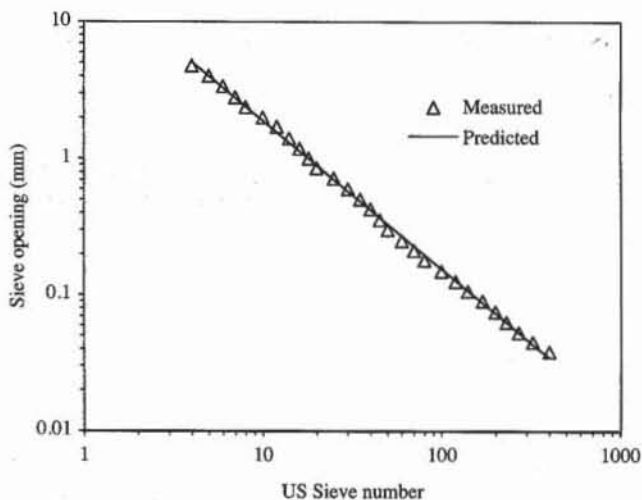


Figure 6 Comparison of data points and results fitted by using TREND.

	B	C	D
41	Slope, Intercept = =LINEST(LOG10(d),LOG10(N))	=LINEST(LOG10(d),LOG10(N))	
42	Slope = =SLOPE(LOG(d),LOG(N))		
43	Intercept = =INTERCEPT(LOG(d),LOG(N))		

Figure 7 Formulas used in Fig. 8.

	A	B	C	D
40	Result of linear regression analysis using LINEST			
41	Slope, Intercept = -1.08461 1.36039			
42	Slope = -1.08461			
43	Intercept = 1.36039			

Figure 8 Results of linear regression analysis with built-in functions LINEST, SLOPE, and INTERCEPT.

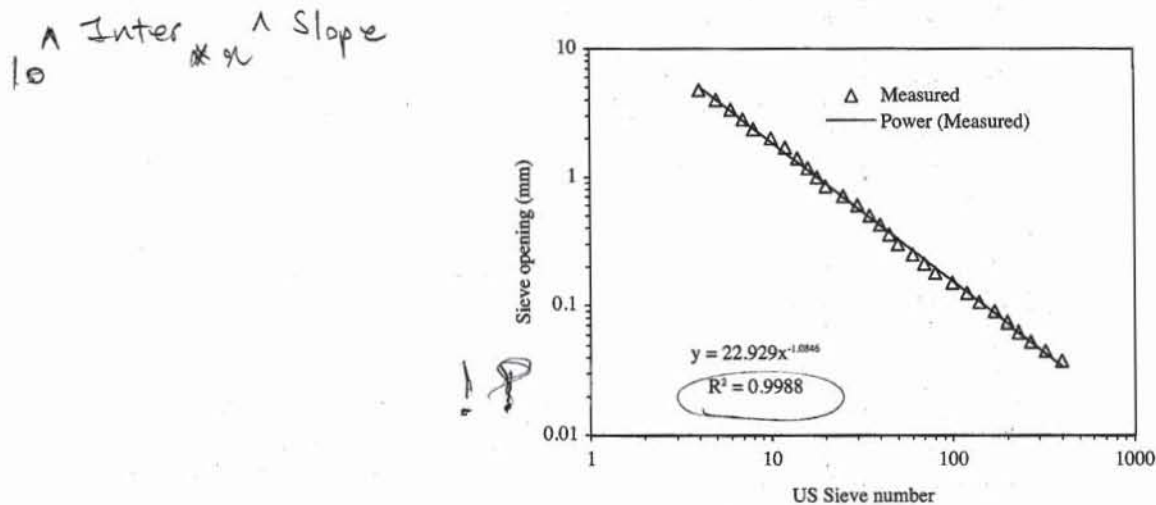


Figure 9 Comparison of data points and results fitted by using Trendline.

EXAMPLE 3: CUBIC POLYNOMIAL FITTING OF DATA POINTS

EXERCISE

Find the two cubic polynomials that describe the variations of water viscosity and water unit mass with temperature. The data measured are listed in Fig. 10. Plot the fitted and measured viscosity and unit mass versus temperature (Fig. 11). Use the method in Chapter 8-1 to determine the polynomial coefficients, and compare your results with those obtained by Trendline.

STEPS

- In a new workbook, enter and format the heading and data of the table in Fig. 10.
- Assign the names T , hw , and rw to cell ranges A8:A23, B8:B23, and C8:C23. Unfortunately, neither the Greek symbols η and ρ nor superscripts or subscripts can be used for variable names.

	A	B	C
6	Temperature (° C)	Viscosity (g/s/cm)	Unit mass (g/cm³)
7	T	T _w	ρ _w
8	4.0	0.01567	1.00000
9	16.0	0.01111	0.99897
10	17.0	0.01083	0.99880
11	18.0	0.01056	0.99862
12	19.0	0.01030	0.99844
13	20.0	0.01005	0.99823
14	21.0	0.00981	0.99802
15	22.0	0.00958	0.99780
16	23.0	0.00936	0.99757
17	24.0	0.00914	0.99733
18	25.0	0.00894	0.99708
19	26.0	0.00874	0.99682
20	27.0	0.00855	0.99655
21	28.0	0.00836	0.99627
22	29.0	0.00818	0.99598
23	30.0	0.00801	0.99568

Figure 10 Measured variations of water viscosity and water unit mass with temperature.

	A	B	C
48	Temperature (° C)	Viscosity (g/s/cm)	Unit mass (g/cm³)
49	T _a		
50	1.0	0.01721	0.99995
51	2.0	0.01668	0.99998
52	3.0	0.01616	1.00000
53	4.0	0.01567	1.00000
54	5.0	0.01520	0.99999
55	6.0	0.01474	0.99996
56	7.0	0.01430	0.99992
57	8.0	0.01389	0.99986
58	9.0	0.01348	0.99980
59	10.0	0.01310	0.99972
60	11.0	0.01273	0.99962
61	12.0	0.01238	0.99951
62	13.0	0.01204	0.99940
63	14.0	0.01172	0.99926
64	15.0	0.01141	0.99912
65	16.0	0.01111	0.99897
66	17.0	0.01083	0.99880
67	18.0	0.01056	0.99862
68	19.0	0.01030	0.99843
69	20.0	0.01005	0.99823
70	21.0	0.00981	0.99802
71	22.0	0.00958	0.99780
72	23.0	0.00936	0.99757
73	24.0	0.00914	0.99733
74	25.0	0.00894	0.99708
75	26.0	0.00874	0.99682
76	27.0	0.00855	0.99655
77	28.0	0.00836	0.99627
78	29.0	0.00818	0.99598
79	30.0	0.00801	0.99568

Figure 11 Fitted variations of water viscosity and water unit mass.

- Define the 16 entries of matrix *A* in cell range A25:D28, as shown in Fig. 12, and assign the name *A* to this range by using $\text{apple}L$.
- Select the range A30:D33, type the formula of cell A30 shown in Fig. 12, and press $\text{apple}Enter$. Assign the name *AI* to the range A30:D33 by using $\text{apple}L$.
- Enter the formulas for the vectors *Bh* and *Br* in cell ranges A36:A39 and A42:A45, as shown in Fig. 12, and assign the names *Bh* and *Br* to these ranges by using $\text{apple}L$.
- Select the range C36:C39, type the contents of cell C36 shown in Fig. 12, and press $\text{apple}Enter$. The coefficients of the cubic polynomial should be as shown in Fig. 13. Assign the names *A_0*, *A_1*, *A_2*, and *A_3* to cells C36 to C39 by using $\text{apple}L$. The names *a1*, *a2*, and *a3* cannot be used because they conflict with cell names.
- Select the range C42:C45, type the contents of cell C42 shown in Fig. 12, and press $\text{apple}Enter$. Assign the names *B_0*, *B_1*, *B_2*, and *B_3* to cells C42 to C45.
- Define the table of Fig. 11 showing cells A48:C79. Use the edit Fill series to generate the temperature data. Enter the formulas in cells B50 and C50, as shown in Fig. 14, and copy them to range B50:C79.

	A	B	C	D
24	Matrix A			
25	=COUNT(T)	=SUM(T)	=SUMPRODUCT(T,T)	=SUMPRODUCT(T,T,T)
26	=B25	=C25	=D25	=SUMPRODUCT(T,T,T)
27	=B26	=C26	=D26	=SUMPRODUCT(T,T,T,T)
28	=B27	=C27	=D27	=SUMPRODUCT(T,T,T,T,T)
29	Inverse matrix A ⁻¹			
30	=MINVERSE(A)	=MINVERSE(A)	=MINVERSE(A)	=MINVERSE(A)
31	=MINVERSE(A)	=MINVERSE(A)	=MINVERSE(A)	=MINVERSE(A)
32	=MINVERSE(A)	=MINVERSE(A)	=MINVERSE(A)	=MINVERSE(A)
33	=MINVERSE(A)	=MINVERSE(A)	=MINVERSE(A)	=MINVERSE(A)
34	Nonlinear regression for viscosity (cubic)			
35	Vector Bh		Polynomial coefficients	
36	=SUM(hw)		a ₀ = =MMULT(AI,Bh)	
37	=SUMPRODUCT(T,hw)		a ₁ = =MMULT(AI,Bh)	
38	=SUMPRODUCT(T,T,hw)		a ₂ = =MMULT(AI,Bh)	
39	=SUMPRODUCT(T,T,T,hw)		a ₃ = =MMULT(AI,Bh)	
40	Nonlinear regression for unit mass (cubic)			
41	Vector Br		Polynomial coefficients	
42	=SUM(rw)		b ₀ = =MMULT(AI,Br)	
43	=SUMPRODUCT(T,rw)		b ₁ = =MMULT(AI,Br)	
44	=SUMPRODUCT(T,T,rw)		b ₂ = =MMULT(AI,Br)	
45	=SUMPRODUCT(T,T,T,rw)		b ₃ = =MMULT(AI,Br)	

Figure 12 Formulas used in Fig. 13.

	A	B	C	D
24	Matrix A			
25		16	349	8231
26		349	8231	201889
27		8231	201889	5095943
28		201889	5095943	131689249
29	Inverse matrix A ⁻¹			
30		6.975278585	-1.6770185	0.1042623
31		-1.677018533	0.4732953	-0.031107
32		0.104262304	-0.0311065	0.0020889
33		-0.001899598	0.0005829	-3.9654E-05
34	Nonlinear regression for viscosity (cubic)			
35	Vector Bh		Polynomial coefficients	
36		0.15719	a ₀ = 0.0177717	
37		3.25593	a ₁ = -0.000568	
38		74.93481	a ₂ = 1.115E-05	
39		1806.32571	a ₃ = -1.02E-07	
40	Nonlinear regression for unit mass (cubic)			
41	Vector Br		Polynomial coefficients	
42		15.96216	b ₀ = 0.99991	
43		348.06384	b ₁ = 5.202E-05	
44		8207.227	b ₂ = -7.51E-06	
45		201271.7513	b ₃ = 3.605E-08	

Figure 13 Results of cubic polynomial regression.

- Use the Chart Wizard to plot the measured and fitted data, as shown in Figs. 15 and 16.

Cubic polynomial fitting with Trendline.

- Use the Chart Wizard to plot the measured data, as shown in Figs. 17 and 18.

	A	B	C
48	Temperature (° C) T_e	Viscosity (g/s/cm)	Unit mass (g/cm³)
49			
50	1	=A_0+A_1*Te+A_2*Te^2+A_3*Te^3	=B_0+B_1*Te+B_2*Te^2+B_3*Te^3
51	2	=A_0+A_1*Te+A_2*Te^2+A_3*Te^3	=B_0+B_1*Te+B_2*Te^2+B_3*Te^3

Figure 14 Formulas used in Fig. 2.

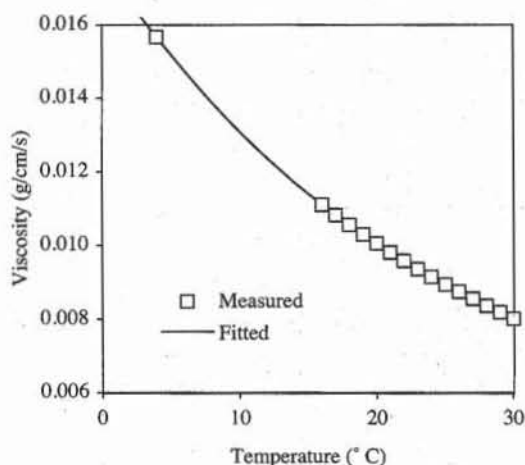


Figure 15 Variation of measured and fitted viscosity with temperature.

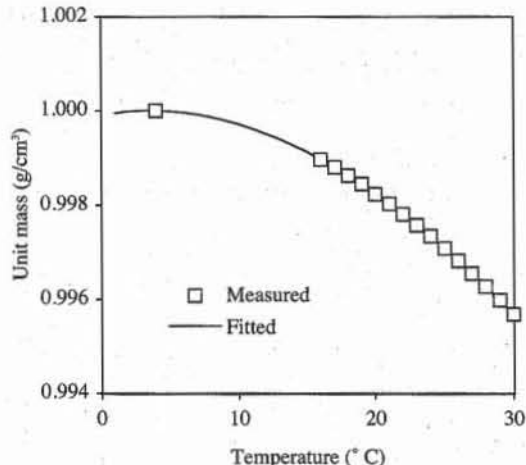


Figure 16 Variation of measured and fitted unit mass with temperature.

- Select the data points, and use **Insert Trendline**. In **Options**, select the display of equation and R^2 value, and in **Type**, select the polynomial fitting with a degree equal to 3. The results obtained by Trendline should be identical to those obtained in the preceding section.

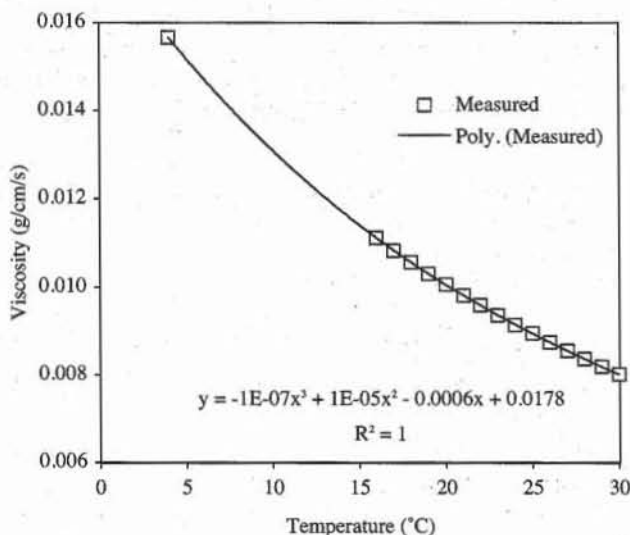


Figure 17 Variation of water viscosity with temperature fitted by using Trendline.

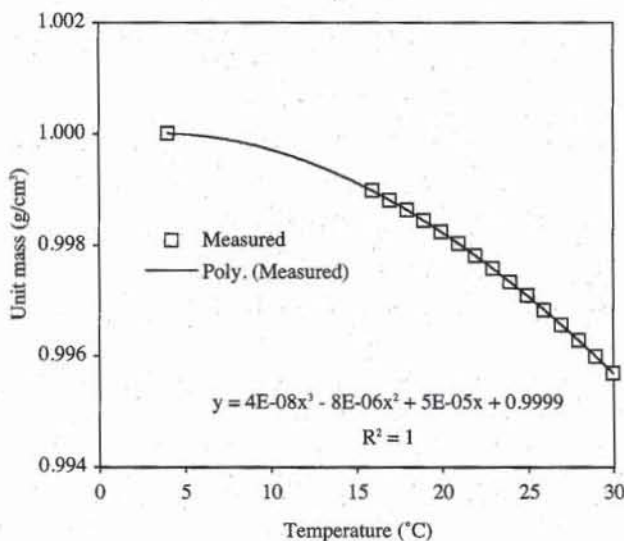


Figure 18 Variation of water unit mass with temperature fitted by using Trendline.

EXAMPLE 4: USER-DEFINED FUNCTIONS FOR UNIT MASS AND VISCOSITY OF WATER

EXERCISE

Write two user-defined functions to calculate the water viscosity η in $\text{g}/\text{cm}\cdot\text{s}$ and the water unit mass ρ_w (g/cm^3) as a function of the temperature T ($^\circ\text{C}$).

$$\eta = 0.0178 - 5.684 \times 10^{-4}T + 1.115 \times 10^{-5}T^2 - 1.017 \times 10^{-7}T^3$$

$$\rho_w = 0.99991 + 5.202 \times 10^{-5}T - 7.512 \times 10^{-6}T^2 + 3.605 \times 10^{-8}T^3$$

Write a user-defined function in the macrosheet and Visual Basic languages. Plot the variations of water viscosity and water unit mass on the same graph with primary and secondary vertical axes.

STEPS

- In a new workbook, use **Insert Macro MS Excel 4.0 Macro** to create a new macrosheet.
- Type the formulas as shown in Fig. 19.
- Assign the name **VISCO** and **DENSI** to cells A1 and A6 by using **AL**. In both cases, check the **Function** option when naming macros.
- Use **Insert Module** to create the Visual Basic functions **VBvisco** and **VBDensi** shown in Fig. 20. The functions are given different names in order not to conflict with the corresponding macrosheet functions. You do not need to define the function names because this is automatically done by Visual Basic.
- In a worksheet created by using **Insert Worksheet**, define the heading

	A	B
1	VISCO	Viscosity of water in g/cm/s
2	=RESULT(1)	
3	=ARGUMENT("T",1)	Temperature in degrees Celsius
4	=RETURN(0.0178-5.684/10^4*T+1.115/10^5*T^2-1.017/10^7*T^3)	
5		
6	DENSI	Density of water in g/cm ³
7	=RESULT(1)	
8	=ARGUMENT("T",1)	Temperature in degrees Celsius
9	=RETURN(0.99991+5.202/10^5*T-7.512/10^6*T^2+3.605/10^8*T^3)	

Figure 19 Macrosheet user-defined function for water viscosity and water unit mass.

```

Viscosity of water in g/cm/s at temperature T in degree Celsius
Function VBvisco(T)
    VBvisco = 0.0178 - 5.684/10^4*T + 1.115/10^5*T^2 - 1.017/10^7*T^3
End Function

'Unit mass of water in g/cm3 at temperature T in degree Celsius
Function VBDensi(T)
    VBDensi = 0.99991 + 5.202/10^5*T - 7.512/10^6*T^2 + 3.605/10^8*T^3
End Function

```

Figure 20 Visual Basic user-defined function for water viscosity and water unit mass.

and column A of Fig. 21 (the formulas used in Fig. 21 are listed in Fig. 22). Use **Edit Fill Series** to generate the temperature data. Assign the name *T* to cells A8:A37 by using **AL**.

- Enter the formulas shown in cells B8 and C8, and copy them onto cells B9:C37.
- Use the Chart Wizard to create the graph of Fig. 23. Introduce the secondary axis for the water viscosity, add legends, and format the graph so that it looks like Fig. 23.
- After having tested the macrosheet functions VISCO and DENSI, you may test the Visual Basic functions. Replace VISCO and DENSI with VBvisco and VBDensi by using **AH**.

EXAMPLE 5: USER-DEFINED FUNCTION FOR LINEAR REGRESSION

EXERCISE

Write a user-defined function that performs a linear regression in the same way as the built-in function LINEST. Write the user-defined function in the macrosheet and Visual Basic languages. Compare the results of LINEST and your own function in the case of a random series.

STEPS

- In a new workbook, use **Insert Macro MS Excel 4.0 Macro** to create a new macrosheet.
- Type the formulas as shown in Fig. 24.

	A	B	C
6	Temperature (° C)	Viscosity (g/s/cm)	Unit mass (g/cm ³)
7	T		
8	1.0	0.01724	0.99995
9	2.0	0.01671	0.99998
10	3.0	0.01619	1.00000
11	4.0	0.01570	1.00000
12	5.0	0.01522	0.99999
13	6.0	0.01477	0.99996
14	7.0	0.01433	0.99992
15	8.0	0.01391	0.99986
16	9.0	0.01351	0.99980
17	10.0	0.01313	0.99972
18	11.0	0.01276	0.99962
19	12.0	0.01241	0.99951
20	13.0	0.01207	0.99940
21	14.0	0.01175	0.99926
22	15.0	0.01144	0.99912
23	16.0	0.01114	0.99897
24	17.0	0.01086	0.99880
25	18.0	0.01059	0.99862
26	19.0	0.01033	0.99843
27	20.0	0.01008	0.99823
28	21.0	0.00984	0.99802
29	22.0	0.00961	0.99780
30	23.0	0.00939	0.99757
31	24.0	0.00917	0.99733
32	25.0	0.00897	0.99708
33	26.0	0.00877	0.99682
34	27.0	0.00858	0.99655
35	28.0	0.00839	0.99627
36	29.0	0.00821	0.99598
37	30.0	0.00804	0.99568

Figure 21 Variation of water unit mass and viscosity with temperature.

	A	B	C
6	Temperature (° C)	Viscosity (g/s/cm)	Unit mass (g/cm ³)
7	T		
8	1	=VISCO(T)	=DENSI(T)
9	2	=VISCO(T)	=DENSI(T)

Figure 22 Formulas used in Fig. 21.

- Assign the name **MYLINEST** to cell B1 by using **⌘L**. Check the **Function** option when defining the name. Assign the names *n*, *Ax*, *AY*, *Axx*, *Axy*, and *D* to cells A5 to A10. These names should be preceded by the macrosheet name and ! for these local variables to be declared only in the macrosheet.
- Use **Insert Module** and create the Visual Basic function VBLINEST of Fig. 25. You do not need to name it.
- In a new worksheet created with **Insert Worksheet**, type cells A5:A15 and B5 as shown in Fig. 26.
- Enter the formula of Fig. 27 in cell B6 and copy it in range B6:B15, as shown in Fig. 26. Assign the names *x* and *y* to the ranges A6:A15 and B6:B15 by using **⌘L**.
- Select range C17:D17, use the Function Wizard to call LINEST, complete the arguments as shown in Fig. 27, and press **⌘Enter**.
- Select range C19:D19, use the Function Wizard to call MYLINEST, complete the arguments as shown in Fig. 27, and press **⌘Enter**. The results of MYLINEST and LINEST should be identical.

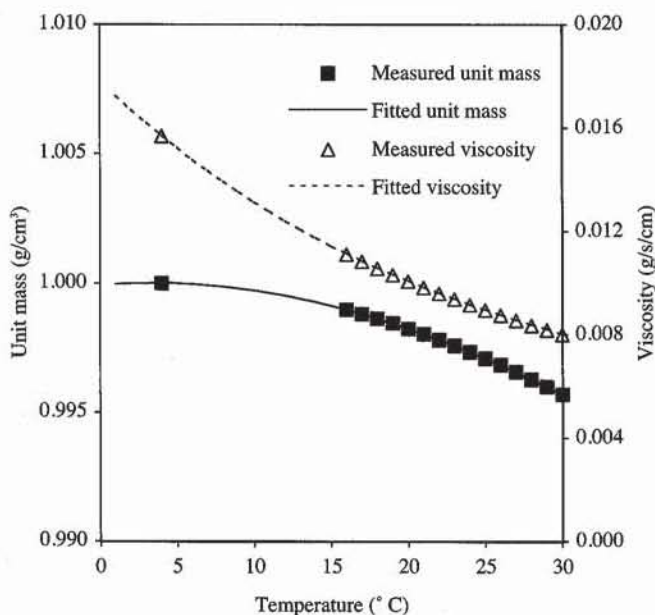


Figure 23 Variation of water unit mass and water viscosity with temperature.

A	B	C
1	MYLINEST	name of function
2	=RESULT(64)	result of function is an array
3	=ARGUMENT("Y",64)	input array y
4	=ARGUMENT("X",64)	input array x
5	n =COUNT(X)	n= number of element in arrays X and Y
6	Ax =SUM(X)	X1+X2+...+Xn
7	Ay =SUM(Y)	Y1+Y2+...+Yn
8	Axx =SUMPRODUCT(X,X)	X1*X1+X2*Y2+...+Xn*Xn
9	Axy =SUMPRODUCT(X,Y)	X1*Y1+X2*Y2+...+Xn*Yn
10	D =n*Axx-Ax^2	
11	=IF(D=0,RETURN("ERR"))	
12	=(n*Axy-Ax*Ay)/D	
13	=(Ay*Axx-Ax*Axy)/D	
14	=RETURN(TRANSPOSE(B12:B13))	return slope and intercept on the same row

Figure 24 Macrosheet user-defined function MYLINEST for linear regression.

- After having tested the macrosheet function MYLINEST, you may test the Visual Basic function VBlinest. Replace MYLYNEST with VBlinest by using **Alt**+**H**.

```

Function VBlinest(Yarray, Xarray) As Variant
    Dim N As Integer, x As Single, y As Single,
    xx As Single, xy As Single, Slope As Single,
    Intercept As Single
    N = 0
    x = 0
    y = 0
    xx = 0
    xy = 0
    For Each c In Xarray
        N = N + 1
        x = x + Xarray(N)
        y = y + Yarray(N)
        xx = xx + Xarray(N)^2
        xy = xy + Xarray(N)*Yarray(N)
    Next
    Slope = (N*xy - x*y) / (N*xx - x^2)
    Intercept = (y*xx - x*xy) / (N*xx - x^2)
    VBlinest = Array(Slope, Intercept)
End Function

```

Figure 25 Visual basic user-defined function VBlinest for linear regression.

	A	B	C	D
5	x	y		
6	1	0.397		
7	2	0.503		
8	3	0.914		
9	4	0.680		
10	5	0.062		
11	6	0.268		
12	7	0.867		
13	8	0.528		
14	9	0.809		
15	10	0.271		
16	Result of built-in function LINEST			
17	Slope, intercept = -0.00090043 0.535050422			
18	Result of user-defined function MYLINEST			
19	Slope, intercept = -0.00090043 0.535050422			

Figure 26 Results of linear regression with LINEST and user-defined function MYLINEST.

	A	B	C	D
5	x	y		
6	1	=RAND()	Slope, intercept = =LINEST(y,x)	=LINEST(y,x)
7	2	=RAND()	Slope, intercept = =MYLINEST(y,x)	=MYLINEST(y,x)

Figure 27 Formulas used in Fig. 26.

EXAMPLE 6: USER-DEFINED FUNCTION FOR UNIT CONVERSION

EXERCISE

Write the user-defined function UNITS that converts the number X from a system of unit U into another unit V . Dimensions and UNITS are covered in Chapter 8-4.

PRINCIPLES OF UNIT CONVERSION

The user-defined function UNITS converts the value X initially in unit U into another compatible unit, V . The unit dimensions include length, area, volume, force, stress, unit weight, time, velocity, and diffusivity. Most metric and English units are considered. The converted value Y in new unit V of the value X in original unit U is obtained as follows:

$$Y = X * \text{UNITS}(U, V) \quad (9)$$

where U is the case-insensitive spelling of the old unit and V is the case-insensitive spelling of the new unit. The spelling of all the units is defined in Fig. 28. For instance, to convert 10 atm into kPa, enter the following formula:

$$= 10 * \text{UNITS}("atm", "kPa") \quad (10)$$

Figure 28 also gives the basic conversion factors used by UNITS. When AU and AV are the conversion factors of units U and V , respectively, then

$$Y = X * AV / AU \quad (11)$$

Figure 29 and 30 show the macrosheet and Visual Basic versions of the user-defined function for unit conversion. New units may be added provided that the new units names are spelt in lowercase, and that the extreme left column and bottom row of the table of unit names and conversion factors is left blank.

STEPS

- In a new workbook, use **Insert Macro MS Excel 4.0 Macro** to create a new macrosheet.
- Type the formulas and data as shown in Figs. 28 and 29. Assign the name UNITS to cell A1 by using **AL**. Check the function option when naming UNITS. Assign the name A to range E2:R20 of Fig. 28. Also assign the names i , j , and Av to cells C5, C6, and B10. The variable names A , i , j , and Av should be preceded by the macrosheet name and ! for having local variables (e.g., Macros!A).
- Use **Insert Module** to create the Visual Basic function VBUNITS shown in Fig. 30. You do not need to define the function name. The third argument of function VBUNITS is the table defined in UNITS.

	D	E	F	G	H	I	J
1	DIMENSION	Table 1					
2	length	inch	ft	ang	micron	mm	cm
3		1	0.083333333333	254000000	25400	25.4	2.54
4	area	inch2	ft2	cm2	m2	ha	acre
5		1	0.0069444	6.4516	0.00064516	0.00000064516	0.000000159423
6	volume	inch3	ft3	cm3	m3	gal	quart
7		1	0.0005787037	16.387064	0.000016387064	0.004329	0.017316
8	force	kg	dyne	gr	pound	tonl	ton
9		1	980665	1000	2.2046223	0.00098420653	0.0011023113
10	stress	atm	bar	cmhg	mmhg	ftwater	kg/cm2
11		1	1.0133	76	760	33.899	1.03323
12	unit weight	gr/cm3	t/m3	kg/m3	pci	pcf	kn/m3
13		1	1	1000	0.036127292	62.427961	9.8039
14	time	ms	s	mn	hr	day	month
15		1	0.001	0.00001666666	0.00000027777777	0.00000011574074	0.00000000038057
16	velocity	cm/s	micron/s	m/mn	ft/mn	mile/hr	ft/yr
17		1	10000	0.6	1.9685	0.022369	1034643.6
18	consolidation	cm2/s	cm2/month	cm2/yr	m2/month	m2/yr	inch2/s
19		1	2628000	31536000	262.8	3153.6	0.155

	D	K	L	M	N	O	P	Q
1	DIMENSION							
2	length	m	yard	mile	km			
3		0.0254	0.02777777	0.0000157	0.0000254			
4	area	mile2						
5		0.00000000249098						
6	volume	pint	l	ml				
7		0.034632	0.0163852	16.3852				
8	force	kip	t	n	kn	ounce		
9		0.0022046223	0.001	9.80665	0.00980665	32.1512		
10	stress	gr/cm2	kg/m2	t/m2	psf	psi	ton/ft2	kpa
11		1033.23	10332.3	10.3323	2116.22	14.696	1.0581	101.325
12	unit weight							
13								
14	time	yr						
15		0.000000003171416						
16	velocity							
17								
18	consolidation	inch2/month	inch2/yr	ft2/month	ft2/yr			
19		4151600	4888200	2882.998	33944.7			

Figure 28 Table of data used in user-defined function UNITS.

A	B	C
1	UNITS	Convert from
2	=RESULT(3)	one unit to another
3	=ARGUMENT("OLD",2)	New unit name in "
4	=ARGUMENT("NEW",2)	Old unit name in "
5	=SET.VALUE(i,1)	9
6	=WHILE(NOT(ISBLANK(INDEX(A,i,1))))	10
7	= SET.VALUE(j,1)	Above space is reserved
8	= WHILE(NOT(ISBLANK(INDEX(A,i,j))))	for counters i and j.
9	= IF(EXACT(INDEX(A,i,j),LOWER(NEW)))	For input, check spelling
10 AV	= INDEX(A,i+1,j)	of unit names in Table 1
11	= SET.VALUE(j,1)	Units may be added
12	= WHILE(NOT(ISBLANK(INDEX(A,i,j))))	into Table 1. However
13	= IF(EXACT(INDEX(A,i,j),LOWER(OLD)))	the named array A
14	= RETURN(AV/INDEX(A,i+1,j))	should have one more
15	= ELSE()	row and column than
16	= SET.VALUE(j,j+1)	Table 1. The unit
17	= END.IF()	names should be in lower
18	= NEXT()	case in Table 1.
19	= RETURN("ERROR")	
20	= ELSE()	
21	= SET.VALUE(j,j+1)	
22	= END.IF()	
23	= NEXT()	
24	= SET.VALUE(i,i+2)	
25	=NEXT()	
26	=RETURN("ERROR")	

Figure 29 User-defined function UNITS for unit conversion.

```

Function VBunits(OldUnit, NewUnit, AllUnits)
    Dim x, i, j
    i = 1
    Do Until IsEmpty(AllUnits(i, 1))
        j = 1
        Do Until IsEmpty(AllUnits(i, j))
            If AllUnits(i, j) = LCase(NewUnit) Then
                x = AllUnits(i + 1, j)
                j = 1
                Do Until IsEmpty(AllUnits(i, j))
                    If AllUnits(i, j) = LCase(OldUnit) Then
                        VBunits = x / AllUnits(i + 1, j)
                        Exit Function
                    Else
                        j = j + 1
                    End If
                Loop
                MsgBox "Check the units"
                Exit Function
            Else
                j = j + 1
            End If
        Loop
        i = i + 2
    Loop
    MsgBox "Check the units"
End Function

```

Figure 30 Visual Basic user-defined function for unit conversion.

	A	B	C	D	E	F	G	H
4	Examples of unit conversion with UNITS							
5	From feet to cm	X =	12.4 ft	= 377.95	cm			
6	From psf to kPa	X =	50 psf	= 2.39	kPa			
7	From pcf to kN/m ³	X =	120 pcf	= 18.85	kN/m ³			
8	From m/s ² to ft ² /yr	X =	0 cm ² /s	= 33.94	ft ² /yr			
							G	
5							=D5*UNITS(E5,H5)	
6							=D6*UNITS(E6,H6)	
7							=D7*UNITS(E7,H7)	
8							=D8*UNITS(E8,H8)	

Figure 31 Example for user-defined function UNITS.

- In a new worksheet, define the table and formulas of Fig. 31. You should find the results of Fig. 31.
- After having tested the macrosheet function UNITS, you may test the Visual Basic function VBunits. Replace UNITS with VBunits by using H . You will also need to add the third argument of VBunits, which contains the table of Fig. 28 [e.g., D5*VBunits(E5,H5,Macros!A) in cell G5 of Fig. 31].

EXAMPLE 7: USER-DEFINED FUNCTION FOR GRADE ASSIGNMENT

EXERCISE

Write a user-defined function that gives the course grade for numeric grades between 0 and 100. The custom function should specify the lower limit to get an A, B, C, and D and should automatically assign + and - in each grade category.

STEPS

- In a new workbook, use **Insert Macro MS Excel 4.0 Macro** to create a new macrosheet.
- Type the formulas as shown in Fig. 32. A_l , B_l , C_l , and D_l are the lower

	A	B
1	Grade	Grading program
2	=RESULT(2)	returns a letter grade
3	=ARGUMENT("G",1)	Number between 0 and 100
4	=ARGUMENT("A_l",1)	Lower limit to get A
5	=ARGUMENT("B_l",1)	Lower limit to get B
6	=ARGUMENT("C_l",1)	Lower limit to get C
7	=ARGUMENT("D_l",1)	Lower limit to get D
8	=IF(G>=(2*100/3+A_l/3),RETURN("A+"))	
9	=IF(G>=(100/3+2*A_l/3),RETURN("A"))	
10	=IF(G>=A_l,RETURN("A-"))	
11	=IF(G>=(2*A_l/3+B_l/3),RETURN("B+"))	
12	=IF(G>=(A_l/3+2*B_l/3),RETURN("B"))	
13	=IF(G>=B_l,RETURN("B-"))	
14	=IF(G>=(2*B_l/3+C_l/3),RETURN("C+"))	
15	=IF(G>=(B_l/3+2*C_l/3),RETURN("C"))	
16	=IF(G>=C_l,RETURN("C-"))	
17	=IF(G>=(2*C_l/3+D_l/3),RETURN("D+"))	
18	=IF(G>=(C_l/3+2*D_l/3),RETURN("D"))	
19	=IF(G>=D_l,RETURN("D-"))	
20	=RETURN("F")	

Figure 32 User-defined function for grade assignment.

	A	B	C	
	Student Name	Exam grade (/100)	Course grade	C
4	Mary Absent	10	F	4 Course grade
5	Joe Doe	85	B+	5 =Grade(B5,90,75,60,50)
6	Kathy Greats	90	A-	6 =Grade(B6,90,75,60,50)
7	Paul Reagan	70	C+	7 =Grade(B7,90,75,60,50)
8	Ian Smith	65	C	8 =Grade(B8,90,75,60,50)
9				9 =Grade(B9,90,75,60,50)

Figure 33 Example for user-defined function Grade and formulas used to call it.

limits to get an A, B, C, and D. Assign the name Grade to cell A1 by using **AL**.

- In a new worksheet, define the example of Fig. 33 and enter the formulas of Fig. 33 to get the course grade.

EXAMPLE 8: USER-DEFINED FUNCTION FOR CUBIC POLYNOMIAL REGRESSION

EXERCISE

Write a user-defined function that calculates the coefficients of cubic polynomial regression. Compare the results obtained with your function with those of Example 3 in the case of the variation of the viscosity and unit mass of water with temperature.

STEPS

- In a new workbook, use **Insert Macro MS Excel 4.0 Macro** to create a new macrosheet.
- Type the formulas and data as shown in Fig. 34. Assign the name FIT3

	A	B
19	FIT3	
20	=RESULT(64)	Fit cubic polynomial by linear regression
21	=ARGUMENT("X",64)	Input X-array
22	=ARGUMENT("Y",64)	Input Y-array
23	=COUNT(X)	349
24	=SUM(X)	8231
25	=SUMPRODUCT(X,X)	201889
26	=SUMPRODUCT(X,X,X)	5095943
27	=SET.VALUE(B23,A24)	Form matrix
28	=SET.VALUE(C23,A25)	
29	=SET.VALUE(D23,A26)	
30	=SET.VALUE(B24,A25)	
31	=SET.VALUE(C24,A26)	
32	=SET.VALUE(D24,SUMPRODUCT(X,X,X,X))	
33	=SET.VALUE(B25,A26)	
34	=SET.VALUE(C25,D24)	
35	=SET.VALUE(D25,SUMPRODUCT(X,X,X,X,X))	
36	=SET.VALUE(B26,D24)	
37	=SET.VALUE(C26,D25)	
38	=SET.VALUE(D26,SUMPRODUCT(X,X,X,X,X,X))	
39	=SET.VALUE(E23,SUM(Y))	
40	=SET.VALUE(E24,SUMPRODUCT(X,Y))	Form vector
41	=SET.VALUE(E25,SUMPRODUCT(X,X,Y))	
42	=SET.VALUE(E26,SUMPRODUCT(X,X,X,Y))	
43	=RETURN(MMULT(MINVERSE(A23:D26),E23:E26))	

Figure 34 User-defined function for cubic fitting.

to cell A19 by using AL . Do not forget to check the function option when naming user-defined functions.

- In a new worksheet, enter and format the heading and data of the table in Fig. 35.
- Assign the names T , hw , and rw to cell ranges A7:A22, B7:B22, and C7:C22 by using AL .
- Select the range B24:B27, type the formula of cell B24 shown in Fig. 36, and press Enter . Same thing for the range B29:B32. You should find the same coefficients as in Example 3.

	A	B	C
5	Temperature (°C)	Viscosity (g/s/cm)	Unit mass (g/cm³)
6	T	η_w	ρ_w
7	4.0	0.01567	1.00000
8	16.0	0.01111	0.99897
9	17.0	0.01083	0.99880
10	18.0	0.01056	0.99862
11	19.0	0.01030	0.99844
12	20.0	0.01005	0.99823
13	21.0	0.00981	0.99802
14	22.0	0.00958	0.99780
15	23.0	0.00936	0.99757
16	24.0	0.00914	0.99733
17	25.0	0.00894	0.99708
18	26.0	0.00874	0.99682
19	27.0	0.00855	0.99655
20	28.0	0.00836	0.99627
21	29.0	0.00818	0.99598
22	30.0	0.00801	0.99568
23	Nonlinear regression for viscosity (cubic)		
24	$a_0 =$	0.017771671	
25	$a_1 =$	-0.000568441	
26	$a_2 =$	1.11479E-05	
27	$a_3 =$	-1.01686E-07	
28	Nonlinear regression for unit mass (cubic)		
29	$b_0 =$	0.999910033	
30	$b_1 =$	5.20192E-05	
31	$b_2 =$	-7.51229E-06	
32	$b_3 =$	3.60518E-08	

Figure 35 Results of cubic polynomial regression for unit mass and viscosity of

A	B
23	Nonlinear
24	$a_0 = =\text{FIT3}(T,hw)$
25	$a_1 = =\text{FIT3}(T,hw)$
26	$a_2 = =\text{FIT3}(T,hw)$
27	$a_3 = =\text{FIT3}(T,hw)$
28	Nonlinear
29	$b_0 = =\text{FIT3}(T,rw)$
30	$b_1 = =\text{FIT3}(T,rw)$
31	$b_2 = =\text{FIT3}(T,rw)$
32	$b_3 = =\text{FIT3}(T,rw)$

Figure 36 Formulas used in Fig. 35.

Appendix:

Conversion Factors

LENGTH

To the unit below, multiply by

	inch	ft	ang	micron	mm	cm	m	yard	mile	km
inch	1	0.08333333	254.000E+6	25400	25.4	2.54	0.0254	0.02777777	15.700E-6	25.400E-6
ft	12	1	3.048E+9	304800	304.8	30.48	0.3048	0.33333324	0.000188	0.0003048
ang	3.937E-9	328.084E-12	1	0.0001	100.000E-9	1E-08	1E-10	109.361E-12	6.18E-14	100.000E-15
micron	39.370E-6	3.281E-6	10.000E+3	1	0.001	0.0001	0.000001	1.094E-6	6.18E-10	1.000E-9
mm	0.03937	0.00328084	10.000E+6	1000	1	0.1	0.001	0.00109361	6.18E-07	0.000001
cm	0.393701	0.0328084	100.000E+6	10000	10	1	0.01	0.01093613	6.18E-06	0.000001
m	39.37008	3.2808399	10.000E+9	1000000	1000	100	1	1.09361299	0.000618	0.001
yard	36.00001	3.000E+0	9.144E+9	914400.3	914.400256	91.44003	0.9144	1	0.000565	0.0009144
mile	63694.27	5307.85563	16.178E+12	1.618E+9	1617834.39	161783.4	1617.834	1769.28471	1	1.617834395
km	39370.08	3280.8399	1E+13	1.000E+9	1000000	100000	1000	1093.61299	0.61811	1

AREA

To the unit below, multiply by

	inch ²	ft ²	cm ²	m ²	ha	acre	mile ²
inch ²	1	0.0069444	6.4516	0.000645	64.516E-9	159.423E-9	249.098E-12
ft ²	144.00092	1	929.036346	0.092904	9.290E-6	22.957E-6	35.870E-9
cm ²	0.155000	0.0010764	1	0.0001	10.000E-9	24.711E-9	38.610E-12
m ²	1550.0031	10.763842	10000	1	0.0001	0.0002471	386.103E-9
ha	15500031	107638.42	100.000E+6	10000	1	2.4710614	0.003861027
acre	6272620.6	43559.587	40.468E+6	4046.844	0.4046844	1	0.001562497
mile ²	4.014E+9	27.878E+6	25.900E+9	2.590E+6	258.99847	640.00112	1

To convert from this unit

To convert from

VOLUME

To convert from this unit

To the unit below, multiply by

	inch ³	ft ³	cm ³	m ³	gal	quart	pint	l	ml
inch ³	1	0.0005787	16.3871	16.387E-6	0.004329	0.01732	0.03463	0.01639	16.3852
ft ³	1728	1	28316.8	0.02831685	7.480512	29.922	59.8441	28.3136	28313.626
cm ³	0.06102	35.315E-6	1	0.000001	0.0002642	0.00106	0.00211	0.001	1
m ³	61023.7	35.314666	1000000	1	264.17179	1056.69	2113.375	1000	1.00E+6
gal	231	0.1336807	3785.42	0.00378542		1	4	8	3.78498
quart	57.7501	0.0334202	946.354	0.00094635		0.25	1	2	0.9462425
pint	28.875	0.0167101	473.177	0.00047318		0.125	0.5	1	0.47312
l	61.0307	0.0353187	1000	0.00100011	0.2642018	1.05681	2.11361	1	1000
ml	0.06103	35.319E-6	1	1.000E-6	264.202E-6	1.057E-3	0.00211	0.001	1

TIME

To convert from

To the unit below, multiply by

	ms	s	mn	hr	day	month	yr
ms	1	0.001	16.667E-6	277.778E-9	11.574E-9	380.570E-12	31.714E-12
s	1000	1	0.0166667	0.00027778	11.574E-6	380.570E-9	31.714E-9
mn	60000.024	60.00002	1	0.0166667	0.00069444	22.834E-6	1.903E-6
hr	3600000.1	3600	59.999978	1	0.04166667	0.001370052	0.0001142
day	86400001	86400	1439.9994	23.9999995	1	0.032881248	0.0027401
month	2.628E+9	2627637	43793.941	729.899283	30.4124708	1	0.0833333
yr	31.532E+9	31531657	525527.4	8758.79323	364.949726	12.00000252	1

VELOCITY

To convert from

To the unit below, multiply by

	cm/s	micron/s	m/mn	ft/mn	mile/hr	ft/yr
cm/s	1	10000	0.6	1.9685	0.022369	1034644
micron/s	0.0001	1	0.00006	0.000197	2.24E-06	103.4644
m/mn	1.666667	16666.67	1	3.280833	0.037282	1724406
ft/mn	0.508001	5080.01	0.304801	1	0.011363	525600
mile/hr	44.70473	447047.3	26.82284	88.00125	1	46253458
ft/yr	9.67E-07	0.009665	5.8E-07	1.9E-06	2.16E-08	1

FORCE

To convert from this unit

	kg	dyne	gr	pound	tonl	ton	kip	t	N	kN	ounce
kg	1	980665	1000	2.204622	0.0009842	0.0011023	0.002205	1.000E-3	9.80665	0.0098067	32.151E+0
dynes	1.020E-6	1	0.00102	2.248E-6	1.004E-9	1.124E-09	2.248E-9	1.020E-9	0.00001	10.000E-9	32.785E-6
gr	0.001	980.665	1	0.002205	984.207E-9	1.102E-6	2.205E-6	0.000001	0.009807	9.807E-6	0.0321512
pound	0.453592	444822.2	453.5924	1	0.0004464	0.0005	0.001	0.0004536	4.448222	0.0044482	14.583541
tonl	1016.047	996.4E+6	1016047	2240	1	1.12	2.24	1.0160469	9964.016	9.9640164	32667.127
ton	907.1847	889.6E+6	907184.7	2000	0.8928572	1	2	0.9071847	8896.443	8.8964433	29167.078
kip	453.5924	444.8E+6	453592.4	1000	0.4464286	0.5000001	1	0.4535924	4448.222	4.4482223	14583.541
t	1000	980.7E+6	1000000	2204.622	0.9842065	1.1023113	2.204622	1	9806.65	9.80665	32151.2
N	0.101972	100000	101.9716	0.224809	0.0001004	0.0001124	0.000225	0.000102	1	0.001	3.27851
kN	101.9716	100.0E+6	101971.6	224.8089	0.1003611	0.1124045	0.224809	0.1019716	1000	1	3278.51
ounce	0.031103	30501.66	31.10304	0.06857	30.612E-6	34.285E-6	68.570E-6	31.103E-6	0.305017	0.000305	1

STRESS AND PRESSURE

To convert from this unit

	atm	bar	cmHg	mmHg	ftwater	kg/cm ²	gr/cm ²	kg/m ²	t/m ²	psf	psi	ton/ft ²	kPa
atm	1	1.0133	76	760	33.899	1.0332	1033.2	10332	10.3323	2116.2	14.696	1.0581	101.32
bar	0.986875	1	75.002	750.02	33.454	1.0197	1019.7	10197	10.1967	2088.4	14.503	1.04421	99.995
cmHg	0.013158	0.0133329	1	10	0.446	0.0136	13.595	135.95	136.0E-3	27.845	0.1934	0.01392	1.3332
mmHg	0.001316	0.0013333	0.1	1	0.0446	0.0014	1.3595	13.595	0.0136	2.7845	0.0193	1.392E-3	0.1333
ftwater	0.029499	0.0298917	2.242	22.42	1	0.0305	30.48	304.8	0.3048	62.427	0.4335	0.03121	2.989
kg/cm ²	0.967839	0.980711	73.556	735.556	32.809	1	1000	10000	10	2048.2	14.223	1.02407	98.066
gr/cm ²	967.8E-6	980.7E-6	0.0736	0.7356	0.0328	0.001	1	10	0.01	2.0482	0.0142	0.00102	0.0981
kg/m ²	96.784E-6	98.071E-6	0.0074	0.0736	0.0033	0.0001	0.1	1	0.001	0.2048	0.0014	0.0001	0.0098
t/m ²	0.096784	98.071E-3	7.3556	73.556	3.2809	0.1	100	1000	1	204.82	1.4223	0.10241	9.8066
psf	472.5E-6	478.825E-6	0.0359	0.3591	0.016	0.0005	0.4882	4.8824	0.00488	1	0.0069	0.0005	0.0479
psi	68.046E-3	0.0689507	5.1715	51.715	2.3067	0.0703	70.307	703.07	0.70307	144	1	0.072	6.8947
ton/ft ²	0.94509	0.95766	71.827	718.27	32.038	0.9765	976.5	9765	9.76496	2000	13.889	1	95.761
kPa	0.00986	10.000E-3	0.75006	7.5006	0.3346	0.0102	10.197	101.97	0.10197	20.885	0.145	0.01044	1

UNIT WEIGHT

To convert from this unit

	gr/cm ³	t/m ³	kg/m ³	pci	pcf	kN/m ³
gr/cm ³	1	1	1000	0.036127	62.42796	9.8039
t/m ³	1	1	1000	0.036127	62.42796	9.8039
kg/m ³	0.001	0.001	1	3.61273E-05	0.062428	0.009804
pci	27.6799	27.6799	27679.9	1	1728	271.3714
pcf	0.016018	0.016018	16.01846	0.000579	1	0.157043
kN/m ³	0.102	0.102	102.0002	0.003685	6.367666	1

DIFFUSIVITY

To the unit below, multiply by

To convert from this unit

	cm ² /s	cm ² /month	cm ² /yr	m ² /month	m ² /yr	inch ² /s	inch ² /month	inch ² /yr	ft ² /month	ft ² /yr
cm ² /s	1	2628000	31536000	262,8	3153,6	0,155	4151600	4888200	2882,998	33944,7
cm ² /month	380,518E-9	1	12	0,0001	0,0012	58,980E-9	1,579756	1,860046	0,001097	0,012917
cm ² /yr	31,710E-9	0,083333	1	8,333E-6	0,0001	4,915E-9	0,131646	0,155004	91,419E-6	0,001076
m ² /month	0,0038052	10000	120000	1	12	589,802E-6	15797,56	18600,46	10,97031	129,1655
m ² /yr	0,0003171	833,3333	10000	0,083333	1	49,150E-6	1316,464	1550,038	0,914193	10,76379
inch ² /s	6,4516129	16954839	203,458E+6	1695,484	20345,81	1	26784516	31536774	18599,99	218998,1
inch ² /month	240,871E-9	0,633009	7,59610752	63,301E-6	0,00076	37,335E-9	1	1,177426	0,000694	0,008176
inch ² /yr	204,574E-9	0,537621	6,45145452	53,762E-6	0,000645	31,709E-9	0,849311	1	0,000589	0,006944
ft ² /month	0,0003469	911,5511	10938,6132	0,091155	1,093861	53,763E-6	1440,029	1695,527	1	11,7741
ft ² /yr	2,94597E-05	77,42004	929,040469	0,007742	0,092904	4,566E-6	122,3048	144,0048	0,084932	1

Data Sheets

- Sieve analysis
- Hydrometer analysis
- Pipette analysis
- Buoyancy analysis
- Liquid limit test
- Plastic limit test
- Shrinkage test
- Determination of unit weight of soils
- Specific gravity test
- Compaction test
- Sand cone method
- Constant head permeability test
- Falling head permeability test
- Consolidation test
- Unconfined compression test
- Direct shear test
- Drained triaxial test
- Undrained triaxial test

Note: Additional datasheets can be printed from the Excel datafiles on the floppy disk provided with Experimental Soil Mechanics.

Sieve analysis

Analyst name: _____

Test date:

Sample description:

Total sample mass = g

Sieve analysis

Analyst name:

Test date:

Sample description:

Total sample mass = _____ g

ASTM Sieve number	Sieve opening (mm)	Mass retained (g)
4	4.750	
5	4.000	
6	3.350	
7	2.800	
8	2.360	
10	2.000	
12	1.700	
14	1.400	
16	1.180	
18	1.000	
20	0.850	
25	0.710	
30	0.600	
35	0.500	
40	0.425	
45	0.355	
50	0.300	
60	0.250	
70	0.212	
80	0.180	
100	0.150	
120	0.125	
140	0.106	
170	0.090	
200	0.075	
230	0.063	
270	0.053	
325	0.045	
400	0.038	

Hydrometer analysis

Analyst name: _____

Test date:

Sample description: _____

Mass in suspension W_0 = _____ g

Specific unit weight $G_s =$

Dispersing agent correction C_d = _____ g/L

Menicus correction $C_m =$

Cylinder diameter d_c = cm

Hydrometer bulb volume V_b = cm^3

Graduation mark on hydrometer stem (g/L)	Distance to bulb center (cm)
R _s	H _s
0	
10	
20	
30	
40	
50	
60	

Hydrometer analysis

Analyst name:

Test date: _____

Sample description:

Mass in suspension = g

Specific unit weight =

Dispersing agent correction = _____ g/L

Menicus correction = g/L

Cylinder diameter = _____ cm

Hydrometer number =

DATA SHEET

Pipette analysis

Analyst name: _____

Test date: _____

Sample description: _____

Dry method

Total mass in suspension = _____ g

Soil specific density =

Volume of pipette = _____ mL

Total volume of suspension = _____ mL

Mass of dry agent and bottle =

Mass of bottle = _____ g

DATA SHEET (cont.)

Pipette analysis

Analyst: _____

Test date:

Sample:

Wet method

Total soil mass in suspension = _____ g

Soil specific gravity =

Pipette volume = _____ mL

Total volume of suspension = _____ mL

Mass of sampled water, agent and bottle = _____ g

Mass of bottle = _____ g

Buoyancy analysis

Analyst name:

Test date:

Sample description: _____

Depth of sampling H = cm

Specific gravity $G_s =$

Total mass of soil in suspension $M_{\text{tot}} =$ g

Total volume of suspension $V_{\text{tot}} =$ cm^3

Mass of sphere in air M_a = _____ g

Mass of sphere in water M_w =

water and dispersing agent $M_r =$

Diameter of sedimentation cylinder d = _____ cm

Journal of Health Politics, Policy and Law, Vol. 30, No. 4, December 2005
DOI 10.1215/03616878-30-4 © 2005 by The University of Chicago

Buoyancy analysis

Analyst name: _____

Test date: _____

Sample description:

Depth of sampling H = _____ cm

Specific gravity G_s = _____

Total mass of soil in suspension $M_{\text{tot}} =$ _____ g

Total volume of suspension $V_{\text{tot}} =$ _____ cm^3

Mass of sphere in air M_a = _____ g

Mass of sphere in water M_w = _____ g

Water and dispersing agent M_r = _____ g

Mass of sphere in water and dispersing agent M_r = _____ g
Diameter of sedimentation cyclinder d = _____ cm

DATA SHEET

Liquid limit

Analyst name: _____

Test date: 12/20/2011

Sample description: _____

Plastic limit

Analyst name:

Test date: _____

Sample description: _____

DATA SHEET (cont.)

Liquid limit

Analyst name:

Test date: _____

Sample description:

Plastic limit

Analyst name: _____

Test date:

Sample description:

Shrinkage Test

Analyst name: _____

Test date: _____

Sample description: _____

WAX METHOD	Sample No.1	Sample No.2
Mass of coated dish (g)		
Mass of coated dish + wet soil (g)		
Mass of coated dish + dry soil (g)		
Volume of wet soil (cm ³)		
Mass of soil and wax (g)		
Buoyant Mass of soil and wax (g)		
Unit mass of wax (g/cm ³)		

Shrinkage Test

Analyst name: _____

Test date: _____

Sample description: _____

WAX METHOD	Sample No.1	Sample No.2
Mass of coated dish (g)		
Mass of coated dish + wet soil (g)		
Mass of coated dish + dry soil (g)		
Volume of wet soil (cm ³)		
Mass of soil and wax (g)		
Buoyant Mass of soil and wax (g)		
Unit mass of wax (g/cm ³)		

Shrinkage Test

Analyst name: _____

Test date: _____

Sample description: _____

MERCURY METHOD	Sample No.1	Sample No.2
Mass of coated dish (g)		
Mass of coated dish + wet soil (g)		
Mass of coated dish + dry soil (g)		
Volume of wet soil (cm ³)		
Mass of dish (g)		
Mass of dish + displaced mercury (g)		
Unit mass of Mercury (g/cm ³)		

Shrinkage Test

Analyst name: _____

Test date: _____

Sample description: _____

MERCURY METHOD	Sample No.1	Sample No.2
Mass of coated dish (g)		
Mass of coated dish + wet soil (g)		
Mass of coated dish + dry soil (g)		
Volume of wet soil (cm ³)		
Mass of dish (g)		
Mass of dish + displaced mercury (g)		
Unit mass of Mercury (g/cm ³)		

Unit Weight of soils

Analyst name: _____

Test date: _____

Sample description: _____

SOIL UNIT WEIGHT	Sample 1	Sample 2	Sample 3
Mass of soil sample (g)			
Mass of waxed soil (g)			
Mass of immersed soil (g)			
Mass of trimmed sample (g)			
Mass of dry sample (g)			

WAX UNIT WEIGHT	Sample 1	Sample 2
Mass of immersed iron block (g)		
Mass of wax block (g)		
Mass of immersed iron and wax blocks (g)		

Unit Weight of soils

Analyst name: _____

Test date: _____

Sample description: _____

SOIL UNIT WEIGHT	Sample 1	Sample 2	Sample 3
Mass of soil sample (g)			
Mass of waxed soil (g)			
Mass of immersed soil (g)			
Mass of trimmed sample (g)			
Mass of dry sample (g)			

WAX UNIT WEIGHT	Sample 1	Sample 2
Mass of immersed iron block (g)		
Mass of wax block (g)		
Mass of immersed iron and wax blocks (g)		

DATA SHEET**Unit Weight of soils**

Analyst name: _____

Test date: _____

Sample description: _____

SOIL UNIT WEIGHT	Sample 1	Sample 2	Sample 3
Mass of soil sample (g)			
Mass of waxed soil (g)			
Mass of immersed soil (g)			
Mass of trimmed sample (g)			
Mass of dry sample (g)			

WAX UNIT WEIGHT	Sample 1	Sample 2
Mass of immersed iron block (g)		
Mass of wax block (g)		
Mass of immersed iron and wax blocks (g)		

Unit Weight of soils

Analyst name: _____

Test date: _____

Sample description: _____

SOIL UNIT WEIGHT	Sample 1	Sample 2	Sample 3
Mass of soil sample (g)			
Mass of waxed soil (g)			
Mass of immersed soil (g)			
Mass of trimmed sample (g)			
Mass of dry sample (g)			

WAX UNIT WEIGHT	Sample 1	Sample 2
Mass of immersed iron block (g)		
Mass of wax block (g)		
Mass of immersed iron and wax blocks (g)		

DATA SHEET

Specific Gravity

Analyst name: _____

Test date: _____

Sample description: _____

	Sample 1	Sample 2
Mass of flask and water (g)		
Mass of flask, soil and water (g)		
Mass of evaporating dish (g)		
Mass of evaporating dish and dry soil (g)		

Specific Gravity

Analyst name: _____

Test date: _____

Sample description: _____

	Sample 1	Sample 2
Mass of flask and water (g)		
Mass of flask, soil and water (g)		
Mass of evaporating dish (g)		
Mass of evaporating dish and dry soil (g)		

Specific Gravity

Analyst name: _____

Test date: _____

Sample description: _____

	Sample 1	Sample 2
Mass of flask and water (g)		
Mass of flask, soil and water (g)		
Mass of evaporating dish (g)		
Mass of evaporating dish and dry soil (g)		

Specific Gravity

Analyst name: _____

Test date: _____

Sample description: _____

	Sample 1	Sample 2
Mass of flask and water (g)		
Mass of flask, soil and water (g)		
Mass of evaporating dish (g)		
Mass of evaporating dish and dry soil (g)		

Specific Gravity

Analyst name: _____

Test date: _____

Sample description: _____

	Sample 1	Sample 2
Mass of flask and water (g)		
Mass of flask, soil and water (g)		
Mass of evaporating dish (g)		
Mass of evaporating dish and dry soil (g)		

Specific Gravity

Analyst name: _____

Test date: _____

Sample description: _____

	Sample 1	Sample 2
Mass of flask and water (g)		
Mass of flask, soil and water (g)		
Mass of evaporating dish (g)		
Mass of evaporating dish and dry soil (g)		

Compaction test

Analyst name:

Test date:

Sample description:

Diameter of mold (cm)

Height of mold (cm) = _____

Mass of mold (g) =

Specific gravity $G_s =$

Compaction test

Analyst name: _____

Test date: _____

Sample description: _____

Diameter of mold (cm)

Height of mold (cm) = _____

Mass of mold (g) = _____

Specific gravity G_s = _____

Sand cone method

Analyst name: _____

Test date: _____

Sample description: _____

Measurement in the field

Mass of jar and sand before use M_f = _____ gMass of jar and sand after use M_e = _____ gMass of collected soil M = _____ g

Water content in the laboratory

Mass of can and wet soil (g) M_w Mass of can and dry soil (g) M_d Mass of can (g) M_c

Sample 1	Sample 2

Calibration in the laboratory

Diameter of mold D = _____ cmHeight of mold H = _____ cmMass of mold and sand (g) M_{ms} Mass of empty mold (g) M_m Mass of jar and sand before filling cone (g) M_{jb} Mass of jar and sand after filling cone (g) M_{ja}

Sample 1	Sample 2

Sand cone method

Analyst name: _____

Test date: _____

Sample description: _____

Measurement in the field

Mass of jar and sand before use M_f = _____ gMass of jar and sand after use M_o = _____ gMass of collected soil M = _____ g

Water content in the laboratory

Mass of can and wet soil (g) M_w Mass of can and dry soil (g) M_d Mass of can (g) M_t

Sample 1	Sample 2

Calibration in the laboratory

Diameter of mold D = _____ cmHeight of mold H = _____ cmMass of mold and sand (g) M_{ms} Mass of empty mold (g) M_m Mass of jar and sand before filling cone (g) M_{jb} Mass of jar and sand after filling cone (g) M_{ja}

Sample 1	Sample 2

Constant Head Permeability

Analyst name:

Test date:

Soil sample:

Specific gravity G_s =Specimen dry mass M_d =

g

Specimen height H =

cm

Specimen diameter D =

cm

Piezometer tap distance L =

cm

Trial	1	2	3	4
Piezometer level distance (cm) Δh				
Duration of sampling (s) t				
Mass of water collected & container (g) M_{wc}				
Mass of container (g) M_c				
Water temperature ($^{\circ}\text{C}$) T_e				

Constant Head Permeability

Analyst name:

Test date:

Soil sample:

Specific gravity G_s =Specimen dry mass M_d =

g

Specimen height H =

cm

Specimen diameter D =

cm

Piezometer tap distance L =

cm

Trial	1	2	3	4
Piezometer level distance (cm) Δh				
Duration of sampling (s) t				
Mass of water collected & container (g) M_{wc}				
Mass of container (g) M_c				
Water temperature ($^{\circ}\text{C}$) T_e				

Constant Head Permeability

Analyst name: _____

Test date: _____

Soil sample: _____

Specific gravity G_s = _____Specimen dry mass M_d = _____ gSpecimen height H = _____ cmSpecimen diameter D = _____ cmPiezometer tap distance L = _____ cm

Trial	1	2	3	4
Piezometer level distance (cm) Δh				
Duration of sampling (s) t				
Mass of water collected & container (g) M_{wc}				
Mass of container (g) M_c				
Water temperature ($^{\circ}\text{C}$) T_e				

Constant Head Permeability

Analyst name: _____

Test date: _____

Soil sample: _____

Specific gravity G_s = _____Specimen dry mass M_d = _____ gSpecimen height H = _____ cmSpecimen diameter D = _____ cmPiezometer tap distance L = _____ cm

Trial	1	2	3	4
Piezometer level distance (cm) Δh				
Duration of sampling (s) t				
Mass of water collected & container (g) M_{wc}				
Mass of container (g) M_c				
Water temperature ($^{\circ}\text{C}$) T_e				

DATA SHEET

Falling Head Permeability

Analyst Name: _____

Test Date: _____

Soil Sample: _____

Specific gravity G_s = _____

Specimen dry mass M = _____ g

Specimen height H = _____ cm

Specimen diameter D = _____ cm

Diameter of standpipe d_s = cm
Initial height in standpipe h_0 = cm

DATA SHEET

Falling Head Permeability

Analyst Name:

Test Date: _____

Soil Sample:

Specific gravity G_s = _____

Specimen dry mass M = _____ g

Specimen height H = _____ cm

Specimen diameter D = _____ cm

Diameter of standpipe d_s = _____ cm

Initial height in standpipe $h_0 =$ _____ cm

DATA SHEET

Consolidation test

Analyst : _____

Test date:

Sample description:

Initial sample height = cm

Sample diameter = cm

Initial sample mass = g

Initial sample mass = _____ g

Final sample mass = _____
mass of dry sample = _____

Initial dial reading = cm

Initial dial reading = _____ cm
Final dial reading = _____ cm

Final dial reading = _____ cm

Consolidation test

Analyst : _____

Test date:

Sample description: _____

Initial sample height = _____ cm

Sample diameter = _____ cm

Initial sample mass = _____ g

Final sample mass = _____ g

Final mass of dry sample = _____ g

Initial dial reading = _____ cm

Final dial reading = _____ cm

Unconfined compression test

Analyst name:

Test date: _____

Sample description:

Initial height h_0 = _____ cm

Initial diameter d_0 = _____ cm

Mass of wet sample and tare M_i = _____ g

Mass of dry sample and tare M_d = _____ g

Mass of tare M_t = _____ g

Specific gravity G_s = _____

Unconfined compression test

Analyst name:

Test date:

Sample description:

Initial height h_0 = _____ cm

Initial diameter d_0 = _____ cm

Mass of wet sample and tare M_i = _____ g

Mass of dry sample and tare M_d = _____ g

Mass of tare M_t = _____ g

Specific gravity G_s = _____

DATA SHEET

Direct Shear Test

Analyst name: _____

Test date: _____

Sample Description: _____

Mass of specimen M = _____ g

Vertical load $N =$ _____ N

Specific gravity G_s = _____

Initial height h_0 = _____ cm

Diameter d_0 = _____ cm

DATA SHEET (cont.)

Direct Shear Test

Analyst name: _____

Test date: _____

Sample Description: _____

Mass of specimen M = _____ g

Vertical load $N =$ _____ N

Specific gravity G_s = _____

Initial height h_0 = _____ cm

Diameter d_0 = _____ cm

DATA SHEET

Drained triaxial test

Analyst name: _____

Date: _____

Sample identification: _____

Weight of dry sample W = _____ g

Initial height of sample h_0 = _____ cm

Initial sample diameter D_0 = _____ cm

Soil specific gravity G_s = _____

Confining pressure σ_3 = _____ kPa

Back pressure σ_b = _____ kPa

Saturation coefficient B = _____ %

Rate of loading $v =$ mm

Volume change during consolidation $\Delta V_c =$ _____ cm^3

Drained triaxial test

Analyst name:

Date:

Sample identification:

Weight of dry sample $W =$ _____ g
 Initial height of sample $h_0 =$ _____ cm
 Initial sample diameter $D_0 =$ _____ cm
 Soil specific gravity $G_s =$ _____
 Confining pressure $\sigma_3 =$ _____ kPa
 Back pressure $\sigma_b =$ _____ kPa
 Saturation coefficient $B =$ _____ %
 Rate of loading $v =$ _____ mm/min
 during consolidation $\Delta V_c =$ _____ cm^3

DATA SHEET

Undrained triaxial test

Analyst name:

Date: _____

Sample identification:

Weight of dry sample W = g

Initial height of sample h_0 = _____ cm

Initial sample diameter D_0 = _____ cm

Soil specific gravity G_s = _____

Confining pressure σ_3 = _____ kPa

Back pressure $\sigma_b =$ _____ kPa

Saturation coefficient B = _____ %

Rate of loading $v =$ mm/s

during consolidation $\Delta V_c =$ _____ cm^3

•

Volume change during consolidation $\Delta V_c =$ _____ cm^3